

David Campillo Pérez

Study of the Reactivity of
Organometallic Platinum and
Palladium Complexes with Basic
Properties Towards Electrophilic
Species

Director/es

Martín Tello, Antonio Jesús

<http://zaguan.unizar.es/collection/Tesis>



Universidad de Zaragoza
Servicio de Publicaciones

ISSN 2254-7606



Tesis Doctoral

STUDY OF THE REACTIVITY OF
ORGANOMETALLIC PLATINUM AND PALLADIUM
COMPLEXES WITH BASIC
PROPERTIES TOWARDS ELECTROPHILIC
SPECIES

Autor

David Campillo Pérez

Director/es

Martín Tello, Antonio Jesús

UNIVERSIDAD DE ZARAGOZA
Escuela de Doctorado

Programa de Doctorado en Química Inorgánica

2022

Study of the Reactivity of Organometallic Platinum and Palladium Complexes with Basic Properties Towards Electrophilic Species

David Campillo Pérez

Tesis Doctoral

Memoria presentada para optar al grado de Doctor con Mención
Internacional por la Universidad de Zaragoza

Departamento de Química Inorgánica

Facultad de Ciencias – ISQCH

Universidad de Zaragoza - CSIC

2022

ANTONIO MARTÍN TELLO, Investigador Científico del CSIC en el Instituto de Síntesis Química y Catálisis Homogénea (Universidad de Zaragoza-CSIC)

CERTIFICA:

Que la presente Memoria titulada “Study of the Reactivity of Organometallic Platinum and Palladium Complexes with Basic Properties Towards Electrophilic Species” ha sido realizada en el Departamento de Química Inorgánica de la Universidad de Zaragoza y en el Instituto de Síntesis Química y Catálisis Homogénea (ISQCH) bajo su supervisión y AUTORIZA su presentación para que sea calificada como Tesis Doctoral. Asimismo, hace constar la realización de una estancia en modalidad online de tres meses en la *Katholieke Universiteit Leuven* (Lovaina, Bélgica), autorizando la solicitud a la mención internacional en el título de Doctor.

Zaragoza, a 10 de enero de 2022.

Fdo. Dr. Antonio Martín Tello

Al finalizar un trayecto tan arduo y desafiante como es una tesis doctoral, considero que es de recibo no dar por hecho que todos los esfuerzos para que el trabajo saliera adelante hayan sido solamente míos, ya que la contribución de muchas personas (directa o indirectamente) ha sido totalmente imprescindible para culminar este trabajo exitosamente. Es por ello que no puedo dejar de expresar un sincero agradecimiento:

Al Dr. Antonio Martín, director de esta Tesis Doctoral, por su supervisión, su continuo apoyo y su valiosa ayuda durante el desarrollo de este trabajo. También por su continua motivación durante todos estos años (unos cuantos ya) para que el trabajo avanzara adecuadamente y por nuestras charlas sobre series de vez en cuando. Quisiera agradecerle también su importantísimo trabajo en la resolución de las estructuras cristalinas incluidas en esta Memoria.

Al Dr. Daniel Escudero de la KU Leuven, supervisor de mi estancia internacional online, por su constante seguimiento, interés y buen hacer para dar mis primeros pasos en el interesante mundo de los cálculos teóricos. A pesar de la situación causada por la pandemia y de no haber podido viajar para desarrollar una estancia presencial, la experiencia ha sido muy gratificante y enriquecedora, gracias también a la existencia de seminarios y reuniones de grupo online.

Al Dr. Miguel Baya, por su inestimable ayuda en la realización de los experimentos de RMN a temperatura variable y por enseñarme los primeros fundamentos de cálculos teóricos durante mi tesis.

Al resto de componentes del grupo. A los Drs. Juan Forniés, José M^a Casas, Babil Menjón, Consuelo Fortuño, Irene Ara, Sara Fuertes y Violeta Sicilia por sus consejos y el inmejorable trato recibido.

Y por supuesto, al resto de *Platineros*: A Daniel por nuestras geniales conversaciones, como aquella sobre el viaje de Holanda que nunca hice, a Lorenzo por su ayuda en todos los campos de la química y más allá de los que ya es experto (Lorenzo, tú que sabes de todo...), a Alberto, que siempre estaba disponible para conversar y ponerme correctamente el cuello de la bata y al que echamos mucho de menos (ya debe tener un nivel C2 de alemán como mínimo) y a Antonio Gimeno, por su amistad y nuestras grandes conversaciones sobre roedores. También me acuerdo del resto de miembros pasados y presentes del grupo como Úrsula, Luis, Sergio, Guillermo, Sara y Nacho.

No me olvido tampoco de mis amigos de fuera de la Universidad. Tengo grandes recuerdos de nuestros geniales sábados de juegos de mesa en los que tan bien lo pasamos con el Imperial Assault, el Blackstone Fortress y el Blomavén; Rafael “Workaholic” Herguedas (el hombre que siempre se llevaba el portátil en nuestras vacaciones), Guillermo “Payoyo” Ríos, Daniel “Citadel” Ríos y D. Javier Branco (¡¿qué has dicho?!). Muchas gracias por vuestra valiosa amistad y por nuestros divertidos viajes veraniegos.

Agradezco también los ánimos, nuestros ya clásicos viajes para el puente del Pilar y la sincera relación de amistad a Samuel Llonga, a quien conozco desde preescolar.

Adicionalmente, me acuerdo mucho de mis amigos de la carrera, *The Walking Freaks*, como Daniel Bafaluy, Daniel Ardaiz, Victor Elía, Cesar Blasco, Miriam Abad, Raquel Díaz, Cristina Espeja y Laura Espada, a quienes no veo tan a menudo como me gustaría.

Muy especialmente querría agradecer también a mis padres, mi hermano y al resto de mi familia por el apoyo durante todo este largo tiempo de tesis doctoral.

Por último, quiero dar las gracias a la D.G.A. por la concesión de un contrato predoctoral para la realización de la tesis.

¡A todos, muchas gracias!

La realización de esta tesis ha sido posible gracias a la financiación a través de los siguientes proyectos:

- Proyecto PGC2018-094749-B-I00 financiado por MCIN/AEI/10.13039/501100011033/ y por FEDER Una manera de hacer Europa.
- Gobierno de Aragón (Grupo E17_20R: Química Inorgánica y de los Compuestos Organometálicos).

A mis padres

A Raúl

Abstract

Reactivity of neutral platinum and palladium (II) complexes with a CNC cyclometallated ligand, [Pt(CNC)(PPh₃)], [Pd(CNC)(PPh₃)] or [Pt(CNC)(dmsO)], has been studied towards several electrophilic species: acidic metallic centers, species containing acidic hydrogens and CH₃⁺.

When the electrophile used is an acidic metallic species, M' (M' = Ag(I), Au(I)), bimetallic clusters with M-M' donor-acceptor bonds of different nuclearities are obtained. In these complexes, the acidic center M' also establishes an interaction with a C_{ipso} of the CNC ligand, which is detected not only in the solid state but also in solution. Structural and computational studies carried out on these polymetallic species suggest that they can be regarded as arrested intermediates of a transmetallation process, in which the process cannot proceed completely due to the pincer nature of the CNC ligand.

When the platinum and palladium (II) compounds are reacted with a protic acid the breakage of a M-C_{ipso} bond and formation of a C-H bond is produced. Depending on the anion of the acid and the ligand present in solution either cationic or neutral M(II) species are obtained. If the reaction of the appropriate starting substrate is carried out with organic ligands with acidic hydrogens and donor atoms, the same result is observed with the coordination of the ligand in a bidentate or bridge fashion.

Finally, if the Pt(II) species [Pt(CNC)(PPh₃)] is reacted towards MeI *via* oxidative addition and followed by a reductive elimination, methylation of the C_{ipso} of the CNC ligand can be achieved. This process can be repeated twice rendering as a global result two methylations of the C_{ipso} of the CNC ligand.

All the complexes of this thesis have been fully characterized and studied by several techniques as IR, multinuclear NMR, MS, X-Ray diffraction and DFT computational studies.

Resumen

La reactividad de los complejos neutros de platino y paladio (II) con un ligando ciclometalado CNC, [Pt(CNC)(PPh₃)], [Pd(CNC)(PPh₃)] o [Pt(CNC)(dmsO)], ha sido estudiada frente a varias especies electrófilas: centros metálicos ácidos, especies con hidrógenos ácidos y CH₃⁺.

Cuando el electrófilo utilizado es un metal ácido, M' (M' = Ag(I), Au(I)), se obtienen clústeres bimetálicos con enlaces dador-aceptor M-M' de diferente nuclearidad. En estos complejos, el centro metálico ácido M' también establece una interacción con un C_{ipso} del ligando CNC, detectada tanto en estado sólido como en disolución. Estudios estructurales y computacionales llevados a cabo en estas especies polimetálicas sugieren que pueden ser consideradas como intermedios congelados de un proceso de transmetalación, en el que éste no puede completarse debido a la naturaleza pincer del ligando CNC.

Cuando se hacen reaccionar los complejos de platino y paladio (II) con un ácido prótico, se produce la ruptura de un enlace M-C_{ipso} y la formación de un enlace C-H. Dependiendo del anión del ácido y del ligando presente en disolución se obtienen complejos M(II) catiónicos o neutros. Si la reacción con el sustrato de partida adecuado se lleva a cabo frente a ligandos orgánicos con hidrógenos ácidos y átomos dadores, se observa el mismo resultado y la coordinación del ligando de forma bidentada o puente.

Por último, si se hace reaccionar la especie de Pt(II) [Pt(CNC)(PPh₃)] con MeI mediante un proceso de adición oxidante seguida de una eliminación reductora, se puede conseguir la metilación de un C_{ipso} del ligando CNC. Este proceso se puede repetir para producir, como resultado global, dos metilaciones de los C_{ipso} del ligando CNC.

Todos los complejos recogidos en esta tesis han sido completamente caracterizados y estudiados por diversas técnicas como IR, RMN multinuclear, espectrometría de masas, difracción de rayos X y estudios computacionales DFT.

List of Abbreviations

CNC	2,6-di(phen-2-ide)-pyridine
dmsO	Dimethyl sulfoxide
PPh ₃	Triphenylphosphane
tht	Tetrahydrothiophene
THF	Tetrahydrofuran
ⁱ PrOH	Propan-2-ol
Me ₂ CO	Acetone
MeOH	Methanol
H ₂ -SPy	Pyridine-2-thiol
HTfO	Trifluoromethanesulfonic acid
8-hqH	8-Hydroxyquinoline
PPh ₂ (C ₆ H ₄ - <i>o</i> -OH)	(2-Hydroxyphenyl)diphenylphosphane
NC ₅ H ₄ - <i>o</i> -COOH	Pyridinecarboxylic acid
PPh ₂ (C ₆ H ₄ - <i>o</i> -COOH)	2-(Diphenylphosphino)benzoic acid
xyl	Xylyl
tol	Tolyl
<i>o</i> -	<i>Ortho</i>
<i>m</i> -	<i>Meta</i>
<i>p</i> -	<i>Para</i>
RT	Room Temperature
IR	
ATR	Attenuated Total Reflection

vs	Very strong
s	Strong
m	Medium
w	Weak
vw	Very weak

NMR

VT	Variable temperature
s	Singlet
br. s	Broad singlet
d	Doublet
dd	Doublet of doublets
dt	Doublet of triplets
t	Triplet
td	Triplet of doublets
tt	Triplet of triplets
m	Multiplet
COSY	Correlation Spectroscopy
APT	Attached Proton Test
HSQC	Heteronuclear Single Quantum Coherence
HMBC	Heteronuclear Multiple Bond Correlation

MS

ESI	Electrospray Ionization
-----	-------------------------

MALDI

Matrix-Assisted Laser Desorption/Ionization

Computational studies

DFT

Density Functional Theory

QTAIM

Quantum Theory of Atoms In Molecules

BP

Bond Path

BCP

Bond Critical Point

$\rho(r)$

Electron density

au

Atomic units

$\nabla^2\rho(r)$

Laplacian

NBO

Natural Bond Orbital

WBI

Wiberg Bond Index

EDA

Energy Decomposition Analysis

SMD

Solvation Model based on Density

CDFT

Conceptual Density Functional Theory

List of Compounds

- 1 [Pt(CNC)(PPh₃)]
- 2 [Pd(CNC)(PPh₃)]
- 3 [Pd(CNC-H)Cl(PPh₃)]
- 4 [(CNC)(PPh₃)PtAu(PPh₃)](ClO₄)
- 5 [(CNC)(PPh₃)PdAu(PPh₃)](ClO₄)
- 6 [{Pt(CNC)(PPh₃)₂Au]}(ClO₄)
- 7 [{Pd(CNC)(PPh₃)₂Au]}(ClO₄)
- 8 [{Pt(CNC)(PPh₃)₂Ag]}(ClO₄)
- 9 [{Pd(CNC)(PPh₃)₂Ag]}(ClO₄)
- 10 [(CNC)(PPh₃)PtAg(PPh₃)](ClO₄)
- 11 [(CNC)(PPh₃)PdAg(PPh₃)](ClO₄)
- 12 [Pt(CNC)(dmsO)]
- 13 [Pt(CNC-H)Cl(PPh₃)]
- 14 [Pt(CNC-H)Cl(dmsO)]
- 15 [Pt(CNC-H)(MeCN)(PPh₃)](ClO₄)
- 16 [Pd(CNC-H)(MeCN)(PPh₃)](ClO₄)
- 17 [Pt(CNC-H)(H₂O)(PPh₃)](ClO₄)
- 18 [Pd(CNC-H)(H₂O)(PPh₃)](ClO₄)
- 19 [Pt(CNC-H)(tht)(PPh₃)](ClO₄)
- 20 [Pd(CNC-H)(tht)(PPh₃)](TfO)
- 21 [Pt(CNC-H)(μ-S-2Py)]₂
- 22A *trans*-(N,O) [Pt(CNC-H)(8-hq)]
- 22B *trans*-(N,N) [Pt(CNC-H)(8-hq)]

- 23 [Pt(CNC-H){PPh₂(C₆H₄-*o*-O)}]
- 24 [Pd(CNC-H){PPh₂(C₆H₄-*o*-O)}]
- 25A *trans*-(N,O) [Pt(CNC-H)(NC₅H₄-*o*-COO)]
- 25B *trans*-(N,N) [Pt(CNC-H)(NC₅H₄-*o*-COO)]
- 26 [Pt(CNC-H){PPh₂(C₆H₄-*o*-COO)}]
- 27 [Pd(CNC-H){PPh₂(C₆H₄-*o*-COO)}]
- 28 [PtMe(CNC)(PPh₃)]
- 29 [Pt(CN-*o*-tol)I(PPh₃)]
- 30 [Pt(CN-*o*-tol)(MeCN)(PPh₃)](ClO₄)
- 31 [Pd(CN-*o*-tol)I(PPh₃)]
- 32 [Pt(CNC-Me)(PPh₃)]
- 33 [Pt(CN-2,6-xyl)I(PPh₃)]
- 34 [PtMe(CNC-Me)(PPh₃)]
- 35 [Pt(CN-*o*-tol)Cl(PPh₃)]

Table of Contents

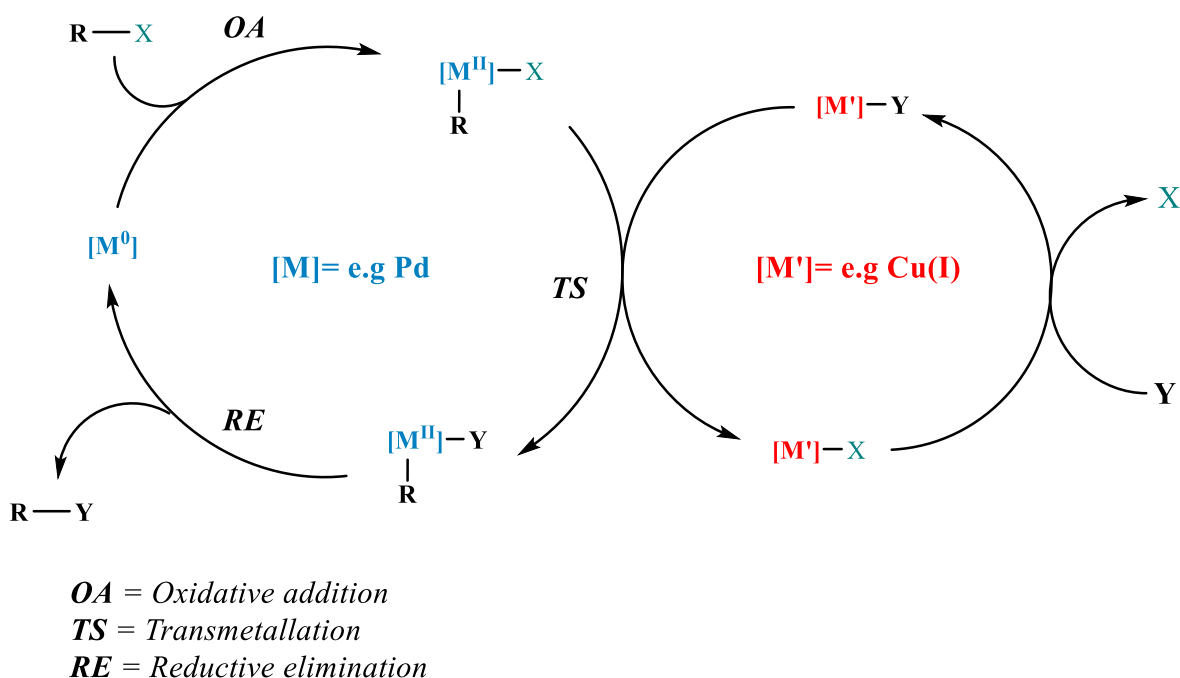
Introduction	1
References.....	14
Chapter 1. Organometallic complexes with M-M' bonds as intermediates for bimetallic catalysis	29
1.1. Preparation and characterization of heterobimetallic platinum-gold and palladium-gold complexes [(CNC)(PPh ₃)MAu(PPh ₃)](ClO ₄) (M = Pt (4), Pd (5)) and [{M(CNC)(PPh ₃) ₂ Au](ClO ₄) (M = Pt (6), Pd (7))	33
1.2. Preparation and characterization of heterobimetallic platinum-silver and palladium-silver complexes [{M(CNC)(PPh ₃) ₂ Ag](ClO ₄) (M = Pt (8), Pd (9)) and [(CNC)(PPh ₃)MAg(PPh ₃)](ClO ₄) (M = Pt (10), Pd (11)).....	47
1.2.1. Characterization of trinuclear complexes [{M(CNC)(PPh ₃) ₂ Ag](ClO ₄) (M = Pt (8), Pd (9)).....	49
1.2.2. Characterization of mixtures 10* and 11*	54
1.3. DFT calculations and structural analysis: degree of transmetallation on the M-M' complexes	60
1.4. Experimental section	79
1.5. References.....	87
Chapter 2. Reactivity of platinum (II) and palladium (II) cyclometallated substrates towards sources of H ⁺	93
2.1. Reactivity of platinum (II) and palladium (II) cyclometallated substrates towards protic acids	95
2.1.1. Reactions with HCl: formation of neutral species	96
2.1.2. Reactions with HClO ₄ , HTfO and HBF ₄ ·OEt ₂ : formation of cationic species	102
2.1.3. Reactions in presence of acetonitrile	104

2.1.4. Reactions in presence of water	106
2.1.5. Reactions in presence of tetrahydrothiophene	109
2.2. Reactivity of platinum (II) and palladium (II) cyclometallated substrates towards organic ligands with acidic hydrogens	112
2.2.1. Reaction with a ligand with -SH group.....	113
2.2.2. Reactions with ligands with -OH groups	117
2.2.3. Reactions with ligands with -COOH groups	128
2.3. Experimental section	138
2.4. References.....	151
Chapter 3. Reactivity of platinum (II) and palladium (II) cyclometallated substrates towards sources of Me ⁺	157
3.1. Reactivity of [Pt(CNC)(PPh ₃)] (1) and [Pd(CNC)(PPh ₃)] (2) towards sources of electrophilic methyl groups	159
3.1.1. First methylation of the CNC ligand with MeI.....	160
3.1.2. Second methylation of the CNC ligand with MeI	172
3.1.3. Reactivity of [Pt(CNC-Me)(PPh ₃)] (32) towards HCl.....	179
3.2. Experimental section	184
3.3. References.....	190
Conclusions / Conclusiones.....	195

Introduction

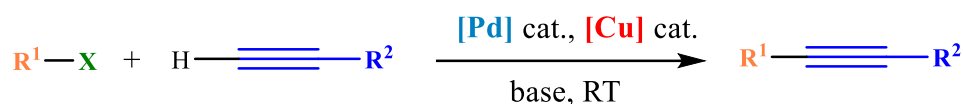
The study of heteropolynuclear complexes with metal-metal interactions between closed or pseudo-closed shell transition metals (d^8 , d^{10} , $d^{10}s^2$) constitutes a very well-studied field of knowledge in inorganic chemistry.¹⁻⁴ The interest on this kind of compounds resides in several possible applications due to their luminescent properties or their potential use in crystal engineering.⁵⁻⁷

Remarkably, this interest has grown lately because species containing these interactions may play an important role in cooperative catalysis, which in the last decade has emerged as a strategy affording novel and more efficient transformations.⁸⁻¹⁵ Thus, polymetallic complexes have attracted attention because it has been recognized that these species may play a crucial role in bimetallic catalysis processes, especially in C-C or C-X coupling reactions.¹⁶ In many of the catalytic reactions involving bimetallic systems, the metallic couples consist of a potential donor metallic center as Pd(II) or Pt(II) and an acceptor center such as Cu(I), Ag(I) or Au(I).^{8,17-20} In fact, these are some of the most typical metallic centers that have a tendency to establish intermetallic donor-acceptor interactions, as they are acids and bases of Lewis. These metallic systems typically operate *via* combined cycles that connect through a necessary intersecting step: the transmetallation step (see TS, Scheme I.1).



Scheme I.1. General mechanistic scheme for a bimetallic catalysis process.

Indeed, in some widely studied catalytic couplings, a transmetalation process in which the metallic centers are able to exchange their ligands is needed to obtain the seek cross-coupling product. A very well-known example is the classic Sonogashira reaction (see Scheme I.2), which allows the coupling of terminal acetylenes with aryl or vinyl halides, and where Pd(II) and M'(I) (M' = Cu, Ag, Au) species are used as catalysts.²¹⁻²⁵



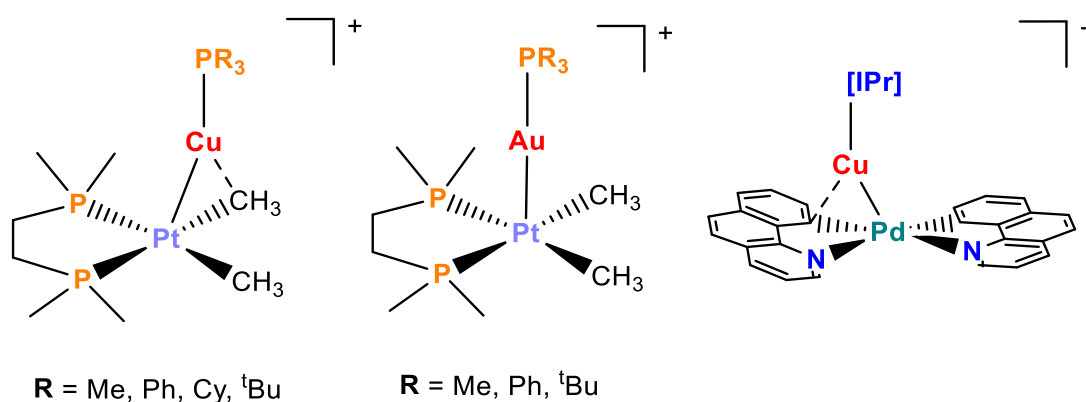
R^1 = aryl

R^2 = aryl or vinyl

X = I, Br, Cl or TfO

Scheme I.2. General scheme for the Sonogashira reaction.

Thus, the understanding of every aspect of the transmetalation step can be of crucial importance for the design of efficient catalytic systems. In the literature, several studies point to the formation of donor-acceptor M-M' interactions as a key feature of the transmetalation process. For example, Chen and coworkers have reported and investigated several heterobimetallic complexes related with this topic (see Scheme I.3 for some examples).²⁶⁻³² This group identified complexes with Pt-M' bonds (M' = Cu, Au) which have been detected in the gas phase or in solution as intermediates in transmetalation reactions involving methyl groups.²⁸ On the other hand, the same group described that the formation of species with Pd-M' bonds (M' = Cu, Ag, Au) plays an important role in the decrease of the energetic barrier on the transmetalation step in Sonogashira reactions.^{29,30}

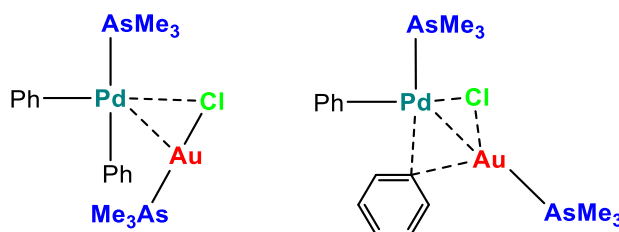


Scheme I.3. Examples of complexes with M-M' bonds reported by Chen *et al.*

Furthermore, Lledós, Khusnutdinova and coworkers found that subtle changes in Pd-Cu distances in heterobimetallic complexes with polydentate ligands affected to the efficiency of Sonogashira processes; complexes with shorter intermetallic bond distances showed to increase its reactivity towards a terminal alkyne.³³

Takita, Uchiyama and coworkers took advantage of the lowered activation energy on transmetallation processes for cross coupling reactions with Pd and Cu systems involving highly sterically hindered structures, due to the existence of Pd-Cu intermetallic interactions.³⁴

Besides, Espinet and coworkers studied the importance of Pd-Au interactions in processes of aryl transmetallation with Pd and Au systems (see Scheme I.4 for some examples of intermediates), in which the formation of these intermetallic interactions seemed to be crucial to stabilize the reaction intermediates.^{35,36}



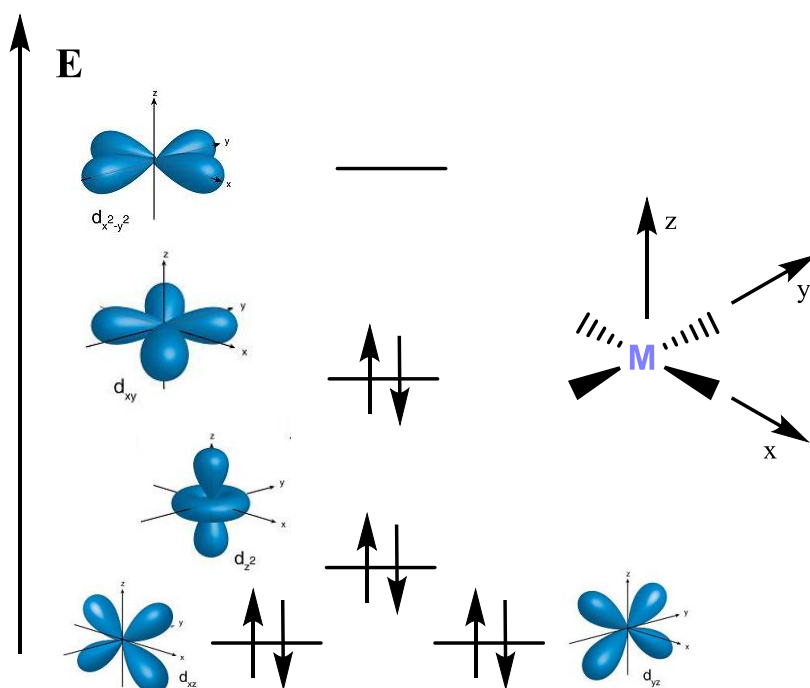
Scheme I.4. Some proposed intermediates for an aryl transmetallation process by Espinet *et al.*

Similar results were observed by Zhang and coworkers in the cross coupling reaction of iodobenzene facilitated by Pd-Au species,³⁷ and by Hashmi and coworkers in several Pd-Au transmetallation scenarios, in which a transition state with short Pd-Au contacts was favored.³⁸

In the literature, the synthesis and characterization of complexes bearing Pt-M donor-acceptor bonds has been extensively studied, being M' an acidic metal as Ag(I),³⁹⁻⁵⁰ Tl(I),^{48,51-57} Au(I),^{47,57-64} Cu(I),^{27,65} Pb(II),^{55,66,67} Cd(II),^{5,68} or Hg(II).⁶⁹⁻⁷¹ Accordingly, square planar Pt(II) d⁸ complexes have been widely regarded as proper starting materials to render heteropolymetallic clusters with interesting structural features and varied nuclearities, as dinuclear,^{41,43,47,59,68} trinuclear,^{39,41,44,45,47} tetranuclear clusters^{39,42,46,48,72,73} or even infinite chains.^{43,48,54,56,57}

Thus, for these Pt(II)-M' compounds, Ag(I) has been typically the most studied acidic metal followed by Tl(I) and to a much lesser extent Au(I). Besides, the same can be applied to Pd(II)-M' complexes, but examples of bimetallic complexes with this kind of bonds are much more scarce than their platinum analogues.^{59,60,74-76}

To understand the nature of this interaction it is necessary to consider the different energies of the d orbitals in square planar Pt(II) and Pd(II) d⁸ complexes (see Scheme I.5). The splitting of the d orbitals of the metal due to the ligand field is strong enough to consider the metallic center as a closed shell species.



Scheme I.5. Schematic d-orbital diagram for Pt(II) and Pd(II) square planar d⁸ species.

On the other hand, the existence of a filled dz^2 orbital oriented on the z-axis direction of the square planar environment of the Pt(II) or the Pd(II) metal, allows the metallic center to act as a Lewis base towards acidic metallic species M'.

The nature of the Pt(II)-M' and Pd(II)-M' donor-acceptor bonds can be described therefore as dative bonds in which an electron rich metallic species, that is, a base of Lewis donates its electron density to an acidic metallic center, which acts as a Lewis acid. As a whole, this bond is participated by the dz^2 orbital of the Pt or Pd center and an empty s-orbital of the acidic metal.^{47,52,76} Concerning the strength of these interactions, they are

considered to be weaker than ionic or covalent bonds, but stronger than other weaker interactions as Van der Waals forces.⁴

The molecular orbital diagram of these complexes shows that the higher in energy the dz^2 orbital of the Pt(II) or Pd(II) centers, the stronger the M-M' interaction. Thus, the presence of strong field ligands in the metal coordination sphere causes an increase in the energy of the dz^2 orbital of the Pt(II) or Pd(II) centers and favor the intermetallic interaction. It is very common to observe intermetallic interactions in cyclometallated complexes with π -conjugated ligands; this sort of ligands exert a strong field effect because they act as σ -donors and π -acceptors. Chelate ligands C^N, CNN, CNC and NCN are a representative example of this kind of π -conjugated ligands, not only because they are widely used to obtain heterobimetallic complexes but also due to the fact that they can be used for luminescent and biological applications.^{5,44,66,77-90}

Due to the participation of the dz^2 orbital of the platinum center in the M-M' bond, there are several examples in the literature of Pt(II) derivatives (see Figure I.1 for some examples) in which the Pt-M' lines are almost perpendicular to the best square planar environment of the platinum center.⁹¹⁻⁹²

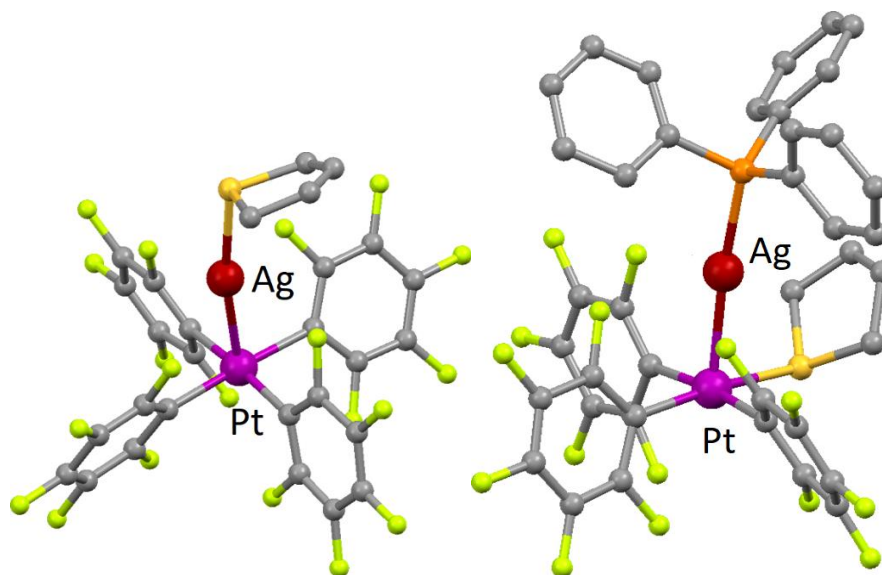


Figure I.1. Pentafluorophenyl platinum(II) complexes with Pt-Ag bonds.

This structural feature changes when there is a cyclometallated ligand coordinated to the metallic center. For example, cyclometallated C^N or CNC ligands in the coordination sphere of the Pt(II) or Pd(II) center (see Figure I.2 for some examples), cause the M-M' line to lean towards the ligand carbon bonded to the metal, due to the existence

of $\eta^1\text{-M}'\text{-C}$ short interactions in the solid state. These $\eta^1\text{-M}'\text{-C}$ interactions have been observed in silver,^{41,47,48} gold,^{47,57} copper^{27,30,33} and zinc³¹ heterobimetallic complexes. Interestingly, for the widely studied Pt-Tl derivatives this interaction is not observed.^{48,53,56,76}

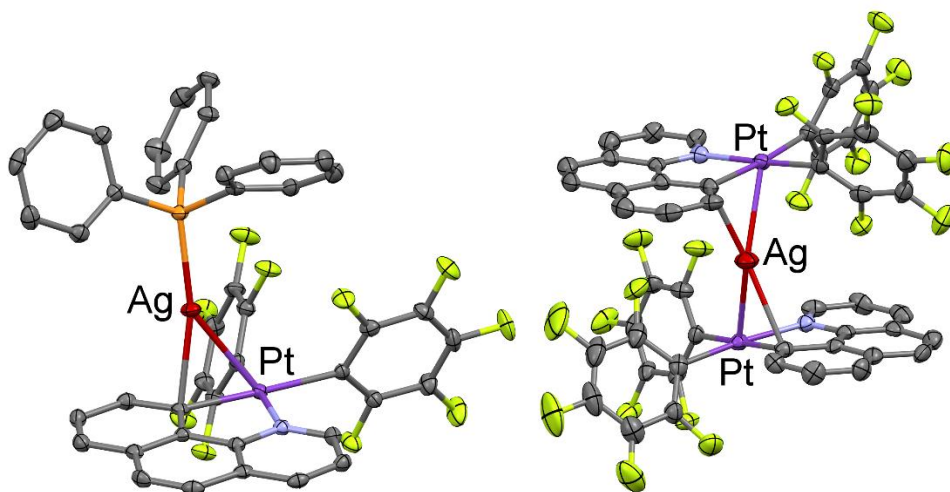


Figure I.2. Examples of benzoquinolate platinum-silver complexes with $\eta^1\text{-M}'\text{-C}$ interactions.

The use of a CNC ligand, such as 2,6-di(phen-2-ide)-pyridine, has also been lately studied in the synthesis of heteropolymetallic complexes.^{47,48,53,54} Again, short $\eta^1\text{-M}'\text{-C}$ interactions are observed in the solid state for silver and gold derivatives (see Figure I.3 for some examples).

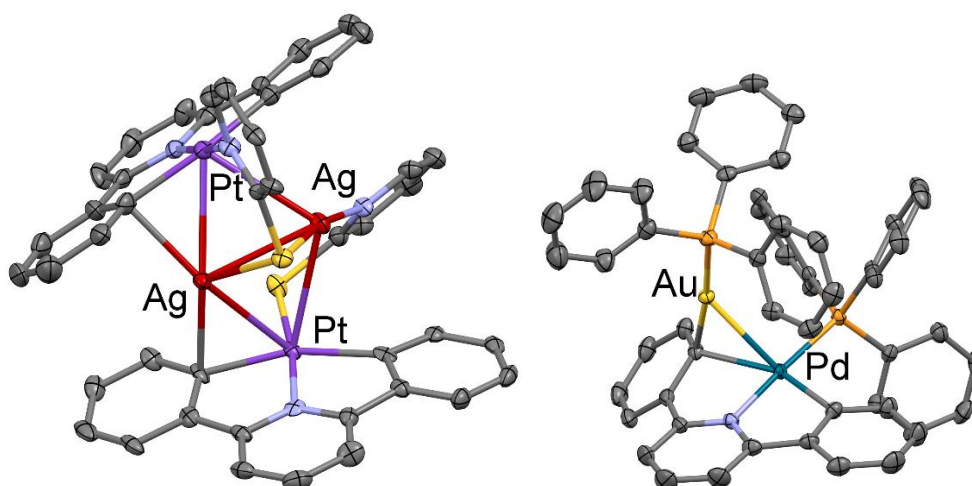
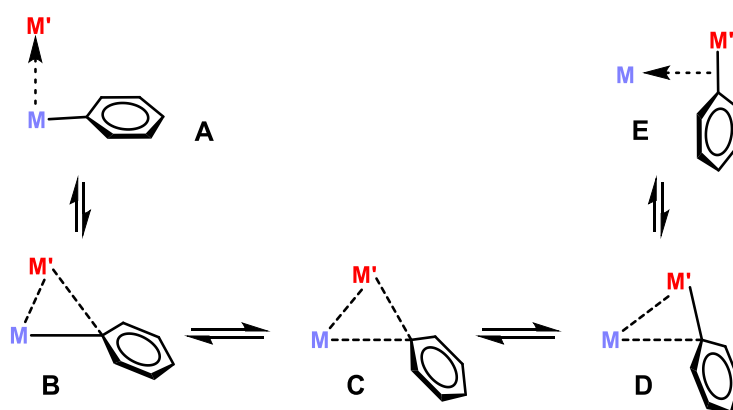


Figure I.3. Examples of M-M' complexes with CNC ligands showing $\eta^1\text{-M}'\text{-C}$ interactions.

The presence of the $\eta^1\text{-M}'\text{-C}$ interaction is also observed for some complexes in solution, where these interactions form and break giving rise to a dynamic intramolecular process.^{47,61}

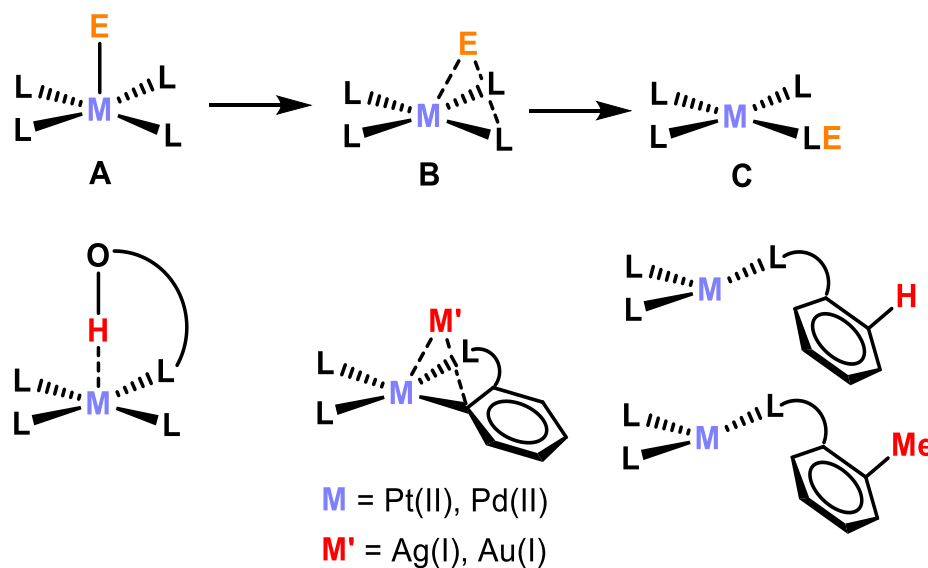
The existence of these remarkable $\eta^1\text{-M}'\text{-C}$ interactions and the previous work in the literature about intermetallic interactions taking place in bimetallic catalysis processes, allow to think that this kind of complexes could be regarded as a frozen snapshot of a transmetallation reaction. In these compounds, the exchange process of a phenyl group between the two different metals has been arrested at different stages, and due to the pincer nature of the tridentate CNC ligand it cannot be completed. Depending on the metallic systems used, this degree of transfer (see Scheme I.6) from one metal to the other is different.



Scheme I.6. Transmetallation process in a heterobimetallic system, showing five different degrees of transfer of a phenyl group.

The chemistry described so far evidences the role of the basic metal (mainly Pt but also Pd) in these complexes as a Lewis base which is able to form adducts with acidic metals that behave as Lewis acids, through dative metal-metal bonds. As described above, this is a key event in some reactions since these $\text{M-M}'$ species can be the initiators of a subsequent process in which transmetallation, that is, ligand exchange between metals, takes place. This exchange involves the cleavage and formation of new bonds, a feature that is paramount in chemistry. Along these lines, the basic properties of these CNC square planar M ($\text{M} = \text{Pt}$ or Pd) complexes can also be activated towards other electrophiles that behave as Lewis acids, other than metals (E). Thus, the formation of adducts M-E may be the starting point for reactions in which E is transferred to ligands (see Scheme I.7, stages A to C), in a similar way to the acidic metals described above,

again involving the breaking and formation of chemical bonds. Two such possible electrophilic species would be the proton and R^+ groups, such as the methyl group.



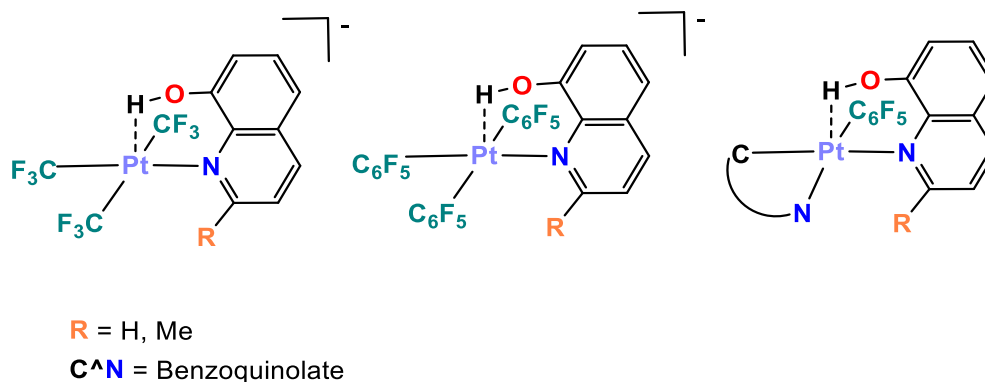
Scheme I.7. Different possible stages of an electrophile (E) transfer to a ligand by interaction with a basic metallic center (upper row) and examples (lower row).

Furthermore, an analogy of the reactivity of basic Pt(II) and Pd(II) complexes towards the acidic Au center and such electrophilic species can be made by means of the isolobality concept, because it is established in the literature that the proton and the methyl group are isolobal with $[Au]^+$ and $[Au-L]^+$ fragments.⁹³⁻⁹⁶

The concept of isolobality was first proposed by Hoffmann in 1982,⁹⁷ defining that two fragments are isolobal when their “number, symmetry properties, approximate energy and shape of the frontier orbitals and the number of electrons in them are similar”. This analogy helped to analyze the structure and bonding situation of more complex compounds by the study of less complicated molecules. It was not, until 1984, that Stone related this concept with gold species being isolobal with the proton and the methyl group.⁹⁸

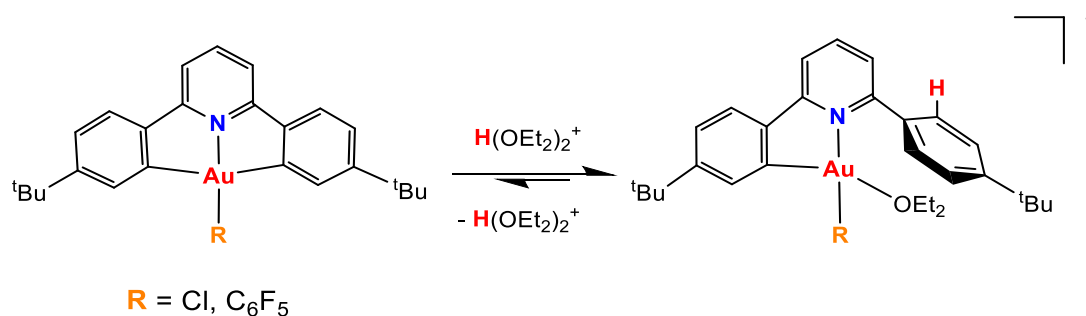
Thus, reactivity of d^8 complexes towards electrophiles is well-known.^{99,100} For example, it has been proposed that d^8 square planar metallic complexes can react with acids through several possible mechanisms, one of which is the oxidative addition of the acid forming M(IV) intermediates that evolve to the final product by a reductive elimination process.¹⁰¹

In addition, there are examples in the literature of Pt(II) metallic centers acting as hydrogen-bonding acceptors.¹⁰²⁻¹⁰⁵ For example, hydroxyl groups supported by a ligand have a tendency to form that kind of interactions^{106,107} (see Scheme I.8 for some examples), disposing the hydroxyl group perpendicular to the square planar metallic environment. This suggests an important participation of the filled dz^2 orbital of the metallic center, giving rise to an interaction between a base and an acid of Lewis.



Scheme I.8. Examples of Pt(II) complexes with hydrogen bonds.

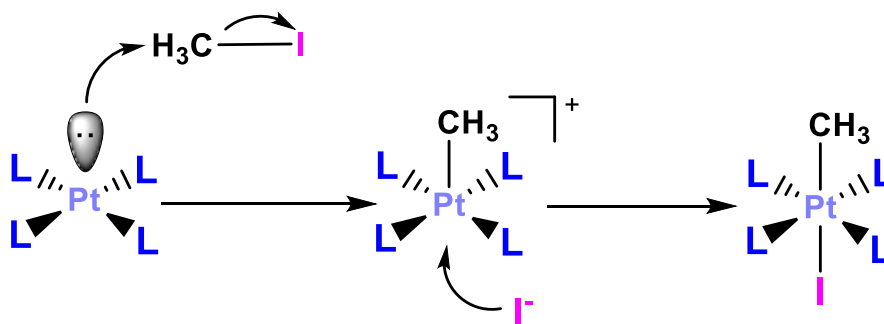
There are some examples in the bibliography about the reactivity of cyclometallated square planar complexes towards acids. For example, Bochmann and coworkers have reported several results on the use of acids on Au(III) (which is isoelectronic with Pt(II)) square planar complexes with a tridentate CNC ligand,¹⁰⁸⁻¹¹⁰ to render for example Au-C reversible protonation processes (see Scheme I.9 for an example).



Scheme I.9. Example of reversible protonation processes on Au(III) derivatives with a CNC ligand.

In these cases, the idea of having first a Au(V)-H species by oxidative addition of a proton to the Au(III) center was ruled out, revealing by computational means that the protonation of the Au-C bond was direct.¹¹⁰

On the other hand, reactivity of basic metallic centers as Pt(II) towards a source of electrophilic methyl groups as MeI has been widely studied and constitutes a classical example of an oxidative addition, which proceeds *via* an S_N2 mechanism (see Scheme I.10).¹¹¹⁻¹³⁰ First, the basic metallic center attacks the methyl fragment of the MeI molecule, forming a $[M-CH_3]^+$ intermediate. In the case of Pt(II) complexes, the nucleophilic attack is produced by the $5dz^2$ orbital of the Pt center on the σ^* LUMO of the carbon atom of MeI. This is followed by a coordination of the resulting iodine ligand to the metallic center, resulting in octahedral Pt(IV) complexes.



Scheme I.10. General mechanism for oxidative addition processes in square planar Pt(II) complexes.

The generated Pt(IV) complexes bear a final disposition of the entering ligands in *trans*, although it is known that *trans* Pt(IV) complexes containing CNC or C[^]N cyclometallated ligands and a phosphane undergo isomerization, being the *cis* isomer the thermodynamically stable species.^{115,121,122,125,130} In such cases, it seems that the rate of this isomerization process is related with the bulkiness of the phosphane ligand, being faster for the bulkier ones.^{114,130}

As a summary of the contents of this thesis, in the first chapter the synthesis, characterization, structural and computational studies of several examples of heteropolymetallic species with Pt-M' and Pd-M' bonds are widely discussed and related with the possibility of regarding them as intermediates for bimetallic catalysis. The degree of transfer of the R group is sensitive to the pair of metals existing in the bimetallic complex.

In the second chapter, the study of the reactivity of basic cyclometallated Pt(II) and Pd(II) substrates is studied towards different protic acids and organic ligands bearing a group with an acidic hydrogen.

In the last chapter the functionalization of a CNC ligand of a basic Pt(II) substrate with methyl groups in *ortho* positions is achieved *via* consecutive oxidative addition and reductive elimination processes.

In the included USB memory, different Supporting Information materials are given for the three chapters containing all the characterization (NMR, IR, MS), computational and crystallographic details for all the complexes discussed. In addition, relevant references for each chapter are given at the end of the Introduction and each different chapter.

References

- (1) Carvajal, M. A.; Alvarez, S.; Novoa, J. J. The Nature of Intermolecular $\text{Cu}^{\text{I}} \cdots \text{Cu}^{\text{I}}$ Interactions: A Combined Theoretical and Structural Database Analysis. *Chem. Eur. J.* **2004**, *10* (9), 2117-2132. DOI: 10.1002/chem.200305249.
- (2) Gade, L. H. Encapsulated, Sandwiched, or Sticking Out: Closed-Shell Interactions of d^{10} Metal Centers with Thallium(I). *Angew. Chem. Int. Ed.* **2001**, *40* (19), 3573-3575. DOI: 10.1002/1521-3773(20011001)40:19<3573::AID-ANIE3573>3.0.CO;2-Y.
- (3) Pyykko, P. Theoretical Chemistry of Gold. *Angew. Chem. Int. Ed.* **2004**, *43* (34), 4412-4456. DOI: 10.1002/anie.200300624.
- (4) Pyykkö, P. Strong Closed-Shell Interactions in Inorganic Chemistry. *Chem. Rev.* **1997**, *97* (3), 597-636. DOI: 10.1021/cr940396v.
- (5) Berenguer, J. R.; Lalinde, E.; Moreno, M. T. Luminescent cyclometalated-pentafluorophenyl Pt^{II} , Pt^{IV} and heteropolynuclear complexes. *Coord. Chem. Rev.* **2018**, *366*, 69-90. DOI: 10.1016/j.ccr.2018.04.002.
- (6) Donamaría, R.; Lippolis, V.; López-de-Luzuriaga, J. M.; Monge, M.; Nieddu, M.; Olmos, M. E. Metallophilic $\text{Au}(\text{I}) \cdots \text{M}(\text{I})$ interactions ($\text{M} = \text{Tl}, \text{Ag}$) in heteronuclear complexes with 1,4,7-triazacyclononane: Structural features and optical properties. *Dalton Trans.* **2020**, *49* (31), 10983-10993. DOI: 10.1039/D0DT01902J.
- (7) Fernandez-Cestau, J.; Rama, R. J.; Rocchigiani, L.; Bertrand, B.; Lalinde, E.; Linnolahti, M.; Bochmann, M. Synthesis and Photophysical Properties of $\text{Au}(\text{III})$ - $\text{Ag}(\text{I})$ Aggregates. *Inorg. Chem.* **2019**, *58* (3), 2020-2030. DOI: 10.1021/acs.inorgchem.8b02987.
- (8) Perez-Temprano, M. H.; Casares, J. A.; Espinet, P. Bimetallic Catalysis using Transition and Group 11 Metals: An Emerging Tool for C-C Coupling and Other Reactions. *Chem. Eur. J.* **2012**, *18* (7), 1864-1884. DOI: 10.1002/chem.201102888.
- (9) Allen, A. E.; MacMillan, D. W. C. Synergistic catalysis: A powerful synthetic strategy for new reaction development. *Chem. Sci.* **2012**, *3* (3), 633-658. DOI: 10.1039/C2SC00907B.
- (10) Inamdar, S. M.; Shinde, V. S.; Patil, N. T. Enantioselective Cooperative Catalysis. *Org. Biomol. Chem.* **2015**, *13* (30), 8116-8162. DOI: 10.1039/C5OB00986C.

- (11) Wu, Y.; Huo, X.; Zhang, W. Synergistic Pd/Cu Catalysis in Organic Synthesis. *Chem. Eur. J.* **2020**, *26* (22), 4895-4916. DOI: 10.1002/chem.201904495.
- (12) Kim, U. B.; Jung, D. J.; Jeon, H. J.; Rathwell, K.; Lee, S.-g. Synergistic Dual Transition Metal Catalysis. *Chem. Rev.* **2020**, *120* (24), 13382-13433. DOI: 10.1021/acs.chemrev.0c00245.
- (13) Chatterjee, B.; Chang, W.-C.; Jena, S.; Werlé, C. Implementation of Cooperative Designs in Polarized Transition Metal Systems—Significance for Bond Activation and Catalysis. *ACS Catal.* **2020**, *10* (23), 14024-14055. DOI: 10.1021/acscatal.0c03794.
- (14) Graziano, B. J.; Vollmer, M. V.; Lu, C. C. Cooperative Bond Activation and Facile Intramolecular Aryl Transfer of Nickel–Aluminum Pincer-type Complexes. *Angew. Chem. Int. Ed.* **2021**, *60* (27), 15087-15094. DOI: 10.1002/anie.202104050.
- (15) Wang, Q.; Brooks, S. H.; Liu, T.; Tomson, N. C. Tuning metal–metal interactions for cooperative small molecule activation. *Chem. Commun.* **2021**, *57* (23), 2839-2853. DOI: 10.1039/D0CC07721F.
- (16) Pye, D. R.; Mankad, N. P. Bimetallic catalysis for C-C and C-X coupling reactions. *Chem. Sci.* **2017**, *8* (3), 1705-1718. DOI: 10.1039/c6sc05556g.
- (17) Hidalgo, N.; Maya, C.; Campos, J. Cooperative activation of X–H (X = H, C, O, N) bonds by a Pt(0)/Ag(I) metal-only Lewis pair. *Chem. Commun.* **2019**, *55* (60), 8812-8815. DOI: 10.1039/C9CC03008E.
- (18) Meana, I.; Espinet, P.; Albéniz, A. C. Heterometallic Complexes by Transmetalation of Alkynyl Groups from Copper or Silver to Allyl Palladium Complexes: Demetalation Studies and Alkynyl Homocoupling. *Organometallics* **2014**, *33* (1), 1-7. DOI: 10.1021/om4005498.
- (19) Deolka, S.; Rivada-Wheeler, O.; Aristizábal, S. L.; Fayzullin, R. R.; Pal, S.; Nozaki, K.; Khaskin, E.; Khusnutdinova, J. R. Metal–metal cooperative bond activation by heterobimetallic alkyl, aryl, and acetylide Pt^{II}/Cu^I complexes. *Chem. Sci.* **2020**, *11* (21), 5494-5502. DOI: 10.1039/D0SC00646G.
- (20) Campos, J. Bimetallic cooperation across the periodic table. *Nat. Rev. Chem.* **2020**, *4* (12), 696-702. DOI: 10.1038/s41570-020-00226-5.
- (21) Bertus, P.; Halbes, U.; Pale, P. Pd/Ag-Catalyzed Direct Coupling of 1-Trimethylsilyl Alkynes with Vinyl Triflates. *Eur. J. Org. Chem.* **2001**, *2001* (23),

- 4391-4393. DOI: 10.1002/1099-0690(200112)2001:23<4391::AID-EJOC4391>3.0.CO;2-D.
- (22) Sonogashira, K. Development of Pd–Cu catalyzed cross-coupling of terminal acetylenes with sp^2 -carbon halides. *J. Organomet. Chem.* **2002**, *653* (1), 46-49. DOI: 10.1016/S0022-328X(02)01158-0.
- (23) Weibel, J.-M.; Blanc, A.; Pale, P. Ag-Mediated Reactions: Coupling and Heterocyclization Reactions. *Chem. Rev.* **2008**, *108* (8), 3149-3173. DOI: 10.1021/cr078365q.
- (24) Panda, B.; Sarkar, T. K. Gold and palladium combined for the Sonogashira-type cross-coupling of arenediazonium salts. *Chem. Commun.* **2010**, *46* (18), 3131-3133. DOI: 10.1039/C001277G.
- (25) Panda, B.; Sarkar, T. K. Gold and Palladium Combined for the Sonogashira Coupling of Aryl and Heteroaryl Halides. *Synthesis* **2013**, *45* (06), 817-829. DOI: 10.1055/s-0032-1318119.
- (26) Moret, M.-E.; Chen, P. Interaction of Organoplatinum(II) Complexes with Monovalent Coinage Metal Triflates. *J. Am. Chem. Soc.* **2009**, *131* (15), 5675-5690. DOI: 10.1021/ja900449y.
- (27) Moret, M.-E.; Serra, D.; Bach, A.; Chen, P. Transmetalation Supported by a Pt^{II} - Cu^I Bond. *Angew. Chem. Int. Ed.* **2010**, *49* (16), 2873-2877. DOI: 10.1002/anie.200906480.
- (28) Serra, D.; Moret, M.-E.; Chen, P. Transmetalation of Methyl Groups Supported by Pt^{II} - Au^I Bonds in the Gas Phase, in Silico, and in Solution. *J. Am. Chem. Soc.* **2011**, *133* (23), 8914-8926. DOI: 10.1021/ja110405q.
- (29) Oeschger, R. J.; Ringger, D. H.; Chen, P. Gas-Phase Investigations on the Transmetalation Step in Sonogashira Reactions. *Organometallics* **2015**, *34* (15), 3888-3892. DOI: 10.1021/acs.organomet.5b00491.
- (30) Oeschger, R. J.; Chen, P. Structure and Gas-Phase Thermochemistry of a Pd/Cu Complex: Studies on a Model for Transmetalation Transition States. *J. Am. Chem. Soc.* **2017**, *139* (3), 1069-1072. DOI: 10.1021/jacs.6b12152.
- (31) Oeschger, R. J.; Chen, P. A Heterobimetallic Pd-Zn Complex: Study of a d^8 - d^{10} Bond in Solid State, in Solution, and in Silico. *Organometallics* **2017**, *36* (8), 1465-1468. DOI: 10.1021/acs.organomet.7b00113.

- (32) Paenurk, E.; Gershoni-Poranne, R.; Chen, P. Trends in Metallophilic Bonding in Pd-Zn and Pd-Cu Complexes. *Organometallics* **2017**, *36* (24), 4854-4863. DOI: 10.1021/acs.organomet.7b00748.
- (33) Rivada-Wheelaghan, O.; Comas-Vives, A.; Fayzullin, R. R.; Lledós, A.; Khusnutdinova, J. R. Dynamic Pd^{II}/Cu^I Multimetallic Assemblies as Molecular Models to Study Metal–Metal Cooperation in Sonogashira Coupling. *Chem. Eur. J.* **2020**, *26* (53), 12168-12179. DOI: 10.1002/chem.202002013.
- (34) Oi, M.; Takita, R.; Kanazawa, J.; Muranaka, A.; Wang, C.; Uchiyama, M. Organocopper cross-coupling reaction for C–C bond formation on highly sterically hindered structures. *Chem. Sci.* **2019**, *10* (24), 6107-6112. DOI: 10.1039/C9SC00891H.
- (35) Pérez-Temprano, M. H.; Casares, J. A.; de Lera, Á. R.; Álvarez, R.; Espinet, P. Strong Metallophilic Interactions in the Palladium Arylation by Gold Aryls. *Angew. Chem. Int. Ed.* **2012**, *51* (20), 4917-4920. DOI: 10.1002/anie.201108043.
- (36) Villar, P.; Pérez-Temprano, M. H.; Casares, J. A.; Álvarez, R.; Espinet, P. Experimental and DFT Study of the [AuAr(AsPh₃)]-Catalyzed *cis/trans* Isomerization of [PdAr₂(AsPh₃)₂] (Ar = C₆F₅ or C₆Cl₂F₃): Alternative Mechanisms and Its Switch upon Pt for Pd Substitution. *Organometallics* **2020**, *39* (12), 2295-2303. DOI: 10.1021/acs.organomet.0c00245.
- (37) Wang, J.; Zhan, L.; Wang, G.; Wei, Y.; Shi, M.; Zhang, J. Pd-promoted cross coupling of iodobenzene with vinylgold *via* an unprecedented phenyl transmetalation from Pd to Au. *Chem. Commun.* **2020**, *56* (46), 6213-6216. DOI: 10.1039/D0CC02645J.
- (38) Hansmann, M. M.; Pernpointner, M.; Döpp, R.; Hashmi, A. S. K. A Theoretical DFT-Based and Experimental Study of the Transmetalation Step in Au/Pd-Mediated Cross-Coupling Reactions. *Chem. Eur. J.* **2013**, *19* (45), 15290-15303. DOI: 10.1002/chem.201301840.
- (39) Vicente, J.; Chicote, M. T.; Huertas, S.; Bautista, D.; Jones, P. G.; Fischer, A. K. Mononuclear (Pd, Pt), Heterodinuclear (PdAg, PtAg), and Tetranuclear (Pd₂Ag₂, Pt₂Ag₂) 1,1-ethylenedithiolato Complexes. *Inorg. Chem.* **2001**, *40* (9), 2051-2057. DOI: 10.1021/ic000996e.
- (40) Alonso, E.; Forniés, J.; Fortuño, C.; Martín, A.; Orpen, A. G. Reactivity of [NBu₄][(C₆F₅)₂M(μ-PPh₂)₂M'(acac-O,O')] (M, M' = Pt, Pd) toward Silver

- Centers. Synthesis of Polynuclear Complexes Containing M–Ag Bonds (M = Pd, Pt). *Organometallics* **2003**, *22* (24), 5011-5019. DOI: 10.1021/om034047f.
- (41) Forniés, J.; Ibañez, S.; Martín, A.; Sanz, M.; Berenguer, J. R.; Lalinde, E.; Torroba, J. Influence of the Pt → Ag Donor-Acceptor Bond and Polymorphism on the Spectroscopic and Optical Properties of Heteropolynuclear Benzoquinolateplatinum(II) Complexes. *Organometallics* **2006**, *25* (18), 4331-4340. DOI: 10.1021/om0604526.
- (42) Jamali, S.; Mazloomi, Z.; Nabavizadeh, S. M.; Milic, D.; Kia, R.; Rashidi, M. Cyclometalated Cluster Complex with a Butterfly-Shaped Pt₂Ag₂ Core. *Inorg. Chem.* **2010**, *49* (6), 2721-2726. DOI: 10.1021/ic9O2O44g.
- (43) Forniés, J.; Ibañez, S.; Lalinde, E.; Martín, A.; Moreno, M. T.; Tsipis, A. C. Benzoquinolateplatinum(II) Complexes as Building Blocks in the Synthesis of Pt–Ag Extended Structures. *Dalton Trans.* **2012**, *41* (12), 3439-3451. DOI: 10.1039/c2dt11885h.
- (44) Fuertes, S.; Woodall, C. H.; Raithby, P. R.; Sicilia, V. Heteropolynuclear Pt(II)–M(I) Clusters with a C^NC Biscyclometalated Ligand. *Organometallics* **2012**, *31* (11), 4228-4240. DOI: 10.1021/om300170j.
- (45) Arias, A.; Forniés, J.; Fortuño, C.; Martín, A.; Mastroilli, P.; Gallo, V.; Latronico, M.; Todisco, S. Donor Behaviour of Anionic and Asymmetric Phosphanido Derivatives of Platinum and Palladium. *Eur. J. Inorg. Chem.* **2014**, *2014* (10), 1679-1693. DOI: 10.1002/ejic.201300808.
- (46) Schneider, L.; Sivchik, V.; Chung, K. Y.; Chen, Y. T.; Karttunen, A. J.; Chou, P. T.; Koshevoy, I. O. Cyclometalated Platinum(II) Cyanometallates: Luminescent Blocks for Coordination Self-Assembly. *Inorg. Chem.* **2017**, *56* (8), 4459-4467. DOI: 10.1021/acs.inorgchem.7b00006.
- (47) Baya, M.; Belío, Ú.; Campillo, D.; Fernandez, I.; Fuertes, S.; Martín, A. Pt–M Complexes (M=Ag, Au) as Models for Intermediates in Transmetalation Processes. *Chem. Eur. J.* **2018**, *24* (52), 13879-13889. DOI: 10.1002/chem.201802542.
- (48) Campillo, D.; Belío, Ú.; Martín, A. New Pt → M (M = Ag or Tl) complexes based on anionic cyclometalated Pt(II) complexes. *Dalton Trans.* **2019**, *48* (10), 3270-3283. DOI: 10.1039/c9dt00121b.
- (49) Han, L.-J.; Wu, X.-X.; Ma, Z.-G.; Li, Y.; Wei, Q.-H. Novel luminescent homo/heterometallic platinum(II) alkynyl complexes based on Y-shaped pyridyl

- diphosphines. *Dalton Trans.* **2020**, *49* (24), 8347-8353. DOI: 10.1039/D0DT01173H.
- (50) Yabune, N.; Nakajima, H.; Nishioka, T. Metal–metal bond formation of triplatinum cores with a silver(I) ion affording a heptanuclear cluster bearing four Pt–Ag bonds. *Dalton Trans.* **2020**, *49* (23), 7680-7683. DOI: 10.1039/D0DT01227K.
- (51) Stork, J. R.; Olmstead, M. M.; Fettinger, J. C.; Balch, A. L. Metal-Metal Interactions in Thallium(I)/Platinum(II) Compounds Involving a Chelating Dicarbene and Various Auxiliary Ligands. *Inorg. Chem.* **2006**, *45* (2), 849-857. DOI: 10.1021/ic051252+.
- (52) Purgel, M.; Maliarik, M.; Glaser, J.; Platas-Iglesias, C.; Persson, I.; Tóth, I. Binuclear Pt–Tl Bonded Complex with Square Pyramidal Coordination around Pt: A Combined Multinuclear NMR, EXAFS, UV–Vis, and DFT/TDDFT Study in Dimethylsulfoxide Solution. *Inorg. Chem.* **2011**, *50* (13), 6163-6173. DOI: 10.1021/ic200417q.
- (53) Belío, Ú.; Fuertes, S.; Martín, A. Synthesis and Characterization of a "Pt₃Tl" Cluster Containing an Unprecedented Trigonal Environment for Thallium(I). *Inorg. Chem.* **2013**, *52* (10), 5627-5629. DOI: 10.1021/ic400167w.
- (54) Belío, Ú.; Fuertes, S.; Martín, A. Preparation of Pt-Tl clusters showing new geometries. X-ray, NMR and luminescence studies. *Dalton Trans.* **2014**, *43* (28), 10828-10843. DOI: 10.1039/c4dt00536h.
- (55) Forniés, J.; Gimenez, N.; Ibañez, S.; Lalinde, E.; Martín, A.; Moreno, M. T. An Extended Chain and Trinuclear Complexes Based on Pt(II)-M (M = Tl(I), Pb(II)) Bonds: Contrasting Photophysical Behavior. *Inorg. Chem.* **2015**, *54* (9), 4351-4363. DOI: 10.1021/acs.inorgchem.5b00083.
- (56) Fuertes, S.; Chueca, A. J.; Martín, A.; Sicilia, V. Pt₂Tl Building Blocks for Two-Dimensional Extended Solids: Synthesis, Crystal Structures, and Luminescence. *Cryst. Growth Des.* **2017**, *17* (8), 4336-4346. DOI: 10.1021/acs.cgd.7b00662.
- (57) Rajabi, S.; Jamali, S.; Naseri, S.; Jamjah, A.; Kia, R.; Samouei, H.; Mastroilli, P.; Shahsavari, H. R.; Raithby, P. R. Pt–M (M = Au and Tl) Dative Bonds Using Bis(cyclometalated)platinum(II) Complexes. *Organometallics* **2019**, *38* (8), 1709-1720. DOI: 10.1021/acs.organomet.8b00907.
- (58) Briant, C. E.; Gilmour, D. I.; Mingos, D. M. P. Synthesis and Structural Characterisation of [Au₂Pt₂(PPh₃)₄(CN-xylyl)₄](PF₆)₂: A Platinum—Gold Cluster

- with a Flattened Butterfly Geometry. *J. Organomet. Chem.* **1984**, 267 (3), c52-c55. DOI: 10.1016/0022-328X(84)80212-0.
- (59) Crespo, O.; Gimeno, M. C.; Laguna, A.; Lehtonen, O.; Ospino, I.; Pyykkö, P.; Villacampa, M. D. Structural and Photophysical Study on Heterobimetallic Complexes with d^8 - d^{10} Interactions Supported by Carborane Ligands: Theoretical Analysis of the Emissive Behaviour. *Chem. Eur. J.* **2014**, 20 (11), 3120-3127. DOI: 10.1002/chem.201303735.
- (60) Goto, E.; Begum, R. A.; Ueno, C.; Hosokawa, A.; Yamamoto, C.; Nakamae, K.; Kure, B.; Nakajima, T.; Kajiwara, T.; Tanase, T. Electron-Deficient $Pt_2M_2Pt_2$ Hexanuclear Metal Strings (M = Pt, Pd) Supported by Triphosphine Ligands. *Organometallics* **2014**, 33 (8), 1893-1904. DOI: 10.1021/om401211d.
- (61) Baya, M.; Belío, Ú.; Fernandez, I.; Fuertes, S.; Martín, A. Unusual Metal-Metal Bonding in a Dinuclear Pt-Au Complex: Snapshot of a Transmetalation Process. *Angew. Chem. Int. Ed.* **2016**, 55 (24), 6978-6982. DOI: 10.1002/anie.201602081.
- (62) Crespo, M.; Sales, J.; Solans, X. Monohydrido-bridged platinum(II)-gold(I) complexes. X-Ray crystal structure of $[(Ph_3P)_2(C_6Cl_5)Pt(\mu-H)Au(PPh_3)]ClO_4 \cdot 2Et_2O$. *J. Chem. Soc., Dalton Trans.* **1989**, (6), 1089-1092. DOI: 10.1039/DT9890001089.
- (63) Vicente, J.; Chicote, M. T.; Huertas, S.; Jones, P. G.; Fischer, A. K. Heterodi- $[M_{Ag}, MAu]$ (M = Pd, Pt), Tri- $[PdAg_2, PtAg_2, PtAu_2, Pt_2M]$ (M = Ni, Pt, Cd, Hg), and Tetranuclear (Pt_2Ag_2, Pt_2Au_2) 1,1-Ethylenedithiolato Complexes. *Inorg. Chem.* **2001**, 40 (24), 6193-6200. DOI: 10.1021/ic010488k.
- (64) Yin, G.-Q.; Wei, Q.-H.; Zhang, L.-Y.; Chen, Z.-N. Luminescent $Pt^{II}-M^I$ (M = Cu, Ag, Au) Heteronuclear Alkynyl Complexes Prepared by Reaction of $[Pt(C:CR)_4]^{2-}$ with $[M_2(dppm)_2]^{2+}$ (dppm = Bis(diphenylphosphino)methane). *Organometallics* **2006**, 25 (3), 580-587. DOI: 10.1021/om050620e.
- (65) Gericke, R.; Bennett, M. A.; Privér, S. H.; Bhargava, S. K. Formation of Heterobimetallic Complexes by Addition of d^{10} -Metal Ions to *cis*- $[(dppe)M(\kappa C-2-C_6F_4PPh_2)_2]$ (M = Ni, Pd, and Pt). *Organometallics* **2017**, 36 (17), 3178-3188. DOI: 10.1021/acs.organomet.7b00145.
- (66) Berenguer, J. R.; Lalinde, E.; Martín, A.; Moreno, M. T.; Ruiz, S.; Sanchez, S.; Shahsavari, H. R. Photophysical Responses in Pt_2Pb Clusters Driven by Solvent Interactions and Structural Changes in the Pb^{II} Environment. *Inorg. Chem.* **2014**, 53 (16), 8770-8785. DOI: 10.1021/ic501458q.

- (67) Forniés, J.; Giménez, N.; Ibáñez, S.; Lalinde, E.; Martín, A.; Moreno, M. T. An Extended Chain and Trinuclear Complexes Based on Pt(II)–M (M = Tl(I), Pb(II)) Bonds: Contrasting Photophysical Behavior. *Inorg. Chem.* **2015**, *54* (9), 4351-4363. DOI: 10.1021/acs.inorgchem.5b00083.
- (68) Forniés, J.; Ibañez, S.; Martín, A.; Gil, B.; Lalinde, E.; Moreno, M. T. Synthesis, Characterization, and Optical Properties of Pentafluorophenyl Complexes with a Pt–Cd Bond. *Organometallics* **2004**, *23* (16), 3963-3975. DOI: 10.1021/om049719w.
- (69) Vicente, J.; Arcas, A.; Gálvez-López, M. D.; Jones, P. G. Bis(2,6-dinitroaryl)platinum Complexes. 2.1 Di- and Trinuclear Complexes Containing Pt–Hg Bonds. *Organometallics* **2004**, *23* (14), 3528-3537. DOI: 10.1021/om049699y.
- (70) Ibáñez, S.; Mihály, B.; Sanz Miguel, P. J.; Steinborn, D.; Pretzer, I.; Hiller, W.; Lippert, B. The Challenge of Deciphering Linkage Isomers in Mixtures of Oligomeric Complexes Derived from 9-Methyladenine and *trans*-(NH₃)₂Pt^{II} Units. *Chem. Eur. J.* **2015**, *21* (15), 5794-5806. DOI: 10.1002/chem.201406378.
- (71) Yamaguchi, T.; Yoshiya, K. Coordination Isomers of Trinuclear Pt₂Hg Complex That Differ in Type of Metal–Metal Bond. *Inorg. Chem.* **2019**, *58* (15), 9548-9552. DOI: 10.1021/acs.inorgchem.9b00978.
- (72) Ebihara, M.; Tokoro, K.; Maeda, M.; Ogami, M.; Imaeda, K.; Sakurai, K.; Masuda, H.; Kawamura, T. Bonding Interaction Between Group-10 and Group-11 Metals- Synthesis, Structure and Properties of [M₃(S₂CNR₂)₆M'₂]²⁺ (M=Pt or Pd; M'=Ag or Cu; R=Et, Prⁱ, Prⁿ, Buⁿ or C₆H₁₁). *J. Chem. Soc., Dalton Trans.* **1994**, (24), 3621-3635. DOI: 10.1039/dt9940003621.
- (73) Arnal, L.; Fuertes, S.; Martín, A.; Sicilia, V. The Use of Cyclometalated NHCs and Pyrazoles for the Development of Fully Efficient Blue Pt^{II} Emitters and Pt/Ag Clusters. *Chem. Eur. J.* **2018**, *24* (37), 9377-9384. DOI: 10.1002/chem.201800646.
- (74) Crespo, O.; Laguna, A.; Fernandez, E. J.; Lopez-de-Luzuriaga, J. M.; Jones, P. G.; Teichert, M.; Monge, M.; Pyykko, P.; Runeberg, N.; Schutz, M.; Werner, H. J. Experimental and Theoretical Studies of the d⁸-d¹⁰ Interaction Between Pd(II) and Au(I): Bis(chloro[(phenylthiomethyl)diphenylphosphine]gold(I))-dichloropalladium(II) and Related Systems. *Inorg. Chem.* **2000**, *39* (21), 4786-4792. DOI: 10.1021/ic000420p.

- (75) Reitsamer, C.; Schuh, W.; Kopacka, H.; Wurst, K.; Peringer, P. Synthesis and Structure of the First Heterodinuclear PCP–Pincer–CDP Complex with a Pd–Au d^8 – d^{10} Pseudo-Closed-Shell Interaction. *Organometallics* **2009**, *28* (22), 6617–6620. DOI: 10.1021/om900686r.
- (76) Sicilia, V.; Forniés, J.; Fuertes, S.; Martín, A. New Dicyano Cyclometalated Compounds Containing Pd(II)-Tl(I) Bonds as Building Blocks in 2D Extended Structures: Synthesis, Structure, and Luminescence Studies. *Inorg. Chem.* **2012**, *51* (20), 10581–10589. DOI: 10.1021/ic300808z.
- (77) Williams, J. A. G.; Beeby, A.; Davies, E. S.; Weinstein, J. A.; Wilson, C. An Alternative Route to Highly Luminescent Platinum(II) Complexes: Cyclometalation with NACAN-Coordinating Dipyridylbenzene Ligands. *Inorg. Chem.* **2003**, *42* (26), 8609–8611. DOI: 10.1021/ic035083+.
- (78) Wang, Z.; Turner, E.; Mahoney, V.; Madakuni, S.; Groy, T.; Li, J. Facile Synthesis and Characterization of Phosphorescent Pt(NACAN)X Complexes. *Inorg. Chem.* **2010**, *49* (24), 11276–11286. DOI: 10.1021/ic100740e.
- (79) Sotoyama, W.; Satoh, T.; Sawatari, N.; Inoue, H. Efficient organic light-emitting diodes with phosphorescent platinum complexes containing NACAN-coordinating tridentate ligand. *Appl. Phys. Lett.* **2005**, *86* (15), 153505. DOI: 10.1063/1.1901826.
- (80) Pike, S.; Lord, R.; Kergreis, A. Influence of Ligand and Nuclearity on the Cytotoxicity of Cyclometallated C^NC Platinum(II) Complexes. *Chem. Eur. J.* **2020**, *26* (65), 14938–14946. DOI: 10.1002/chem.202002517.
- (81) Liu, J.; Sun, R. W.-Y.; Leung, C.-H.; Lok, C.-N.; Che, C.-M. Inhibition of TNF- α stimulated nuclear factor-kappa B (NF- κ B) activation by cyclometalated platinum(II) complexes. *Chem. Commun.* **2012**, *48* (2), 230–232. DOI: 10.1039/C1CC15317J.
- (82) Koshevoy, I. O.; Sivchik, V.; Kochetov, A.; Eskelinen, T.; Kisel, K. S.; Solomatina, A. I.; Grachova, E. V.; Tunik, S. P.; Hirva, P. Modulation of metallophilic and π – π interactions in platinum cyclometalated luminophores with halogen bonding. *Chem. Eur. J.* **2021**, *27* (5), 1787–1794. DOI: 10.1002/chem.202003952.
- (83) Garner, K. L.; Parkes, L. F.; Piper, J. D.; Williams, J. A. G. Luminescent Platinum Complexes with Terdentate Ligands Forming 6-Membered Chelate Rings:

- Advantageous and Deleterious Effects in N_4N_4 and $\text{N}_2\text{C}_2\text{N}_2$ -Coordinated Complexes. *Inorg. Chem.* **2010**, *49* (2), 476-487. DOI: 10.1021/ic9016323.
- (84) Garbe, S.; Krause, M.; Klimpel, A.; Neundorf, I.; Lippmann, P.; Ott, I.; Brünink, D.; Strassert, C. A.; Doltsinis, N. L.; Klein, A. Cyclometalated Pt Complexes of CNC Pincer Ligands: Luminescence and Cytotoxic Evaluation. *Organometallics* **2020**, *39* (5), 746-756. DOI: 10.1021/acs.organomet.0c00015.
- (85) Fuertes, S.; Brayshaw, S. K.; Raithby, P. R.; Schiffers, S.; Warren, M. R. New $\text{C}^2\text{N}^2\text{C}$ Bis-Cyclometalated Platinum(II) Complexes: Synthesis, Structures, and Photophysical Properties. *Organometallics* **2012**, *31* (1), 105-119. DOI: 10.1021/om200589q.
- (86) Bryant, M. J.; Skelton, J. M.; Hatcher, L. E.; Stubbs, C.; Madrid, E.; Pallipurath, A. R.; Thomas, L. H.; Woodall, C. H.; Christensen, J.; Fuertes, S.; Robinson, T. P.; Beavers, C. M.; Teat, S. J.; Warren, M. R.; Pradaux-Caggiano, F.; Walsh, A.; Marken, F.; Carbery, D. R.; Parker, S. C.; McKeown, N. B.; Malpass-Evans, R.; Carta, M.; Raithby, P. R. A rapidly-reversible absorptive and emissive vapochromic Pt(II) pincer-based chemical sensor. *Nat. Commun.* **2017**, *8* (1), 1800. DOI: 10.1038/s41467-017-01941-2.
- (87) Berenguer, J. R.; Lalinde, E.; Moreno, M. T.; Sanchez, S.; Torroba, J. Facile Metalation of Hbzq by $[\text{cis-Pt}(\text{C}_6\text{F}_5)_2(\text{thf})_2]$: A Route to a Pentafluorophenyl Benzoquinolate Solvate Complex That Easily Coordinates Terminal Alkynes. Spectroscopic and Optical Properties. *Inorg. Chem.* **2012**, *51* (21), 11665-11679. DOI: 10.1021/ic301563u.
- (88) Aoki, R.; Kobayashi, A.; Chang, H.-C.; Kato, M. Structures and Luminescence Properties of Cyclometalated Dinuclear Platinum(II) Complexes Bridged by Pyridinethiolate Ions. *Bull. Chem. Soc. Jpn.* **2011**, *84* (2), 218-225. DOI: 10.1246/bcsj.20100304.
- (89) Vivancos, Á.; Bautista, D.; González-Herrero, P. Luminescent Platinum(IV) Complexes Bearing Cyclometalated 1,2,3-Triazolylidene and Bi- or Tridentate 2,6-Diarylpyridine Ligands. *Chem. Eur. J.* **2019**, *25* (23), 6014-6025. DOI: 10.1002/chem.201900489.
- (90) von der Stück, R.; Krause, M.; Brünink, D.; Buss, S.; Doltsinis, N. L.; Strassert, C. A.; Klein, A. Luminescent Pd(II) Complexes with Tridentate – Aryl-pyridine-(benzo)thiazole Ligands. *Z. Anorg. Allg. Chem.* **2021**, *648*. DOI: 10.1002/zaac.202100278.

- (91) Cotton, F. A.; Falvello, L. R.; Usón, R.; Forniés, J.; Tomás, M.; Casas, J. M.; Ara, I. Heterobinuclear PtAg Compounds with Platinum-Silver Bonds Unsupported by Covalent Bridges. Molecular Structure of $(C_6F_5)_3(SC_4H_8)PtAgPPh_3$. *Inorg. Chem.* **1987**, *26* (9), 1366-1370. DOI: 10.1021/ic00256a006.
- (92) Usón, R.; Forniés, J.; Tomás, M.; Ara, I.; Casas, J. M.; Martín, A. Neutral and Anionic Binuclear Perhalogenophenyl Platinum–Silver Complexes with Pt→Ag Bonds Unsupported by Covalent Bridges. Molecular Structures of $[(tth)(C_6Cl_5)(C_6F_5)_2-PtAg(PPh_3)]$, $[NBu_4][[(C_6F_5)_4PtAg(tth)]]$ and $[NBu_4][[cis-(C_6Cl_5)_2(C_6F_5)_2PtAg(tth)]]$ (tth = tetrahydrothiophene). *J. Chem. Soc., Dalton Trans.* **1991**, (9), 2253-2264. DOI: 10.1039/DT9910002253.
- (93) Raubenheimer, H. G.; Schmidbaur, H. Gold Chemistry Guided by the Isolobality Concept. *Organometallics* **2012**, *31* (7), 2507-2522. DOI: 10.1021/om2010113.
- (94) Kickelbick, G.; Schubert, U. $CIMPH_3$ and $[MPH_3]^+$ (M=Cu, Ag, Au); a density functional study. *Inorg. Chim. Acta* **1997**, *262* (1), 61-64. DOI: 10.1016/S0020-1693(97)05484-4.
- (95) Hashmi, A. S. K. Homogeneous gold catalysis: The role of protons. *Catal. Today* **2007**, *122* (3), 211-214. DOI: 10.1016/j.cattod.2006.10.006.
- (96) Böttcher, H.-C.; Graf, M.; Mayer, P.; Scheer, M. Synthesis and Characterization of a Novel Triangular Rh_2Au Cluster Compound Inspired by the Isolobality Concept. *ChemistryOpen* **2020**, *9* (10), 991-995. DOI: 10.1002/open.202000217.
- (97) Hoffmann, R. Building Bridges Between Inorganic and Organic Chemistry (Nobel Lecture). *Angew. Chem. Int. Ed.* **1982**, *21* (10), 711-724. DOI: 10.1002/anie.198207113.
- (98) Stone, F. G. A. Metal-Carbon and Metal-Metal Multiple Bonds as Ligands in Transition-Metal Chemistry: The Isolobal Connection. *Angew. Chem. Int. Ed.* **1984**, *23* (2), 89-99. DOI: 10.1002/anie.198400893.
- (99) Canty, A. J.; van Koten, G. Mechanisms of d^8 organometallic reactions involving electrophiles and intramolecular assistance by nucleophiles. *Acc. Chem. Res.* **1995**, *28* (10), 406-413. DOI: 10.1021/ar00058a002.
- (100) Belluco, U.; Giustiniani, M.; Graziani, M. Mechanism of electrophilic reactions of carbon-metal bonded platinum(II) complexes. Comparison between transition and post-transition organometallic compounds. *J. Am. Chem. Soc.* **1967**, *89* (25), 6494-6500. DOI: 10.1021/ja01001a021.

- (101) Stahl, S. S.; Labinger, J. A.; Bercaw, J. E. Exploring the Mechanism of Aqueous C–H Activation by Pt(II) through Model Chemistry: Evidence for the Intermediacy of Alkylhydridoplatinum(IV) and Alkane σ -Adducts. *J. Am. Chem. Soc.* **1996**, *118* (25), 5961-5976. DOI: 10.1021/ja960110z.
- (102) Brammer, L.; Charnock, J. M.; Goggin, P. L.; Goodfellow, R. J.; Orpen, A. G.; Koetzle, T. F. The role of transition metal atoms as hydrogen bond acceptors: a neutron diffraction study of $[\text{NPr}^n_4]_2[\text{PtCl}_4] \cdot \text{cis-}[\text{PtCl}_2(\text{NH}_2\text{Me})_2]$ at 20 K. *J. Chem. Soc., Dalton Trans.* **1991**, (7), 1789-1798. DOI: 10.1039/DT9910001789.
- (103) Wehman-Ooyevaar, I. C. M.; Grove, D. M.; Kooijman, H.; Van der Sluis, P.; Spek, A. L.; Van Koten, G. A hydrogen atom in an organoplatinum-amine system. 1. Synthesis and spectroscopic and crystallographic characterization of novel zwitterionic complexes with a Pt(II)···H-N⁺ unit. *J. Am. Chem. Soc.* **1992**, *114* (25), 9916-9924. DOI: 10.1021/ja00051a025.
- (104) Rizzato, S.; Bergès, J.; Mason, S. A.; Albinati, A.; Kozelka, J. Dispersion-Driven Hydrogen Bonding: Predicted Hydrogen Bond between Water and Platinum(II) Identified by Neutron Diffraction. *Angew. Chem. Int. Ed.* **2010**, *49* (41), 7440-7443. DOI: 10.1002/anie.201001892.
- (105) Behnia, A.; Fard, M. A.; Boyle, P. D.; Puddephatt, R. J. Complexes Containing a Phenol–Platinum(II) Hydrogen Bond: Synthons for Supramolecular Self-Assembly and Precursors for Hydridoplatinum(IV) Complexes. *Eur. J. Inorg. Chem.* **2019**, *2019* (24), 2899-2906. DOI: 10.1002/ejic.201900480.
- (106) Baya, M.; Belío, Ú.; Martín, A. Synthesis, Characterization, And Computational Study of Complexes Containing Pt···H Hydrogen Bonding Interactions. *Inorg. Chem.* **2014**, *53* (1), 189-200. DOI: 10.1021/ic402036p.
- (107) Pérez-Bitrián, A.; Baya, M.; Casas, J. M.; Martín, A.; Menjón, B. Hydrogen bonding to metals as a probe for an inverted ligand field. *Dalton Trans.* **2021**, *50* (16), 5465-5472. DOI: 10.1039/D1DT00597A.
- (108) Smith, D. A.; Rosca, D.-A.; Bochmann, M. Selective Au-C Cleavage in ((C^NC)Au(III) Aryl and Alkyl Pincer Complexes. *Organometallics* **2012**, *31* (17), 5998-6000. DOI: 10.1021/om300666j.
- (109) Rocchigiani, L.; Budzelaar, P. H. M.; Bochmann, M. Heterolytic bond activation at gold: evidence for gold(III) H-B, H-Si complexes, H-H and H-C cleavage. *Chem. Sci.* **2019**, *10* (9), 2633-2642. DOI: 10.1039/c8sc05229h.

- (110) Rocchigiani, L.; Fernandez-Cestau, J.; Budzelaar, P. H. M.; Bochmann, M. Arene C-H activation by gold(III): solvent-enabled proton shuttling, and observation of a pre-metallation Au-arene intermediate. *Chem. Commun.* **2017**, 53 (31), 4358-4361. DOI: 10.1039/c7cc01628j.
- (111) Hamidzadeh, P.; Nabavizadeh, S. M.; Hoseini, S. J. Effects of the number of cyclometalated rings and ancillary ligands on the rate of MeI oxidative addition to platinum(II)-pincer complexes. *Dalton Trans.* **2019**, 48 (10), 3422-3432. DOI: 10.1039/C9DT00205G.
- (112) Nabavizadeh, S. M.; Aseman, M. D.; Ghaffari, B.; Rashidi, M.; Hosseini, F. N.; Azimi, G. Kinetics and mechanism of oxidative addition of MeI to binuclear cycloplatinated complexes containing biphosphine bridges: Effects of ligands. *J. Organomet. Chem.* **2012**, 715, 73-81. DOI: 10.1016/j.jorganchem.2012.05.026.
- (113) Nabavizadeh, S. M.; Shahsavari, H. R.; Sepehrpour, H.; Hosseini, F. N.; Jamali, S.; Rashidi, M. Oxidative addition reaction of diarylplatinum(II) complexes with MeI in ionic liquid media: a kinetic study. *Dalton Trans.* **2010**, 39 (33), 7800-7805. DOI: 10.1039/C0DT00282H.
- (114) Shaw, P. A.; Clarkson, G. J.; Rourke, J. P. Long-Lived Five-Coordinate Platinum(IV) Intermediates: Regiospecific C-C Coupling. *Organometallics* **2016**, 35 (21), 3751-3762. DOI: 10.1021/acs.organomet.6b00697.
- (115) Shahsavari, H. R.; Babadi Aghakhanpour, R.; Babaghasabha, M.; Golbon Haghghi, M.; Nabavizadeh, S. M.; Notash, B. Combined Kinetic-Mechanistic and Theoretical Elucidation of the Oxidative Addition of Iodomethane to Cycloplatinated(II) Complexes: Controlling the Rate of *trans/cis* Isomerization. *Eur. J. Inorg. Chem.* **2017**, 2682-2690. DOI: 10.1002/ejic.201700088.
- (116) Rashidi, M.; Fakhroei, Z.; Puddephatt, R. J. Studies of binuclear methyl and phenyl derivatives of platinum(II). *J. Organomet. Chem.* **1991**, 406 (1), 261-267. DOI: 10.1016/0022-328X(91)83191-6.
- (117) Hosseini, F. N. Theoretical studies of methyl iodide oxidative addition to adjacent metal centers in diplatinum(II) complexes. *Polyhedron* **2015**, 100, 67-73. DOI: 10.1016/j.poly.2015.07.041.
- (118) Jamali, S.; Nabavizadeh, S. M.; Rashidi, M. Oxidative Addition of Methyl Iodide to a New Type of Binuclear Platinum(II) Complex: a Kinetic Study. *Inorg. Chem.* **2005**, 44 (23), 8594-8601. DOI: 10.1021/ic0511064.

- (119) Hashemi, M. Comparison of reactivity of Pt(II) center in the mononuclear and binuclear organometallic diimineplatinum complexes toward oxidative addition of methyl iodide. *J. Mol. Struct.* **2016**, *1103*, 132-139. DOI: 10.1016/j.molstruc.2015.09.017.
- (120) Rendina, L. M.; Puddephatt, R. J. Oxidative Addition Reactions of Organoplatinum(II) Complexes with Nitrogen-Donor Ligands. *Chem. Rev.* **1997**, *97* (6), 1735-1754. DOI: 10.1021/cr9704671.
- (121) Nabavizadeh, S. M.; Amini, H.; Jame, F.; Khosraviolya, S.; Shahsavari, H. R.; Hosseini, F. N.; Rashidi, M. Oxidative addition of MeI to some cyclometalated organoplatinum(II) complexes: Kinetics and mechanism. *J. Organomet. Chem.* **2012**, *698*, 53-61. DOI: 10.1016/j.jorganchem.2011.10.028.
- (122) Hamidizadeh, P.; Rashidi, M.; Nabavizadeh, S. M.; Samaniyan, M.; Aseman, M. D.; Owczarzak, A. M.; Kubicki, M. Secondary kinetic deuterium isotope effect in oxidative addition reaction of cycloplatinated(II) complexes with MeI. *J. Organomet. Chem.* **2015**, *791*, 258-265. DOI: 10.1016/j.jorganchem.2015.06.001.
- (123) Habibzadeh, S.; Rashidi, M.; Nabavizadeh, S. M.; Mahmoodi, L.; Hosseini, F. N.; Puddephatt, R. J. Steric and Solvent Effects on the Secondary Kinetic α -Deuterium Isotope Effects in the Reaction of Methyl Iodide with Organoplatinum(II) Complexes: Application of a Second-Order Technique in Measuring the Rates of Rapid Processes. *Organometallics* **2010**, *29* (1), 82-88. DOI: 10.1021/om900778u.
- (124) Fatemeh, N. H.; Farasat, Z.; Nabavizadeh, S. M.; Wu, G.; Abu-Omar, M. M. N-methylation versus oxidative addition using MeI in the reaction of organoplatinum(II) complexes containing pyrazine ligand. *J. Organomet. Chem.* **2019**, *880*, 232-240. DOI: 10.1016/j.jorganchem.2018.11.002.
- (125) Dolatyari, V.; Shahsavari, H. R.; Habibzadeh, S.; Babadi Aghakhanpour, R.; Paziresh, S.; Golbon Haghighi, M.; Halvagar, M. R. Photophysical Properties and Kinetic Studies of 2-Vinylpyridine-Based Cycloplatinated(II) Complexes Containing Various Phosphine Ligands. *Molecules* **2021**, *26* (7), 2034. DOI: 10.3390/molecules26072034.
- (126) Crespo, M.; Martínez, M.; Nabavizadeh, S. M.; Rashidi, M. Kinetic-mechanistic studies on CX (X=H, F, Cl, Br, I) bond activation reactions on organoplatinum(II) complexes. *Coord. Chem. Rev.* **2014**, *279*, 115-140. DOI: 10.1016/j.ccr.2014.06.010.

- (127) Aghakhanpour, R. B.; Rashidi, M.; Hosseini, F. N.; Raoof, F.; Nabavizadeh, S. M. Oxidation of a rollover cycloplatinated(II) dimer by MeI: a kinetic study. *RSC Adv.* **2015**, *5* (82), 66534-66542. DOI: 10.1039/C5RA12201E.
- (128) Aghakhanpour, R. B.; Nabavizadeh, S. M.; Mohammadi, L.; Jahromi, S. A.; Rashidi, M. A kinetic approach to carbon-iodide bond activation by rollover cycloplatinated(II) complexes containing monodentate phosphine ligands. *J. Organomet. Chem.* **2015**, *781*, 47-52. DOI: 10.1016/j.jorganchem.2015.01.015.
- (129) Shaw, P. A.; Rourke, J. P. Selective C-C coupling at a Pt(IV) centre: 100% preference for sp^2-sp^3 over sp^3-sp^3 . *Dalton Trans.* **2017**, *46* (14), 4768-4776. DOI: 10.1039/C7DT00328E.
- (130) Shahsavari, H. R.; Babadi Aghakhanpour, R.; Fereidoonzehad, M. An in-depth investigation on the C-I bond activation by rollover cycloplatinated(II) complexes bearing monodentate phosphane ligands: kinetic and kinetic isotope effect. *New J. Chem.* **2018**, *42* (4), 2564-2573. DOI: 10.1039/C7NJ04159D.

Chapter 1

Organometallic complexes with M-
M' bonds as intermediates for
bimetallic catalysis

This chapter focuses on the synthesis, characterization, computational and structural studies of several trinuclear and dinuclear bimetallic clusters with M-M' bonds with formula [(CNC)(PPh₃)MM'(PPh₃)](ClO₄) and [{M(CNC)(PPh₃)₂M'}](ClO₄) (being M = Pt(II), Pd(II) and M' = Ag(I), Au(I); CNC = 2,6-di(phen-2-ide)-pyridine) which could be regarded as possible models for a transmetallation reaction.

As indicated in the introduction, in bimetallic catalysis processes there is necessary step in which the two catalytic cycles of the metals intersect; the transmetallation process.¹⁻⁴ In this step, the two metallic centers exchange their ligands in order to render the seek product. In the literature it has been discussed whether in this process both metals need to establish an intermetallic interaction in order to proceed, and for some examples the existence of an intermetallic bond has been proved to stabilize the intermediates of the transmetallation process.⁵⁻¹⁰ Accordingly, several clusters with M-M' bonds have been proposed as intermediates for a transmetallation reaction.^{6,7,9,11-17}

Thus, the obtention of complexes with donor-acceptor bonds involving d⁸-d¹⁰ metals has been studied in this chapter. The initial proposal for this line of work of this thesis is the study of reactivity of starting materials [Pt(CNC)(PPh₃)] (**1**) and [Pd(CNC)(PPh₃)] (**2**) as suitable candidates for the formation of donor-acceptor bonds with Ag(I) and Au(I). The creation of short interactions between the acidic metal and the C_{ipso} of the CNC cyclometallated ligand allow them, therefore, to be regarded as a frozen snapshot of a phenyl ring transfer between the metals, which cannot be completed because of the pincer nature of the CNC ligand. In addition, it is possible to modulate the degree of transfer of this organic group depending on the pair of metals involved.

While syntheses and characterization of the complexes discussed in this chapter are explained with detail in Sections 1.1 and 1.2, the computational and structural studies that allow them to be considered as arrested intermediates of a transmetallation process are discussed in Section 1.3.

Thus, the first task was the preparation of the starting materials [Pt(CNC)(PPh₃)] (**1**) and [Pd(CNC)(PPh₃)] (**2**). However, while **1** was prepared according to the literature,¹⁶ the absence of a facile method for the synthesis of palladium CNC starting substrates forced to explore a new route for the obtaining of the palladium starting material **2**. Thus, a suspension of complex [Pd(CNC-H)Cl(PPh₃)] (**3**) was reacted with excess of the base KHMDS (potassium bis(trimethylsilyl)amide) in THF under argon. After work-up a yellow solid identified as [Pd(CNC)(PPh₃)] (**2**) was obtained with 59% yield. The structure of **2** was determined by single crystal X-Ray diffraction (see Figure 1.1 for a view of the structure of **2** and Table 1.1 for a selection of distances and angles). This structure confirmed the cyclometallation of the two aromatic rings, showing the expected square planar Pd(II) complex where the CNC ligand was coordinated in a tridentate fashion.

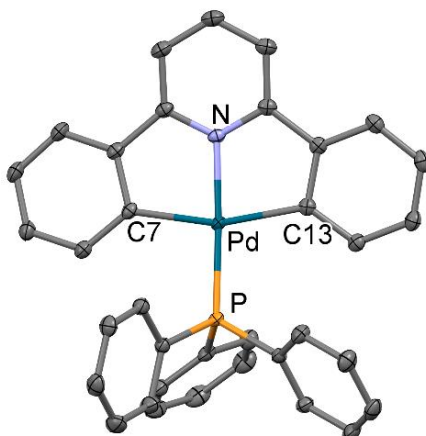


Figure 1.1. Molecular structure of complex [Pd(CNC)(PPh₃)] (**2**).

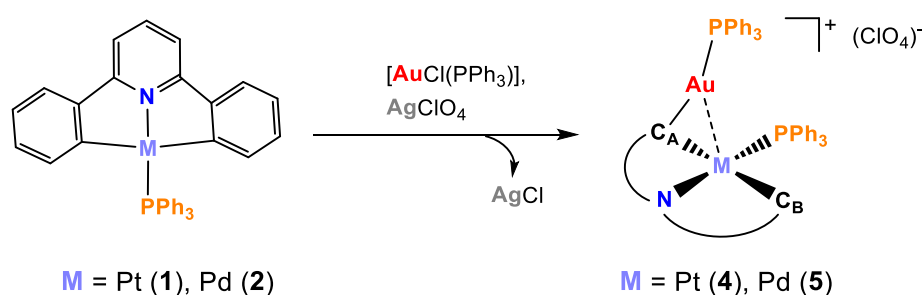
Table 1.1. Selected bond lengths (Å) and angles (°) for **2**.

Pd-C7	2.0787(14)	N-Pd-C13	80.58(5)
Pd-C13	2.0788(14)	N-Pd-C7	80.73(5)
Pd-P	2.2250(4)	C7-Pd-C13	160.74(6)
Pd-N	2.0109(12)		

1.1. Preparation and characterization of heterobimetallic platinum-gold and palladium-gold complexes $[(CNC)(PPh_3)MAu(PPh_3)](ClO_4)$ ($M = Pt$ (4), Pd (5)) and $\{[M(CNC)(PPh_3)]_2Au\}(ClO_4)$ ($M = Pt$ (6), Pd (7))

Reactivity of platinum and palladium cyclometallated starting materials $[Pt(CNC)(PPh_3)]$ (1) and $[Pd(CNC)(PPh_3)]$ (2) towards gold substrates $[AuCl(PPh_3)]$ and $[AuCl(tht)]$ (tht = tetrahydrothiophene, SC_4H_8) was studied in order to achieve the synthesis of clusters with Pt-Au and Pd-Au bonds. Given the different nature of the ligands bonded to these two Au complexes, the stoichiometry of the reaction is determined by the gold precursors used.¹⁷⁻²⁰ Thus, reactions with equimolar amounts of starting material with $[AuCl(PPh_3)]$ result in dinuclear clusters, while ratios 2:1 of basic metallic substrate with $[AuCl(tht)]$ afford trinuclear clusters.

When equimolar quantities of $[AuCl(PPh_3)]$ were reacted towards complexes $[Pt(CNC)(PPh_3)]$ (1) or $[Pd(CNC)(PPh_3)]$ (2), the products obtained were identified as dinuclear bimetallic clusters with M-Au bonds (see Scheme 1.1). To carry out these reactions, the gold complex $[AuCl(PPh_3)]$ was dissolved in THF and $AgClO_4$ was added at low temperatures (see Experimental section for details) under argon. Then, a white solid appeared, namely $AgCl$, giving rise in solution to the gold (I) species $[Au(thf)(PPh_3)]^+$. After 60 minutes of reaction, $AgCl$ was removed and $[Pt(CNC)(PPh_3)]$ (1) or $[Pd(CNC)(PPh_3)]$ (2) were added. After some time, removal of the solvent allowed to obtain the expected complexes $[(CNC)(PPh_3)PtAu(PPh_3)](ClO_4)$ (4) and $[(CNC)(PPh_3)PdAu(PPh_3)](ClO_4)$ (5) as yellow solids.

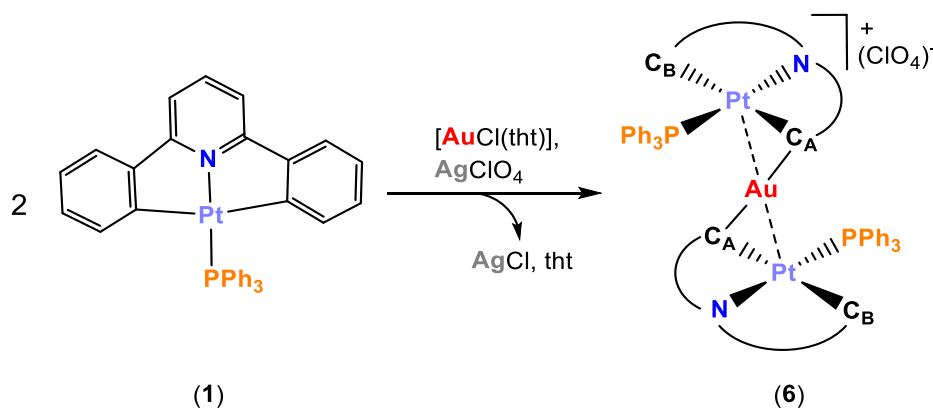


Scheme 1.1. Synthesis of complexes with formula $[(CNC)(PPh_3)MAu(PPh_3)](ClO_4)$.

On the other hand, the obtaining of trinuclear complexes with formula $\{[M(CNC)(PPh_3)]_2Au\}(ClO_4)$ was also investigated. For these syntheses, $[AuCl(tht)]$ was chosen as a source of “naked” Au(I). The same reaction procedure was followed in

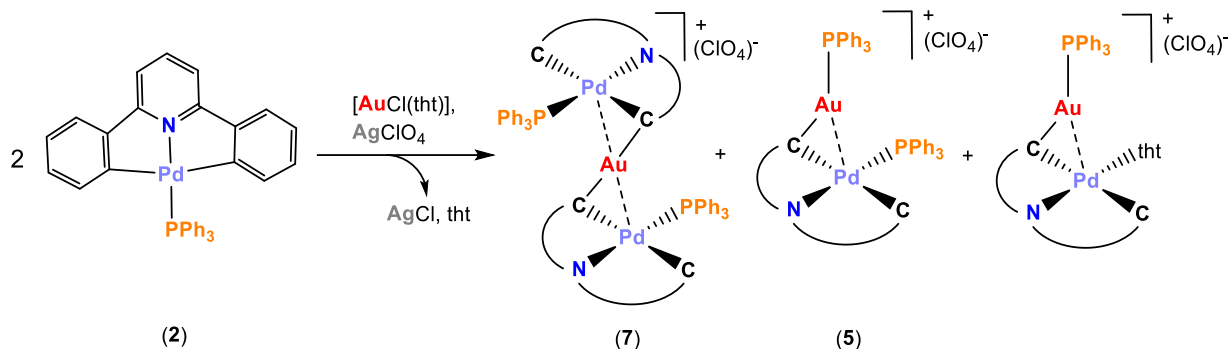
order to prepare complexes with formula $[\{M(\text{CNC})(\text{PPh}_3)\}_2\text{Au}](\text{ClO}_4)$ ($M = \text{Pt}$ (**6**), Pd (**7**)) with slight variations (see Experimental section). Thus, equimolar amounts of $[\text{AuCl}(\text{tht})]$ and AgClO_4 were dissolved in THF at low temperature under argon and kept protected from light. Then, AgCl precipitated and species $[\text{Au}(\text{thf})(\text{tht})]^+$ formed in solution. Ligand tht is known to behave usually as a labile ligand that can be displaced easily by other species.^{17,21-23} Then, two equivalents of complex $[\text{M}(\text{CNC})(\text{PPh}_3)]$ ($M = \text{Pt}$ (**1**), Pd (**2**)) were added. The resulting solutions were kept at low temperature and after some time they were concentrated, and the resulting solids filtrated.

These syntheses afforded different results. While in the case of the platinum reaction (see Scheme 1.2) the seek trinuclear $[\{\text{Pt}(\text{CNC})(\text{PPh}_3)\}_2\text{Au}](\text{ClO}_4)$ (**6**) was the only complex obtained, in the case of the palladium solid, **7***, this was identified as a mixture of complexes.



Scheme 1.2. Synthesis of complex $[\{\text{Pt}(\text{CNC})(\text{PPh}_3)\}_2\text{Au}](\text{ClO}_4)$ (**6**).

Several attempts to prepare complex $[\{\text{Pd}(\text{CNC})(\text{PPh}_3)\}_2\text{Au}](\text{ClO}_4)$ (**7**) as a pure solid varying the reaction conditions, namely temperature and reaction times, always resulted in a mixture of three different species in different proportions (NMR). These species were the dinuclear $[(\text{CNC})(\text{PPh}_3)\text{PdAu}(\text{PPh}_3)](\text{ClO}_4)$ (**5**), the expected $[\{\text{Pd}(\text{CNC})(\text{PPh}_3)\}_2\text{Au}](\text{ClO}_4)$ (**7**) and other unknown product that was not unequivocally identified and tentatively assigned to a dinuclear complex with formula “ $[(\text{CNC})(\text{tht})\text{PdAu}(\text{PPh}_3)](\text{ClO}_4)$ ” (see Scheme 1.3).



Scheme 1.3. Reaction of complex $[\text{Pd}(\text{CNC})(\text{PPh}_3)]$ (**2**) with $[\text{AuCl}(\text{tht})]$ and AgClO_4 .

It is noteworthy that when solutions containing the proposed $[(\text{CNC})(\text{tht})\text{PdAu}(\text{PPh}_3)](\text{ClO}_4)$ dinuclear complex were kept for a day at room temperature, its aromatic signals in the ^1H NMR spectrum disappeared and a blue colour and black particles appeared in the NMR tube. This information indicated that the stability of this dinuclear complex was very low at room temperature. However, a small batch of yellow crystals of complex $[\{\text{Pd}(\text{CNC})(\text{PPh}_3)\}_2\text{Au}](\text{ClO}_4)$ (**7**) could be obtained and used for its characterization through NMR and X-Ray diffraction studies (see below).

Solids corresponding to complexes $[(\text{CNC})(\text{PPh}_3)\text{PtAu}(\text{PPh}_3)](\text{ClO}_4)$ (**4**), $[(\text{CNC})(\text{PPh}_3)\text{PdAu}(\text{PPh}_3)](\text{ClO}_4)$ (**5**), $[\{\text{Pt}(\text{CNC})(\text{PPh}_3)\}_2\text{Au}](\text{ClO}_4)$ (**6**) and $[\{\text{Pd}(\text{CNC})(\text{PPh}_3)\}_2\text{Au}](\text{ClO}_4)$ (**7**) were characterized using the habitual techniques as can be seen in the Supporting Information. IR spectra of complexes **4**, **5** and **6** (see Figures S1.18, S1.24 and S1.33, Supporting Information) showed the typical signals of the CNC, PPh_3 ligands and ClO_4^- , being in agreement with the proposed formula for these clusters.

X-Ray diffraction studies could be performed on crystals of **4**, **5**, **6** and **7** confirming the expected nuclearities. Figures 1.2 and 1.3 display the structures of the cations of these complexes and relevant distances and angles for these complexes are listed in Table 1.2.

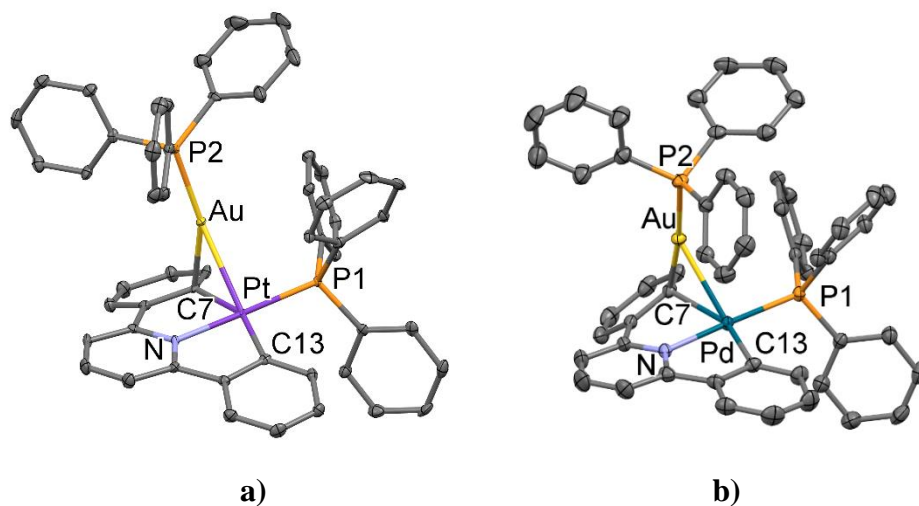


Figure 1.2. Molecular structures of the cations of complexes $[(\text{CNC})(\text{PPh}_3)\text{PtAu}(\text{PPh}_3)](\text{ClO}_4)$ (**4**) (a) and $[(\text{CNC})(\text{PPh}_3)\text{PdAu}(\text{PPh}_3)](\text{ClO}_4)$ (**5**) (b).

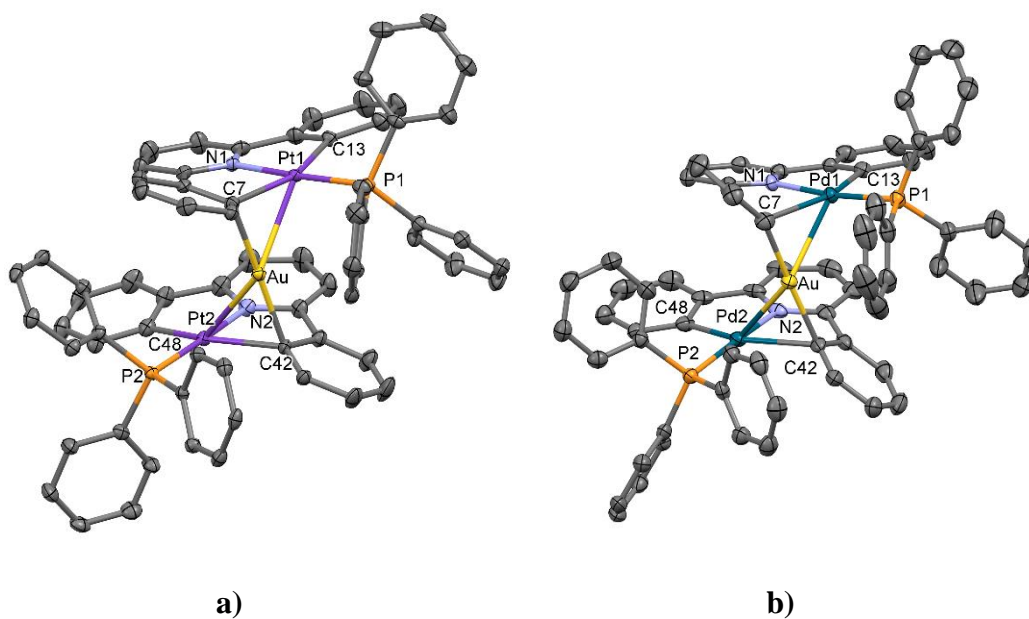


Figure 1.3. Molecular structures of the cations of complexes $[\{\text{Pt}(\text{CNC})(\text{PPh}_3)\}_2\text{Au}](\text{ClO}_4)$ (**6**) (a) and $[\{\text{Pd}(\text{CNC})(\text{PPh}_3)\}_2\text{Au}](\text{ClO}_4)$ (**7**) (b).

Table 1.2. Selected bond lengths (Å) and angles (°) for **4**, **5**, **6** and **7**. See Schemes 1.1-1.2 for the definition of C_A and C_B.

	M = Pt (4)	M = Pd (5)	M = Pt (6)	M = Pd (7)
M-Au	2.7222(2)	2.7422(3)	2.7297(2) 2.7426(2)	2.7366(4) 2.7491(4)
M-C _A	2.158(3)	2.393(3)	2.212(3) 2.244(3)	2.498(5) 2.419(5)
M-C _B	2.063(3)	2.031(3)	2.051(3) 2.045(3)	2.020(5) 2.029(5)
Au-C _A	2.225(3)	2.119(3)	2.174(3) 2.157(3)	2.098(5) 2.108(5)
C _A -M-C _B	156.30(14)	157.68(12)	157.99(13) 157.71(12)	157.3(2) 157.9(2)
C _A -M-Au	52.71(9)	48.16(7)	50.90(8) 50.04(8)	46.98(11) 47.61(12)

The crystal structures show in all four cases short Pt-Au and Pd-Au interactions, varying from 2.7222(2) to 2.7491(4) Å. In the case of the palladium clusters, these are remarkable values, since the number of Pd(II)-Au complexes structurally characterized is very small and always with bridging ligands between the metals and longer intermetallic distances.^{19,20,24,25} The only shorter Pd-Au distance reported (2.6174(9) Å) belongs to an electron deficient polynuclear complex.²⁶

Dinuclear clusters consisted of one platinum or palladium subunit bonded to a [Au(PPh₃)]⁺ fragment, while trinuclear complexes revealed a gold center sandwiched by two [M(CNC)(PPh₃)] (M = Pt or Pd) moieties.

More importantly, M-Au lines are not perpendicular with respect to the square planar environment of the Pt or Pd centers. Instead, in all cases the gold center leans towards a C_{ipso} (C_A, see Schemes 1.1 and 1.2) of the CNC cyclometallated ligand, giving short Au-C_A interactions. Similar interactions between the acidic metal and a

cyclometalated carbon have been reported for other M-M' complexes.^{6,7,12,18,27-30} These distances between Au and C_A are sensitive to the basic metal existing in the cluster. In the case of palladium, shorter distances than for the platinum clusters are found, exhibiting the trinuclear complex **7**, the shortest ones (2.098(5) and 2.108(5) Å). This Au-C interaction causes an elongation of the Pt and Pd-C_A distances, corresponding the longest ones again to the trinuclear [$\{\text{Pd}(\text{CNC})(\text{PPh}_3)\}_2\text{Au}\](\text{ClO}_4)$ (**7**). In fact, the Au-C_A distances for the palladium-gold complexes **5** and **7** are comparable to those reported for gold (I) aryl compounds in which an ordinary σ Au-C(aryl) bond is present.³¹⁻³³

It is noteworthy that the phenylene ring interacting with the gold center displayed a remarkable deviation with respect to the best Pt(II) or Pd(II) square planar environments. This distortion was found out very significant in the palladium clusters, especially in [$\{\text{Pd}(\text{CNC})(\text{PPh}_3)\}_2\text{Au}\](\text{ClO}_4)$ (**7**). An overlay of the two trinuclear structures can be seen in Figure 1.4, where this effect can be noticed.

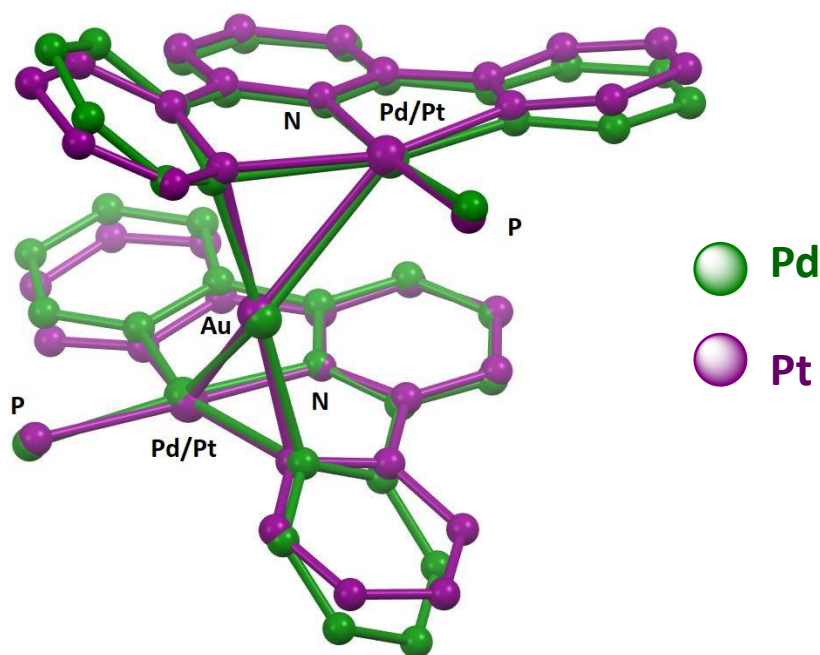


Figure 1.4. Overlay of the structures of [$\{\text{Pt}(\text{CNC})(\text{PPh}_3)\}_2\text{Au}\](\text{ClO}_4)$ (**6**) and [$\{\text{Pd}(\text{CNC})(\text{PPh}_3)\}_2\text{Au}\](\text{ClO}_4)$ (**7**).

To sum up, all that structural information suggested that there was an important interaction between metallic fragments on these Pt/Pd-Au complexes. These “[$(\text{CNC})\text{M}$]-Au” interactions were noticed to be stronger when the basic metal is palladium, giving

rise to a tighter bonding situation. This statement was later confirmed through NMR studies and DFT calculations.

Heterobimetallic gold complexes $[(\text{CNC})(\text{PPh}_3)\text{PtAu}(\text{PPh}_3)](\text{ClO}_4)$ (**4**), $[(\text{CNC})(\text{PPh}_3)\text{PdAu}(\text{PPh}_3)](\text{ClO}_4)$ (**5**), $[\{\text{Pt}(\text{CNC})(\text{PPh}_3)\}_2\text{Au}](\text{ClO}_4)$ (**6**) and a small batch of crystals of $[\{\text{Pd}(\text{CNC})(\text{PPh}_3)\}_2\text{Au}](\text{ClO}_4)$ (**7**) were also characterised through multinuclear and variable temperature (VT) NMR studies. Thus, ^1H NMR spectrum of complex $[(\text{CNC})(\text{PPh}_3)\text{PtAu}(\text{PPh}_3)](\text{ClO}_4)$ (**4**) in CD_2Cl_2 (see Figure 1.5) shows at 273K a pattern of signals that indicates that both halves of the CNC ligand are equivalent for the NMR timescale, displaying for example only one signal at around 6 ppm for the H2 protons of this cyclometallated ligand (see the numbering of the protons in Chart 1.1).

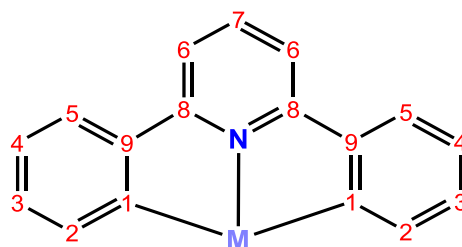


Chart 1.1. Numbering of the positions of the CNC ligand.

This observation is not compatible with the X-Ray structure described above, in which the two phenylene rings of the CNC ligand are different. Interestingly, by lowering the temperature, H2 signal suffers coalescence between 213 and 183K. At 173K the ^1H NMR spectrum of $[(\text{CNC})(\text{PPh}_3)\text{PtAu}(\text{PPh}_3)](\text{ClO}_4)$ (**4**) gives a more complex pattern of signals than at room temperature (see Figure 1.5). This spectrum reveals for example two signals with integration of 1 at 6.4 and 5.1 ppm corresponding to different signals of H2. This observation is in agreement with the presence in solution of a CNC ligand bearing two inequivalent halves at the NMR timescale.

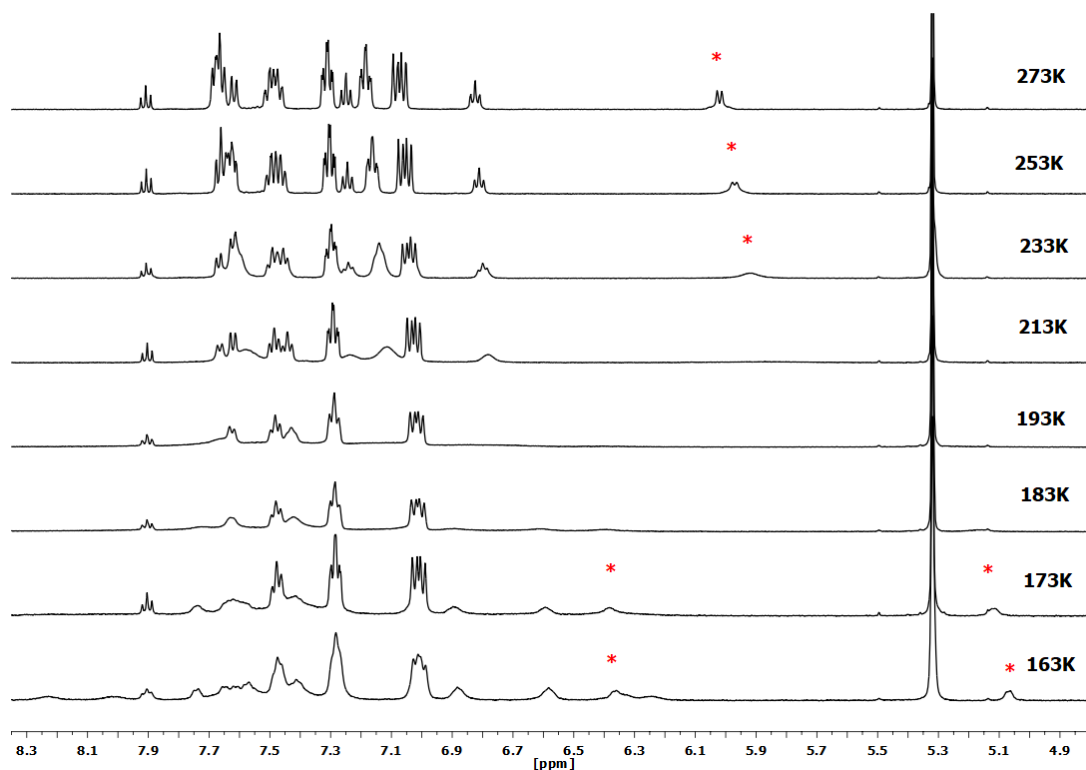
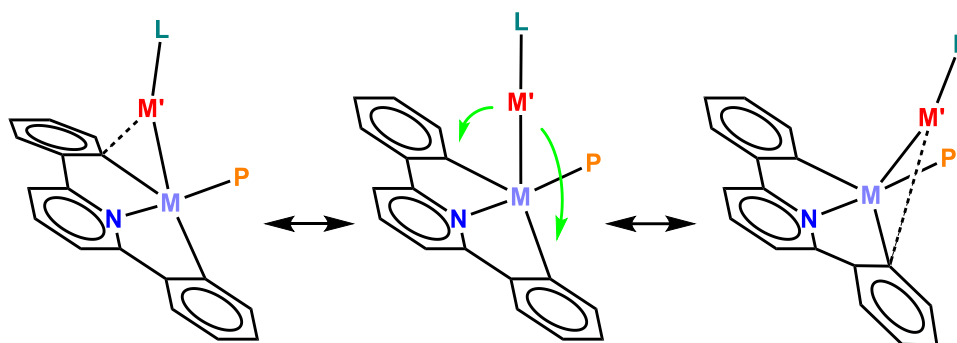


Figure 1.5. VT ^1H NMR spectra (CD_2Cl_2) of complex $[(\text{CNC})(\text{PPh}_3)\text{PtAu}(\text{PPh}_3)](\text{ClO}_4)$ (**4**) (red asterisks, H2 signals).

With this information and the one gathered from X-Ray diffraction studies, it can be stated that there is an intramolecular dynamic process, that can be named as a “metronome-like” movement,^{16,17} which operates in solution at room temperature. By lowering the temperature this movement is slowed down and therefore, the symmetry of the CNC ligand is broken during the NMR timescale. This process consists of the movement of the “[Au(PPh₃)]⁺” fragment along the C-M-C axis of the basic platinum or palladium subunit, with formation and breakage of interactions between the gold center and the C_{ipso} of a phenylene ring of the CNC ligand (see Scheme 1.4 for a general graphical depiction of this process).



Scheme 1.4. Proposed “metronome-like” dynamic process for heterobimetallic complexes of this chapter.

$^{31}\text{P}\{^1\text{H}\}$ NMR spectrum of platinum complex $[(\text{CNC})(\text{PPh}_3)\text{PtAu}(\text{PPh}_3)](\text{ClO}_4)$ (**4**) at RT (see Figure 1.6) displays two signals, one singlet with platinum satellites ($^2J_{\text{P}(\text{Au})-\text{Pt}} = 254$ Hz) at 34.6 ppm corresponding to the phosphane ligand attached to the gold center and another singlet with platinum satellites ($^1J_{\text{P-Pt}} = 3680$ Hz) at 22.5 ppm which is assigned to the phosphane ligand coordinated to the platinum center. At 173K, $^{31}\text{P}\{^1\text{H}\}$ NMR spectrum of **4** displays the same signals than at RT. These spectra indicate that the Pt-Au bond remains in solution.

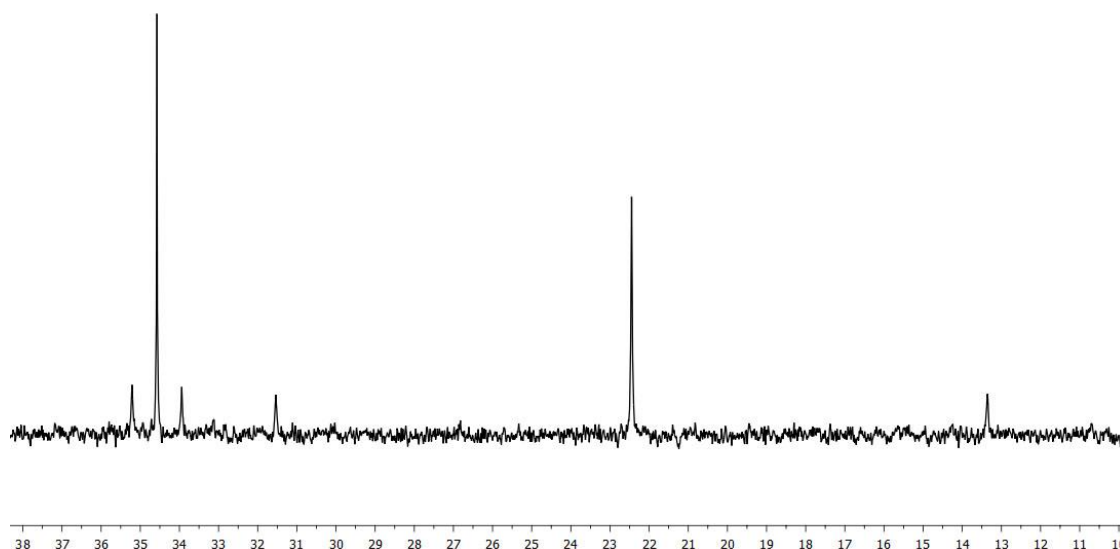


Figure 1.6. $^{31}\text{P}\{^1\text{H}\}$ NMR spectrum (CD_2Cl_2 , 293K) of complex $[(\text{CNC})(\text{PPh}_3)\text{PtAu}(\text{PPh}_3)](\text{ClO}_4)$ (**4**).

Furthermore, the recorded $^{195}\text{Pt}\{^1\text{H}\}$ NMR spectrum of platinum complex $[(\text{CNC})(\text{PPh}_3)\text{PtAu}(\text{PPh}_3)](\text{ClO}_4)$ (**4**) (see Figure 1.7) presents a doublet of doublets centered at -4017 ppm ($^1J_{\text{Pt-P}} = 3680$ Hz, $^2J_{\text{Pt-P}(\text{Au})} = 254$ Hz), which also confirms the

existence of the intermetallic interaction in solution at 293K. It is noteworthy that this signal is displaced downfield with respect to the starting material [Pt(CNC)(PPh₃)] (**1**) around 200 ppm. This finding could be related with the electron-withdrawing capacity of the acidic gold center, which has been also observed for other acidic metals.^{16,17,30,34}

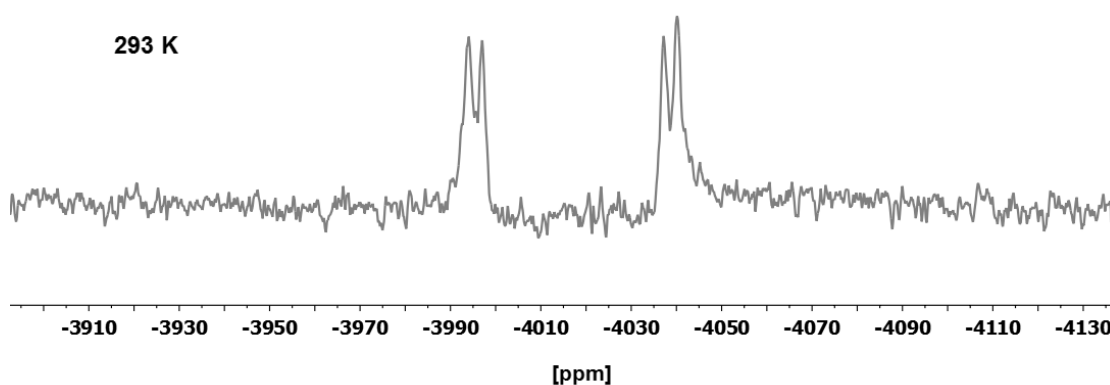


Figure 1.7. $^{195}\text{Pt}\{^1\text{H}\}$ NMR spectrum (CD_2Cl_2 , 293K) of complex $[(\text{CNC})(\text{PPh}_3)\text{PtAu}(\text{PPh}_3)](\text{ClO}_4)$ (**4**).

On the other hand, ^1H NMR spectrum of complex $[(\text{CNC})(\text{PPh}_3)\text{PdAu}(\text{PPh}_3)](\text{ClO}_4)$ (**5**) in CD_2Cl_2 exhibits a more complex pattern of signals than that of **4** at room temperature, revealing for example two signals with integration of 1 (one of them around 5.3 ppm) for the H2 of the cyclometallated ligand (see Figure 1.8). Thus, in this case both halves of the CNC ligand are already inequivalent at room temperature. As expected, lowering the temperature of solutions of complex $[(\text{CNC})(\text{PPh}_3)\text{PdAu}(\text{PPh}_3)](\text{ClO}_4)$ (**5**) does not cause the apparition of new signals. The most remarkable observation is the displacement of one of the H2 signals from 5.4 ppm to 4.9 ppm (Figure 1.8, red asterisks). This could be related to the more rigid disposition of this Pd-Au cluster at low temperature, being the Au-C_{ipso} interactions tighter than at RT, consequently causing a shielding of one H2 signal.

The analysis of the behaviour of this mixture at higher temperatures as 313K was also tried, to study whether the halves CNC ligand became equivalent, but nothing significant was observed.

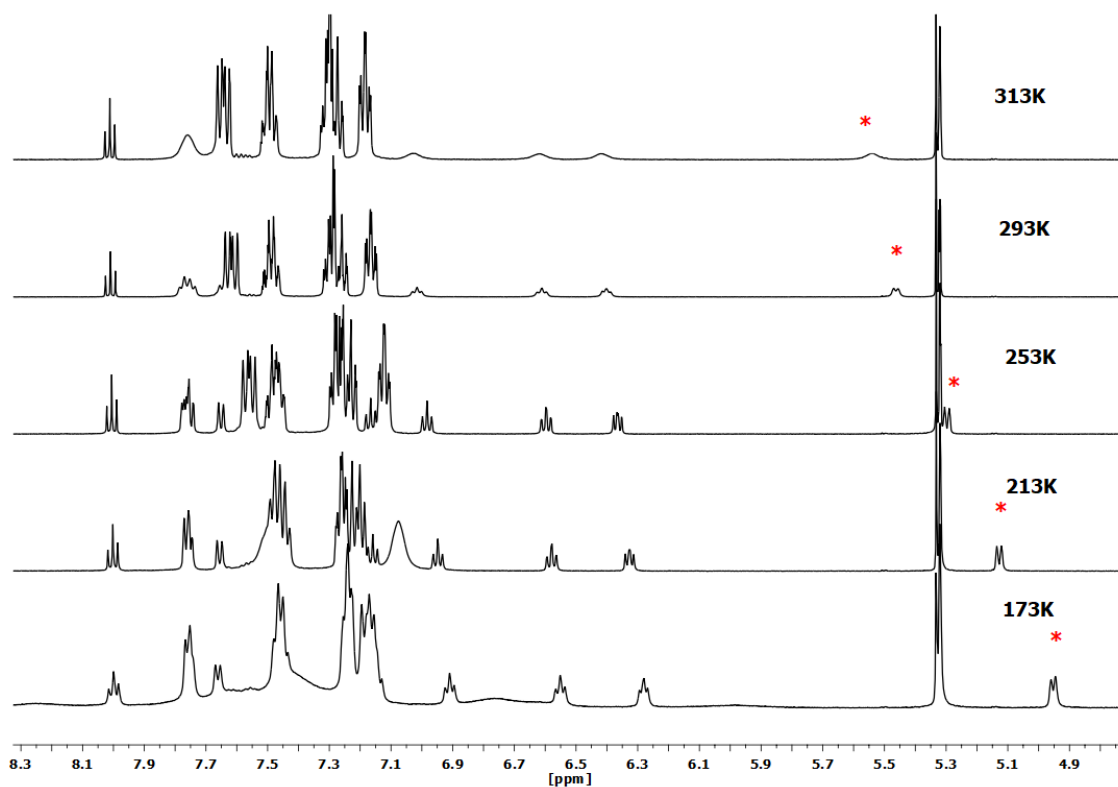


Figure 1.8. VT ^1H NMR spectra (CD_2Cl_2) of complex $[(\text{CNC})(\text{PPh}_3)\text{PdAu}(\text{PPh}_3)](\text{ClO}_4)$ (**5**) (red asterisks, inequivalent H2 signal).

After observing the peculiar behaviour of **5** at room temperature, it can be concluded that the intramolecular “metronome-like” process previously observed for $[(\text{CNC})(\text{PPh}_3)\text{PtAu}(\text{PPh}_3)](\text{ClO}_4)$ (**4**) at room temperature seems to be already slowed down for **5** at that temperature, exhibiting an inequivalent CNC tridentate ligand.

The $^3\text{P}\{^1\text{H}\}$ NMR spectrum of palladium complex $[(\text{CNC})(\text{PPh}_3)\text{PdAu}(\text{PPh}_3)](\text{ClO}_4)$ (**5**) at RT (see Figure 1.9) also shows two singlets at 41.9 and 40.3 ppm, the former corresponding to the $[\text{Au}(\text{PPh}_3)]^+$ fragment and the latter to the PPh_3 bonded to the palladium center.

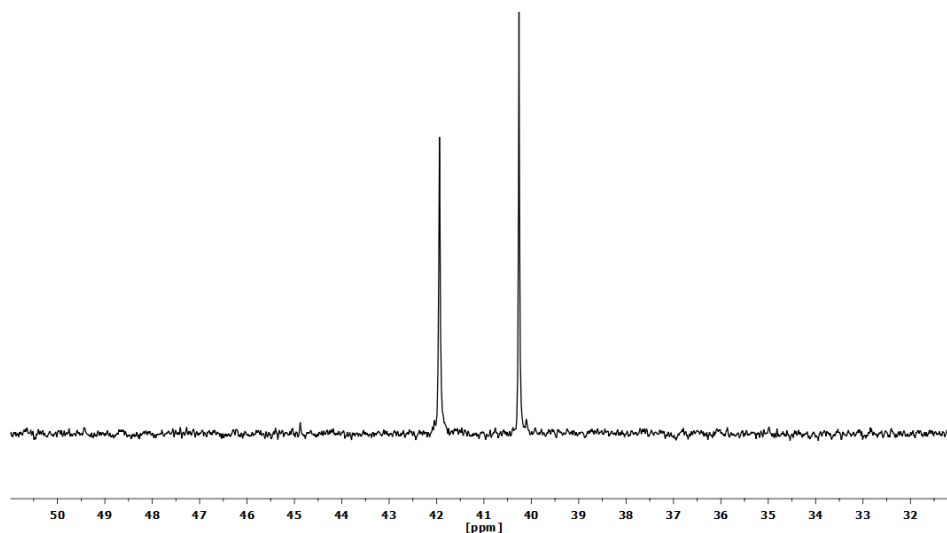


Figure 1.9. $^{31}\text{P}\{^1\text{H}\}$ NMR spectrum (CD_2Cl_2 , 293K) of complex $[(\text{CNC})(\text{PPh}_3)\text{PdAu}(\text{PPh}_3)](\text{ClO}_4)$ (**5**).

The behavior in solution of trinuclear complex $[\{\text{Pt}(\text{CNC})(\text{PPh}_3)\}_2\text{Au}](\text{ClO}_4)$ (**6**) is very similar to that of dinuclear platinum-gold complex **4**. Aromatic signals in the ^1H NMR spectrum of **6** evidence that both halves of the CNC ligand are also equivalent at room temperature within the NMR timescale. When lowering the temperature to 193K new aromatic signals appear, according to the asymmetry of the CNC ligand (see Figure 1.10). Again, two characteristic signals for the different H2 signals appear at 6.3 and 5.4 ppm, with integration of 1.

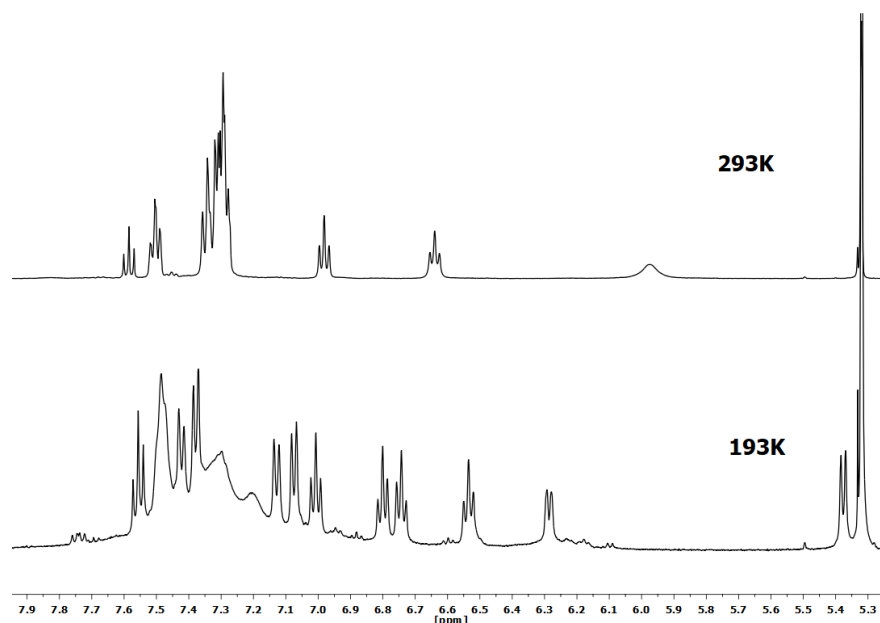


Figure 1.10. ^1H NMR spectrum (CD_2Cl_2 , 293K, top; 193K, bottom) of complex $[\{\text{Pt}(\text{CNC})(\text{PPh}_3)\}_2\text{Au}](\text{ClO}_4)$ (**6**).

This information points out that the “metronome-like” movement operates at room temperature, but at low temperature this intramolecular process slows, as observed previously for [(CNC)(PPh₃)PtAu(PPh₃)](ClO₄) (**4**).

On the other hand, ³¹P{¹H} NMR spectrum of cluster [{Pt(CNC)(PPh₃)₂Au}](ClO₄) (**6**) is very simple, only one singlet from the phosphane attached to the basic metallic center is observed at 20.9 ppm with platinum satellites (¹J_{Pt} = 3794 Hz) (see Figure S1.36, Supporting Information).

In addition to this, the ¹⁹⁵Pt{¹H} NMR spectrum of **6** at 293K (see Figure 1.11) displays a doublet at -4006 ppm (¹J_{Pt-P} = 3813 Hz). This signal displaces downfield with respect to the starting material [Pt(CNC)(PPh₃)] (**1**) as happens in the case of [(CNC)(PPh₃)PtAu(PPh₃)](ClO₄) (**4**). This deshielding of the signal suggests again the persistence of the Pt-Au interaction in solution.

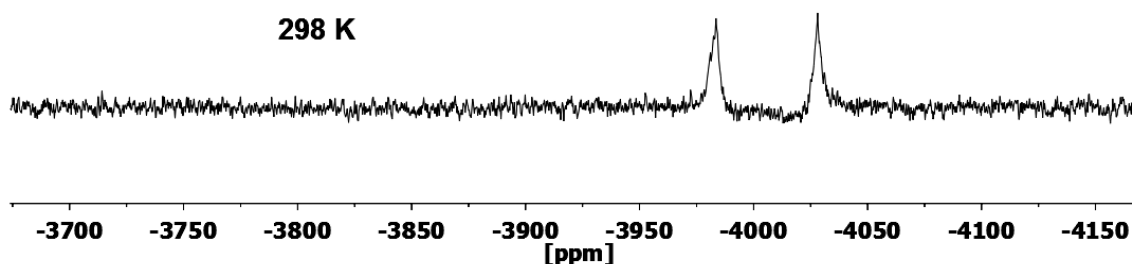


Figure 1.11. ¹⁹⁵Pt{¹H} NMR spectrum (CD₂Cl₂, RT) of complex [{Pt(CNC)(PPh₃)₂Au}](ClO₄) (**6**).

The analogous trinuclear [{Pd(CNC)(PPh₃)₂Au}](ClO₄) (**7**) shows the same behaviour in ¹H NMR as the one observed for [(CNC)(PPh₃)PdAu(PPh₃)](ClO₄) (**5**) at room temperature (see Figure 1.12). The ¹H NMR spectrum of cluster **7** evidences that both halves of the CNC ligand exhibit a complex distribution of signals in agreement with the inequivalence of the phenylene rings of the CNC tridentate ligand. Lowering the temperature for a solution of **7** does not give much information; only the displacement of one H₂ signal upfield is again observed (see Figure 1.12).

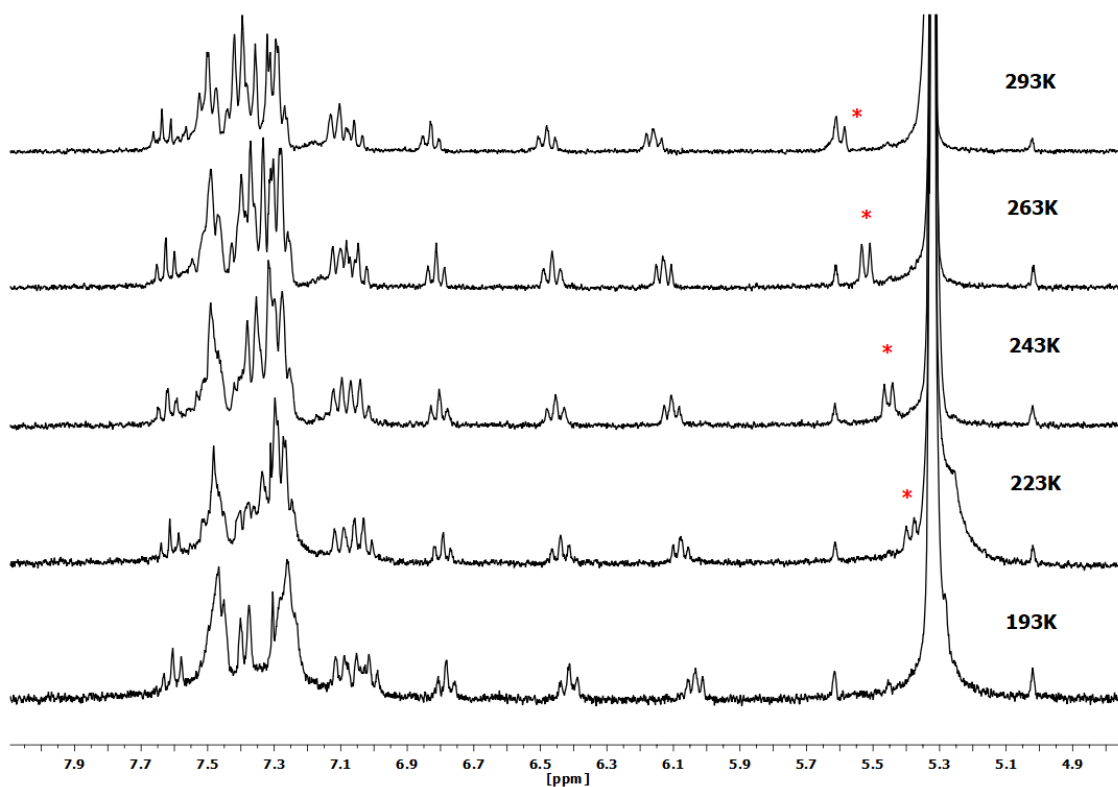


Figure 1.12. VT ^1H NMR spectra (CD_2Cl_2) of complex $[\{\text{Pd}(\text{CNC})(\text{PPh}_3)\}_2\text{Au}](\text{ClO}_4)$ (**7**) (red asterisk, inequivalent H_2 signal).

Again, this information indicates that the “metronome” process is already slowed down at room temperature for the NMR timescale, as happened for the previously described dinuclear Pd-Au cluster **5**.

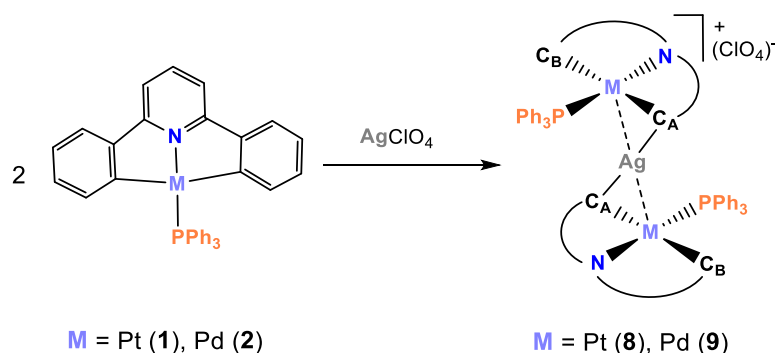
On the other hand, $^{31}\text{P}\{^1\text{H}\}$ NMR spectrum of **7** is very simple, showing only one singlet from the phosphane attached to the palladium center at 40.2 ppm (see Figure S1.41, Supporting Information).

This different behaviour in solution between the Pt-Au and the Pd-Au clusters indicates that the metronome movement is operating faster at RT in the platinum compounds during the NMR timescale. When lowering the temperature for these complexes, this intramolecular process slows down, evidencing inequivalent phenylene rings in the CNC ligands. It is quite remarkable that this process is already slowed down at RT for the palladium-gold complexes, indicating that a stronger interaction between the metallic fragments might be existing in these heterobimetallic compounds. This proposal was later studied and confirmed through DFT calculations.

1.2. Preparation and characterization of heterobimetallic platinum-silver and palladium-silver complexes $[\{M(\text{CNC})(\text{PPh}_3)\}_2\text{Ag}](\text{ClO}_4)$ ($M = \text{Pt}$ (8), Pd (9)) and $[(\text{CNC})(\text{PPh}_3)\text{M}(\text{PPh}_3)](\text{ClO}_4)$ ($M = \text{Pt}$ (10), Pd (11))

As it is already mentioned in the introduction, Ag(I) is one of the most common acidic centers used to form complexes containing intermetallic bonds of donor-acceptor type. Thus, after having investigated the reactivity of cyclometallated complexes $[\text{Pt}(\text{CNC})(\text{PPh}_3)]$ (1) and $[\text{Pd}(\text{CNC})(\text{PPh}_3)]$ (2) towards gold (I) substrates, this study was extended to Ag(I), which could establish interactions with the platinum or palladium centers giving rise to new complexes with M-Ag bonds. The Ag(I) sources used were AgClO_4 and $[\text{Ag}(\text{OCIO}_3)(\text{PPh}_3)]$, two species used frequently in this role. In the former, the silver center is “naked”, while the latter has previously proven to be a suitable compound to obtain dinuclear complexes,^{17,28-30,35} as in this linear silver complex, Ag is coordinated to a bulky ligand and has one free-coordination site available to establish bonds with a basic metallic center.

Therefore, when 2 equivalents of starting materials $[\text{Pt}(\text{CNC})(\text{PPh}_3)]$ (1) or $[\text{Pd}(\text{CNC})(\text{PPh}_3)]$ (2) were reacted with 1 equivalent of AgClO_4 at room temperature protected from light, the expected trinuclear clusters with formula $[\{M(\text{CNC})(\text{PPh}_3)\}_2\text{Ag}](\text{ClO}_4)$ ($M = \text{Pt}$ (8), Pd (9)) were rendered (see Scheme 1.5). When those reactions were carried out with equimolar amounts of the platinum or palladium substrate and the silver salt, a mixture of $[\{M(\text{CNC})(\text{PPh}_3)\}_2\text{Ag}](\text{ClO}_4)$ and unreacted AgClO_4 was obtained.

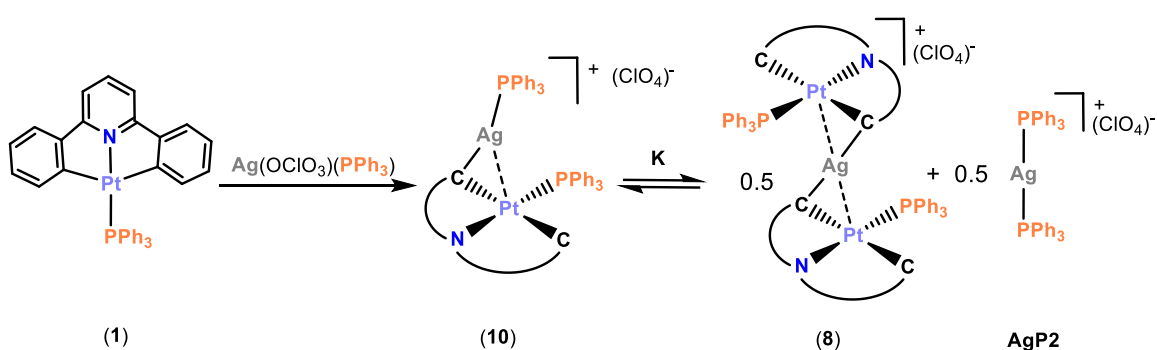


Scheme 1.5. General synthesis of $[\{M(\text{CNC})(\text{PPh}_3)\}_2\text{Ag}](\text{ClO}_4)$ complexes.

On the other hand, the addition of equimolar amounts of silver complex $[\text{Ag}(\text{OCIO}_3)(\text{PPh}_3)]$ to solutions of cyclometallated neutral Pt(II) and Pd(II) substrates $[\text{Pt}(\text{CNC})(\text{PPh}_3)]$ (1) or $[\text{Pd}(\text{CNC})(\text{PPh}_3)]$ (2) in dichloromethane at low temperatures,

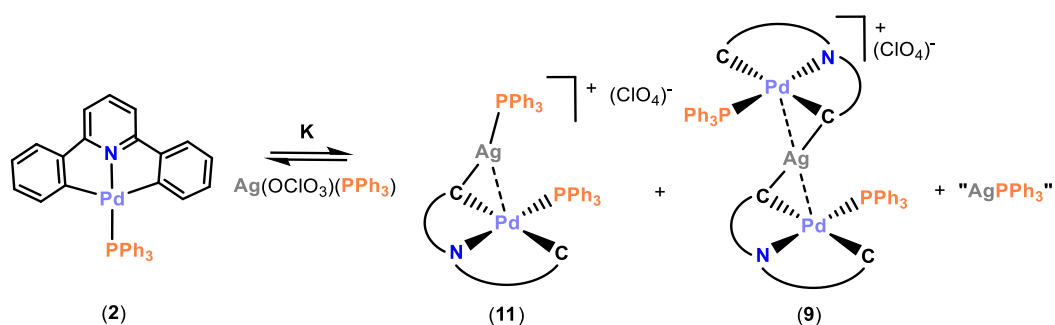
gave rise after short reactions times (see Experimental section for details) to the formation of yellow solids (platinum-silver **10*** and palladium-silver **11***), which were identified by NMR as mixtures of several complexes.

From the platinum starting material, species $[(\text{CNC})(\text{PPh}_3)\text{PtAg}(\text{PPh}_3)](\text{ClO}_4)$ (**10**) and equimolar amounts of trinuclear platinum-silver complex $[\{\text{Pt}(\text{CNC})(\text{PPh}_3)\}_2\text{Ag}](\text{ClO}_4)$ (**8**) and silver complex $[\text{Ag}(\text{PPh}_3)_2](\text{ClO}_4)$ (**AgP2**)³⁶ were detected (NMR) (see Scheme 1.6).



Scheme 1.6. Reaction of $[\text{Pt}(\text{CNC})(\text{PPh}_3)]$ (**1**) with $[\text{Ag}(\text{OCIO}_3)(\text{PPh}_3)]$.

On the other hand the reaction of the palladium starting substrate $[\text{Pd}(\text{CNC})(\text{PPh}_3)]$ (**2**) afforded an even more varied mixture of metallic complexes consisting of the expected dinuclear $[(\text{CNC})(\text{PPh}_3)\text{PdAg}(\text{PPh}_3)](\text{ClO}_4)$ (**11**), the trinuclear complex $[\{\text{Pd}(\text{CNC})(\text{PPh}_3)\}_2\text{Ag}](\text{ClO}_4)$ (**9**), mononuclear silver complexes with Ag-PPh₃ bonds³⁶ and the starting material $[\text{Pd}(\text{CNC})(\text{PPh}_3)]$ (**2**) (see Scheme 1.7).



Scheme 1.7. Reaction of $[\text{Pd}(\text{CNC})(\text{PPh}_3)]$ (**2**) with $[\text{Ag}(\text{OCIO}_3)(\text{PPh}_3)]$.

All the resulting solids from this section were characterized through elemental analysis, IR, MS, multinuclear NMR spectroscopy (^1H , $^{31}\text{P}\{^1\text{H}\}$, $^{13}\text{C}\{^1\text{H}\}$, $^{195}\text{Pt}\{^1\text{H}\}$; platinum complexes) and X-Ray diffraction studies when possible (see Supporting Information).

1.2.1. Characterization of trinuclear complexes $[\{M(\text{CNC})(\text{PPh}_3)\}_2\text{Ag}](\text{ClO}_4)$ ($M = \text{Pt}$ (**8**), Pd (**9**))

For the trinuclears $[\{\text{Pt}(\text{CNC})(\text{PPh}_3)\}_2\text{Ag}](\text{ClO}_4)$ (**8**) and $[\{\text{Pd}(\text{CNC})(\text{PPh}_3)\}_2\text{Ag}](\text{ClO}_4)$ (**9**) X-Ray diffraction studies were possible. Structures of the cations of both complexes and relevant distances and angles are shown in Figure 1.13 and Table 1.3 respectively.

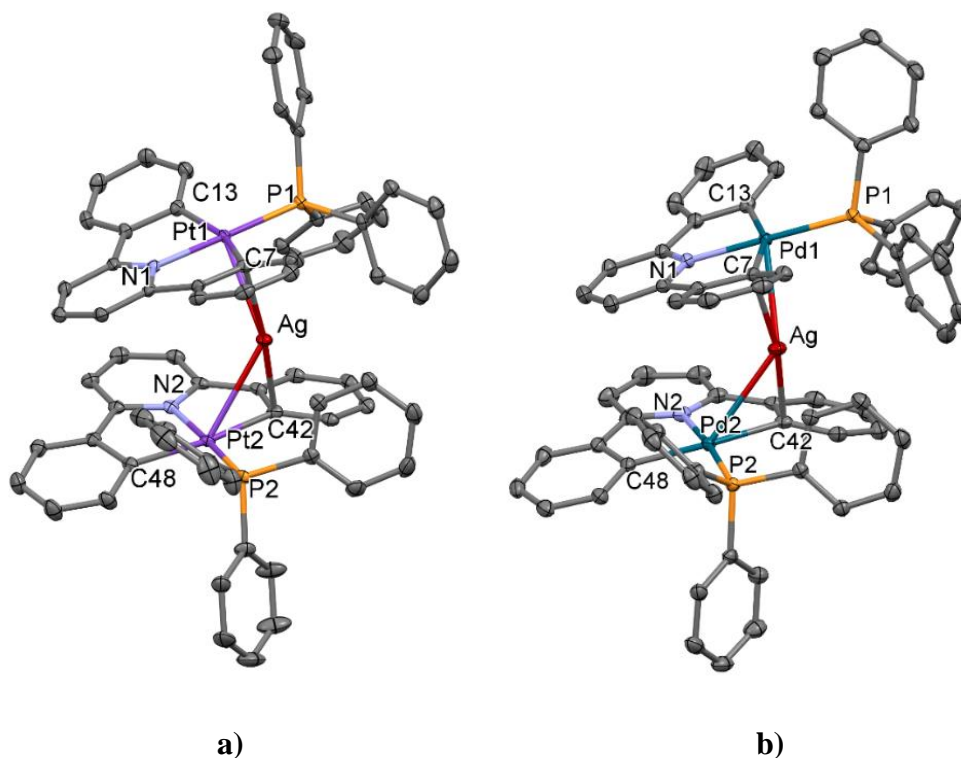


Figure 1.13. Molecular structures of the cations of complexes $[\{\text{Pt}(\text{CNC})(\text{PPh}_3)\}_2\text{Ag}](\text{ClO}_4)$ (**8**) (a) and $[\{\text{Pd}(\text{CNC})(\text{PPh}_3)\}_2\text{Ag}](\text{ClO}_4)$ (**9**) (b).

Table 1.3. Selected bond lengths (\AA) and angles ($^\circ$) for **8** and **9**. See Scheme 1.5 for the definition of C_A and C_B .

	8 ($M = \text{Pt}$)	9 ($M = \text{Pd}$)
M-Ag	2.8549(3)	2.8597(2)
	2.9078(3)	2.9419(2)
M- C_A	2.128(3)	2.143(2)
	2.125(3)	2.164(2)

M-C _B	2.055(3)	2.072(2)
	2.056(3)	2.071(2)
Ag-C _A	2.277(3)	2.239(2)
	2.258(3)	2.212(2)
C _A -Ag-C _A	173.96(12)	168.32(9)
M-Ag-M	126.83(1)	132.774(8)

These structures correspond to trinuclear clusters in which the acidic metallic Ag center is sandwiched (in an analogous way than in the gold clusters) by two square planar platinum or palladium CNC subunits. Dihedral angles between the square planar platinum and palladium environments show that those were almost parallel.

In these silver complexes the M-Ag and η^1 -Ag-C_{ipso} (CNC) interactions are also observed. Due to the latter, the M-Ag lines are not perpendicular to the best square planar environment of Pt and Pd, as occurred in the M-Au clusters. These interactions are not as short as the ones detected for the trinuclear gold complexes [$\{\text{Pt}(\text{CNC})(\text{PPh}_3)_2\text{Au}\}(\text{ClO}_4)$ (**6**) and [$\{\text{Pd}(\text{CNC})(\text{PPh}_3)_2\text{Au}\}(\text{ClO}_4)$ (**7**), in agreement with the known high carbophilicity of gold.^{17,37} In addition to this, the deviation observed for the phenyl ring of the CNC ligand interacting with the silver center is not as pronounced and distances M-C_A are not as long as the ones identified for the gold complexes.

Finally, it is remarkable to indicate, that there are not many examples of Pd-Ag bonds as complex [$\{\text{Pd}(\text{CNC})(\text{PPh}_3)_2\text{Ag}\}(\text{ClO}_4)$ (**9**) reported in the literature.³⁸⁻⁴³

Solutions of complexes [$\{\text{Pt}(\text{CNC})(\text{PPh}_3)_2\text{Ag}\}(\text{ClO}_4)$ (**8**) and [$\{\text{Pd}(\text{CNC})(\text{PPh}_3)_2\text{Ag}\}(\text{ClO}_4)$ (**9**) were also investigated through ¹H NMR spectroscopy. Both complexes (see Figure 1.14) show at RT similar groups of signals, whose pattern and integration indicates that both halves of the CNC ligand are equivalent at the NMR timescale, and, therefore are not consistent with the structural information obtained through X-Ray diffraction.

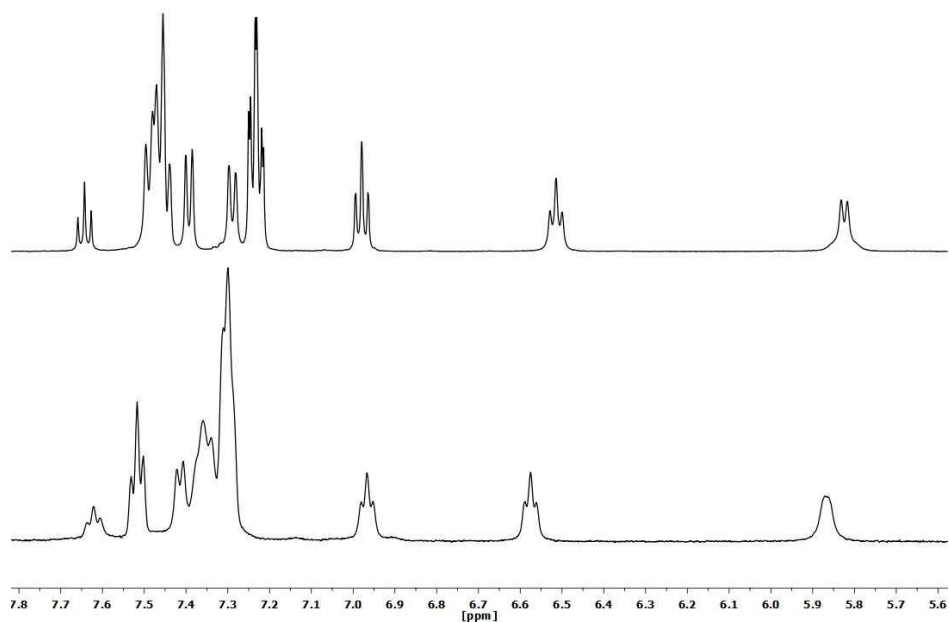


Figure 1.14. ^1H NMR spectra (CD_2Cl_2 , 293K) of complexes $[\{\text{Pt}(\text{CNC})(\text{PPh}_3)\}_2\text{Ag}](\text{ClO}_4)$ (**8**) (top) and $[\{\text{Pd}(\text{CNC})(\text{PPh}_3)\}_2\text{Ag}](\text{ClO}_4)$ (**9**) (bottom).

VT ^1H NMR experiments were also performed on these two systems observing different behaviors in solution for the platinum and palladium species. At 173K no new signals in the platinum silver trinuclear **8** are observed and the existing ones are not well resolved. On the contrary, the spectrum recorded at this temperature for **9** shows a much richer pattern (see Figure 1.15).

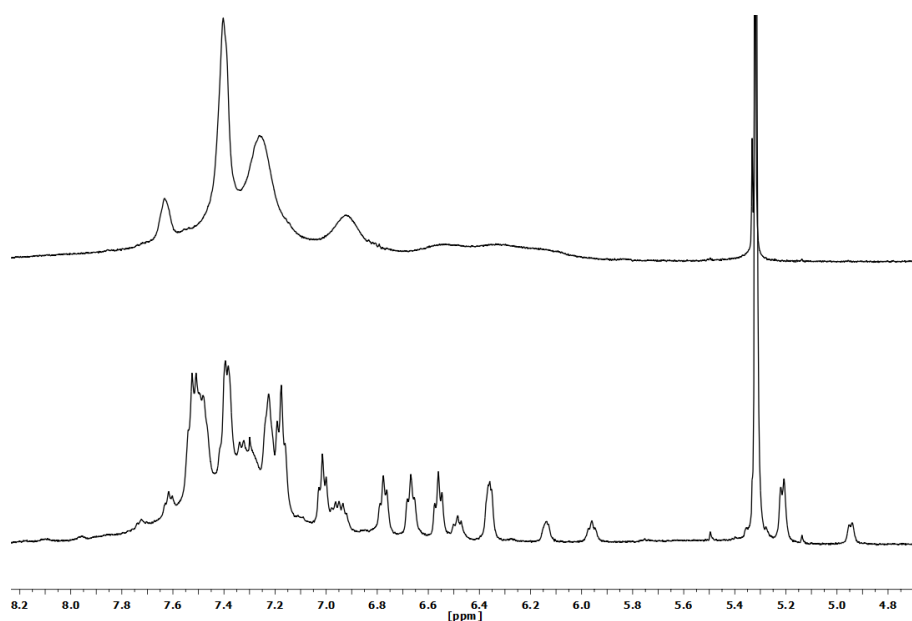


Figure 1.15. ^1H NMR spectra (CD_2Cl_2 , 173K) of complexes $[\{\text{Pt}(\text{CNC})(\text{PPh}_3)\}_2\text{Ag}](\text{ClO}_4)$ (**8**) (top) and $[\{\text{Pd}(\text{CNC})(\text{PPh}_3)\}_2\text{Ag}](\text{ClO}_4)$ (**9**) (bottom).

A VT NMR row of experiments for $[\{\text{Pd}(\text{CNC})(\text{PPh}_3)\}_2\text{Ag}](\text{ClO}_4)$ (**9**) (see Figure 1.16 for a selection of temperatures) reveals that between 233K and 193K the coalescence of some signals occurs.

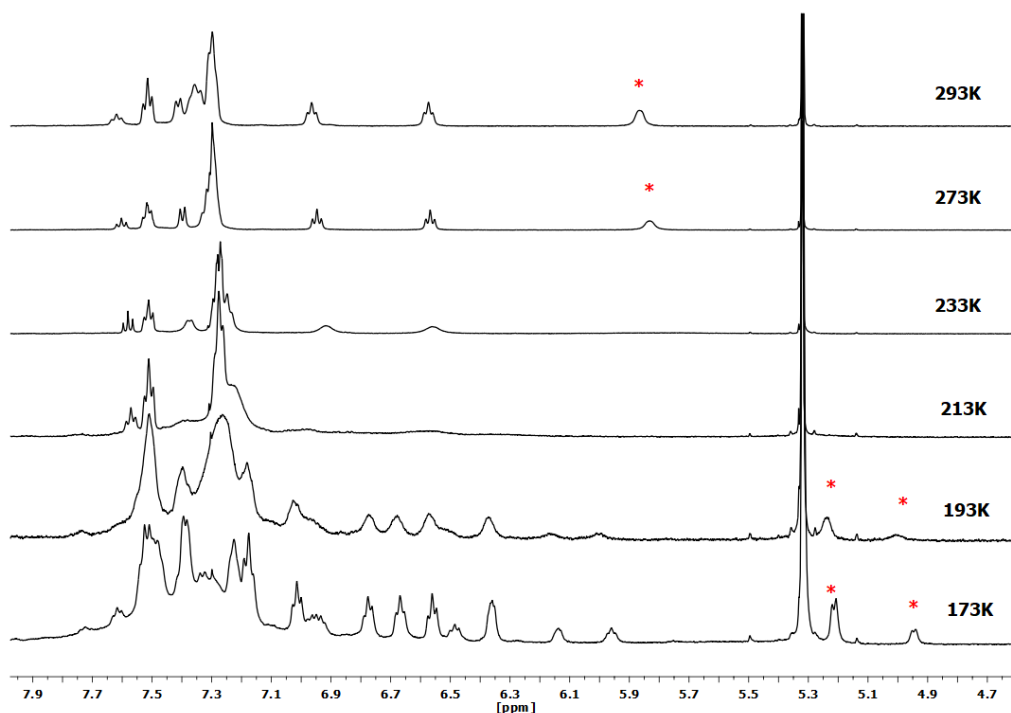


Figure 1.16. VT ^1H NMR spectra (CD_2Cl_2) of complex $[\{\text{Pd}(\text{CNC})(\text{PPh}_3)\}_2\text{Ag}](\text{ClO}_4)$ (**9**) (red asterisks, H2 signals).

Those observations seem to point out that for both trinuclear complexes $[\{\text{Pt}(\text{CNC})(\text{PPh}_3)\}_2\text{Ag}](\text{ClO}_4)$ (**8**) and $[\{\text{Pd}(\text{CNC})(\text{PPh}_3)\}_2\text{Ag}](\text{ClO}_4)$ (**9**), an analogous “metronome-like” dynamic process, as the one explained for the gold clusters, might be operating in solution. It is noteworthy, that in the case of **8** no inequivalency of the CNC ligand is detected even at 173K, which means that this process is still functioning in solution at a considerable speed for the NMR timescale.

On the other hand, a slowdown of this process is detected at that temperature for palladium complex **9**. The different behaviour of **9** at 173K is also reflected in the apparition of additional signals which could be attributed to two different unsymmetrical CNC ligands, with different integration and values of displacement. A possible explanation of this observation could be the presence of two conformers which differentiates in the relative disposition of the two “Pd(CNC)(PPh₃)” fragments. The transformation barrier between the geometry of these two conformers have been investigated by means of theoretical calculations (see Section 1.3) and its interconversion

found to be energetically very favorable at higher temperatures but might be stopped at this lower temperature (173K) allowing the two different conformers to be detectable by NMR.

This difference in the behavior of complexes $[\{\text{Pt}(\text{CNC})(\text{PPh}_3)_2\text{Ag}\}(\text{ClO}_4)]$ (**8**) and $[\{\text{Pd}(\text{CNC})(\text{PPh}_3)_2\text{Ag}\}(\text{ClO}_4)]$ (**9**) in solution suggests that for the dynamic process, the barrier of energy might be higher for the palladium-silver cluster **9**, as the slowdown of the “metronome-like” movement of the platinum-silver complex **10** is not possible even at 173K.

$^{31}\text{P}\{^1\text{H}\}$ NMR spectra of $[\{\text{Pt}(\text{CNC})(\text{PPh}_3)_2\text{Ag}\}(\text{ClO}_4)]$ (**8**) and $[\{\text{Pd}(\text{CNC})(\text{PPh}_3)_2\text{Ag}\}(\text{ClO}_4)]$ (**9**) at RT are not very informative, showing both only a singlet, with platinum satellites in the case of **8**. More interestingly at 193K the $^{31}\text{P}\{^1\text{H}\}$ NMR spectrum of **9** (see Figure 1.17) reveals two singlets at 43.4 and 44.5 ppm of different intensities, which agrees with the existence of two conformers of **9** detected in the ^1H NMR spectrum at low temperature.

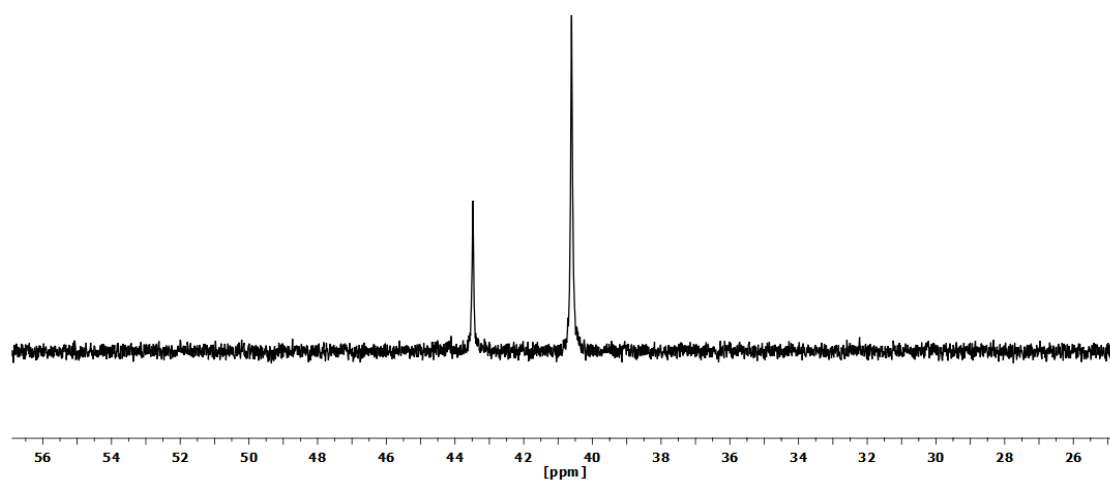


Figure 1.17. $^{31}\text{P}\{^1\text{H}\}$ NMR spectrum (CD_2Cl_2 , 193K) of complex $[\{\text{Pd}(\text{CNC})(\text{PPh}_3)_2\text{Ag}\}(\text{ClO}_4)]$ (**9**).

For the platinum complex **8**, additional $^{195}\text{Pt}\{^1\text{H}\}$ NMR experiments could be carried out (see Figure 1.18). At 193K only one signal centered at 4144 ppm appears, indicating the equivalence of the two Pt atoms. This signal is a doublet of doublets because of the coupling of Pt with P ($^1J_{\text{Pt-P}} = 3670$ Hz) and Ag ($^1J_{\text{Pt-Ag}} = 530$ Hz). This Pt-Ag coupling implies that the Pt-Ag interaction persists in solution at this temperature. It is also remarkable that the signal shifts downfield according to the starting material;

around 200 ppm. This finding could be related with the electron-withdrawing capacity of the acidic silver center.^{17,30,34,44}

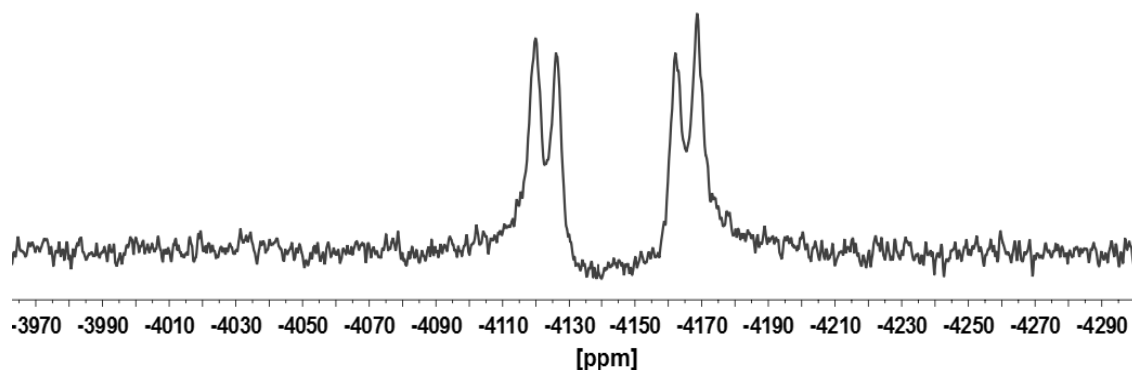


Figure 1.18. $^{195}\text{Pt}\{^1\text{H}\}$ NMR spectrum (CD_2Cl_2 , 193K) of complex $[\{\text{Pt}(\text{CNC})(\text{PPh}_3)\}_2\text{Ag}](\text{ClO}_4)$ (**8**).

1.2.2. Characterization of mixtures **10*** and **11***

Attempts to obtain crystals suitable for X-Ray diffraction studies of $[(\text{CNC})(\text{PPh}_3)\text{PtAg}(\text{PPh}_3)](\text{ClO}_4)$ (**10**) and $[(\text{CNC})(\text{PPh}_3)\text{PdAg}(\text{PPh}_3)](\text{ClO}_4)$ (**11**) were unsuccessful and led to the formation of mixtures of crystals. For the platinum-silver mixture **10***, some well-formed orange crystals were obtained this way and identified as the trinuclear $[\{\text{Pt}(\text{CNC})(\text{PPh}_3)\}_2\text{Ag}](\text{ClO}_4)$ (**8**). In addition to this, there was a second batch formed by poor quality, yellow crystals which were not suitable for X-Ray diffraction studies but behaved in solution as **10*** and a finally a third group of colorless specimens which corresponded to the silver species $[\text{Ag}(\text{PPh}_3)_2](\text{ClO}_4)$ (see Supporting Information). In the case of the palladium-silver mixture **11***, only crystals corresponding to the trinuclear $[\{\text{Pd}(\text{CNC})(\text{PPh}_3)\}_2\text{Ag}](\text{ClO}_4)$ (**9**) could be identified. As it was impossible to prepare single crystals of both complexes with formula “ $[(\text{CNC})(\text{PPh}_3)\text{M}\text{Ag}(\text{PPh}_3)](\text{ClO}_4)$ ”, DFT calculations were performed to model their structures (see Section 1.3).

Characterization of platinum-silver **10*** and palladium-silver **11*** mixtures was challenging due to their rich behaviour in solution. In this way, VT NMR studies in CD_2Cl_2 on these mixtures allowed to identify all species involved.

At room temperature ^1H NMR spectrum of platinum mixture **10*** reflects broad signals which do not give much information. However, by lowering the temperature to

253K, a well-defined ^1H NMR spectrum is obtained (see Figure 1.19). It shows three sets of signals corresponding to $[(\text{CNC})(\text{PPh}_3)\text{PtAg}(\text{PPh}_3)](\text{ClO}_4)$ (**10**), the previously studied $[\{\text{Pt}(\text{CNC})(\text{PPh}_3)\}_2\text{Ag}](\text{ClO}_4)$ (**8**) and $[\text{Ag}(\text{PPh}_3)_2](\text{ClO}_4)$ (**AgP2**).

In the 313-253K temperature range, a dynamic process with a coalescence temperature of 293K is observed (see Figure 1.19). There is, therefore, coalescence of signals corresponding to **10**, **8** and **AgP2** highlighted by three sets of signals in the 5.6-6.6 ppm range at 253K, which at 313K become one broad signal at 5.9 ppm. Below 253K resonances due to $[(\text{CNC})(\text{PPh}_3)\text{PtAg}(\text{PPh}_3)](\text{ClO}_4)$ (**10**) and $[\{\text{Pt}(\text{CNC})(\text{PPh}_3)\}_2\text{Ag}](\text{ClO}_4)$ (**8**) can be individually observed.

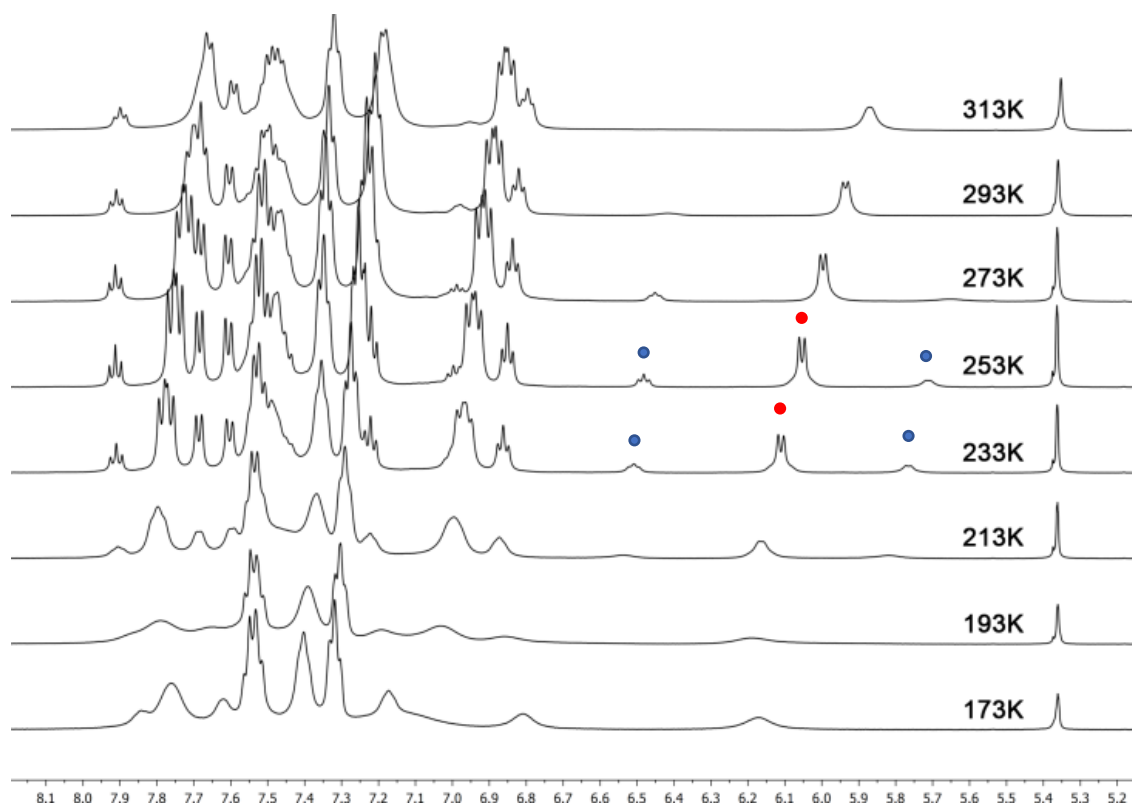


Figure 1.19. VT ^1H NMR spectra (CD_2Cl_2) of mixture **10*** (at 253 and 233K: red dot, H2 signal of **10**; blue dots, signals of **8**).

$^{31}\text{P}\{^1\text{H}\}$ NMR experiments performed on mixture **10*** are more informative and reveal the rich behaviour of this preparation in solution. Thus, the spectrum at room temperature displays a singlet at 24.1 ppm with platinum satellites ($^1J_{\text{P-Pt}} = 3662$ Hz) corresponding to a PPh_3 ligand bonded to a platinum center, and a doublet of broad peaks at 15.1 ppm assigned to the phosphane coordinated to the silver ($^1J_{\text{P-Ag}} = 672$ Hz). These

signals become sharper by lowering the temperature, appearing the signal due to the “Ag(PPh₃)” fragment better resolved at 163K (see Figure 1.20). Then, two doublets (coupling due to the two active isotopes of Ag; ¹⁰⁷Ag, 51.8% abundance and ¹⁰⁹Ag, 48.2% abundance) centered at 15.5 ppm can be observed with ¹J_{P-Ag} coupling constants of 730 and 623 Hz. It is noteworthy to indicate that platinum satellites appear on these two signals (²J_{P(Ag)-Pt} = 122 Hz). Finally this spectrum depicts a low-intensity doublet of doublets, not detected at room temperature, with a typical pattern for an “Ag-PPh₃” system, which is assigned to [Ag(PPh₃)₂](ClO₄) (**AgP2**) complex. A singlet corresponding to trinuclear [{Pt(CNC)(PPh₃)₂Ag](ClO₄) (**8**) is difficult to distinguish, as its chemical shift is similar to that of [(CNC)(PPh₃)PtAg(PPh₃)](ClO₄) (**10**), but at some temperatures a small shoulder on the “Pt-PPh₃” signal of **8** can be seen.

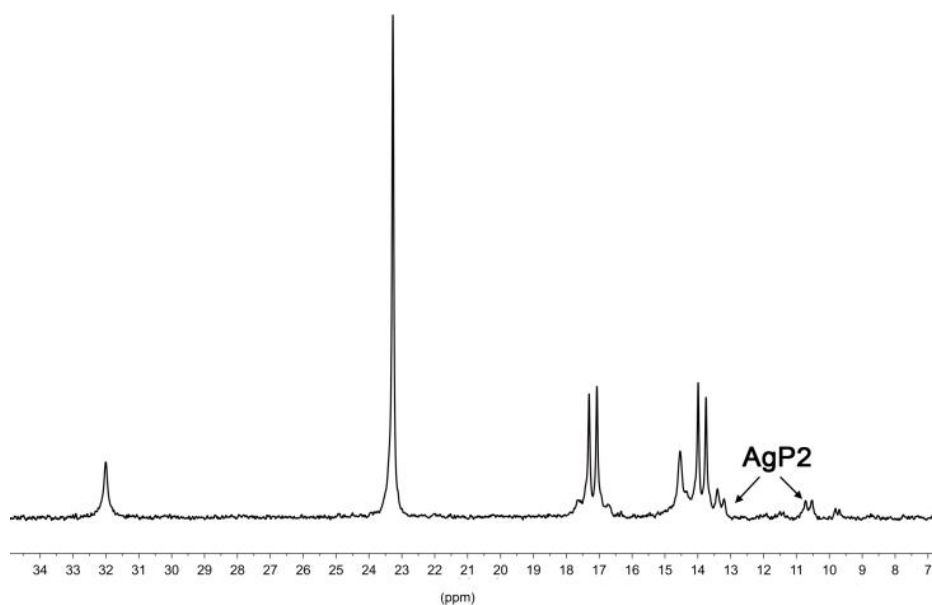


Figure 1.20. ³¹P{¹H} NMR spectrum (CD₂Cl₂, 163K) of mixture **10***.

¹⁹⁵Pt{¹H} NMR studies of solutions of **10*** also give very valuable data. At 193K a resolved signal centered at -4171 ppm appears (see Figure 1.21), being attributed to the dinuclear platinum-silver complex. Coupling of the platinum center with the silver and both P atoms of the phosphane ligands (¹J_{Pt-P} = 3561 Hz, ¹J_{Pt-Ag} = 438 Hz, ²J_{Pt-P(Ag)} = 115 Hz) causes a complex pattern that can be seen in Figure 1.21.

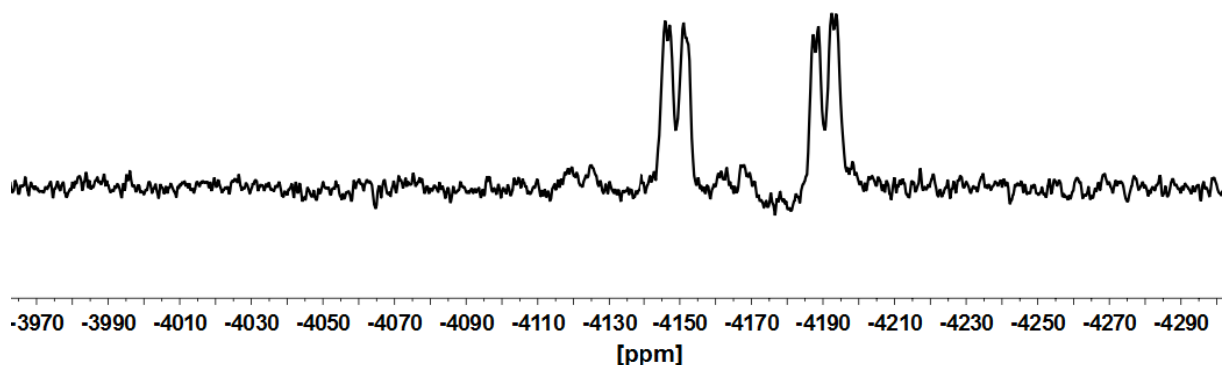


Figure 1.21. $^{195}\text{Pt}\{^1\text{H}\}$ NMR spectrum (CD_2Cl_2 , 193K) of mixture **10***.

Along with this signal, a doublet of doublets with a much lower intensity is observed and assigned to trinuclear silver complex $[\{\text{Pt}(\text{CNC})(\text{PPh}_3)\}_2\text{Ag}](\text{ClO}_4)$ (**8**), described in the previous section. At 293K the signal of the dinuclear $[(\text{CNC})(\text{PPh}_3)\text{PtAg}(\text{PPh}_3)](\text{ClO}_4)$ (**10**) complex appears as a broad doublet and the intensity of the signal of **8** increases (see Figure 1.22).

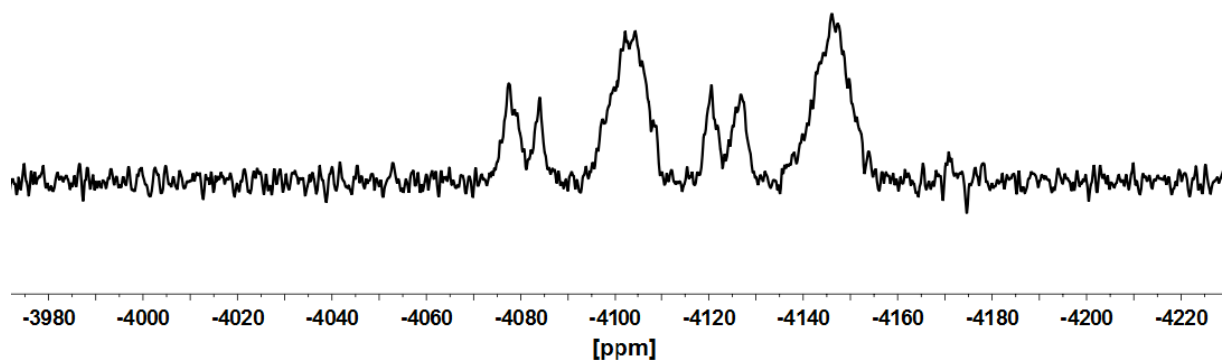


Figure 1.22. $^{195}\text{Pt}\{^1\text{H}\}$ NMR spectrum (CD_2Cl_2 , 293K) of mixture **10***.

All these $^{31}\text{P}\{^1\text{H}\}$ and $^{195}\text{Pt}\{^1\text{H}\}$ NMR observations for the mixture **10*** point out that at room temperature a dynamic process is taking place, in which the three species $[(\text{CNC})(\text{PPh}_3)\text{PtAg}(\text{PPh}_3)](\text{ClO}_4)$ (**10**), $[\{\text{Pt}(\text{CNC})(\text{PPh}_3)\}_2\text{Ag}](\text{ClO}_4)$ (**8**) and **AgP2** are involved. Moreover, when low temperature experiments are performed on this mixture, Pt-Ag couplings are detected, indicating that Pt-Ag interactions still exist for **10** in solution. Therefore, rearrangement equilibria between $[(\text{CNC})(\text{PPh}_3)\text{PtAg}(\text{PPh}_3)](\text{ClO}_4)$ (**10**), $[\{\text{Pt}(\text{CNC})(\text{PPh}_3)\}_2\text{Ag}](\text{ClO}_4)$ (**8**) and $[\text{Ag}(\text{PPh}_3)_2](\text{ClO}_4)$ (**AgP2**), in which Pt-Ag and Ag-P bonds would be breaking, could be operating in solution.

^1H NMR spectrum of palladium mixture **11*** reflects also similar broad signals at room temperature. By lowering the temperature, the recording of a better resolved spectrum is not possible, but instead new signals appear, showing for example the

coalescence of a H2 signal around 5.8 ppm (red asterisk in Figure 1.23) at 213K, which splits at 173K into two new H2 signals at 5.9 and 5.2 ppm. One additional signal around 4.9 ppm is attributed to the trinuclear complex $[\{\text{Pd}(\text{CNC})(\text{PPh}_3)\}_2\text{Ag}](\text{ClO}_4)$ (**9**) present in solution.

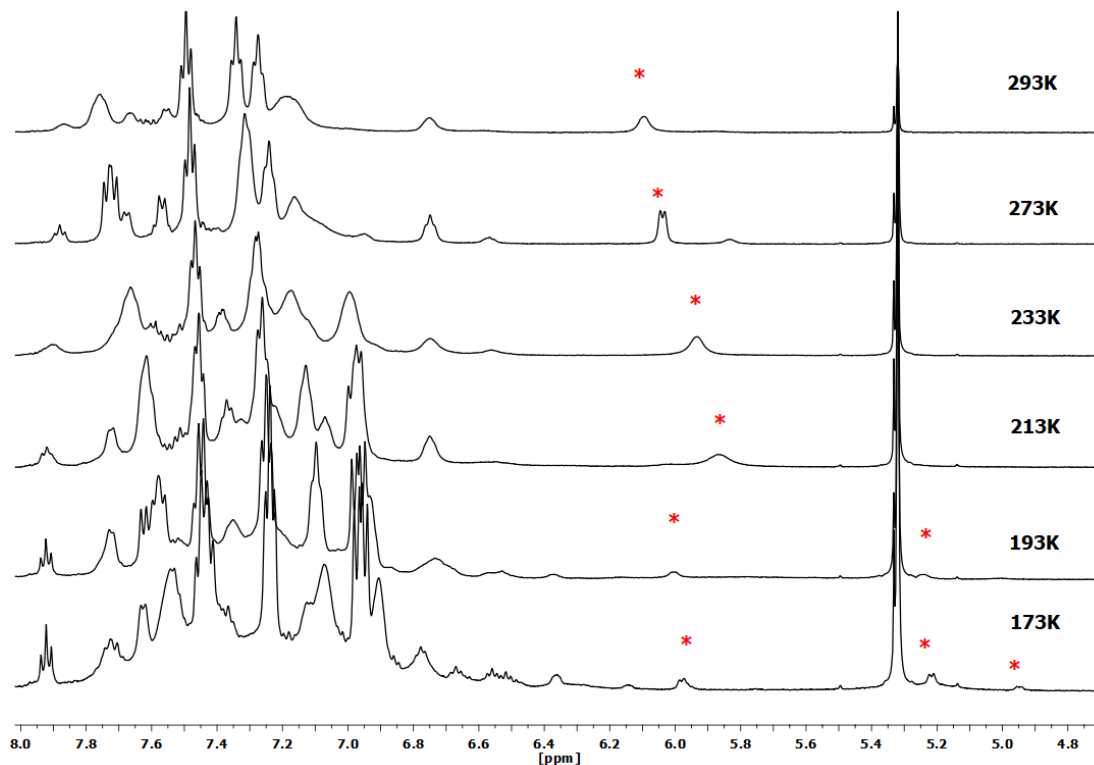


Figure 1.23. VT ^1H NMR spectra (CD_2Cl_2) of mixture **11*** (red asterisks, H2 signals).

VT $^{31}\text{P}\{^1\text{H}\}$ NMR experiments of **11*** give very valuable information (see Figure 1.24). $^{31}\text{P}\{^1\text{H}\}$ NMR spectrum of palladium-silver mixture **11*** at 293K, shows a sharp singlet at around 44 ppm. By lowering the temperature to 173K all the species involved in solution can be identified. A singlet is detected at 44.5 ppm corresponding to the starting palladium substrate $[\text{Pd}(\text{CNC})(\text{PPh}_3)]$ (**2**), a singlet over 43.5 ppm which can be assigned to the phosphorus atom coordinated to the palladium center on the dinuclear complex $[(\text{CNC})(\text{PPh}_3)\text{PdAg}(\text{PPh}_3)](\text{ClO}_4)$ (**11**), a sharp singlet at 40.6 ppm assigned to the previously characterized trinuclear complex $[\{\text{Pd}(\text{CNC})(\text{PPh}_3)\}_2\text{Ag}](\text{ClO}_4)$ (**9**), a doublet of doublets centered at 18.7 ppm which corresponds to the “Ag(PPh₃)” fragment of **11** ($^1J_{\text{P-Ag}} = 678$ Hz and $^1J_{\text{P-Ag}} = 585$ Hz) and two sets of signals with a typical pattern for P coupled with Ag centered at 10.7 and 6.0 ppm ($^1J_{\text{P-Ag}} = 346$ Hz and $^1J_{\text{P-Ag}} = 327$ Hz respectively) possibly due to mononuclear silver species with Ag-PPh₃ bonds.³⁶

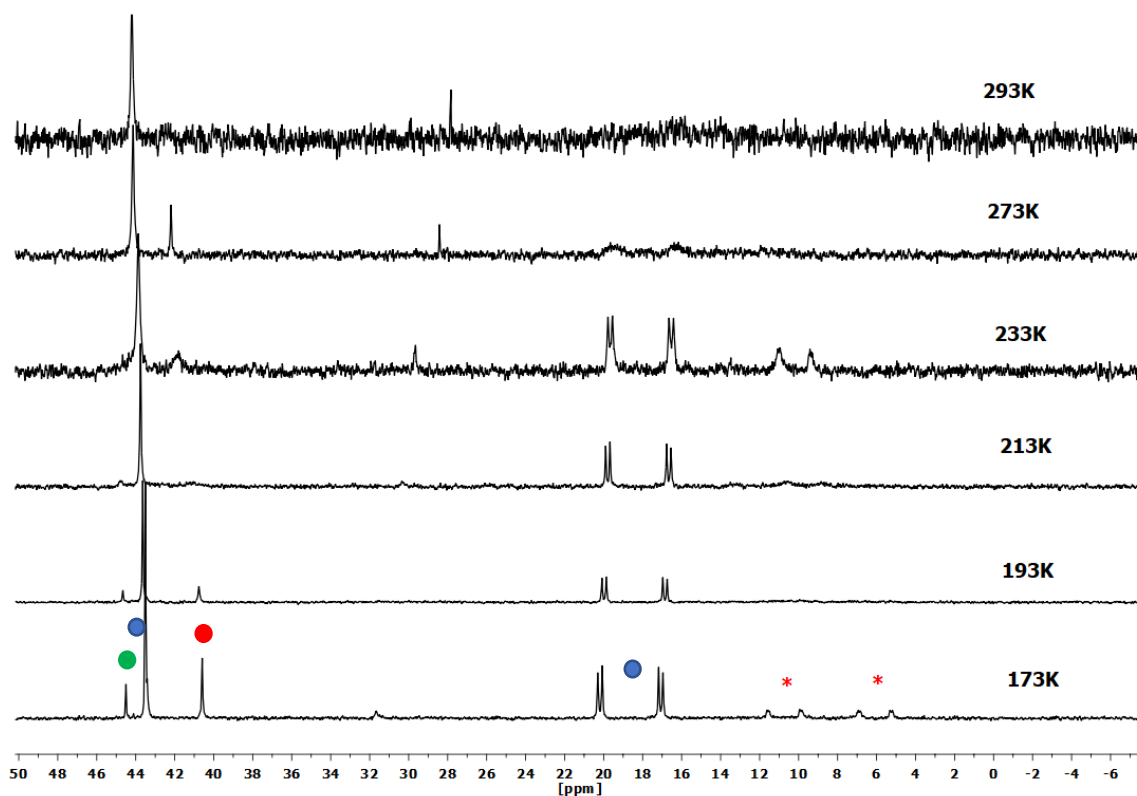
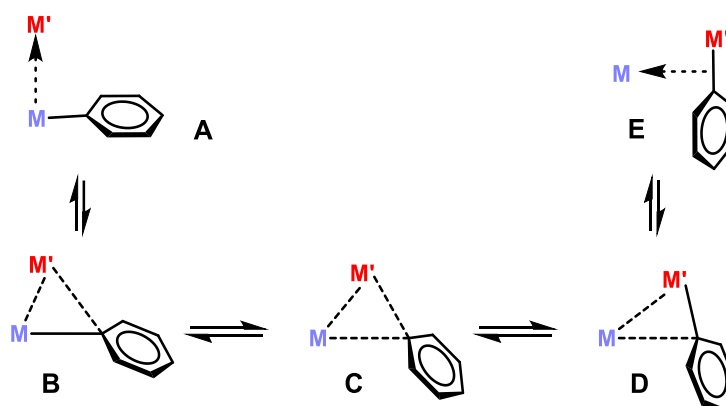


Figure 1.24. VT $^{31}\text{P}\{^1\text{H}\}$ NMR spectra (CD_2Cl_2) of mixture **11*** (173K: green dot, signal of **2**; blue dots, signals of **11**; red dot, signal of **9**; red asterisks, signals of “Ag-PPh₃” species).

Therefore, the behaviour of palladium-silver mixture **11*** in solution is even richer than that of platinum-silver **10***, with signals corresponding to the starting substrate $[\text{Pd}(\text{CNC})(\text{PPh}_3)]$ (**2**) being also identified. This suggests that complex **11** could revert to the starting material by releasing the “[Ag(PPh₃)⁺” moiety. Therefore, two additional signals with Ag-P coupling pattern are observed and tentatively assigned to “Ag(PPh₃)” species.

1.3. DFT calculations and structural analysis: degree of transmetallation on the M-M' complexes

All the heteropolymetallic complexes described in this chapter formed by group 10 and 11 metals can be regarded as frozen snapshots of a transmetallation process, in which the acidic metallic center establishes an interaction with the C_{ipso} (CNC). Due to the pincer nature of the CNC ligand this process cannot occur completely, giving rise to complexes that can be studied as models for arrested intermediates of transmetallation reactions. Intermetallic interactions and differences on the degree of the transmetallation (see Scheme 1.8) on these complexes were studied widely through DFT calculations (see Computational details, Supporting Information).



Scheme 1.8. Transmetallation process in a M-M' heterobimetallic system, showing five different degrees of transfer (A to E).

Thus, the optimized structures of complexes [(CNC)(PPh₃)MAu(PPh₃)](ClO₄) (M = Pt (**4-DFT**), Pd (**5-DFT**)), [{M(CNC)(PPh₃)₂Au}](ClO₄) (M = Pt (**6-DFT**), Pd (**7-DFT**)) and [{M(CNC)(PPh₃)₂Ag}](ClO₄) (M = Pt (**8-DFT**), Pd (**9-DFT**)) are in good agreement with the experimental X-Ray ones (see Tables S1.3 and S1.4, Supporting Information). Structures of dinuclear silver complexes [(CNC)(PPh₃)PtAg(PPh₃)]ClO₄ (**10-DFT**) and [(CNC)(PPh₃)PdAg(PPh₃)]ClO₄ (**11-DFT**) were also modelled but the absence of X-Ray structures for them does not allow this comparison (see Figure 1.25 for a view of these structures and Table 1.4 for a selection of distances).

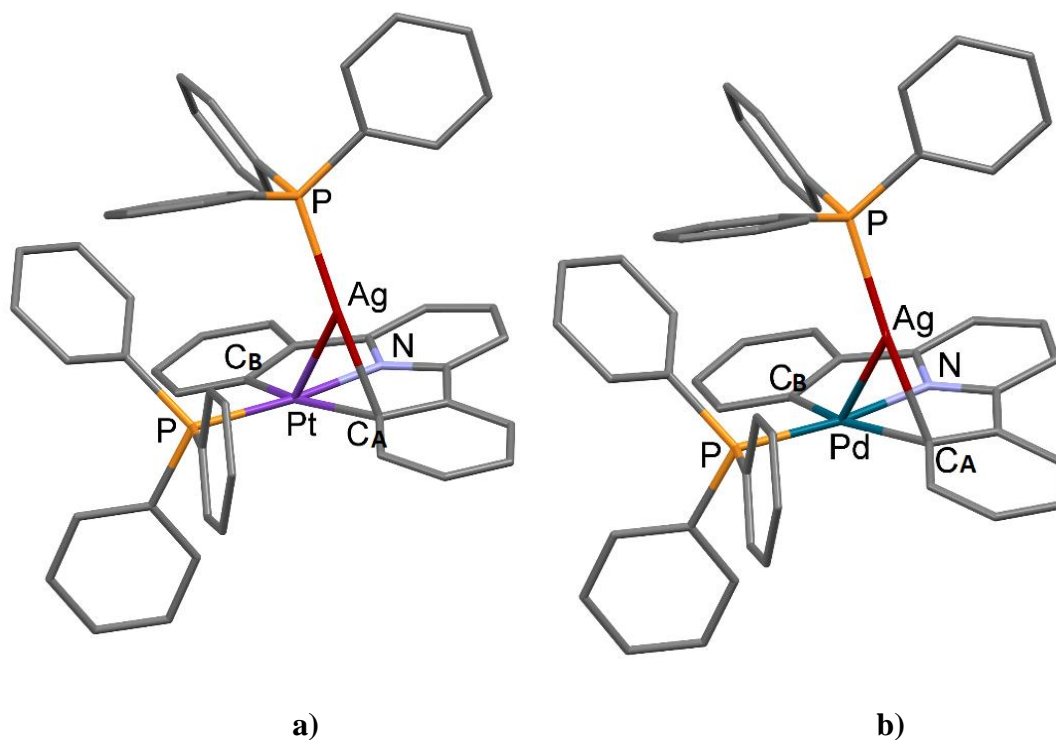


Figure 1.25. DFT optimized structures of **10-DFT** (a) and **11-DFT** (b).

Table 1.4. Selected bond lengths (Å) and angles (°) for **10-DFT** and **11-DFT**.

	10 (M = Pt)	11 (M = Pd)
M-Ag	2.798	2.753
M-C _A	2.075	2.067
M-C _B	2.177	2.206
Ag-C _A	2.246	2.216
M-Ag-P(Ag)	125.41	126.33
C _A -Ag-P(Ag)	171.32	172.94

Thus, comparison of the palladium complexes with the analogous platinum ones is of interest, observing more prominent deformations of the M-CNC moiety when the basic metallic center is palladium in almost all the cases; this deformation is very similar for the trinuclear M-Ag complexes **8-DFT** and **9-DFT**. The overlays of the DFT optimized structures of palladium complexes **5**, **7**, **9** and **11** with their corresponding

platinum counterparts allow to identify these deformations on the planarity of the CNC ligand (see Figures 1.26 and 1.27).

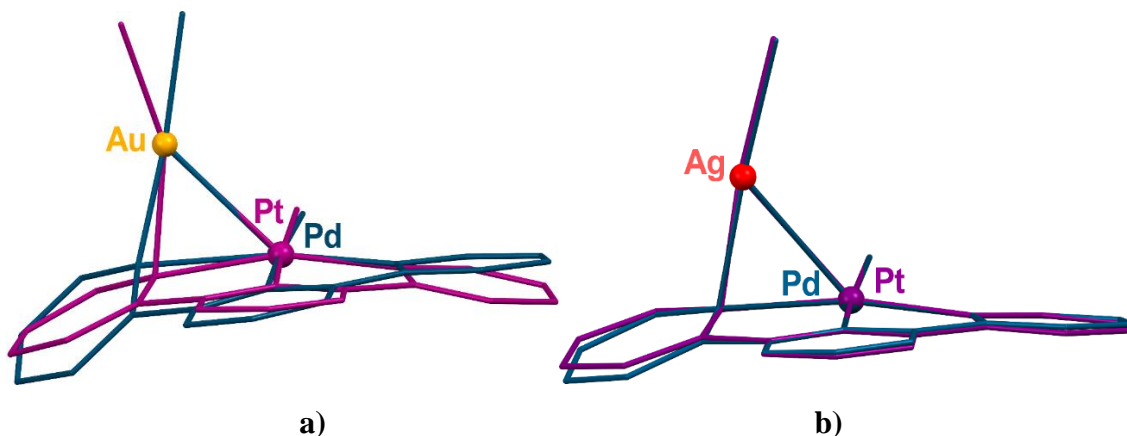


Figure 1.26. Overlay of the structures **5-DFT** (Pd-Au) and its Pt homologue **4-DFT** (Pt-Au) (a) and **11-DFT** (Pd-Ag) and its Pt homologue **10-DFT** (Pt-Ag) (b).

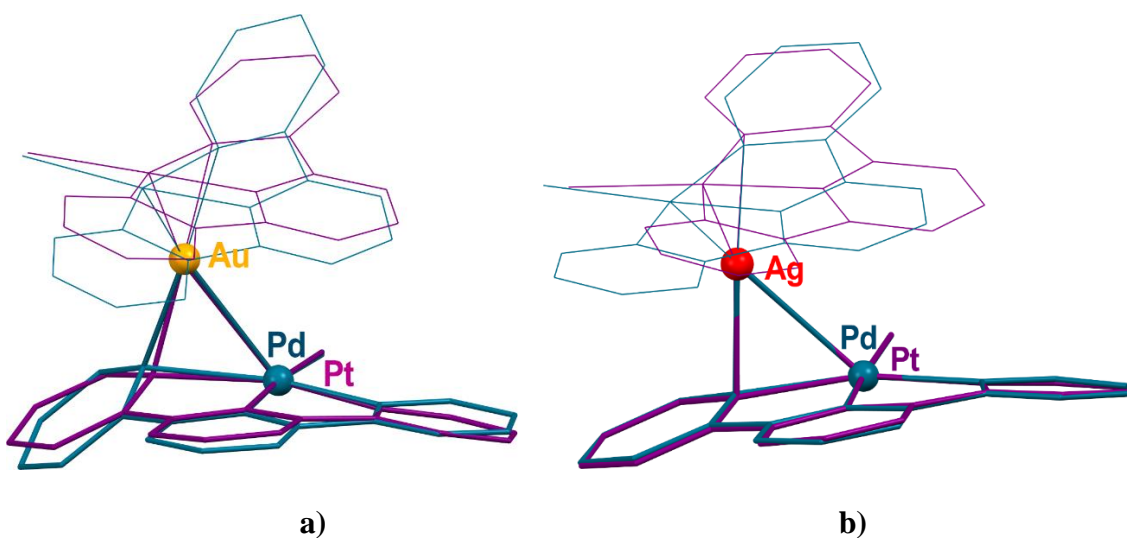


Figure 1.27. Overlay of the structures **7-DFT** (Pd-Au-Pd) and its Pt homologue **6-DFT** (Pt-Au-Pt) (a) and **9-DFT** (Pd-Ag-Pd) and its Pt homologue **8-DFT** (Pt-Ag-Pt).

On the other hand, the overlay of the optimized structures of each Pt-M' and Pd-M' pair shows that the systems with gold experience more marked deformations than the silver analogs (see Figures 1.28 and 1.29).

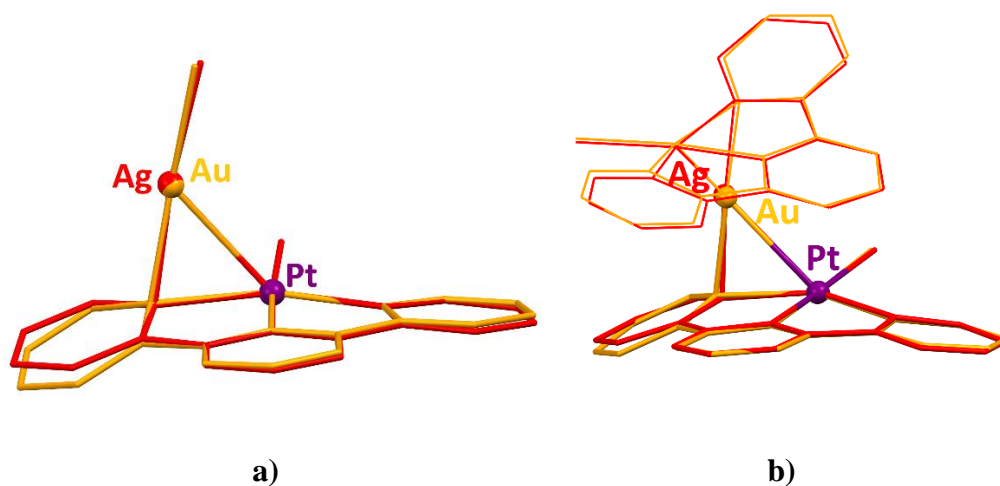


Figure 1.28. Overlay of the structures **4-DFT** (Pt-Au) and **10-DFT** (Pt-Ag) (a) and structures **6-DFT** (Pt-Au-Pt) and **8-DFT** (Pt-Ag-Pt).

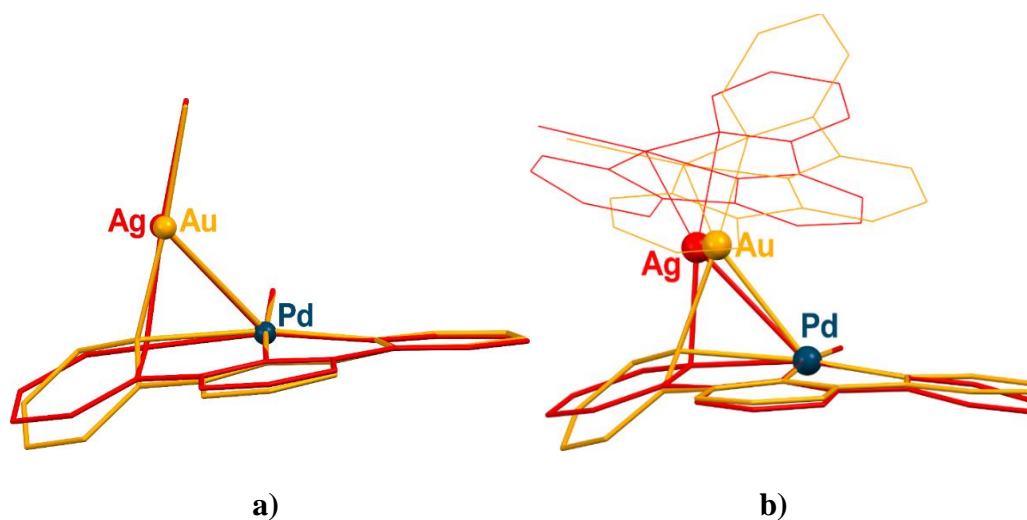
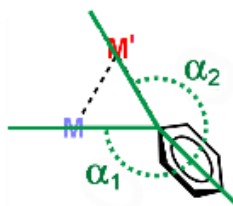


Figure 1.29. Overlay of the structures **5-DFT** (Pd-Au) and **11-DFT** (Pd-Ag) (a) and structures **7-DFT** (Pd-Au-Pd) and **9-DFT** (Pd-Ag-Pd) (b).

With all this structural information, additional geometrical analysis focusing on the $M \cdots R \cdots M'$ unit affords deeper insight. The intermetallic transfer process can be analyzed by establishing and comparing several geometrical descriptors (see Table S1.5, Supporting Information). Two of these informative parameters are the $M-C_{\text{ipso}}-C_{\text{para}}$ (α_1) and $M'-C_{\text{ipso}}-C_{\text{para}}$ (α_2) angles (see Scheme 1.9 and Table 1.5). The value of these angles gives an idea of the distortion of the interacting phenylene plane with respect to the rest of the CNC ligand and the square plane environment of the basic metal.



Scheme 1.9. Graphical depiction of α_1 and α_2 descriptors.

Table 1.5. M-C_{ipso}-C_{para} (α_1) and M'-C_{ipso}-C_{para} (α_2) angles (°) of the compounds of this chapter. Data collected from X-Ray diffraction (cursive) and DFT calculations.

Angle	M'	Pt systems		Pd systems	
		PtM'	Pt ₂ M'	PdM'	Pd ₂ M'
M-C _{ipso} -C _{para} (α_1)	Au	<i>160.5(2)</i>	<i>152.9(2)</i>	<i>140.7(2)</i>	<i>133.2(4)</i>
		152.8	156.6	138.3	134.7
	Ag	-	<i>162.1(2)</i>	-	<i>161.6(2)</i>
		163.0	164.0	157.7	160.9
M'-C _{ipso} -C _{para} (α_2)	Au	<i>120.1(2)</i>	<i>128.2(2)</i>	<i>143.1(2)</i>	<i>152.7(4)</i>
		128.5	123.3	147.0	152.4
	Ag	-	<i>108.5(2)</i>	-	<i>111.5(2)</i>
		115.7	111.9	123.2	118.6

It is remarkable to indicate that the M-C_{ipso}-C_{para} angles of the starting materials [Pt(CNC)(PPh₃)] (**1**) and [Pd(CNC)(PPh₃)] (**2**), in which no R transfer has started yet, are not of 180° (they are 168.1(2) and 167.4(1)° respectively), which is caused by the pincer nature of the CNC cyclometallated ligand. On the other hand, a situation in which the transfer to a M' center is completed would give M'-C_{ipso}-C_{para} angles of 180°. These two values define the boundaries of the R transfer process.

In the complexes of this chapter, gold systems give rise to the highest degree of transfer (yellow marks, Figure 1.30) compared the silver ones (red marks, Figure 1.30). Thus, M-C_{ipso}-C_{para} angles in the PdAu and Pd₂Au clusters are 138.3 and 134.7° respectively (152.8 and 156.6° in their PtAu and Pt₂Au counterparts). In addition to this,

palladium complexes (dot marks, Figure 1.30) display higher degrees of transfer than the platinum analogs (square marks, Figure 1.30), giving values of $M-C_{\text{ipso}}-C_{\text{para}}$ angles of 157.7 and 160.9° respectively (163.0 and 164.0° in the Pt analogs).

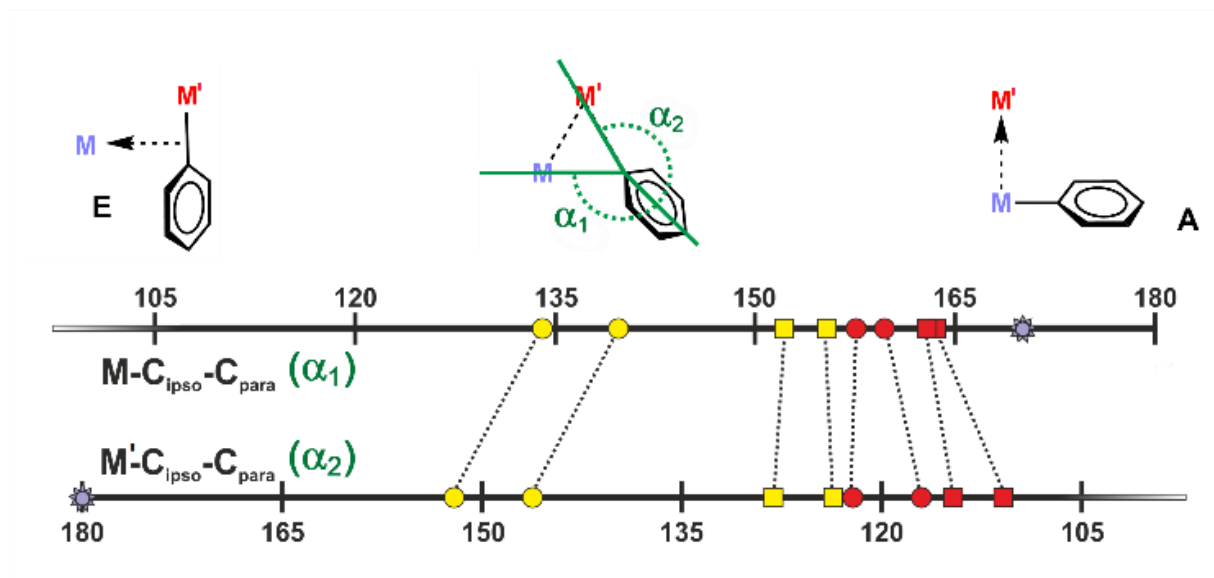
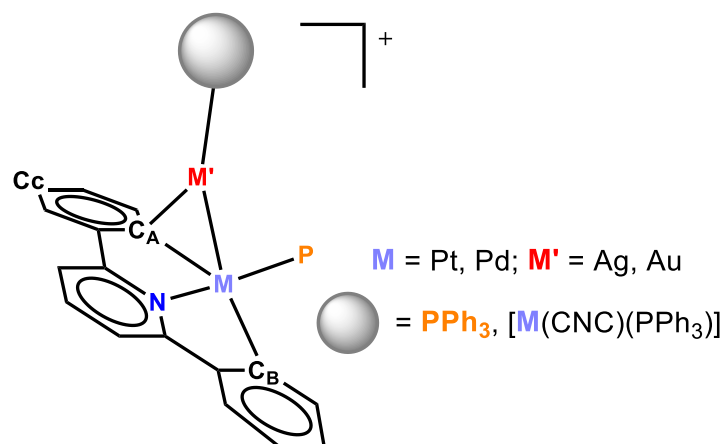


Figure 1.30. Different degrees of transfer achieved in the $M-M'-P$ and $M-M'-M$ systems of this chapter (square = Pt; dot = Pd; red = Ag, yellow = Au; Stars: reference compounds for both boundaries of the transmetalation process). Descriptors used: $M-C_{\text{ipso}}-C_{\text{para}}$ and $M'-C_{\text{ipso}}-C_{\text{para}}$ angles ($^\circ$) obtained from DFT calculations.

Besides, another pair of very informative descriptors can also be represented to study the progression of the frustrated transmetalation process, which are distances $M-C_A$ and $M'-C_A$ (see Scheme 1.10).



Scheme 1.10. Graphical depiction for the established descriptors of complexes of this chapter.

Graphical depiction of that pair of descriptors generates one plot (see Figure 1.31) which pointing in the same direction of the observations on the previously discussed descriptors α_1 and α_2 , indicate higher transmetalation degrees for the palladium gold complexes.

Thus, larger M-C_A distances are always paired with shorter M'-C_A distances, and *vice versa*. The shorter M'-C_A (and thus the longer M-C_A) the higher degree of transfer, as is observed for the Pd-Au complexes.

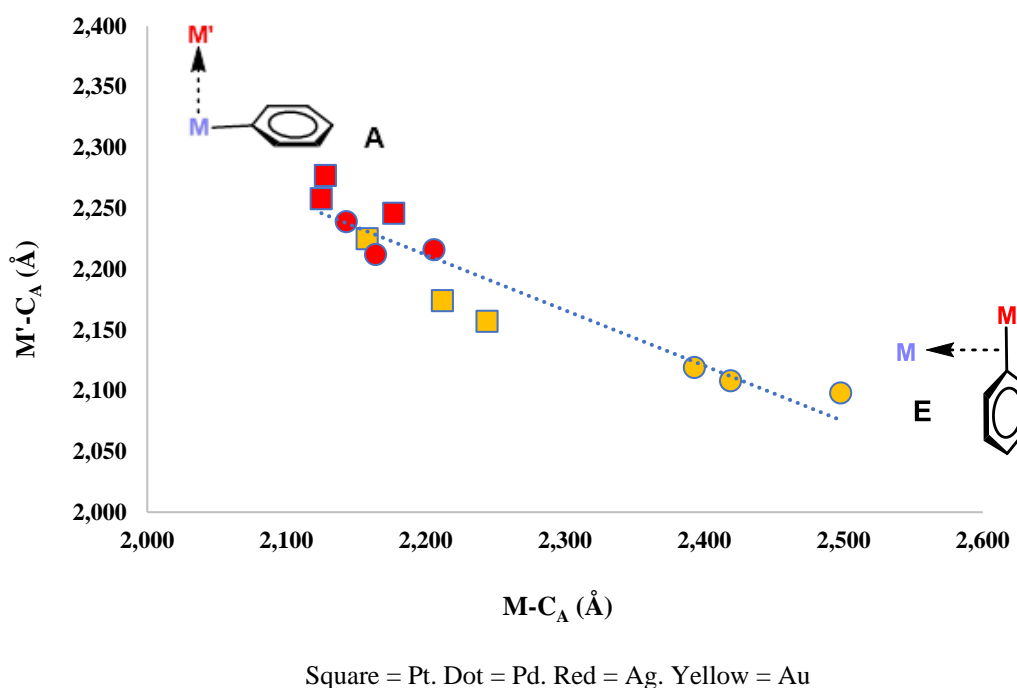
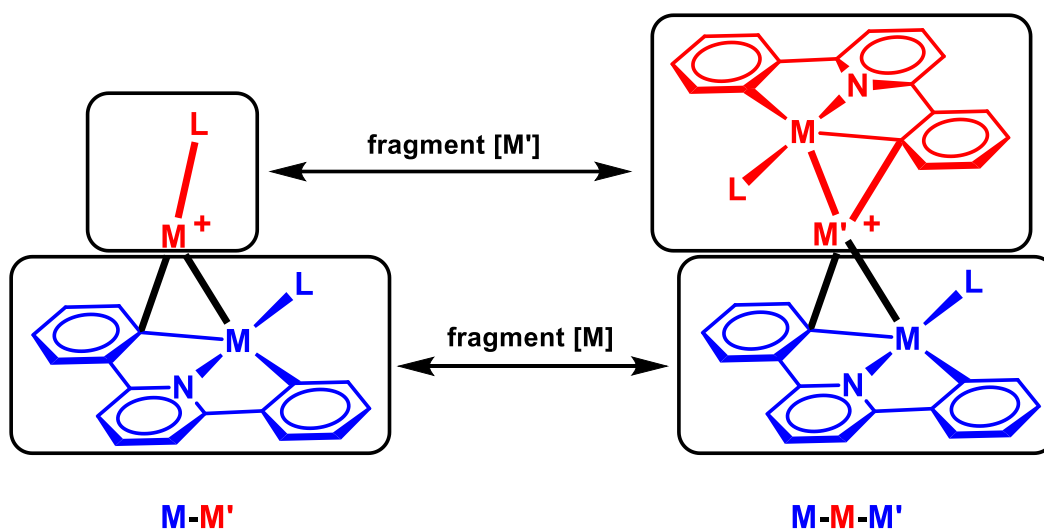


Figure 1.31. Plot of the M-C_A distances *vs.* M'-C_A distances showing a linear correlation of both.

Further understanding of this process can be gained by means of DFT calculations. Energy Decomposition Analysis (EDA) allows to compute the interaction energy (E_{int}) of the M donor and M' acceptor fragments (see Scheme 1.11), corresponding to the [M-(M'-PPh₃)]⁺ and [M-(M'-M)]⁺ adducts (M = Pd, Pt; M' = Ag, Au; see Table 1.6). Trends observed for these data agree with the structural observations described before. Firstly, the M-Au interactions are found to be stronger than the M-Ag, which can be related with the observed lability of the silver systems through NMR studies; secondly, the Pd-M' interactions are more important than the Pt-M' ones (with one exception; the M₂Ag trinuclear complexes). Finally, stronger interactions take place in the trinuclear than in

the dinuclear adducts, possibly due to the better donor ability of the triphenylphosphane ligand of the acidic metal, compared to that of the “[M(CNC)(PPh₃)]⁺” moiety.



Scheme 1.11. Definition of the fragments of heteropolynuclear complexes of this chapter for EDA studies.

Table 1.6. Total interaction energies (ΔE_{int}), electrostatic (ΔE_{ele}), exchange-repulsion (ΔE_{exrep}), polarization (ΔE_{pol}), correlation (ΔE_{corr}) and dispersion (ΔE_{disp}) energies (DFT/BP86-D3 level, gas phase) in kcal/mol of the heteropolynuclear complexes of this chapter ($\Delta E_{\text{int}} = \Delta E_{\text{ele}} + \Delta E_{\text{exrep}} + \Delta E_{\text{pol}} + \Delta E_{\text{corr}} + \Delta E_{\text{disp}}$).

M = Pt	4-DFT Pt-Au	10-DFT Pt-Ag	8-DFT Pt-Ag-Pt	6-DFT Pt-Au-Pt
ΔE_{int}	-92.6	-80.6	-88.0	-98.9
ΔE_{ele}	21.0	15.9	45.7	44.5
ΔE_{exrep}	-35.6	-21.3	-17.6	-28.5
ΔE_{pol}	0.0	0.0	0.0	0.0
ΔE_{corr}	-41.5	-38.9	-54.7	-55.3
ΔE_{disp}	-36.5	-36.3	-61.4	-59.6

M = Pd	5-DFT Pd-Au	11-DFT Pd-Ag	9-DFT Pd-Ag-Pd	7-DFT Pd-Au-Pd
ΔE_{int}	-108.0	-83.2	-85.6	-112.6
ΔE_{ele}	12.5	10.3	38.3	34.5
ΔE_{exrep}	-39.4	-19.0	-14.1	-36.5
ΔE_{pol}	0.0	0.0	0.0	0.0
ΔE_{corr}	-43.7	-38.7	-51.5	-54.5
ΔE_{disp}	-37.4	-35.8	-58.3	-56.2

Furthermore, Natural Bond Orbital (NBO) analysis of the complexes of this chapter shows illuminating trends in agreement with those observed before. Wiberg Bond Indices (WBI) point in coherent directions with respect to the different interactions observed in these clusters. See Tables 1.7 and 1.8 for the WBI found for the relevant bonds of the eight bimetallic clusters.

Values due to the M-M' bond are found larger for the M-Au complexes, indicating therefore stronger bonds. Secondly, WBI of the M'-C_A bonds are larger when M' is gold and M is palladium. Finally, computed values for the M-C_A bonds are smaller when M is palladium and M' is gold, meaning that this bond is weaker in these complexes. As suggested by EDA studies and all the previous structural discussion, these values indicate that the strongest interactions between the metallic fragments exist when M = Pd and M' = Au.

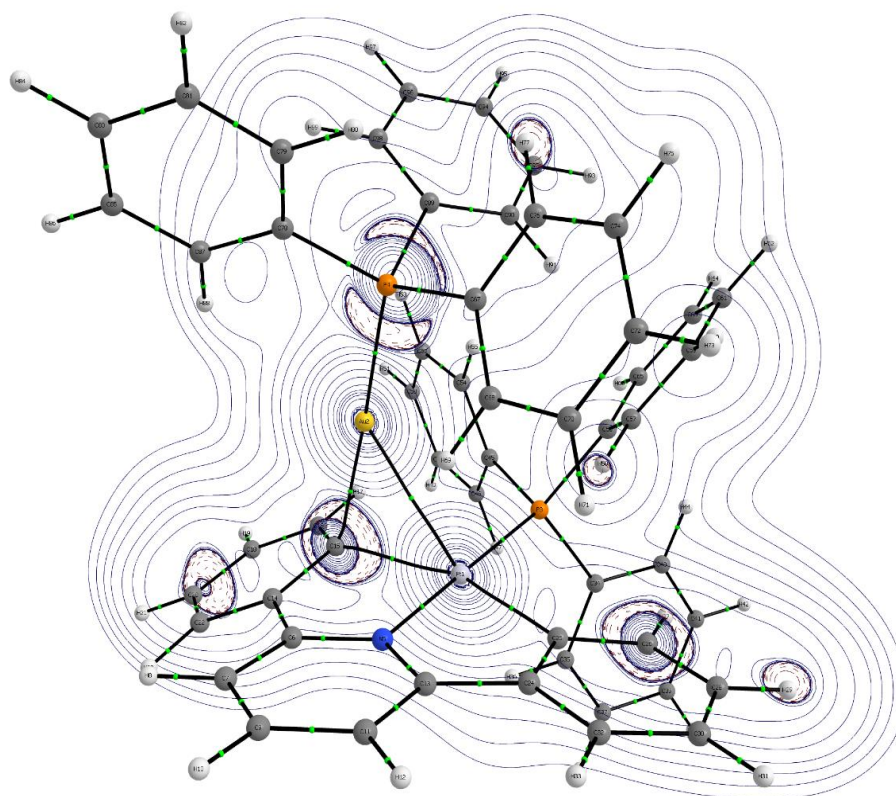
Table 1.7. Calculated WBI (DFT/BP86-D3 level, gas phase) in the heteropolynuclear platinum complexes of this chapter. Data collected from mononuclear derivative [Pt(CNC)(PPh₃)] are also included as reference.

WBI	[Pt(CNC)PPh ₃]	4-DFT Pt-Au	10-DFT Pt-Ag	8-DFT Pt-Ag-Pt	6-DFT Pt-Au-Pt
M-M'	-	0.24	0.20	0.21	0.25
M-C _A	0.66	0.46	0.55	0.55	0.46
M'-C _A	-	0.31	0.21	0.19	0.33

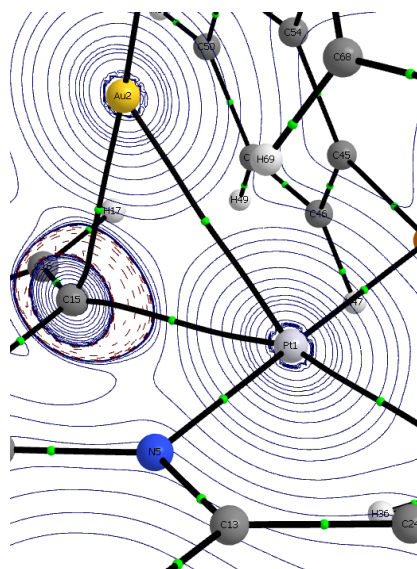
Table 1.8. Calculated WBI (DFT/BP86-D3 level, gas phase) in the heteropolynuclear palladium complexes of this chapter. Data collected from mononuclear derivative [Pd(CNC)(PPh₃)] are also included as reference.

WBI	[Pd(CNC)PPh ₃]	5-DFT Pd-Au	11-DFT Pd-Ag	9-DFT Pd-Ag-Pd	7-DFT Pd-Au-Pd
M-M'	-	0.24	0.19	0.19	0.25
M-C _A	0.60	0.32	0.48	0.49	0.26
M'-C _A	-	0.40	0.25	0.21	0.42

The computational and structural results previously discussed encourage to focus on the bonding situation of these systems by means of the Quantum Theory of Atoms in Molecules (QTAIM) (DFT/BP86-D3 level, gas phase). Interestingly for the Pt-M' complexes (see Tables S1.6 and S1.7, Supporting Information) the QTAIM method locates bond critical points (BCP) between the Pt and the adjacent carbon atoms as well as between the Ag or Au and the C_{ipso} (CNC). In addition to this, bond paths between Pt and Au centers are found for **4-DFT** and **6-DFT** (see Figures 1.32 and S1.75, Supporting Information). However, no BCPs between the Pt and the Ag centers are located for **8-DFT** and **10-DFT** (see Figures 1.33 and S1.76, Supporting Information). These studies again suggest that stronger interactions between the metallic fragments exist for the Pt-Au systems, also indicating that Pt-C_A bonds are more weakened when the acidic metallic center is gold.



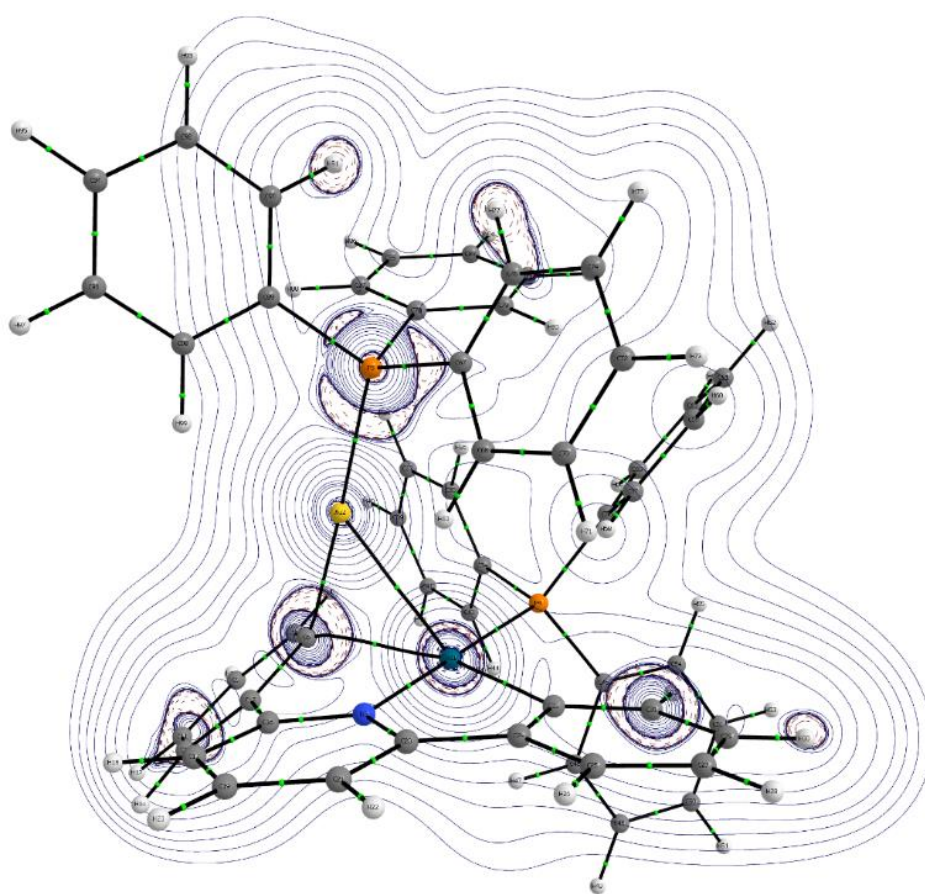
a)



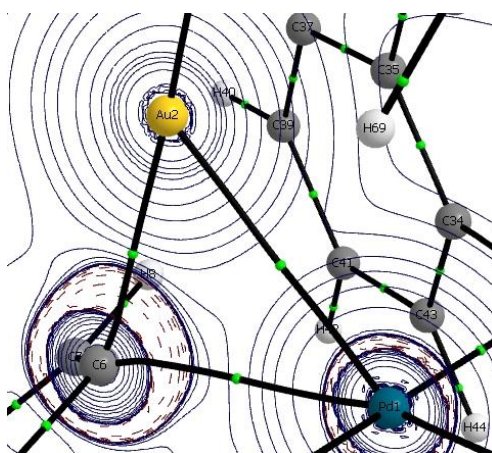
b)

Figure 1.32. Contour line diagrams $\nabla^2\rho(r)$ for the cation of complex **4-DFT** in the Au–C–Pt plane (solid lines connecting nuclei: Bond Paths; green dots: Bond Critical Points) (a). Detail of the complex core (b).

Same results are observed for the palladium analogues (see Tables S1.8 and S1.9, Supporting Information). Pd-M' bond paths are only found for the dinuclear and trinuclear Au complexes **5-DFT** and **7-DFT** (see Figures 1.34 and S1.77, Supporting Information) which again highlight stronger Pd-Au interactions compared to the Pd-Ag ones **9-DFT** and **11-DFT** (see Figures 1.35 and S1.78, Supporting Information). Moreover, the data extracted from this analysis at the Pd-C_A, Pd-C_B, Au-C_A and Ag-C_A BCPs also support a more marked weakening of the Pd-C_A bonds upon interaction with the Au centers.

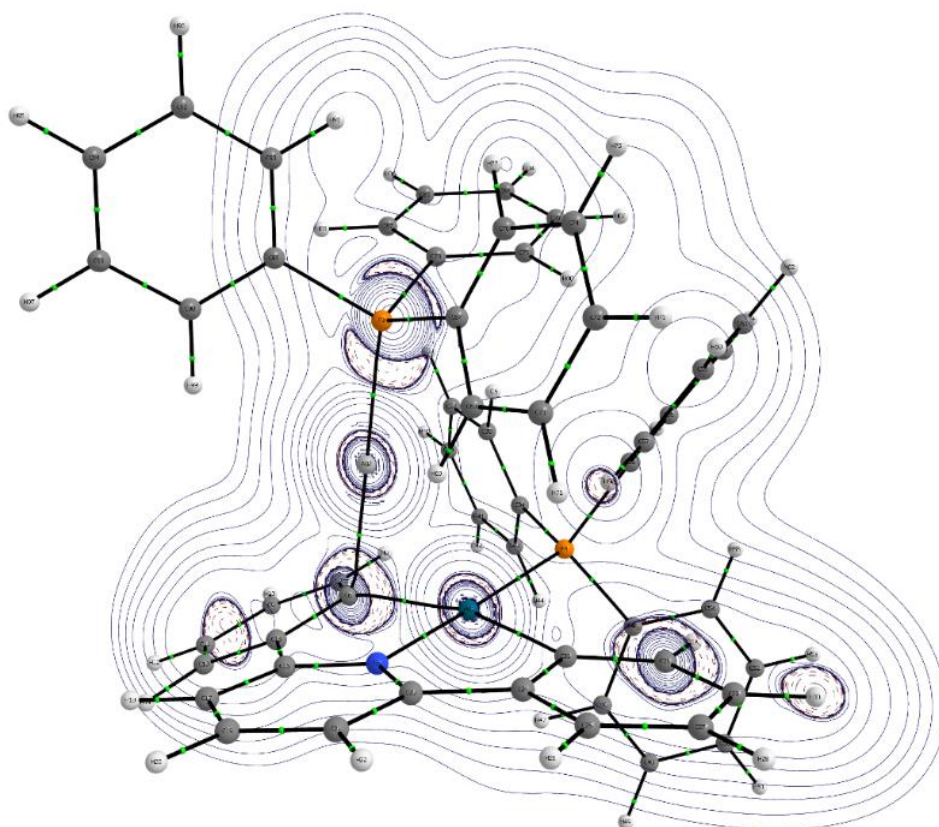


a)



b)

Figure 1.34. Contour line diagrams $\nabla^2\rho(r)$ for the cation of complex **5-DFT** in the Au–C–Pd plane (solid lines connecting nuclei: Bond Paths; green dots: BCP) (a), detail of the complex core (b).



a)

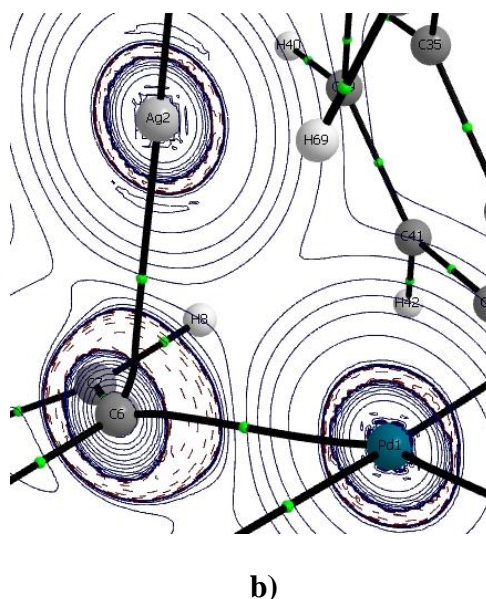
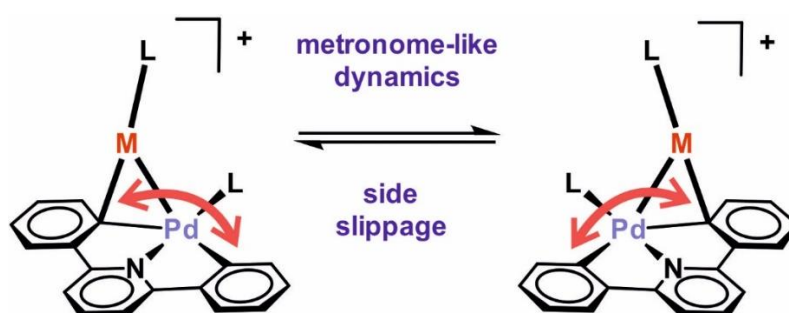
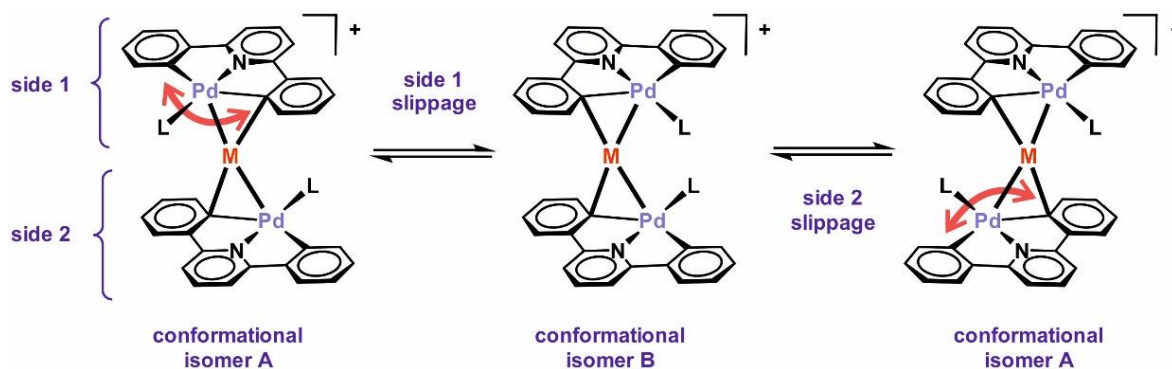


Figure 1.35. Contour line diagrams $\nabla^2\rho(r)$ for the cation of complex **11-DFT** in the Ag–C–Pd plane (solid lines connecting nuclei: Bond Paths; green dots: BCP) (a), detail of the complex core (b).

Finally, the “metronome-like” dynamics in the Pd–M’ systems (see Schemes 1.12 and 1.13) were also carefully studied through DFT calculations, in good agreement with the experimental behavior observed through NMR for these complexes. Thus, the “metronome-like” process (see Figures 1.36 and 1.37) presents higher energy barriers in the Pd–Au complexes (14.2 kcal/mol for **5** and 14.5 kcal/mol for **7**) than in the Pd–Ag ones (11.7 kcal/mol for **11** and 11.4 for **9**). This could explain why only the latter reaches fast exchange temperatures at RT and displays coalescence at around 203–213K.



Scheme 1.12. “Metronome-like” dynamics operating in the heterodinuclear complexes **5** (Pd–Au) and **11** (Pd–Ag).



Scheme 1.13. “Metronome-like” dynamics operating in the heterotrinnuclear complexes **7** (Pd-Au-Pd) and **9** (Pd-Ag-Pd). The double side mechanism generated two different conformers (A and B).

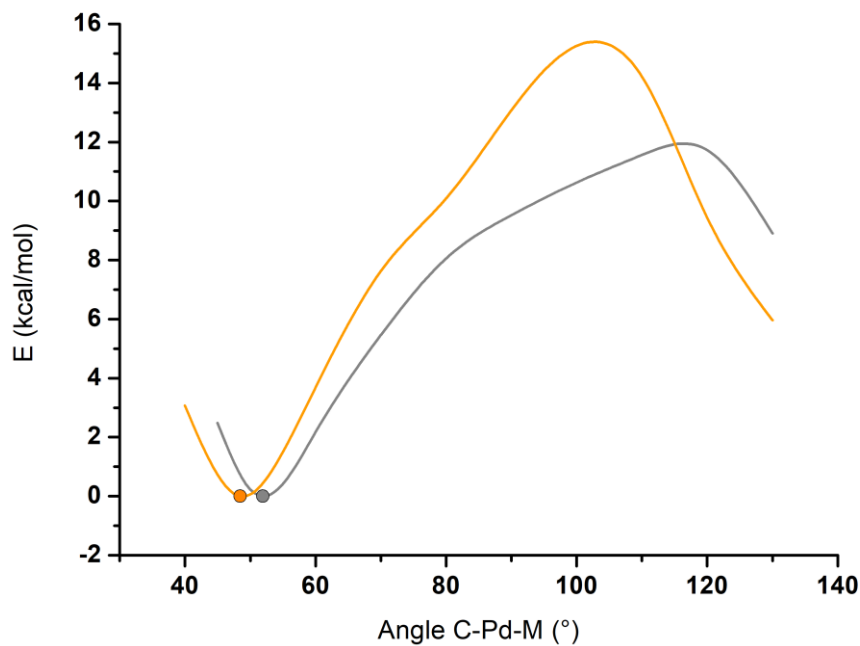


Figure 1.36. Calculated energy profile (relaxed scan, DFT/BP86-D3 level, dichloromethane solution) for the “metronome-like” dynamics operating in **5-DFT** (orange, Pd-Au) and **11-DFT** (grey, Pd-Ag).

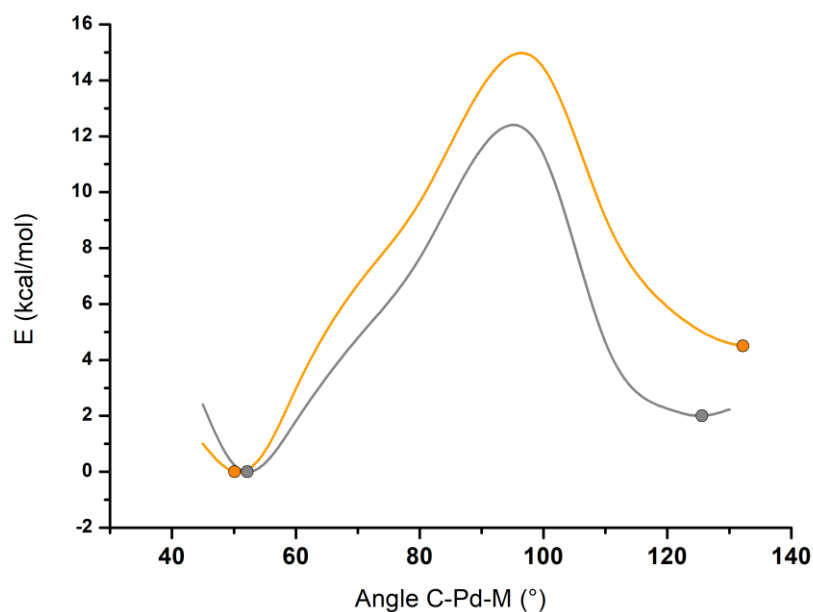


Figure 1.37. Calculated energy profile (relaxed scan, DFT/BP86-D3 level, dichloromethane solution) for the “metronome-like” dynamics operating in **7-DFT** (orange, Pd-Au-Pd) and **9-DFT** (grey, Pd-Ag-Pd).

Moreover, for trinuclear complexes $[\{\text{Pd}(\text{CNC})(\text{PPh}_3)\}_2\text{Au}](\text{ClO}_4)$ (**7**) and $[\{\text{Pd}(\text{CNC})(\text{PPh}_3)\}_2\text{Ag}](\text{ClO}_4)$ (**9**) additional conformational isomers have been found (see Scheme 1.13). DFT data suggests that only in the case of the silver complex this isomer is present in enough concentration to be detected by NMR at low temperatures, which is compatible with the two sets of signals of ^1H NMR and the two different signals of $^{31}\text{P}\{^1\text{H}\}$ NMR observed for two different conformers of $[\{\text{Pd}(\text{CNC})(\text{PPh}_3)\}_2\text{Ag}](\text{ClO}_4)$ (**9**) at 193K.

In this chapter, the synthesis, characterization and structural study of several Pt-M' and Pd-M' complexes has been undertaken. These complexes constitute a representative selection of donor acceptor systems with all the combinations of basic [Pt/Pd] and [Au/Ag] fragments in dinuclear and trinuclear forms. Altogether they provide a good amount of interconnected data from which some conclusions can be extracted.

Thus, the careful analysis of the behavior of the different heterobimetallic complexes of this chapter in solution (“metronome-like” motion) is in good agreement with the structural observations and computational studies on the interaction between the metallic fragments, confirming that indeed, all the heteropolymetallic clusters of this chapter can be regarded as arrested intermediates of a transmetallation process, which, given the tridentate nature of the CNC ligand, cannot progress further. The ^1H NMR spectra at several temperatures suggest that the energetic barrier, related with the strength of the M'-C_{ipso} interactions, is maximum for the Pd-Au complexes and minimum for the Pt-Ag complexes.

Several geometrical descriptors related with the M-R-M' fragment have been used to evaluate the progression of the frustrated transmetallation, in particular the deviation of the interacting phenylene ring from the rest of the CNC plane, quantified in the Section 1.3 with α_1 and α_2 angles and the M-C_{ipso} and M'-C_{ipso} distances, which can be visually compared in Figure 1.38.

Structural and computational studies helped to establish that Au promotes the highest degrees of transfer from the M-CNC systems. Also, that the Pd systems are more prone to the transfer of the R group than their Pt analogues. Thus, an order on the degree of transfer depending on the metals involved can be proposed, which is Pd-Au > Pt-Au > Pd-Ag > Pt-Ag.

The results of this chapter propose therefore, useful ideas that can be of interest in the design of bimetallic systems for bimetallic catalysis, an emerging and evolving field in chemical science.

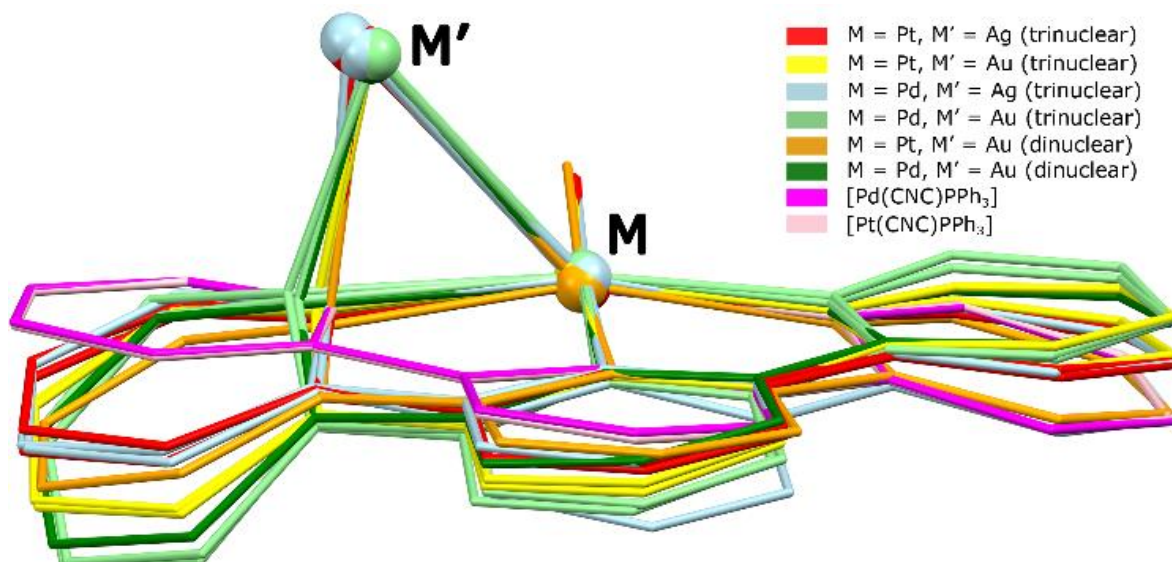


Figure 1.38. Overlay representation of the “P(CNC)MM” fragments in all the M-M’ (M = Pt, Pd; M’ = Ag, Au) structures of the bimetallic complexes of this chapter. For comparative purposes the structures of **1** and **2** are also included.

1.4. Experimental section

General Comments. Literature methods were used to prepare the starting material [Pt(CNC)(PPh₃)] (**1**) (CNC = 2,6-di(phen-2-ide)-pyridine).¹⁶ Elemental analyses were carried out with a Perkin-Elmer 2400 CHNS analyzer. IR spectra were recorded on a Perkin-Elmer Spectrum 100 FT-IR spectrometer (ATR in the range 250-4000 cm⁻¹). Mass spectrometry was performed with the Microflex matrix-assisted laser desorption ionization-time-of-flight (MALDI-TOF) Bruker or an Autoflex III MALDI-TOF Bruker instruments. ¹H, ¹³C{¹H}, ³¹P{¹H} and ¹⁹⁵Pt{¹H} NMR spectra were recorded on Bruker ARX-300, AV-400 and AV-500 spectrometers using the standard references: SiMe₄, 85% H₃PO₄ and Na₂PtCl₆ in D₂O for references for ¹H and ¹³C, ³¹P and ¹⁹⁵Pt respectively. The signal attributions and coupling constant assessment was made on the basis of a multinuclear NMR analysis of each compound including, besides 1D spectra, ¹H-¹H COSY, ¹H-¹³C HSQC, ¹H-¹³C HMBC and ¹³C{¹H} APT.

Safety Note: Perchlorate salts of metal complexes with organic ligands are potentially explosive. Only small amounts of material should be prepared, and these should be handled with great caution.

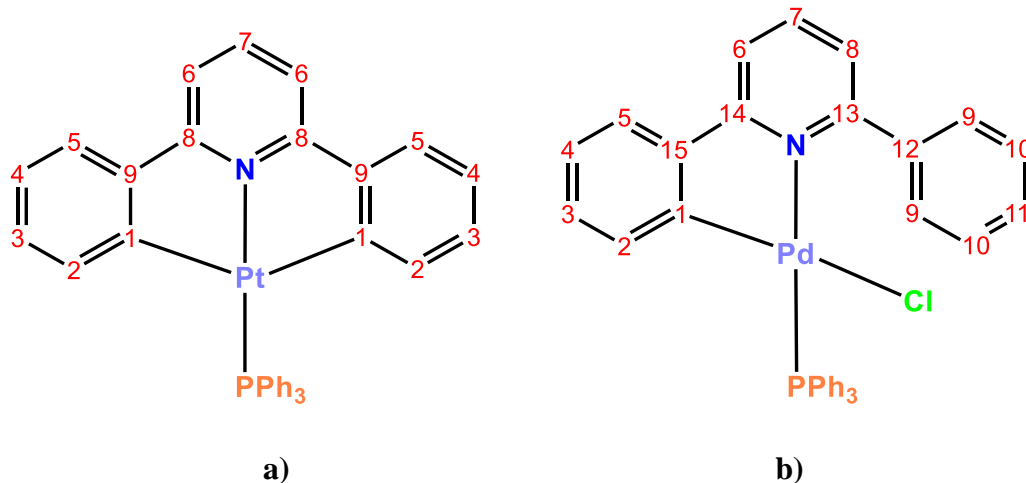


Chart 1.2. ¹H and ¹³C numbering scheme for the [M(CNC)] fragment.

Preparation of complex [Pd(CNC-H)(μ-Cl)]₂. To a solution of [PdCl₂(PhCN)₂] (0.400 g, 1.043 mmol) in 90 mL of MeOH, 2,6-diphenylpyridine (0.265 g, 1.147 mmol) was added. The reaction was kept under reflux for 2 days. As a result, a green solid was formed. The suspension was filtered, and the green product was washed with diethylether (10 mL) and air dried (Yield: 0.382 g, 98%).

Preparation of complex [Pd(CNC)(PPh₃)] (2). To a solution of KHMDS (0.072 g, 0.362 mmol) under argon in THF (20 mL) at room temperature, [Pd(CNC-H)Cl(PPh₃)] (3) (0.200 g, 0.315 mmol). After 45 minutes of stirring the mixture was evaporated to dryness and 20 mL of CH₂Cl₂ were added. The solution was filtered through celite, and the filtrate was evaporated to dryness. The yellow solid was extracted with *n*-hexane (10 mL), filtered, washed with MeOH (10 mL) and air dried (Yield: 0.112 g, 59%). Anal. Found: C, 70.01; H, 4.48; N, 2.39. Anal. Calcd. for C₃₅H₂₆NPPd: C, 70.30; H, 4.38; N, 2.34. IR (ATR, cm⁻¹): 1592 (m, ν(N-C)), 1565 (m, ν(N-C)), 1544 (w, ν(N-C)), 531 (vs, ν(P-C)), 511 (vs, ν(P-C)), 503 (vs, ν(P-C)). ¹H NMR (400.132 MHz, CD₂Cl₂, 293K, see Chart 1.2 a) for the H numbering scheme): δ = 7.83 (6H, m, *o*-PPh₃), 7.74 (1H, t, ³J_{H7-H6} = 7.9 Hz, H7), 7.47 (5H, m, H5 and *p*-PPh₃), 7.40 (8H, m, H6 and *m*-PPh₃), 6.89 (2H, td, ³J_{H4-H3} = ³J_{H4-H5} = 7.5 Hz, ⁴J_{H4-H2} = 1.3 Hz, H4), 6.57 (2H, td, ³J_{H3-H2} = ³J_{H3-H4} = 7.5 Hz, ⁴J_{H3-H5} = 1.3 Hz, H3), 6.16 (2H, dd, ³J_{H2-H3} = 7.5 Hz, ⁴J_{H2-H4} = 1.3 Hz, H2) ppm. ³¹P{¹H} NMR (161.923 MHz, CD₂Cl₂, 293K): δ = 45.2 (s) ppm. ¹³C{¹H} NMR plus HSQC and HMBC (100.624 MHz, CD₂Cl₂, 293K, see Chart 1.2 a) for the C numbering scheme): δ = 170.0 (d, ²J_{C-P} = 9.6 Hz, C1), 165.8 (s, C8), 151.9 (s, C9), 140.0 (s, C7), 139.4 (d, ³J_{C-P} = 5.3 Hz, C2), 135.7 (d, ²J_{C-P} = 13.1 Hz, *o*-PPh₃), 133.0 (d, ¹J_{C-P} = 46.9 Hz, *q*-PPh₃), 130.8 (d, ⁴J_{C-P} = 2.2 Hz, *p*-PPh₃), 128.8 (d, ⁴J_{C-P} = 1.7 Hz, C3), 128.6 (d, ³J_{C-P} = 10.4 Hz, *m*-PPh₃), 124.3 (s, C4), 123.6 (s, C5), 115.5 (s, C6) ppm. MS ESI+: m/z = 598.1 [[Pd(CNC)(PPh₃)]+H]⁺.

Preparation of complex [Pd(CNC-H)Cl(PPh₃)] (3). To a suspension of [Pd(CNC-H)(μ-Cl)]₂ (0.200 g, 0.269 mmol) under argon in CH₂Cl₂ (20 mL), PPh₃ (0.159 g, 0.606 mmol) was added. The reaction was carried out in reflux of CH₂Cl₂. After 60 minutes of stirring the resulting solution was filtered through celite. The filtered solution was concentrated *ca.* 2 mL, 15 mL of *n*-hexane were added obtaining a yellow precipitate. That solid was extracted with diethylether (10 mL), filtered, washed with more diethylether (5 mL) and air dried (Yield: 0.326 g, 96%). Anal. Found: C, 66.15; H, 4.62; N, 1.92. Anal. Calcd. for C₃₅H₂₇ClNPPd: C, 66.26; H, 4.29; N, 2.21. IR (ATR, cm⁻¹): 1595 (w, ν(N-C)), 1575 (m, ν(N-C)), 1564 (m, ν(N-C)), 1553 (m, ν(N-C)), 529 (vs, ν(P-C)), 514 (vs, ν(P-C)), 498 (vs, ν(P-C)), 276 (m, ν(Pd-Cl)). ¹H NMR (400.132 MHz, CD₂Cl₂, 293K, see Chart 1.2 b) for the H numbering scheme): δ = 8.07 (2H, dd, ³J_{H9-H10} = 6.9 Hz, ⁴J_{H9-H11} = 3.0 Hz, H9), 7.96 (1H, t, ³J_{H7-H6} = ³J_{H7-H8} = 7.9 Hz, H7), 7.83 (1H, d, ³J_{H6-H7} =

7.9 Hz, H6), 7.75 (6H, m, *o*-PPh₃), 7.61 (1H, d, ³J_{H5-H4} = 7.8 Hz, H5), 7.52 (1H, d, ³J_{H8-H7} = 7.9 Hz, H8), 7.44 (6H, m, *p*-PPh₃, H10 and H11), 7.36 (6H, m, *m*-PPh₃), 6.98 (1H, t, ³J_{H4-H5} = ³J_{H4-H3} = 7.8 Hz, H4), 6.54 (2H, m, H2 and H3) ppm. ³¹P{¹H} NMR (161.923 MHz, CD₂Cl₂, 293K): δ = 42.2 (s) ppm. ¹³C{¹H} NMR plus HSQC and HMBC (100.624 MHz, CD₂Cl₂, 293K, see Chart 1.2 b) for the C numbering scheme): δ = 163.9 (s, C14), 161.6 (s, C13), 156.2 (s, C1), 147.9 (s, C15), 140.8 (s, C12), 139.5 (s, C7), 138.1 (d, ³J_{C-P} = 12.0 Hz, C2), 135.3 (d, ²J_{C-P} = 12.0 Hz, *o*-PPh₃), 131.8 (d, ¹J_{C-P} = 52.0 Hz, *q*-PPh₃), 130.9 (s, *p*-PPh₃), 129.7 (s, C11), 129.4 (s, C9), 128.3 (d, ³J_{C-P} = 14.0 Hz, *m*-PPh₃), 128.2 (s, C10), 128.1 (s, C3), 125.1 (s, C5), 124.6 (s, C4), 123.5 (s, C8), 117.0 (s, C6) ppm. MS MALDI+ DCTB: m/z = 598.1 [Pd(CNC-H)(PPh₃)]⁺.

Preparation of the complex [(CNC)(PPh₃)PtAu(PPh₃)](ClO₄) (4). To a solution of [AuCl(PPh₃)] (0.076 g, 0.150 mmol) in tetrahydrofuran (20 mL) under argon at -40°C, AgClO₄ (0.032 g, 0.150 mmol) was added. After 75 minutes of stirring in the absence of light the suspension was filtered. To the collected solution, complex [Pt(CNC)(PPh₃)] (1) (0.100 g, 0.150 mmol) was added. After 3 hours of stirring at room temperature, the resulting solution was evaporated to dryness. Addition of MeOH (5 mL) caused a precipitate which was decanted, washed with diethyl ether (10 mL), and air dried (Yield: 0.116 g, 64%). Anal. Found: C, 50.88; H, 3.21; N, 1.26. Anal. Calcd. for C₅₃H₄₁AuClN₂O₄P₂Pt: C, 51.12; H, 3.32; N, 1.12. IR (ATR, cm⁻¹): 1597 (w, ν(N-C)), 1562 (vw, ν(N-C)), 1079 (s, ν(ClO₄⁻)), 689 (s, ν(P-C)), 621 (m, ν(ClO₄⁻)), 536 (vs, ν(P-C)), 513 (vs, ν(P-C)), 497 (vs, ν(P-C)). ¹H NMR (400.132 MHz, CD₂Cl₂, 293K): δ = 7.92 (1H, t, ³J_{H7-H6} = 8.0 Hz, H7), 7.72 (2H, dd, ³J_{H5-H4} = 7.6 Hz, ⁴J_{H5-H3} = 1.3 Hz, H5), 7.70-7.67 (6H, m, ³J_{H_o-H_m} = 8.3 Hz, ⁴J_{H_o-H_p} = 1.2 Hz, *o*-PPh₃(Pt)), 7.62 (2H, d, ³J_{H6-H7} = 8.0 Hz, H6), 7.53-7.47 (6H, m, overlapped signals of *p*-PPh₃(Pt) and *p*-PPh₃(Au)), 7.32 (6H, td, ³J_{H_m-H_o} = 8.3 Hz, ³J_{H_m-H_p} = 2.7 Hz, *m*-PPh₃(Au)), 7.26 (2H, ddd, ³J_{H4-H5} = 7.6 Hz, ³J_{H4-H3} = 7.6 Hz, ⁴J_{H4-H2} = 1.0 Hz, H4), 7.21 (6H, td, ³J_{H_m-H_o} = 8.3 Hz, ³J_{H_m-H_p} = 2.5 Hz, *m*-PPh₃(Pt)), 7.09 (6H, td, ³J_{H_o-H_m} = 8.3 Hz, ⁴J_{H_o-H_p} = 1.2 Hz, *o*-PPh₃(Au)), 6.84 (2H, ddd, ³J_{H3-H4} = ³J_{H3-H2} = 7.6 Hz, ⁴J_{H3-H5} = 1.3 Hz, H3), 6.08 (2H, dd, ³J_{H2-H3} = 7.6 Hz, ⁴J_{H2-H4} = 1.0 Hz, ³J_{H2-Pt} = 25.9 Hz, H2) ppm. ¹³C{¹H} NMR plus HSQC and HMBC (100.624 MHz, CD₂Cl₂, 293K): δ = 164.4 (s, C8), 154.2 (s, C9), 146.1 (s, ¹J_{C-Pt} = 654 Hz, C1), 143.0 (s, C7), 142.1 (s, C2), 136.1 (d, ²J_{C-P} = 11.5 Hz, ³J_{C-Pt} = 25.4 Hz, *o*-PPh₃(Pt)), 134.1 (d, ²J_{C-P} = 13.9 Hz, *o*-PPh₃(Au)), 132.8-132.4 (d, ⁴J_{C-P} = 2.1 Hz, d, ⁴J_{C-P} = 1.6 Hz, *p*-

PPh₃(Au) and *p*-PPh₃(Pt)), 130.5 (s, ³J_{C-Pt} = 33.2 Hz, C3), 129.9 (d, overlapped signals of *m*-PPh₃(Au) and C5), 129.3 (d, ³J_{C-P} = 11.1 Hz, *m*-PPh₃(Pt)), 125.9 (s, ⁴J_{C-Pt} = 22.9 Hz, C4), 117.6 (d, ⁴J_{C-P(Pt)} = 3.1 Hz, C6) ppm. ³¹P{¹H} NMR (161.923 MHz, CD₂Cl₂): δ = 34.6 (s, ²J_{P(Au)-Pt} = 254 Hz) (293K), 22.5 (s, ¹J_{P-Pt} = 3680 Hz) (293K); 35.8 (s, ²J_{P(Au)-Pt} = 242 Hz) (193K), 22.1 (s, ¹J_{P-Pt} = 3660 Hz) (193K) ppm. ¹⁹⁵Pt{¹H} NMR (85.679 MHz, CD₂Cl₂): δ = -4017 (dd, ¹J_{Pt-P} = 3680 Hz, ²J_{Pt-P(Au)} = 254 Hz) (293K), -4060 (dd, ¹J_{Pt-P} = 3660 Hz, ²J_{Pt-P(Au)} = 242 Hz) (193K) ppm. MS MALDI+ DCTB: m/z = 1145.1 [(CNC)(PPh₃)PtAu(PPh₃)]⁺.

Preparation of complex [(CNC)(PPh₃)PdAu(PPh₃)](ClO₄) (5). To a solution of [AuCl(PPh₃)] (0.059 g, 0.119 mmol) in 30 mL of THF at -60°C, AgClO₄ (0.025 g, 0.119 mmol) was added. The reaction was kept under argon and protected from the light for 70 minutes. Then, the resulting solution was filtered through celite and [Pd(CNC)(PPh₃)] (2) (0.065 g, 0.108 mmol) was added. The mixture was kept at room temperature and stirred for 30 minutes. After that, the solution was evaporated to dryness and the resulting yellow solid was extracted with *n*-hexane. The solid was filtered and air dried. (Yield: 0.113 g, 90%). Anal. Found: C, 54.67; H, 3.71; N, 1.37. Anal. Calcd. for C₅₃H₄₁AuClNO₄P₂Pd: C, 55.03; H, 3.57; N, 1.21. IR (ATR, cm⁻¹): 1596 (m, ν(N-C)), 1575 (m, ν(N-C)), 1566 (w, ν(N-C)), 1087 (s, ν(ClO₄⁻)), 621 (m, ν(ClO₄⁻)), 530 (vs, ν(P-C)), 510 (s, ν(P-C)). ¹H NMR (400.132 MHz, CD₂Cl₂, 293K, inequivalent H2-H6 protons could not be identified): δ = 8.01 (1H, t, ³J_{H7-H6} = ³J_{H7-H6*} = 8.0 Hz, H7), 7.76 (3H, m, H6/H6*, H5/H5* and H2/H2*), 7.62 (7H, m, *o*-PPh₃ and H6/H6*), 7.48 (7H, m, *p*-PPh₃ and H4/H4*), 7.28 (12H, m, *o*-PPh₃ and *m*-PPh₃), 7.17 (7H, m, *m*-PPh₃ and H3/H3*), 7.02 (1H, t, ³J_{H3-H2} = ³J_{H3-H4} = 6.8 Hz, H3/H3*), 6.61 (1H, t, ³J_{H4-H3} = ³J_{H4-H5} = 6.8 Hz, H4/H4*), 6.41 (1H, d, ³J_{H5-H6} = 6.0 Hz, H5/H5*), 5.47 (1H, d, ³J_{H2-H3} = 6.9 Hz, H2/H2*) ppm. ³¹P{¹H} NMR (161.923 MHz, CD₂Cl₂, 293K): δ = 41.9 (s, P(Au)), 40.3 (s, P(Pd)) ppm. ¹³C{¹H} NMR plus HSQC and HMBC (100.624 MHz, CD₂Cl₂, 293K, inequivalent C1-C9 carbons could not be identified): δ = 164.6 (s, C8/C8*), 163.6 (s, C8/C8*), 157.8 (s, C9/C9*), 155.9 (s, C9/C9*), 148.5 (s, C2/C2*), 141.8 (s, C7), 139.2 (s, C5/C5*), 135.8 (d, ²J_{C-P} = 12.9 Hz, *o*-PPh₃), 134.2 (d, ²J_{C-P} = 13.5 Hz, *o*-PPh₃), 133.2 (s, C4/C4*), 132.5 (d, ⁴J_{C-P} = 2.6 Hz, *p*-PPh₃), 132.1 (d, ⁴J_{C-P} = 2.6 Hz, *p*-PPh₃), 131.0 (d, ¹J_{C-P} = 51.8 Hz, *q*-PPh₃), 129.7 (d, ³J_{C-P} = 11.5 Hz, *m*-PPh₃), 129.1 (d, ³J_{C-P} = 10.9 Hz, *m*-PPh₃), 129.0 (m, overlapped with *m*-PPh₃, *q*-PPh₃), 128.3 (s, C4/C4*), 126.6 (s, C2/C2* and C5/C5*), 125.4 (s, C3/C3*),

118.9 (s, C6/C6*), 117.9 (s, C6/C6*) ppm. MS MALDI+ DCTB: $m/z = 1056.1$ $[(\text{CNC})(\text{PPh}_3)\text{PdAu}(\text{PPh}_3)]^+$.

Preparation of the complex $[\{\text{Pt}(\text{CNC})(\text{PPh}_3)\}_2\text{Au}](\text{ClO}_4)$ (6). To a solution of $[\text{AuCl}(\text{tht})]$ (0.052 g, 0.162 mmol) in THF (20 mL) at 0°C and under argon, tht (15 μl , 0.162 mmol) and AgClO_4 (0.033 g, 0.162 mmol) were added. After 60 minutes of stirring in absence of light, the complex $[\text{Pt}(\text{CNC})(\text{PPh}_3)]$ (1) (0.212 g, 0.308 mmol) was added to the solution. After 2 hours of stirring, the resulting solution was concentrated to *ca.* 5 mL and kept to -30°C to give an orange precipitate that was filtered off, washed with diethyl ether (10 mL) and finally air dried (Yield: 0.153 g, 60%). Anal. Found: C, 49.94; H, 3.05; N, 1.80. Anal. Calcd. for $\text{C}_{70}\text{H}_{52}\text{AuClN}_2\text{O}_4\text{P}_2\text{Pt}_2$: C, 50.35; H, 3.14; N, 1.68. IR (ATR, cm^{-1}): 1597 (w, $\nu(\text{N-C})$), 1576 (vw, $\nu(\text{N-C})$), 1563 (vw, $\nu(\text{N-C})$), 1544 (vw, $\nu(\text{N-C})$), 1092 (s, $\nu(\text{ClO}_4^-)$), 692 (s, $\nu(\text{P-C})$), 620 (m, $\nu(\text{ClO}_4^-)$), 540 (vs, $\nu(\text{P-C})$), 513 (s, $\nu(\text{P-C})$), 507 (s, $\nu(\text{P-C})$). ^1H NMR (500.130 MHz, CD_2Cl_2 , 293K): $\delta = 7.58$ (2H, t, $^3J_{\text{H7-H6}} = 7.9$ Hz, H7), 7.50 (6H, t, $^3J_{\text{Hp-Hm}} = 7.1$ Hz, *p*- PPh_3), 7.34 (12H, t, $^3J_{\text{Hm-Ho}} = 7.0$ Hz, *m*- PPh_3), 7.33-7.27 (20H, m, overlapped signals of H5 and H6 and *o*- PPh_3), 6.98 (4H, t, $^3J_{\text{H4-H5}} = ^3J_{\text{H4-H3}} = 7.4$ Hz, H4), 6.64 (4H, t, $^3J_{\text{H3-H4}} = ^3J_{\text{H3-H2}} = 7.4$ Hz, H3), 5.98 (4H, broad singlet signal, H2) ppm. $^{13}\text{C}\{^1\text{H}\}$ NMR plus HSQC and HMBC (100.624 MHz, CD_2Cl_2 , 293K): $\delta = 165.3$ (s, C8), 154.2 (s, C9), 146.1 (s, C1), 142.7 (s, C2), 141.9 (s, C7), 135.6 (d, $^3J_{\text{C-P}} = 11.4$ Hz, *m*- PPh_3), 131.8 (d, $^4J_{\text{C-P}} = 2.4$ Hz, *p*- PPh_3), 129.0 (d, $^3J_{\text{C-Pt}} = 25.9$ Hz, $^2J_{\text{C-P}} = 11.0$ Hz, overlapped signals of *o*- PPh_3 and C3 and C4), 125.6 (s, C5), 116.8 (d, $^4J_{\text{C-P}} = 3.2$ Hz, C6) ppm. $^{31}\text{P}\{^1\text{H}\}$ NMR (202.461 MHz, CD_2Cl_2 , 203K): $\delta = 20.8$ (s, $^1J_{\text{P-Pt}} = 3794$ Hz) ppm. $^{195}\text{Pt}\{^1\text{H}\}$ NMR (85.679 MHz, CD_2Cl_2): $\delta = -4006$ (d, $^1J_{\text{Pt-P}} = 3813$ Hz) (293K), -4018 (d, $^1J_{\text{Pt-P}} = 3773$ Hz) (193K) ppm. MS MALDI+ DCTB: $m/z = 1569$ $[\{\text{Pt}(\text{CNC})(\text{PPh}_3)\}_2\text{Au}]^+$, 1307 $[(\text{CNC})(\text{PPh}_3)\text{PtAuPt}(\text{CNC})]^+$, 1145 $[(\text{CNC})(\text{PPh}_3)\text{PtAu}(\text{PPh}_3)]^+$, 893 $[(\text{CNC})(\text{PPh}_3)\text{PtAu}]^+$, 687 $[(\text{CNC})\text{Pt}(\text{PPh}_3)]^+$.

Preparation of mixture 7*. Complex $[\{\text{Pd}(\text{CNC})(\text{PPh}_3)\}_2\text{Au}](\text{ClO}_4)$ (7) could not be synthesized as a pure solid. $[\text{AuCl}(\text{tht})]$ (0.0177 g, 0.055 mmol) was dissolved in 20 mL of THF at -70°C and AgClO_4 (0.0114 g, 0.055 mmol) was added. The reaction was kept under argon and protected from the light for 30 minutes. Then, $[\text{Pd}(\text{CNC})(\text{PPh}_3)]$ (2) (0.065 g, 0.108 mmol) was added. The mixture was kept 2 hours until it reached -

15°C. After that, 60 mL of cold *n*-hexane were added, and the resulting yellow solid was filtered under argon. This solid was then dissolved under argon in CH₂Cl₂, *n*-hexane was added, and this mixture was kept away from light and at -30°C for several days. A small batch of crystals of **7** were identified and analyzed through X-Ray diffraction, MS and VT NMR experiments. ¹H NMR (300.131 MHz, CD₂Cl₂, 293K, inequivalent H2-H6 protons could not be identified): δ = 7.61 (2H, t, ³J_{H7-H6} = 8.2 Hz, H7), 7.39 (36H, m, *o*-PPh₃, *m*-PPh₃, *p*-PPh₃, H2/H2*, H5/H5*, H6/H6*), 7.09 (6H, m, H6/H6*, H4/H4* and H3/H3*), 6.83 (2H, td, ³J_{H3-H2} = ³J_{H3-H4} = 7.5 Hz, ⁴J_{H3-H5} = 1.1 Hz, H3/H3*), 6.48 (2H, td, ³J_{H4-H3} = ³J_{H4-H5} = 7.5 Hz, ⁴J_{H4-H2} = 1.3 Hz, H4/H4*), 6.16 (2H, d, ³J_{H5-H4} = 6.6 Hz, H5/H5*), 5.60 (2H, d, ³J_{H2-H3} = 7.5 Hz, H2/H2*) ppm. ³¹P NMR (121.498 MHz, CD₂Cl₂, 293K): 40.3 (s) ppm. MS MALDI+ DCTB: m/z = 1392.9 [(CNC)(PPh₃)Pd]₂Au⁺.

Preparation of the complex [(Pt(CNC)(PPh₃))₂Ag](ClO₄) (8**).** To a solution of [Pt(CNC)(PPh₃)] (**1**) (0.100 g, 0.146 mmol) in CH₂Cl₂ (20 mL) at room temperature, AgClO₄ (0.015 g, 0.146 mmol) was added. After 120 minutes of stirring in absence of light the solution was evaporated to dryness. ⁱPrOH (3 mL) was added to the orange solid and the resulting suspension was filtered off, washed with *n*-hexane (10 mL) and air dried (Yield: 0.090 g, 78%). Anal. Found: C, 52.79; H, 3.24; N, 1.44. Anal. Calcd. for C₇₀H₅₂AgClN₂O₄P₂Pt₂: C, 53.19; H, 3.32; N, 1.77. IR (ATR, cm⁻¹): 1598 (m, ν(N-C)), 1564 (w, ν(N-C)), 1547 (w, ν(N-C)), 1090 (m, ν(ClO₄⁻)), 693 (s, ν(P-C)), 622 (m, ν(ClO₄⁻)), 539 (vs, ν(P-C)), 513 (m, ν(P-C)), 501 (m, ν(P-C)). ¹H NMR (500.130 MHz, CD₂Cl₂, 293K): δ = 7.64 (2H, t, ³J_{H7-H6} = 7.9 Hz, H7), 7.51-7.43 (18H, m, overlapped signals of *m*-PPh₃ and *p*-PPh₃), 7.39 (4H, d, ³J_{H5-H4} = 7.6 Hz, H5), 7.29 (4H, d, ³J_{H6-H7} = 7.9 Hz, H6), 7.23 (12H, m, *o*-PPh₃), 6.97 (4H, t, ³J_{H4-H5} = ³J_{H4-H3} = 7.6 Hz, H4), 6.51 (4H, t, ³J_{H3-H4} = ³J_{H3-H2} = 7.6 Hz, H3), 5.83 (4H, d, ³J_{H2-H3} = 7.6 Hz, H2) ppm. ¹³C{¹H} NMR plus HSQC and HMBC (100.624 MHz, CD₂Cl₂, 293K): δ = 165.5 (s, C8), 152.8 (s, C9), 149.6 (s, C1), 142.2 (s, C7), 139.7 (s, C2), 135.5 (d, ²J_{C-P} = 11.4 Hz, ³J_{C-Pt} = 34.5 Hz, *o*-PPh₃), 132.1 (s, *p*-PPh₃), 130.5 (s, C3), 129.2 (d, ³J_{C-P} = 10.9 Hz, *m*-PPh₃), 127.5 (s, C4), 125.6 (s, C5), 116.7 (s, C6) ppm. ³¹P{¹H} NMR (202.461 MHz, CD₂Cl₂): δ = 24.1 (s, ¹J_{P-Pt} = 3670 Hz) (293K), 23.6 (s, ¹J_{P-Pt} = 3617 Hz) (193K) ppm. ¹⁹⁵Pt{¹H} NMR (85.679 MHz, CD₂Cl₂): δ = -4102 (dd, ¹J_{Pt-P} = 3711 Hz, ¹J_{Pt-Ag} = 513 Hz) (293K), -4144 (dd, ¹J_{Pt-P} = 3631 Hz, ¹J_{Pt-Ag} = 530 Hz) (193K) ppm. MS MALDI+ DIT: m/z = 1479 [(Pt(CNC)(PPh₃))₂Ag]⁺, 793 [(CNC)(PPh₃)PtAg]⁺, 687 [Pt(CNC)(PPh₃)]+H]⁺.

Preparation of the complex $[\{\text{Pd}(\text{CNC})(\text{PPh}_3)\}_2\text{Ag}](\text{ClO}_4)$ (9). To a solution of $[\text{Pd}(\text{CNC})(\text{PPh}_3)]$ (2) (0.040 g, 0.067 mmol) in 15 mL of acetone at room temperature, AgClO_4 (0.007 g, 0.034 mmol) was added and the reaction was stirred and protected from light for 30 minutes. The yellow solution was then evaporated to *ca.* 1 mL and 15 mL of *n*-hexane were added. As a result, a yellow precipitate was obtained. The solid was filtered, washed with more *n*-hexane (5 mL) and air dried (Yield: 0.032 g, 72%). Anal. Found: C, 59.56; H, 3.60; N, 1.92. Anal. Calcd. for $\text{C}_{70}\text{H}_{52}\text{AgClN}_2\text{O}_4\text{P}_2\text{Pd}_2$: C, 59.91; H, 3.74; N, 2.00. IR (ATR, cm^{-1}): 1593 (m, $\nu(\text{N-C})$), 1565 (m, $\nu(\text{N-C})$), 1091 (s, $\nu(\text{ClO}_4^-)$), 622 (m, $\nu(\text{ClO}_4^-)$), 531 (vs, $\nu(\text{P-C})$), 511 (s, $\nu(\text{P-C})$). ^1H NMR (400.132 MHz, CD_2Cl_2 , 293K): $\delta = 7.63$ (2H, t, $^3J_{\text{H7-H6}} = 7.9$ Hz, H7), 7.51 (6H, t, $^3J_{\text{Hp-Ho}} = 7.1$ Hz, *p*-PPh₃), 7.42 (4H, d, $^3J_{\text{H5-H4}} = 7.5$ Hz, H5), 7.34 (28H, m, H6, *o*-PPh₃ and *m*-PPh₃), 6.97 (4H, t, $^3J_{\text{H4-H3}} = ^3J_{\text{H4-H5}} = 7.5$ Hz, H4), 6.57 (4H, t, $^3J_{\text{H3-H2}} = ^3J_{\text{H3-H4}} = 7.5$ Hz, H3), 5.87 (4H, br. s, H2) ppm. $^{31}\text{P}\{^1\text{H}\}$ NMR (202.461 MHz, CD_2Cl_2): $\delta = 42.5$ (s) (293K) ppm; 43.4 (s), 40.5 (s) (193K) ppm. $^{13}\text{C}\{^1\text{H}\}$ NMR plus HSQC and HMBC (100.624 MHz, CD_2Cl_2 , 293K): $\delta = 164.4$ (s, C8), 153.6 (s, C9), 141.0 (s, C2, C7), 135.3 (d, $^2J_{\text{C-P}} = 12.4$ Hz, *o*-PPh₃), 131.7 (d, $^4J_{\text{C-P}} = 2.4$ Hz, *p*-PPh₃), 131.3 (d, $^1J_{\text{C-P}} = 49.8$ Hz, *q*-PPh₃), 129.2 (d, $^3J_{\text{C-P}} = 10.8$ Hz, *m*-PPh₃), 128.4 (s, C4 and C3), 125.4 (s, C5), 117.0 (s, C6) ppm. MS MALDI+ DCTB: $m/z = 1303.4$ $[\{\text{Pd}(\text{CNC})(\text{PPh}_3)\}_2\text{Ag}]^+$, 598.1 $[[\text{Pd}(\text{CNC})(\text{PPh}_3)]+\text{H}]^+$.

Preparation of mixture 10*. To a solution of $[\text{Pt}(\text{CNC})(\text{PPh}_3)]$ (1) (0.150 g, 0.219 mmol) in CH_2Cl_2 (20 mL) under argon at -70°C , $[\text{Ag}(\text{OCIO}_3)(\text{PPh}_3)]$ (0.102 g, 0.219 mmol) was added. After 30 minutes of stirring in the absence of light the solution was evaporated dryness. *n*-hexane (10 mL) was added to the orange solid and the resulting suspension was filtered off and air dried (Yield: 0.207 g, 82%). Anal. Found: C, 55.02; H, 3.96; N, 1.31. Anal. Calcd. for $\text{C}_{53}\text{H}_{41}\text{AgClNO}_4\text{P}_2\text{Pt}$: C, 55.06; H, 3.57; N, 1.21. IR (ATR, cm^{-1}): 1598 (m, $\nu(\text{N-C})$), 1564 (w, $\nu(\text{N-C})$), 1547 (w, $\nu(\text{N-C})$), 1088 (s, $\nu(\text{ClO}_4^-)$), 690 (vs, $\nu(\text{P-C})$), 620 (s, $\nu(\text{ClO}_4^-)$), 539 (vs, $\nu(\text{P-C})$), 514 (vs, $\nu(\text{P-C})$), 499 (vs, $\nu(\text{P-C})$). ^1H NMR (500.130 MHz, CD_2Cl_2 , 243K): $\delta = 7.87$ (1H, t, $^3J_{\text{H7-H6}} = 8.0$ Hz, H7), 7.72 (6H, m, $^3J_{\text{Ho-Hm}} = 7.8$ Hz, $^3J_{\text{Ho-Hp}} = 1.0$ Hz, *o*-PPh₃), 7.64 (2H, d, $^3J_{\text{H5-H4}} = 7.6$ Hz, H5), 7.56 (2H, d, $^3J_{\text{H6-H7}} = 8.0$ Hz, H6), 7.54-7.40 (6H, m, PPh₃), 7.31 (6H, t, $^3J_{\text{Hp-Hm}} = 7.2$ Hz, *p*-PPh₃), 7.22 (6H, m, PPh₃), 7.18 (2H, t, $^3J_{\text{H4-H5}} = ^3J_{\text{H4-H3}} = 7.6$ Hz, H4), 6.91 (6H, m, PPh₃), 6.81 (2H, t, $^3J_{\text{H3-H4}} = 7.6$ Hz, $^3J_{\text{H3-H2}} = 7.6$ Hz, H3), 6.04 (2H, d, $^3J_{\text{H2-H3}} = 7.6$ Hz, H2)

ppm. $^{31}\text{P}\{^1\text{H}\}$ NMR (202.461 MHz, CD_2Cl_2): $\delta = 24.1$ (s, $^1J_{\text{P-Pt}} = 3662$ Hz) (293K), 15.1 (d, $^1J_{\text{P-Ag}} = 672$ Hz) (293K); 23.6 (s, $^1J_{\text{P-Pt}} = 3548$ Hz) (183K), 15.3 (dd, $^1J_{\text{P-Ag}} = 717$ Hz, $^1J_{\text{P-Ag}} = 624$ Hz, $^2J_{\text{P(Ag)-Pt}} = 122$ Hz) (183K) ppm. $^{195}\text{Pt}\{^1\text{H}\}$ NMR (85.679 MHz, CD_2Cl_2 , 193K): $\delta = -4171$ (ddd, $^1J_{\text{Pt-P}} = 3561$ Hz, $^1J_{\text{Pt-Ag}} = 438$ Hz, $^2J_{\text{Pt-P(Ag)}} = 115$ Hz) ppm. MS MALDI+ DCTB: $m/z = 1055.0$ [(CNC)(PPh₃)PtAg(PPh₃)]⁺, 793.0 [(CNC)(PPh₃)PtAg]⁺, 687.0 [[Pt(CNC)(PPh₃)]+H]⁺, 389.0 [Ag(PPh₃)]⁺.

Preparation of mixture 11*. To a solution of [Pd(CNC)(PPh₃)] (**2**) (0.036 g, 0.060 mmol) in 15 mL of CH_2Cl_2 at -70°C , [Ag(OCIO₃)(PPh₃)] (0.028 g, 0.060 mmol) was added and the reaction was stirred and protected from light for 5 minutes. Then, the mixture was evaporated to dryness and the resulting yellow solid was extracted with *n*-hexane (10 mL). The solid was filtered and air dried. (Yield: 0.039 g, 61%). Anal. Found: C, 59.42; H, 3.98; N, 1.44. Anal. Calcd. for $\text{C}_{53}\text{H}_{41}\text{AgClNO}_4\text{P}_2\text{Pd}$: C, 59.63; H, 3.87; N, 1.31. IR (ATR, cm^{-1}): 1594 (m, $\nu(\text{N-C})$), 1565 (m, $\nu(\text{N-C})$), 1548 (w, $\nu(\text{N-C})$), 1090 (s, $\nu(\text{ClO}_4^-)$), 621 (m, $\nu(\text{ClO}_4^-)$), 532 (vs, $\nu(\text{P-C})$), 511 (s, $\nu(\text{P-C})$). Low resolution signals of ^1H NMR (400.130 MHz, CD_2Cl_2 , 293K) for this solid did not allow to assign signals of complex **11** unequivocally. $^{31}\text{P}\{^1\text{H}\}$ NMR (202.461 MHz, CD_2Cl_2 , 173K): 44.5 (s), 43.5 (s), 40.6 (s), 18.7 (d, $^1J_{\text{P-Ag}} = 678$ Hz, $^1J_{\text{P-Ag}} = 585$ Hz), 10.7 (d, $^1J_{\text{P-Ag}} = 346$ Hz), 6.0 (d, $^1J_{\text{P-Ag}} = 327$ Hz) ppm. MS MALDI+ DCTB: $m/z = 966.1$ [(CNC)(PPh₃)PdAg(PPh₃)]⁺, 598.1 [[Pd(CNC)(PPh₃)]+H]⁺.

1.5. References

- (1) Perez-Temprano, M. H.; Casares, J. A.; Espinet, P. Bimetallic Catalysis using Transition and Group 11 Metals: An Emerging Tool for C-C Coupling and Other Reactions. *Chem. Eur. J.* **2012**, *18* (7), 1864-1884. DOI: 10.1002/chem.201102888.
- (2) Pye, D. R.; Mankad, N. P. Bimetallic catalysis for C-C and C-X coupling reactions. *Chem. Sci.* **2017**, *8* (3), 1705-1718. DOI: 10.1039/c6sc05556g.
- (3) Deolka, S.; Rivada-Wheelaghan, O.; Aristizábal, S. L.; Fayzullin, R. R.; Pal, S.; Nozaki, K.; Khaskin, E.; Khusnutdinova, J. R. Metal-metal cooperative bond activation by heterobimetallic alkyl, aryl, and acetylide Pt^{II}/Cu^I complexes. *Chem. Sci.* **2020**, *11* (21), 5494-5502. DOI: 10.1039/D0SC00646G.
- (4) Kim, U. B.; Jung, D. J.; Jeon, H. J.; Rathwell, K.; Lee, S.-g. Synergistic Dual Transition Metal Catalysis. *Chem. Rev.* **2020**, *120* (24), 13382-13433. DOI: 10.1021/acs.chemrev.0c00245.
- (5) Pérez-Temprano, M. H.; Casares, J. A.; de Lera, Á. R.; Álvarez, R.; Espinet, P. Strong Metallophilic Interactions in the Palladium Arylation by Gold Aryls. *Angew. Chem. Int. Ed.* **2012**, *51* (20), 4917-4920. DOI: 10.1002/anie.201108043.
- (6) Oeschger, R. J.; Chen, P. Structure and Gas-Phase Thermochemistry of a Pd/Cu Complex: Studies on a Model for Transmetalation Transition States. *J. Am. Chem. Soc.* **2017**, *139* (3), 1069-1072. DOI: 10.1021/jacs.6b12152.
- (7) Oeschger, R. J.; Chen, P. A Heterobimetallic Pd-Zn Complex: Study of a d⁸-d¹⁰ Bond in Solid State, in Solution, and in Silico. *Organometallics* **2017**, *36* (8), 1465-1468. DOI: 10.1021/acs.organomet.7b00113.
- (8) Oi, M.; Takita, R.; Kanazawa, J.; Muranaka, A.; Wang, C.; Uchiyama, M. Organocopper cross-coupling reaction for C-C bond formation on highly sterically hindered structures. *Chem. Sci.* **2019**, *10* (24), 6107-6112. DOI: 10.1039/C9SC00891H.
- (9) Rivada-Wheelaghan, O.; Comas-Vives, A.; Fayzullin, R. R.; Lledós, A.; Khusnutdinova, J. R. Dynamic Pd^{II}/Cu^I Multimetallic Assemblies as Molecular Models to Study Metal-Metal Cooperation in Sonogashira Coupling. *Chem. Eur. J.* **2020**, *26* (53), 12168-12179. DOI: 10.1002/chem.202002013.
- (10) Wang, J.; Zhan, L.; Wang, G.; Wei, Y.; Shi, M.; Zhang, J. Pd-promoted cross coupling of iodobenzene with vinylgold *via* an unprecedented phenyl

- transmetalation from Pd to Au. *Chem. Commun.* **2020**, 56 (46), 6213-6216. DOI: 10.1039/D0CC02645J.
- (11) Moret, M.-E.; Chen, P. Interaction of Organoplatinum(II) Complexes with Monovalent Coinage Metal Triflates. *J. Am. Chem. Soc.* **2009**, 131 (15), 5675-5690. DOI: 10.1021/ja900449y.
- (12) Moret, M.-E.; Serra, D.; Bach, A.; Chen, P. Transmetalation Supported by a Pt^{II}-Cu^I Bond. *Angew. Chem. Int. Ed.* **2010**, 49 (16), 2873-2877. DOI: 10.1002/anie.200906480.
- (13) Serra, D.; Moret, M.-E.; Chen, P. Transmetalation of Methyl Groups Supported by Pt^{II}-Au^I Bonds in the Gas Phase, in Silico, and in Solution. *J. Am. Chem. Soc.* **2011**, 133 (23), 8914-8926. DOI: 10.1021/ja110405q.
- (14) Oeschger, R. J.; Ringger, D. H.; Chen, P. Gas-Phase Investigations on the Transmetalation Step in Sonogashira Reactions. *Organometallics* **2015**, 34 (15), 3888-3892. DOI: 10.1021/acs.organomet.5b00491.
- (15) Paenurk, E.; Gershoni-Poranne, R.; Chen, P. Trends in Metallophilic Bonding in Pd-Zn and Pd-Cu Complexes. *Organometallics* **2017**, 36 (24), 4854-4863. DOI: 10.1021/acs.organomet.7b00748.
- (16) Baya, M.; Belío, Ú.; Fernandez, I.; Fuertes, S.; Martín, A. Unusual Metal-Metal Bonding in a Dinuclear Pt-Au Complex: Snapshot of a Transmetalation Process. *Angew. Chem. Int. Ed.* **2016**, 55 (24), 6978-6982. DOI: 10.1002/anie.201602081.
- (17) Baya, M.; Belío, U.; Campillo, D.; Fernandez, I.; Fuertes, S.; Martín, A. Pt-M Complexes (M=Ag, Au) as Models for Intermediates in Transmetalation Processes. *Chem. Eur. J.* **2018**, 24 (52), 13879-13889. DOI: 10.1002/chem.201802542.
- (18) Rajabi, S.; Jamali, S.; Naseri, S.; Jamjah, A.; Kia, R.; Samouei, H.; Mastroilli, P.; Shahsavari, H. R.; Raithby, P. R. Pt-M (M = Au and Tl) Dative Bonds Using Bis(cyclometalated)platinum(II) Complexes. *Organometallics* **2019**, 38 (8), 1709-1720. DOI: 10.1021/acs.organomet.8b00907.
- (19) Reitsamer, C.; Schuh, W.; Kopacka, H.; Wurst, K.; Peringer, P. Synthesis and Structure of the First Heterodinuclear PCP-Pincer-CDP Complex with a Pd-Au d⁸-d¹⁰ Pseudo-Closed-Shell Interaction. *Organometallics* **2009**, 28 (22), 6617-6620. DOI: 10.1021/om900686r.
- (20) Crespo, O.; Gimeno, M. C.; Laguna, A.; Lehtonen, O.; Ospino, I.; Pyykkö, P.; Villacampa, M. D. Structural and Photophysical Study on Heterobimetallic

- Complexes with d^8 – d^{10} Interactions Supported by Carborane Ligands: Theoretical Analysis of the Emissive Behaviour. *Chem. Eur. J.* **2014**, *20* (11), 3120-3127. DOI: 10.1002/chem.201303735.
- (21) Vicente, J.; Chicote, M. T.; Saura-Llamas, I.; Turpin, J.; Fernandez-Baeza, J. Keto-stabilized phosphorus ylide gold(I) and gold(III) complexes. *J. Organomet. Chem.* **1987**, *333* (1), 129-137. DOI: 10.1016/S0022-328X(00)99038-7.
- (22) Monkowius, U.; Zabel, M.; Fleck, M.; Yersin, H. Gold(I) Complexes Bearing P∩N-Ligands: An Unprecedented Twelve-membered Ring Structure Stabilized by Aurophilic Interactions *Z. Naturforsch. B* **2009**, *64* (11-12), 1513-1524. DOI: 10.1515/znb-2009-11-1235.
- (23) Hashmi, A. S. K.; Hengst, T.; Lothschütz, C.; Rominger, F. New and Easily Accessible Nitrogen Acyclic Gold(I) Carbenes: Structure and Application in the Gold-Catalyzed Phenol Synthesis as well as the Hydration of Alkynes. *Adv. Synth. Catal.* **2010**, *352* (8), 1315-1337. DOI: 10.1002/adsc.201000126.
- (24) Crespo, O.; Laguna, A.; Fernandez, E. J.; Lopez-de-Luzuriaga, J. M.; Jones, P. G.; Teichert, M.; Monge, M.; Pyykko, P.; Runeberg, N.; Schutz, M.; Werner, H. J. Experimental and Theoretical Studies of the d^8 - d^{10} Interaction Between Pd(II) and Au(I): Bis(chloro[(phenylthiomethyl)diphenylphosphine]gold(I))-dichloropalladium(II) and Related Systems. *Inorg. Chem.* **2000**, *39* (21), 4786-4792. DOI: 10.1021/ic000420p.
- (25) Gericke, R.; Bennett, M. A.; Privér, S. H.; Bhargava, S. K. Formation of Heterobimetallic Complexes by Addition of d^{10} -Metal Ions to *cis*-[(dppe)M(κ C-2-C₆F₄PPh₂)₂] (M = Ni, Pd, and Pt). *Organometallics* **2017**, *36* (17), 3178-3188. DOI: 10.1021/acs.organomet.7b00145.
- (26) Goto, E.; Begum, R. A.; Ueno, C.; Hosokawa, A.; Yamamoto, C.; Nakamae, K.; Kure, B.; Nakajima, T.; Kajiwara, T.; Tanase, T. Electron-Deficient Pt₂M₂Pt₂ Hexanuclear Metal Strings (M = Pt, Pd) Supported by Triphosphine Ligands. *Organometallics* **2014**, *33* (8), 1893-1904. DOI: 10.1021/om401211d.
- (27) Berenguer, J. R.; Lalinde, E.; Moreno, M. T. Luminescent cyclometalated-pentafluorophenyl Pt^{II}, Pt^{IV} and heteropolynuclear complexes. *Coord. Chem. Rev.* **2018**, *366*, 69-90. DOI: 10.1016/j.ccr.2018.04.002.
- (28) Forniés, J.; Ibañez, S.; Martín, A.; Sanz, M.; Berenguer, J. R.; Lalinde, E.; Torroba, J. Influence of the Pt → Ag Donor-Acceptor Bond and Polymorphism on the Spectroscopic and Optical Properties of Heteropolynuclear

- Benzoquinolateplatinum(II) Complexes. *Organometallics* **2006**, *25* (18), 4331-4340. DOI: 10.1021/om0604526.
- (29) Forniés, J.; Ibañez, S.; Lalinde, E.; Martín, A.; Moreno, M. T.; Tsipis, A. C. Benzoquinolateplatinum(II) Complexes as Building Blocks in the Synthesis of Pt-Ag Extended Structures. *Dalton Trans.* **2012**, *41* (12), 3439-3451. DOI: 10.1039/c2dt11885h.
- (30) Campillo, D.; Belío, Ú.; Martín, A. New Pt → M (M = Ag or Tl) complexes based on anionic cyclometalated Pt(II) complexes. *Dalton Trans.* **2019**, *48* (10), 3270-3283. DOI: 10.1039/c9dt00121b.
- (31) Croix, C.; Balland-Longeau, A.; Allouchi, H.; Giorgi, M.; Duchêne, A.; Thibonnet, J. Organogold(I) complexes: Synthesis, X-ray crystal structures and aurophilicity. *J. Organomet. Chem.* **2005**, *690* (21), 4835-4843. DOI: 10.1016/j.jorganchem.2005.07.080.
- (32) Ferrer, M.; Gutiérrez, A.; Rodríguez, L.; Rossell, O.; Ruiz, E.; Engeser, M.; Lorenz, Y.; Schilling, R.; Gómez-Sal, P.; Martín, A. Self-Assembly of Heterometallic Metallomacrocycles via Ditopic Fluoroaryl Gold(I) Organometallic Metalloligands. *Organometallics* **2012**, *31* (4), 1533-1545. DOI: 10.1021/om201028q.
- (33) Wing-Wah Yam, V.; Cheung, K.-L.; Yip, S.-K.; Zhu, N. Synthesis, characterisation, electrochemistry and luminescence studies of 9-anthrylgold(I) complexes. *Photochem. Photobiol. Sci.* **2005**, *4* (1), 149-153. DOI: 10.1039/B410667A.
- (34) Fuertes, S.; Woodall, C. H.; Raithby, P. R.; Sicilia, V. Heteropolynuclear Pt(II)-M(I) Clusters with a C^NC Biscyclometalated Ligand. *Organometallics* **2012**, *31* (11), 4228-4240. DOI: 10.1021/om300170j.
- (35) Martín, A.; Belío, Ú.; Fuertes, S.; Sicilia, V. Luminescent PtAg Clusters Based on Neutral Benzoquinolate Cyclometalated Platinum Complexes. *Eur. J. Inorg. Chem.* **2013**, *2013* (12), 2231-2247. DOI: 10.1002/ejic.201201528.
- (36) Gimeno, M. C.; Laguna, A. Silver and Gold. In *Comprehensive Coordination Chemistry II*, McCleverty, J. A., Meyer, T. J. Eds.; Pergamon, 2003; pp 911-1145.
- (37) Lo, V. K.-Y.; Chan, A. O.-Y.; Che, C.-M. Gold and silver catalysis: from organic transformation to bioconjugation. *Org. Biomol. Chem.* **2015**, *13* (24), 6667-6680. DOI: 10.1039/C5OB00407A.

- (38) Vicente, J.; Chicote, M. T.; Huertas, S.; Bautista, D.; Jones, P. G.; Fischer, A. K. Mononuclear (Pd, Pt), Heterodinuclear (PdAg, PtAg), and Tetranuclear (Pd₂Ag₂, Pt₂Ag₂) 1,1-ethylenedithiolato Complexes. *Inorg. Chem.* **2001**, *40* (9), 2051-2057. DOI: 10.1021/ic000996e.
- (39) Alonso, E.; Forniés, J.; Fortuño, C.; Martín, A.; Orpen, A. G. Reactivity of [NBu₄][(C₆F₅)₂M(μ-PPh₂)₂M'(acac-O,O')] (M, M' = Pt, Pd) toward Silver Centers. Synthesis of Polynuclear Complexes Containing M–Ag Bonds (M = Pd, Pt). *Organometallics* **2003**, *22* (24), 5011-5019. DOI: 10.1021/om034047f.
- (40) Heckenroth, M.; Kluser, E.; Neels, A.; Albrecht, M. Neutral Ligands with Exceptional Donor Ability for Palladium-Catalyzed Alkene Hydrogenation. *Angew. Chem. Int. Ed.* **2007**, *46* (33), 6293-6296. DOI: 10.1002/anie.200702199.
- (41) Heckenroth, M.; Neels, A.; Garnier, M. G.; Aebi, P.; Ehlers, A. W.; Albrecht, M. On the Electronic Impact of Abnormal C4-Bonding in N-Heterocyclic Carbene Complexes. *Chem. Eur. J.* **2009**, *15* (37), 9375-9386. DOI: 10.1002/chem.200900249.
- (42) Micksch, M.; Herdtweck, E.; Strassner, T. Synthesis and Structure of a Trinuclear Pd-Ag-Pd Carbene Acetato Complex. *Z. Anorg. Allg. Chem.* **2013**, *639* (7), 1237-1241. DOI: 10.1002/zaac.201300158.
- (43) Agarwal, P.; Thomas, J. M.; Sivasankar, C.; Nethaji, M.; Thirupathi, N. Six-membered cyclopalladated N,N',N''-triarylguanidines, [κ^2 (C,N)Pd]₂(μ-OAc)(μ-Pz), [κ^2 (C,N)Pd(μ-Pz)]₂ and a novel [AgNO₃⊂{ κ^2 (C,N)Pd}₂(μ-NO₃)(μ-Pz)}]: Syntheses, reactivity studies, structural aspects, and solution behavior. *Polyhedron* **2016**, *117*, 679-694. DOI: 10.1016/j.poly.2016.07.008.
- (44) Arnal, L.; Fuertes, S.; Martín, A.; Sicilia, V. The Use of Cyclometalated NHCs and Pyrazoles for the Development of Fully Efficient Blue Pt^{II} Emitters and Pt/Ag Clusters. *Chem. Eur. J.* **2018**, *24* (37), 9377-9384. DOI: 10.1002/chem.201800646.

Chapter 2

Reactivity of platinum (II) and
palladium (II) cyclometallated
substrates towards sources of H⁺

Starting materials [Pt(CNC)(PPh₃)] (**1**) and [Pd(CNC)(PPh₃)] (**2**) can be regarded as Lewis bases that can be reacted towards other electrophiles (E) that act as Lewis acids, other than metals. As indicated in the introduction, the formation of M-E adducts can be the starting point for a transference process of the E group to ligands, with creation and breakage of bonds. One of such potential electrophiles suitable for study are hydrogen atoms with acidic characteristics. It is known that such kind of hydrogen atoms have an isolobal relationship with fragments “Au⁺ and Au(PPh₃)⁺”,¹⁻⁴ which is of interest given that both precursors **1** and **2** have shown to react with these gold fragments as described in Chapter 1.

Thus, in this chapter the reactivity of platinum and palladium starting materials [Pt(CNC)(PPh₃)] (**1**), [Pt(CNC)(dmsO)] (**12**)⁵ (dmsO = dimethylsulfoxide) and [Pd(CNC)(PPh₃)] (**2**) is investigated towards acidic substrates, namely, strong acids with coordinating or low-coordinating anions (hydrochloric, perchloric, tetrafluoroboric or trifluoromethanesulfonic acid) and organic ligands with acidic hydrogens. DFT calculations have been also performed to establish a possible mechanism for some of these reactions.

While the results corresponding to the reactions of with protic acids are discussed in Section 2.1, the reactivity of starting substrates towards organic ligands with acidic hydrogens is analyzed in Section 2.2.

2.1. Reactivity of platinum (II) and palladium (II) cyclometallated substrates towards protic acids

The reactions of [Pt(CNC)(PPh₃)] (**1**) and [Pd(CNC)(PPh₃)] (**2**) towards strong protic acids always lead to the cleavage of a Pt-C or Pd-C bond corresponding to one of the phenylene rings of the CNC ligand and the formation of a new C-H bond. The formed coordinative vacant in the metal can be occupied by the anion of the acid, if this has coordinating capabilities (HCl), or by other neutral dative molecules present in the reaction medium in the case of low-coordinating anions (HClO₄, HTfO and HBF₄·OEt₂). Thus, the Pt(II) and Pd(II) complexes resulting from these reactions are expected to be neutral or cationic depending on the acid used.

X-Ray diffraction studies were carried out for these three chloro complexes, [Pt(CNC-H)Cl(PPh₃)] (**13**), [Pd(CNC-H)Cl(PPh₃)] (**3**) and [Pt(CNC-H)Cl(dmsO)] (**14**) confirming that the protonation process had taken place. Figure 2.1 displays structures for **3**, **13** and **14** and Table 2.1 indicates selected distances and angles.

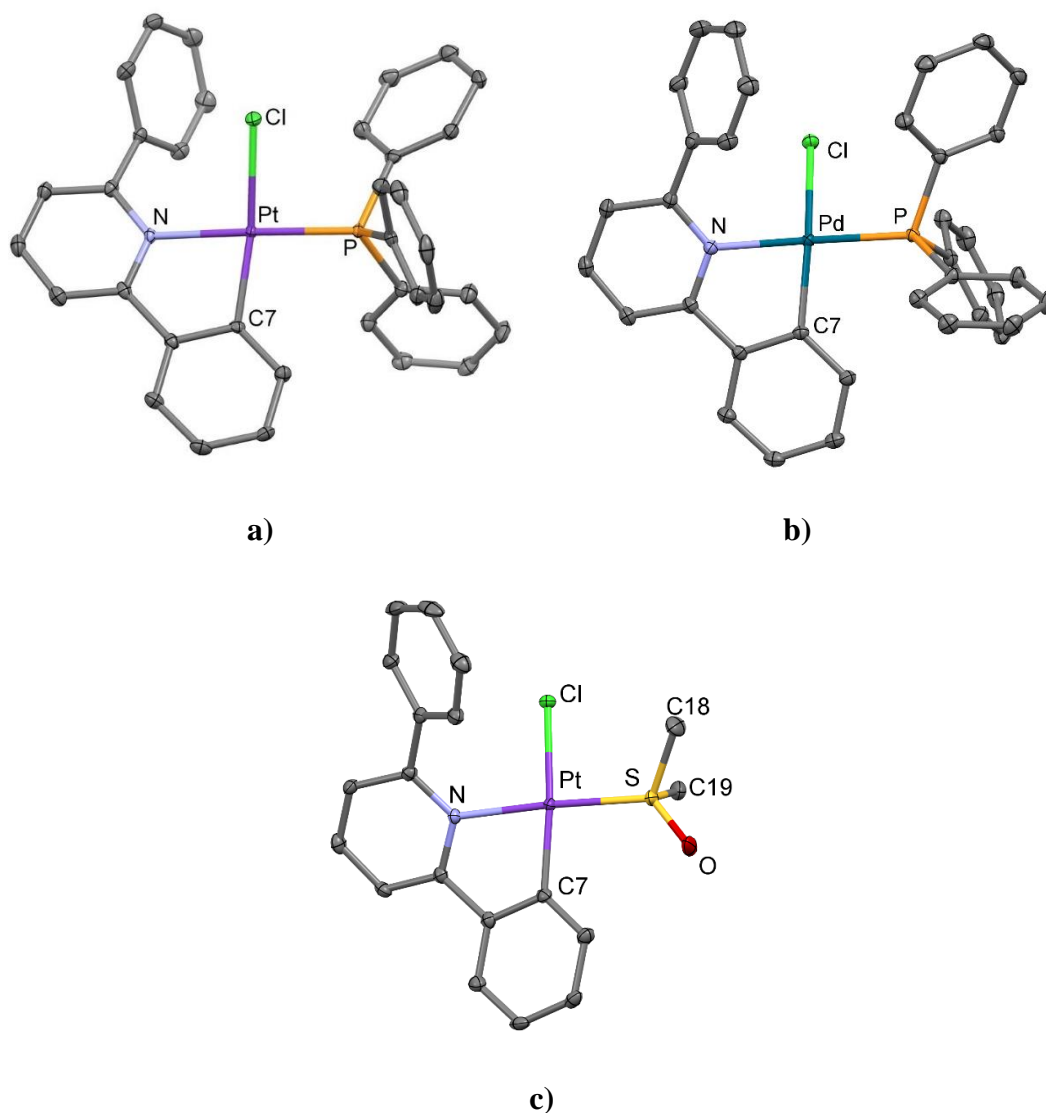


Figure 2.1. Molecular structures of complexes [Pt(CNC-H)Cl(PPh₃)] (**13**) (a), [Pd(CNC-H)Cl(PPh₃)] (**3**) (b) and [Pt(CNC-H)Cl(dmsO)] (**14**) (c).

Table 2.1. Selection of bond lengths (Å) and angles (°) for **3**, **13** and **14**.

	13 (M = Pt)	3 (M = Pd)	14 (M = Pt)
M-Cl	2.3640(7)	2.4182(5)	2.4177(8)
M-N	2.117(2)	2.103(2)	2.080(3)
M-C7	2.004(3)	2.001(2)	2.005(3)
M-P	2.2306(7)	2.2497(5)	-
Pt-S	-	-	2.2142(8)
C7-M-N	80.77(10)	80.99(7)	80.07(12)
C7-M-Cl	165.66(8)	153.80(6)	166.33(10)

Structures of complexes **13**, **3** and **14** can be described as mononuclear metallic complexes where the CNC-H ligand is coordinated in a bidentate way. The phenyl ring resulting from the protonation reaction, is not coplanar with respect to the platinum or palladium planes, no doubt due to steric factors. These rings show torsion angles with respect to the pyridine ring of 44.1 (**13**), 49.8 (**3**) and 36.4° (**14**). Furthermore, the coordination environment of the metallic centers is completed by a chloro ligand, which, possibly due to steric factors is not coplanar with the square planar M(II) environment (C7-M-Cl angles of *ca.* 166° for the platinum complexes **13** and **14** and around 154° for complex **3**). This ligand remains in the three cases *trans* to the cyclometallated carbon atom of the bidentate C^N ligand, as reported for several similar complexes in the literature.⁶⁻¹⁵ The fourth coordination position is completed by the triphenylphosphane ligand in **13** and **3** and by a S-coordinated dmsoligand in *trans* to the N of the pyridine ligand in **14**.

This *trans*-(N,P) disposition of [Pt(CNC-H)Cl(PPh₃)] (**13**) and [Pd(CNC-H)Cl(PPh₃)] (**3**) found for more complexes of this chapter, was examined through DFT calculations (see Computational details, Supporting Information), showing that these isomers are slightly more stable than the respective *trans*-(N,Cl) (around 5.8 and 3.9 kcal/mol respectively). This could be due to steric factors related with the bulkiness of the phosphane ligand, since this ligand in the *trans*-(N,Cl) isomer would be very close to the phenyl group of the CNC-H ligand. Furthermore, it should be noted that to render the

trans-(N,Cl) complexes, an isomerization process would be required after the protonation and creation of the vacant coordination site.

In the case of complex [Pt(CNC-H)Cl(dmsO)] (**14**), only the *trans*-(N,S) isomer was observed. There are several examples of similar Pt(II) complexes in the literature with this disposition of ligands.¹⁰⁻¹³ DFT calculations indicated that the *trans*-(N,S) isomer was 4.2 kcal/mol more stable than the not detected *trans*-(N,Cl) isomer.

The ¹H NMR spectra of complexes **3**, **13** and **14** are in agreement with their X-Ray structures. Thus, the signal patterns are more complex than the ones observed for the starting materials **1**, **2** and **12**. This is consistent with a lower degree of symmetry of the ligand CNC-H with respect to the CNC of the starting materials. Besides, the signal corresponding to a new hydrogen incorporated to the ligand is apparent (see Chart 2.1 for the numbering of the CNC-H ligand and Figures 2.2 and 2.3 for ¹H NMR spectra of [Pt(CNC-H)Cl(PPh₃)] (**13**) and [Pd(CNC-H)Cl(PPh₃)] (**3**)).

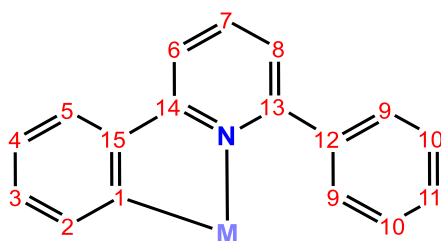


Chart 2.1. Numbering scheme of positions for bidentate C^N complexes.

The new phenyl ring shows three different signals, corresponding to H9 (characteristic signal at around 8.0 ppm), H10 and H11 with a relative integration of 2, 2 and 1 respectively. Furthermore, due to the now asymmetric ligand, H6 and H8 become inequivalent and show two different doublet signals at around 7.9 and 7.6 ppm.

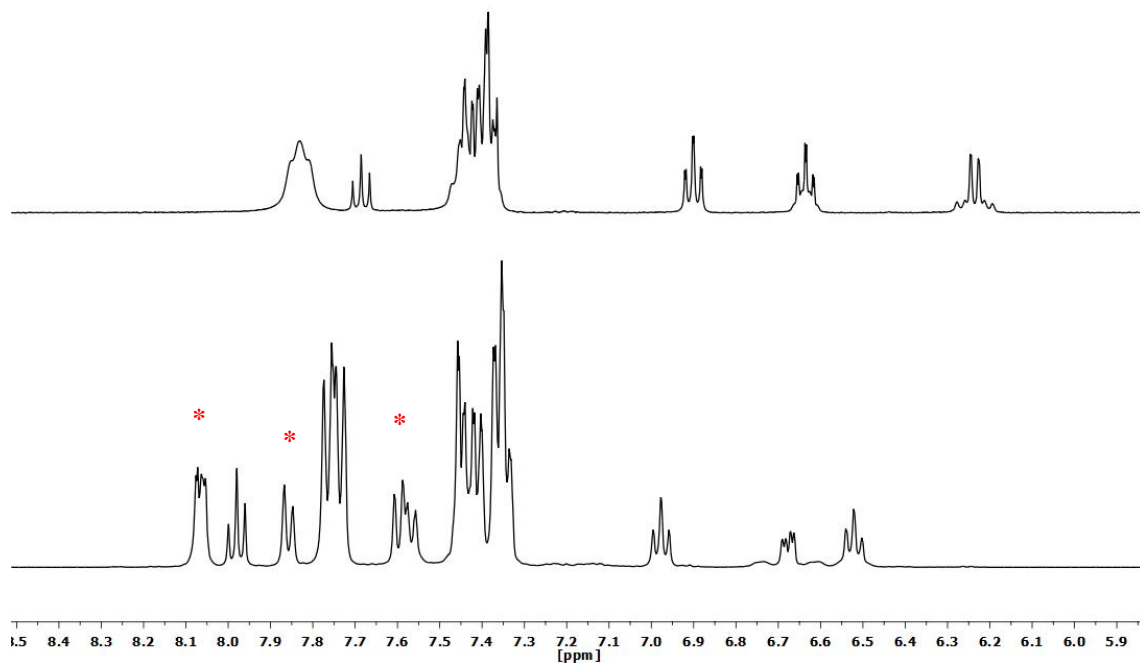


Figure 2.2. ¹H NMR spectra (CD₂Cl₂, RT) of [Pt(CNC)(PPh₃)] (**1**) (top) and [Pt(CNC-H)Cl(PPh₃)] (**13**) (bottom: red asterisks, H9, H6 and H8 signals).

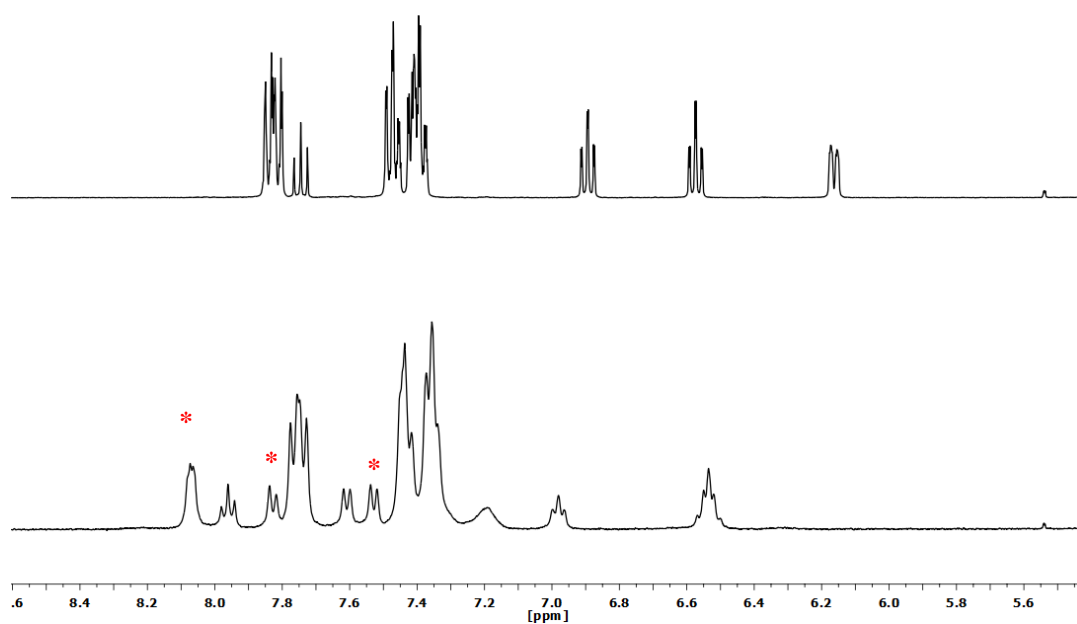


Figure 2.3. ¹H NMR spectra (CD₂Cl₂, RT) of [Pd(CNC)(PPh₃)] (**2**) (top) and [Pd(CNC-H)Cl(PPh₃)] (**3**) (bottom: red asterisks, H9, H6 and H8 signals).

The $^{31}\text{P}\{^1\text{H}\}$ NMR of $[\text{Pt}(\text{CNC-H})\text{Cl}(\text{PPh}_3)]$ (**13**) (see Figure S2.4, Supporting Information) shows a singlet signal corresponding to the phosphane ligand at 20.7 ppm with platinum satellites ($^1J_{\text{P-Pt}} = 4525$ Hz). This resonance value represents an upfield displacement of around 5 ppm with respect of the starting material. This upfield shift had also been previously observed for the Pd complex **3**.

On the other hand, the ^1H NMR spectrum of complex $[\text{Pt}(\text{CNC-H})\text{Cl}(\text{dmsO})]$ (**14**) reveals a more complex pattern of signals compared to that of starting substrate $[\text{Pt}(\text{CNC})(\text{dmsO})]$ (**12**) and a singlet with platinum satellites at 3.4 ppm ($^3J_{\text{Me-Pt}} = 25.0$ Hz), corresponding to the methyl groups of the dmsO ligand (see Figure 2.4). This signal shifted 0.2 ppm upfield with respect to the analogous one in the starting material.

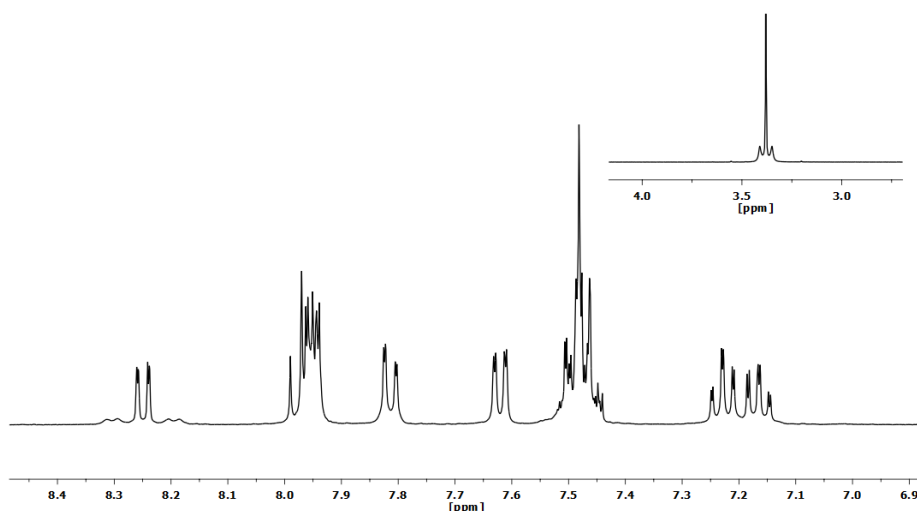


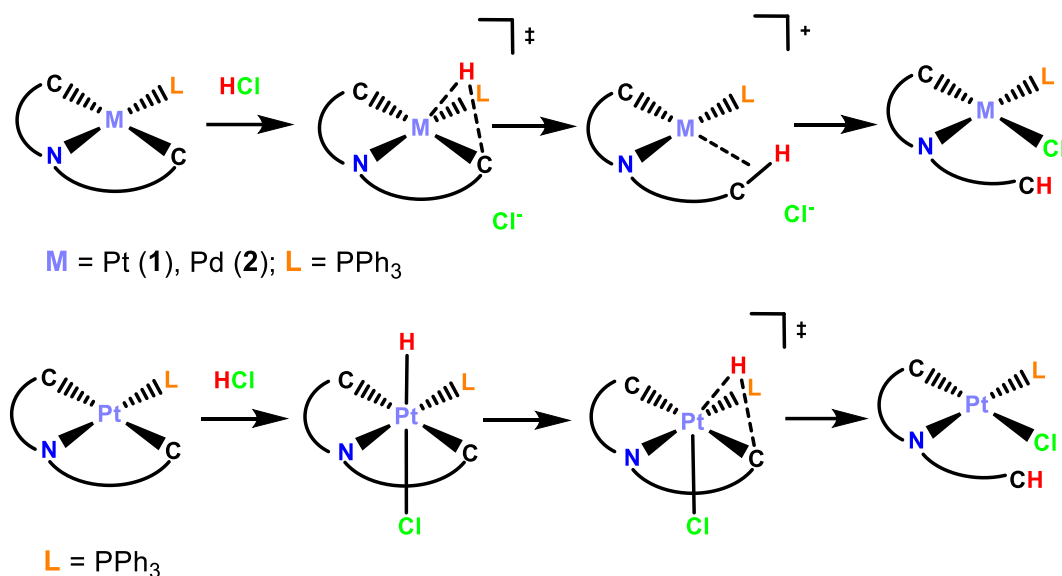
Figure 2.4. ^1H NMR spectrum (CD_2Cl_2 , RT) of complex $[\text{Pt}(\text{CNC-H})\text{Cl}(\text{dmsO})]$ (**14**).

In order to gain more knowledge on these reactions, DFT calculations were carried out to model one possible mechanism for the reaction of $[\text{Pt}(\text{CNC})(\text{PPh}_3)]$ (**1**) and $[\text{Pd}(\text{CNC})(\text{PPh}_3)]$ (**2**) with HCl in dichloromethane solution (see Scheme 2.3, top).

This way, the first modelled step was a transition state in which the proton is interacting with the metallic center and the C_{ipso} (CNC). Then, the protonation process takes place, with the release of a phenyl group giving rise to a coordinative vacant. Finally, the chlorine ligand coordinates, rendering the final product.

Interestingly, the energy profile of the mentioned mechanism showed that these processes are completely barrierless energetically, which is in agreement with the rapidity of the experimental reactions.

Another possible mechanism for this protonation reaction was studied for the formation of platinum complex **13** (see Scheme 2.3, bottom). It was computed for the formation of an octahedral Pt(IV) complex *via* oxidative addition of HCl, and subsequent reductive elimination of the hydrogen atom with the C_{ipso} (CNC) to render **13**. Analogously, it was also found energetically very favorable.



Scheme 2.3. Possible mechanisms modeled for the reaction with HCl.

2.1.2. Reactions with HClO₄, HTfO and HBF₄·OEt₂: formation of cationic species

With the intention to explore what kind of intermediates could intervene in the formation of these cyclometallated C^N complexes, reactivity of complex [Pt(CNC)(PPh₃)] (**1**) with an acid with a low-coordinating anion, HBF₄·OEt₂, was investigated through NMR. Thus, to a solution of 0.007 g of complex [Pt(CNC)(PPh₃)] (**1**) in dry CD₂Cl₂, 6 μL of HBF₄·OEt₂ were added, and its ¹H NMR spectrum recorded immediately. However, only the spectrum attributable to the protonation of one of the phenylene rings of **1** is observed (see Figure 2.5), indicating that this process is very fast and no intermediate could be detected in this experiment. Furthermore, only signals of Et₂O assigned to the HBF₄·OEt₂ reagent are observed.

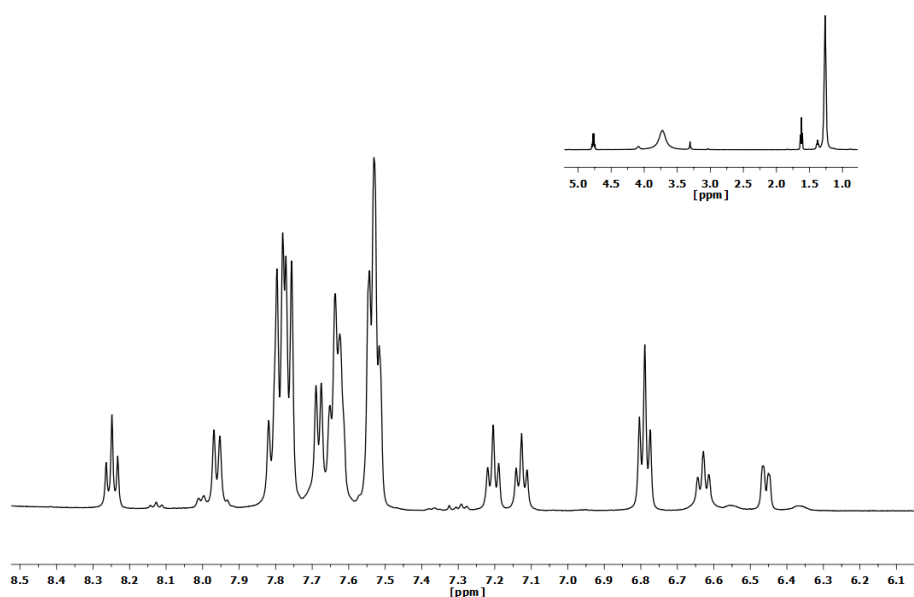


Figure 2.5. ^1H NMR spectrum (CD_2Cl_2 , RT) of the reaction of **1** with $\text{HBF}_4 \cdot \text{OEt}_2$.

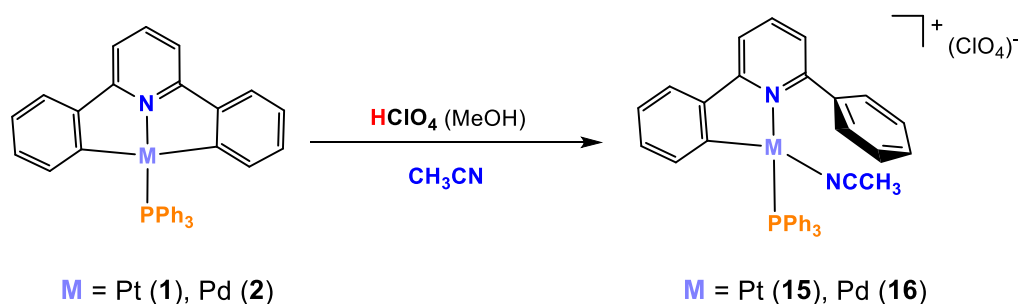
When two drops of acetonitrile are added to the same NMR tube, the formation of the later studied cationic complex $[\text{Pt}(\text{CNC}-\text{H})(\text{MeCN})(\text{PPh}_3)]^+$ (**15**) is identified (see Section 2.1.3 for a complete characterization of this complex).

All this behavior is consistent with the formation of a coordinative vacant due to the breaking of a Pt-C bond during the protonation of one of the rings in **1**. This free coordination site could be occupied either by diethylether or other molecules as water present in the solvent. The complex formed is not isolable and can only be observed in solution. Furthermore, only the addition of a better ligand as acetonitrile (which coordinates instantly), can result in the obtention of an isolable complex. Because of the rapidity of these reactions with acids, the detection of any intermediate was not possible. As indicated before, DFT calculations for the possible mechanism of this process indicate that it is barrierless.

In view of this result, the reactions of $[\text{M}(\text{CNC})(\text{PPh}_3)]$ ($\text{M} = \text{Pt}$ (**1**), Pd (**2**)) with HClO_4 or HTfO were performed in the presence of a ligand that could stabilize the free coordination site resulting from the protonation processes. Depending on the solvent used in the reaction or the additional ligand added to the mixture, the preparation of several cationic complexes with N, O and S-donor ligands was achieved. These complexes were characterized by IR, MS, multinuclear NMR and X-Ray diffraction studies.

2.1.3. Reactions in presence of acetonitrile

First, reaction of starting materials [Pt(CNC)(PPh₃)] (**1**) and [Pd(CNC)(PPh₃)] (**2**) with a methanolic solution of HClO₄ using MeCN as solvent (see Experimental section for details), gave rise to, as expected, protonation of a M-C_{ipso} (CNC) bond and the formation of bidentate cyclometallated complexes with formula [M(CNC-H)(MeCN)(PPh₃)](ClO₄) (M = Pt (**15**), Pd (**16**)) (see Scheme 2.4). IR spectra of these compounds (see Figures S2.16 and S2.24, Supporting Information) exhibited two small bands at around 2300 and 2290 cm⁻¹, that indicated the presence of acetonitrile.



Scheme 2.4. Synthesis of complexes **15** and **16**.

Good quality crystals of these complexes were grown in order to determine the structures of **15** and **16**. Figure 2.6 presents a view of both structures and Table 2.2 a selection of distances and angles.

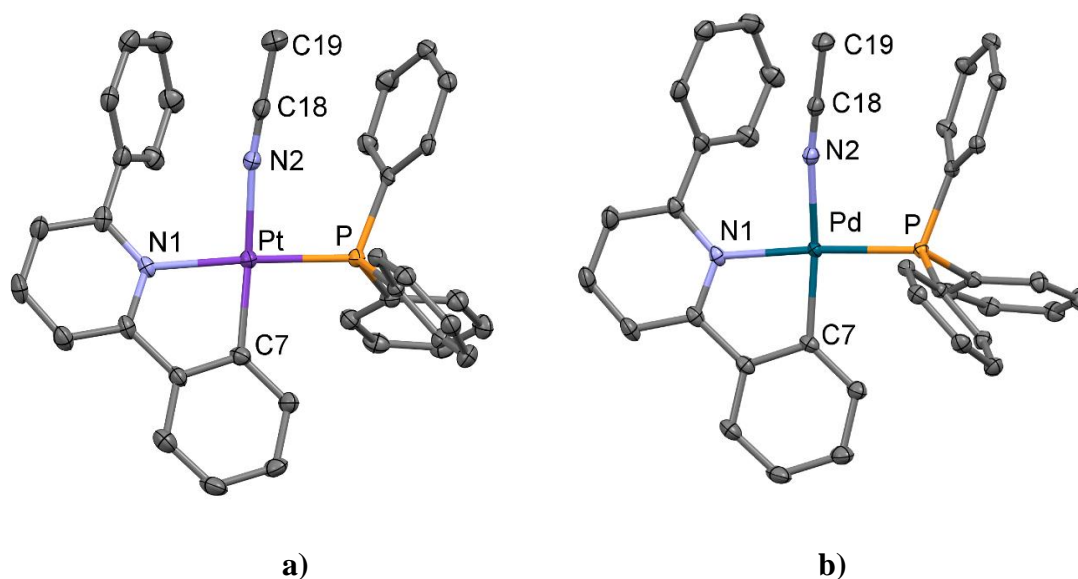


Figure 2.6. Molecular structures of cations of [Pt(CNC-H)(MeCN)(PPh₃)](ClO₄) (**15**) (a) and [Pd(CNC-H)(MeCN)(PPh₃)](ClO₄) (**16**) (b).

Table 2.2. Selection of bond lengths (Å) and angles (°) for **15** and **16**.

	15 (M = Pt)	16 (M = Pd)
M-N1	2.113(3)	2.1193(11)
M-N2	2.083(3)	2.1152(11)
M-C7	2.010(4)	2.0036(13)
M-P	2.2446(10)	2.2736(4)
N2-C18	1.127(5)	1.1392(18)
C18-C19	1.454(6)	1.4593(19)
C7-M-N2	167.37(14)	165.63(5)
M-N2-C18	171.6(3)	172.19(11)

The structures of cations $[\text{Pt}(\text{CNC-H})(\text{MeCN})(\text{PPh}_3)]^+$ and $[\text{Pd}(\text{CNC-H})(\text{MeCN})(\text{PPh}_3)]^+$ can be described as mononuclear square planar complexes, with a bidentate ligand $\text{C}^{\wedge}\text{N}$ occupying two coordination positions. Both structures are very similar regarding distances and angles. The N atom and the P atom of the phosphane ligand are located mutually *trans*. Also, the linear acetonitrile ligand is not coplanar with the metallic platinum or palladium plane, showing for **15** and **16** angles C7-M-N2 of 167.37(14) and 165.63(5)°.

The formation only of these *trans*-(N,P) complexes can be related again with the steric requirements of the phosphane. Similar reported complexes in the literature also display this disposition of ligands.^{16,17} Again, DFT calculations performed on these two systems show that their corresponding *trans*-(N,N) isomers would be around 9 kcal/mol higher in energy.

These complexes were also characterized by NMR experiments, confirming the protonation of one of the cyclometallated carbon atoms and the coordination of one molecule of acetonitrile to the metallic center. Thus, ^1H NMR spectra of complexes $[\text{Pt}(\text{CNC-H})(\text{MeCN})(\text{PPh}_3)](\text{ClO}_4)$ (**15**) and $[\text{Pd}(\text{CNC-H})(\text{MeCN})(\text{PPh}_3)](\text{ClO}_4)$ (**16**) display one multiplet around 7.9 ppm characteristic of the H9 of the phenyl ring (see

Chart 2.1) and one singlet around 1.1 ppm, identified as the methyl group of the acetonitrile coordinated molecule (see Figure 2.7).

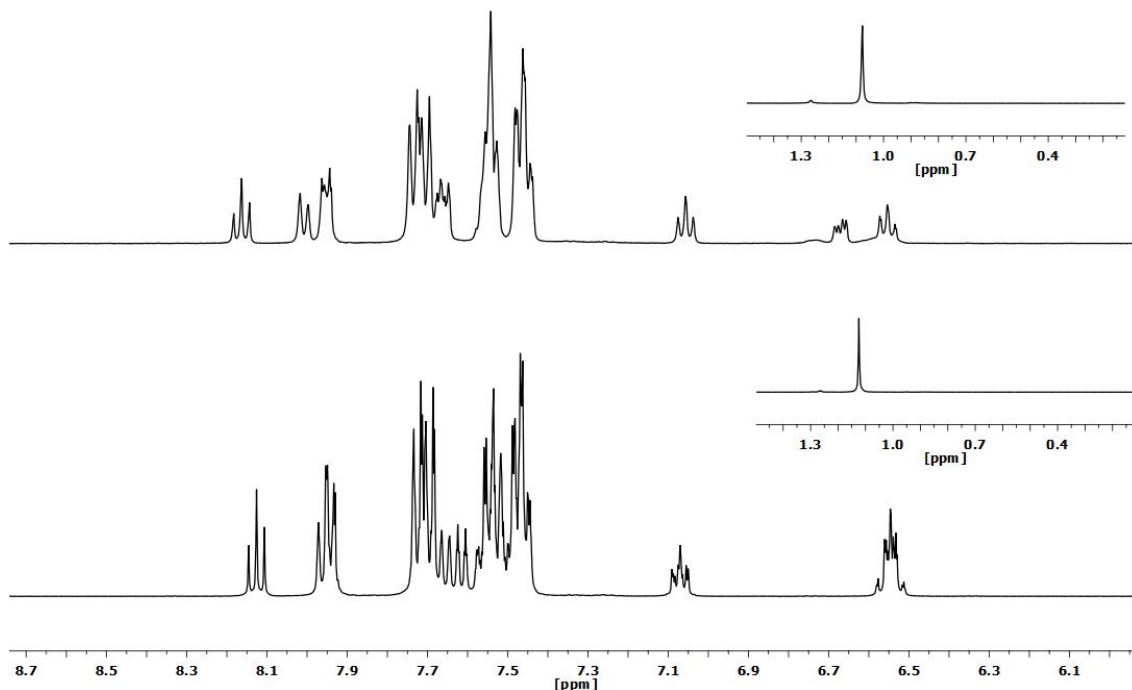


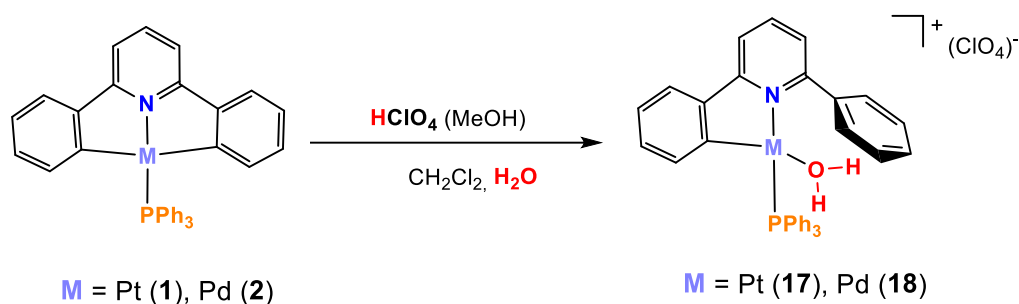
Figure 2.7. ^1H NMR spectra (CD_2Cl_2 , RT) of complexes $[\text{Pt}(\text{CNC-H})(\text{MeCN})(\text{PPh}_3)](\text{ClO}_4)$ (**15**) (top) and $[\text{Pd}(\text{CNC-H})(\text{MeCN})(\text{PPh}_3)](\text{ClO}_4)$ (**16**) (bottom).

The $^{31}\text{P}\{^1\text{H}\}$ NMR spectra of these complexes (see Figures S2.19 and S2.27, Supporting Information) are also consistent with the protonation process. Spectrum of **15** shows one singlet at 20.9 ppm with platinum satellites ($^1J_{\text{P-Pt}} = 4297$ Hz), while **16** displays one singlet at 43.3 ppm. These signals are displaced upfield 4 and 2 ppm with respect to those of $[\text{Pt}(\text{CNC})(\text{PPh}_3)]$ (**1**) and $[\text{Pd}(\text{CNC})(\text{PPh}_3)]$ (**2**), respectively. The value of the Pt-P coupling in $[\text{Pt}(\text{CNC-H})(\text{MeCN})(\text{PPh}_3)](\text{ClO}_4)$ (**15**) is again around 300 Hz larger with respect to the one observed for the starting material, as it was already observed for complex $[\text{Pt}(\text{CNC-H})\text{Cl}(\text{PPh}_3)]$ (**13**).

2.1.4. Reactions in presence of water

After having studied what happened to complexes $[\text{M}(\text{CNC})(\text{PPh}_3)]$ ($\text{M} = \text{Pt}$ (**1**), Pd (**2**)) when the solvent used was acetonitrile, the use of a low-coordinative solvent as CH_2Cl_2 in the presence of water was investigated. Thus, when a solution of HClO_4 in

MeOH was added to solutions of **1** and **2** in CH₂Cl₂ with 0.05 mL of water, after short times of reaction (see Experimental section for details), the formation of aquo compounds with formula [M(CNC-H)(H₂O)(PPh₃)](ClO₄) (M = Pt (**17**), Pd (**18**)) as isolable solids after workup took place (see Scheme 2.5). IR spectra of these solids (see Figures S2.32 and S2.36, Supporting Information) show a broad signal around 3100 cm⁻¹ typical for -OH groups.



Scheme 2.5. Synthesis of complexes **17** and **18**.

X-Ray diffraction studies were carried out on monocrystals of **17** and **18** (see Figure 2.8 for a view of both structures and Table 2.3 for some relevant distances and angles).

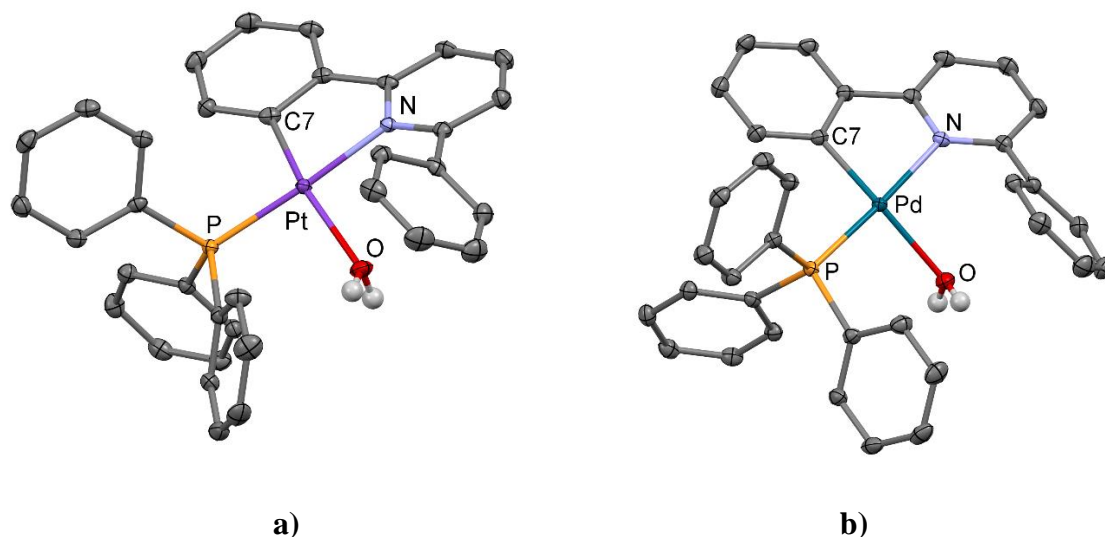


Figure 2.8. Molecular structures of the cations of [Pt(CNC-H)(H₂O)(PPh₃)](ClO₄) (**17**) (a) and [Pd(CNC-H)(H₂O)(PPh₃)](ClO₄) (**18**) (b).

Table 2.3. Selection of bond lengths (Å) and angles (°) for **17** and **18**.

	17 (M = Pt)	18 (M = Pd)
M-N	2.0975(18)	2.1008(11)
M-C7	1.991(2)	1.9894(13)
M-O	2.1870(18)	2.2011(11)
M-P	2.2358(6)	2.2629(4)
C7-M-O	162.58(9)	160.26(5)
C7-M-N	81.19(8)	81.52(5)

Thus, these structures depict mononuclear platinum and palladium compounds, exhibiting again a distorted square planar environment. Both structures show a bidentate C^N ligand with triphenylphosphane and an aquo ligands occupying the other two coordination positions, being the phosphane ligand *trans* to the N atom of the pyridine ring. This ligand environment has also been reported for several aquo complexes.^{18,19} The metal environment depicts a noticeable distortion from planarity, with values of around 160°. DFT calculations indicate that these *trans*-(N,P) complexes are around 15 kcal/mol more stable than their *trans*-(N,O) possible isomers, being in agreement with lesser steric repulsions.

The ¹H NMR spectra of [Pt(CNC-H)(H₂O)(PPh₃)](ClO₄) (**17**) and [Pd(CNC-H)(H₂O)(PPh₃)](ClO₄) (**18**) are in agreement with the structures (see Figure 2.9). Therefore, characteristic signal of H9 (see Chart 2.1) of **17** and **18** at around 7.9 ppm can be observed. Also, the existence of a singlet with integration of 2 at 1.8 and 1.6 ppm for **17** and **18** respectively, indicates the existence of a coordinated water molecule to the metallic center.

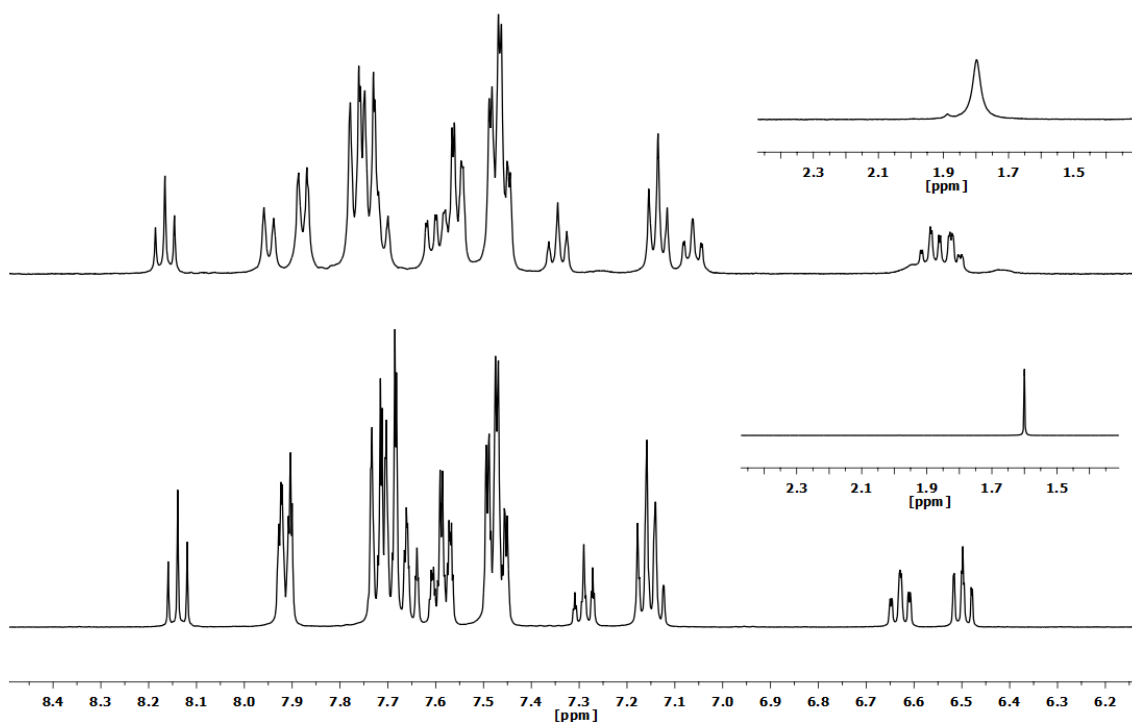


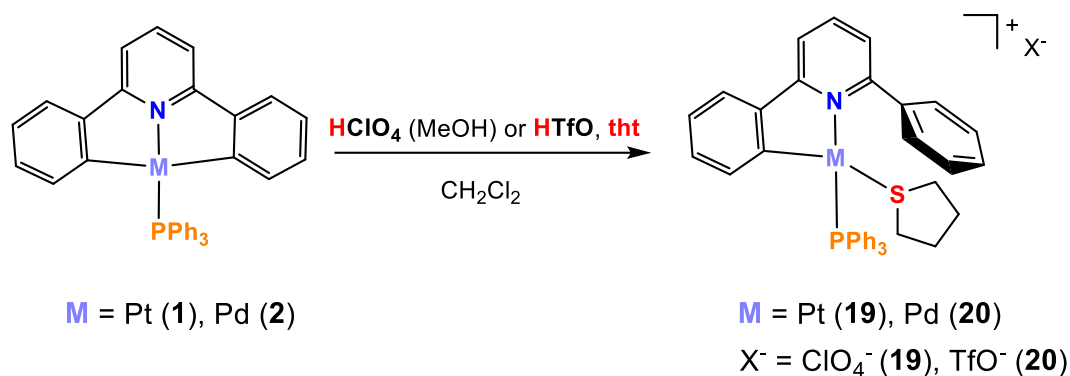
Figure 2.9. ^1H NMR spectra (CD_2Cl_2 , RT) of complexes $[\text{Pt}(\text{CNC-H})(\text{H}_2\text{O})(\text{PPh}_3)](\text{ClO}_4)$ (**17**) (top) and $[\text{Pd}(\text{CNC-H})(\text{H}_2\text{O})(\text{PPh}_3)](\text{ClO}_4)$ (**18**) (bottom).

The $^{31}\text{P}\{^1\text{H}\}$ NMR spectra of **17** and **18** show singlet signals, with platinum satellites in the case of **17** ($^1J_{\text{P-Pt}} = 4405$ Hz) (see Figures S2.34 and S2.39, Supporting Information). These signals again show upfield displacements with respect to the initial complexes **1** and **2** (around 2 and 5 ppm respectively). Again, Pt-P coupling in the signal of **17** is found around 300 Hz larger than the one in the starting substrate $[\text{Pt}(\text{CNC})(\text{PPh}_3)]$ (**1**).

It is noteworthy that $[\text{Pt}(\text{CNC-H})(\text{H}_2\text{O})(\text{PPh}_3)](\text{ClO}_4)$ (**17**) is not stable for long times in solution, decomposing in complex mixtures that prevent the recording of its ^{13}C NMR spectrum.

2.1.5. Reactions in presence of tetrahydrothiophene

Following the study of the synthesis of protonated complexes with different ligands, the reactions of the starting materials $[\text{Pt}(\text{CNC})(\text{PPh}_3)]$ (**1**) and $[\text{Pd}(\text{CNC})(\text{PPh}_3)]$ (**2**) with acids in the presence of a widely used S-donor ligand, such as tetrahydrothiophene (tht) were performed (see Scheme 2.6).



Scheme 2.6. Synthesis of complexes **19** and **20**.

Thus, the reaction of **1** with HClO_4 in CH_2Cl_2 in presence of an excess of tht gave rise to the complex formula $[\text{Pt}(\text{CNC-H})(\text{tht})(\text{PPh}_3)](\text{ClO}_4)$ (**19**). On the other hand, in the case of the palladium complex **2**, HTfO was chosen as a source of protons because the reaction with HClO_4 led to the formation of non-viable oily residues. However, the use of HTfO led to the formation of the sought after complex $[\text{Pd}(\text{CNC-H})(\text{tht})(\text{PPh}_3)](\text{TfO})$ (**20**) efficiently.

While the growing of suitable single crystals for X-Ray studies was successful for the Pt complex **19**, all the attempts for **20** were fruitless. Thus, the crystal structure of **19** is displayed in Figure 2.10 and a selection of distances and angles is listed in Table 2.4.

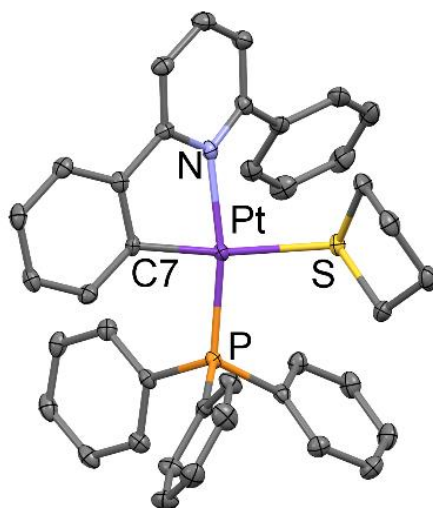


Figure 2.10. Molecular structure of the cation of $[\text{Pt}(\text{CNC-H})(\text{tht})(\text{PPh}_3)](\text{ClO}_4)$ (**19**).

Table 2.4. Selection of bond lengths (Å) and angles (°) for **19**.

Pt-N	2.110(2)	Pt-S	2.4221(7)
Pt-C7	2.020(3)	C7-Pt-N	80.12(10)
Pt-P	2.2380(7)	C7-Pt-S	161.95(8)

As expected, the structure of **19** corresponds to a square planar Pt(II) complex with a bidentate ligand C[^]N, resulting from the protonation of one of the phenylene rings. The coordinative vacant is occupied by the S atom of the incoming tht ligand. As in all the similar complexes described so far, the N and P atoms are located mutually *trans*, in agreement with some examples reported in the literature.²⁰⁻²² Also, the square planar environment of the metal atoms is somewhat distorted from the ideal geometry, with C7-Pt-N and C7-Pt-S angles of 80.12(10) and 161.95(8)°, respectively. This deviation from planarity could be due to the steric repulsions of the phenyl group and the tht ligand. This *trans*-(N,P) isomer is found to be 11 kcal/mol more stable than the *trans*-(N,S) isomer by DFT calculations, which is again in agreement with the existence of lesser steric repulsions in the *trans*-(N,P) isomer.

The ¹H NMR spectra of complexes [Pt(CNC-H)(tht)(PPh₃)](ClO₄) (**19**) and [Pd(CNC-H)(tht)(PPh₃)](TfO) (**20**) confirm the protonation of an aromatic cyclometallated carbon of the CNC tridentate ligand (see Figure 2.11). Also, the coordination of the tht ligand can be confirmed by the existence of two broad singlets with integration of 4 (2.1 and 1.6 ppm for **19**; 2.5 and 1.8 ppm for **20**), corresponding to the H α and H β of the tht ligand. Despite lowering the temperature of the sample, better resolved signals of tht could not be observed in NMR, and the broadness of the signals prevent the detection of any Pt-H coupling for **19**.

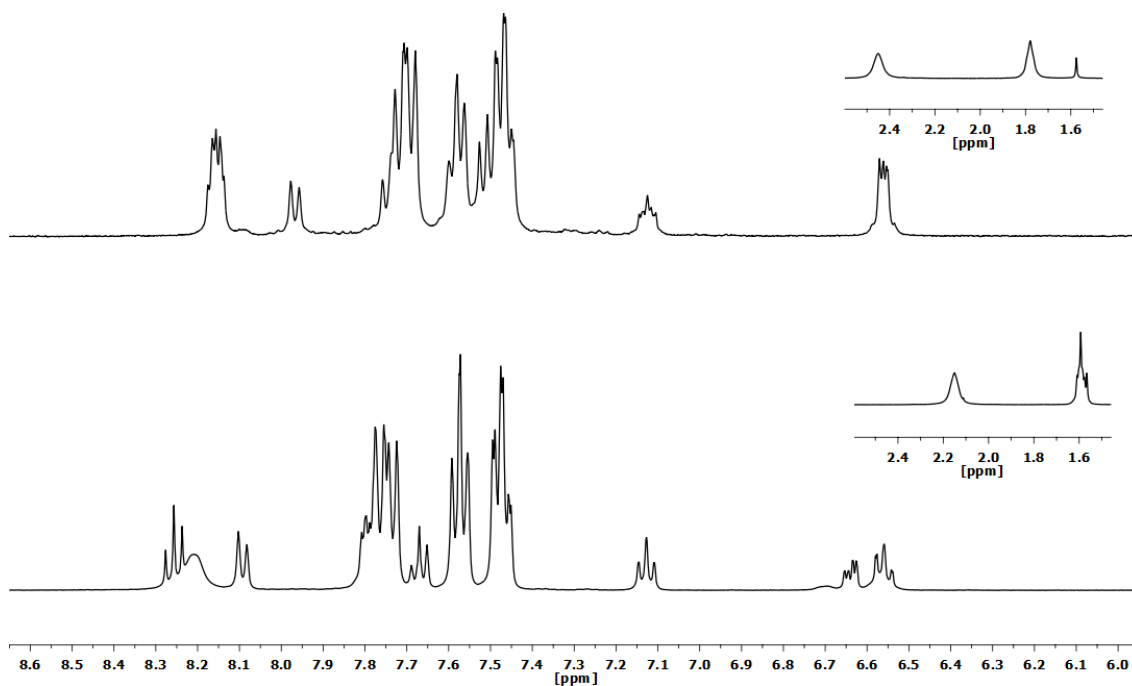


Figure 2.11. ^1H NMR spectra (CD_2Cl_2 , RT) of complexes $[\text{Pt}(\text{CNC-H})(\text{tth})(\text{PPh}_3)](\text{ClO}_4)$ (**19**) (top) and $[\text{Pd}(\text{CNC-H})(\text{tth})(\text{PPh}_3)](\text{TfO})$ (**20**) (bottom).

The $^{31}\text{P}\{^1\text{H}\}$ NMR spectra of **19** and **20** show singlet signals with platinum satellites for **19** ($^1J_{\text{P-Pt}} = 4353$ Hz) (see Figures S2.47 and S2.55, Supporting Information). As in previous cases, they appear upfield when compared to those of the starting substrates **1** and **2**. Also, Pt-P coupling is found to be around 300 Hz larger than in the starting substrate $[\text{Pt}(\text{CNC})(\text{PPh}_3)]$ (**1**).

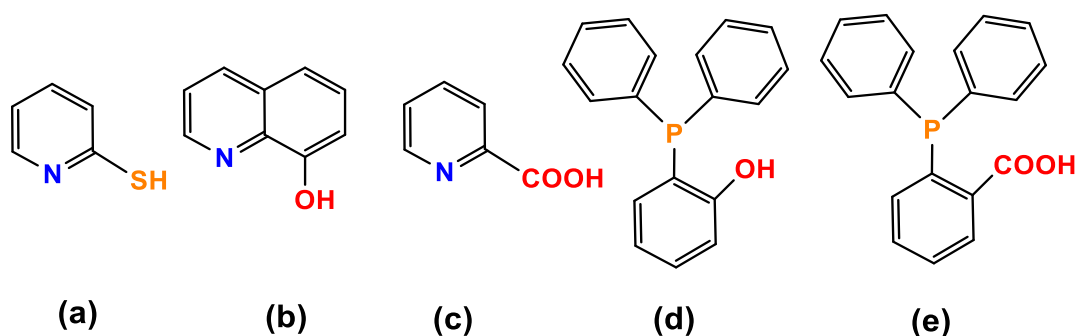
In this case, the Pd complex **20** is not very stable in solution and evolves to complex mixtures, and therefore, its ^{13}C NMR spectrum could not be recorded.

2.2. Reactivity of platinum (II) and palladium (II) cyclometallated substrates towards organic ligands with acidic hydrogens

After having examined the behavior of complexes $[\text{Pt}(\text{CNC})(\text{PPh}_3)]$ (**1**) and $[\text{Pd}(\text{CNC})(\text{PPh}_3)]$ (**2**) in the presence of protic acids, the investigation of the reactivity of platinum substrate $[\text{Pt}(\text{CNC})(\text{dmsO})]$ (**12**) towards some organic ligands with acidic hydrogens and donor atoms was carried out. Complex **12** was chosen for this task since dmsO is known to be a labile ligand whose substitution with other molecules with donor atoms seems to be facile.^{23,24} The application of this strategy to similar Pd substrates is

considerably handicapped by the lack to a synthetic route to the analogous starting complex “[Pd(CNC)(dmsO)]”. For this reason, [Pd(CNC)(PPh₃)] (**2**) was used as starting material when possible.

Thus, some appropriate ligands with -SH, -OH or -COOH functional groups and N- or P- donor atoms were selected (see Scheme 2.7), such as pyridine-2-thiol (a), 8-hydroxyquinoline (b), 2-pyridinecarboxylic acid (c), (2-hydroxyphenyl)diphenylphosphane (d) and 2-(diphenylphosphino)benzoic acid (e).

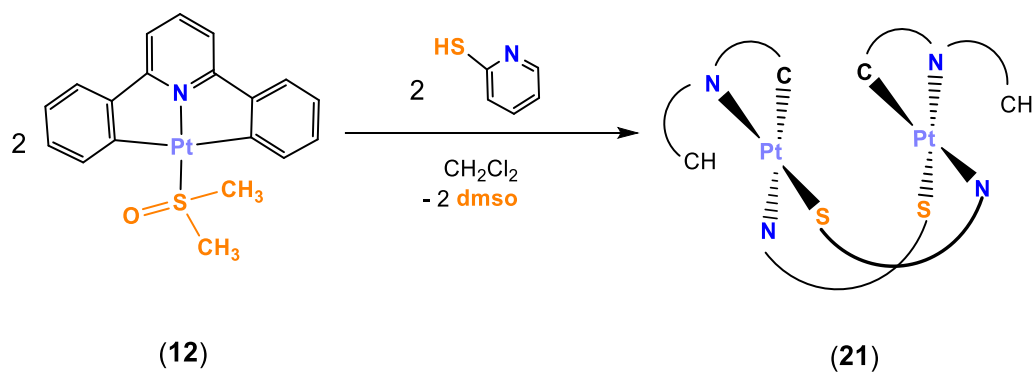


Scheme 2.7. Ligands with donor atoms and acidic hydrogens.

2.2.1. Reaction with a ligand with -SH group

The use of pyridine-2-thiolate (S-2Py) as a N⁺S bidentate ligand is widely reported in the literature.²⁴⁻²⁹ Thiol group of pyridine-2-thiol can be easily deprotonated in basic media to form *in situ* a thiolate that can bond to a metallic center. These acidic properties make this ligand a suitable candidate to be confronted with a basic platinum substrate. Besides, the nitrogen atom of the pyridine moiety enables this ligand to behave as a bidentate ligand, and therefore, it can act as a bridge between metallic centers, forming dinuclear complexes.^{26,28,30-35} Given that, the displacement of the dmsO ligand in complex [Pt(CNC)(dmsO)] (**12**) by pyridine-2-thiol can be attained either through its N- or S- donor atoms to the metallic center, *via* deprotonation of the thiol group.

Thus, the reaction of [Pt(CNC)(PPh₃)] (**1**) with an equimolar amount of pyridine-2-thiol was carried out in CH₂Cl₂ under argon for 1 hour (see Scheme 2.8), yielding an orange solid, whose IR and MS spectra (see Figures S2.58 and S2.61, Supporting Information) were consistent with the formula [Pt(CNC-H)(S-2Py)]₂ (**21**).



Scheme 2.8. Synthesis of complex **21**.

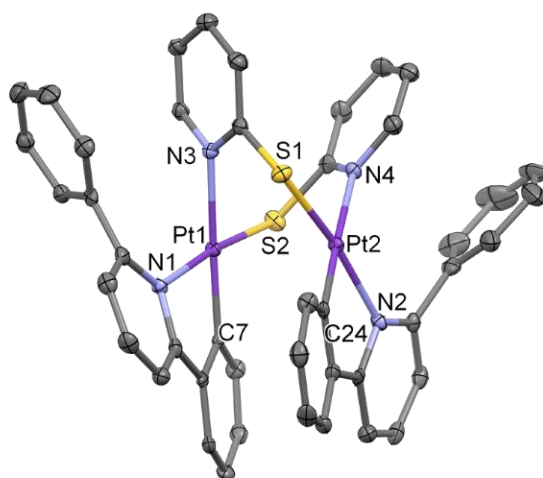


Figure 2.12. Molecular structure of complex $[\text{Pt}(\text{CNC-H})(\mu\text{-S-2Py})]_2$ (**21**).

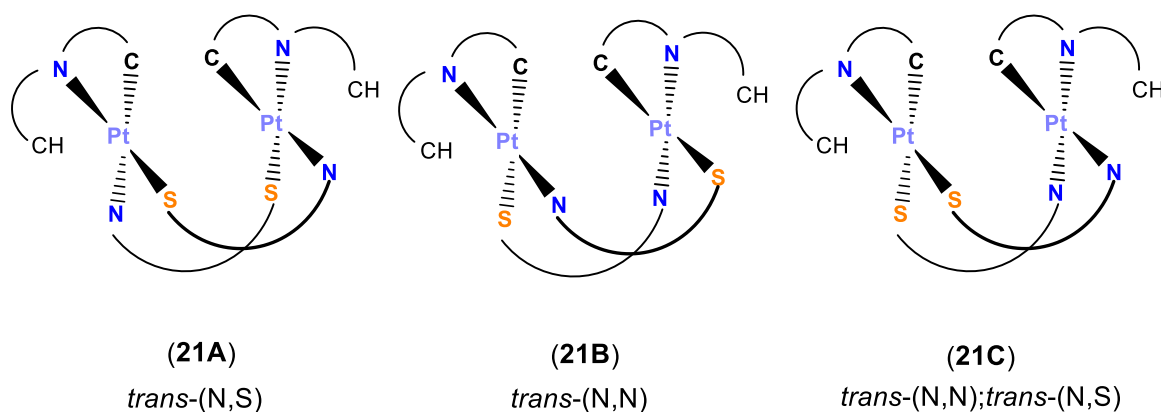
Table 2.5. Selection of bond lengths (Å) and angles (°) for **21**.

Pt1-N1	2.082(4)	Pt2-N4	2.160(4)
Pt2-N2	2.086(4)	Pt1-Pt2	3.0149(3)
Pt1-C7	1.998(5)	N1-Pt1-C7	80.5(2)
Pt2-C24	1.977(5)	N2-Pt2-C24	80.3(2)
Pt1-S2	2.2799(14)	C7-Pt1-N3	177.9(2)
Pt2-S1	2.2801(14)	C24-Pt2-N4	176.1(2)
Pt1-N3	2.162(4)		

The X-Ray diffraction structure of **21** (see Figure 2.12 and Table 2.5) reveals that it is a dinuclear complex, where two “[Pt(CNC-H)]” subunits are symmetrically bridged

with two pyridine-2-thiolate ligands through their N and S atoms. These subunits bear phenyl rings resulting of the protonation of a C_{ipso} of the CNC ligand previously coordinated in a tridentate fashion. Thus, the square planar environment of the platinum centers is completed with a nitrogen or sulfur atom of different thiolate ligands. In both subunits S atoms are located *trans* to the N atoms of the C^N ligands and the N atoms of the pyridine-2-thiolate ligands are situated *trans* to the C7 atoms of the C^N ligands. This disposition of ligands has been previously observed for other platinum (II) dinuclear complexes in the literature.^{30,33-35}

In principle, apart from the one observed in the X-Ray structure (symmetrical *trans*-(N,S)), two other possible isomers could be envisaged (see Scheme 2.9). Another symmetrical one with a *trans*-(N,N) disposition in both metallic units (**21B**), and an unsymmetrical one with a *trans*-(N,N) disposition for one Pt and a *trans*-(N,S) for the other (**21C**).



Scheme 2.9. Possible isomers of complex **21**.

DFT calculations indicate that the symmetrical **21A** according to the X-Ray structure is 7 kcal/mol more stable than the unsymmetrical **21C** and 15 kcal/mol more stable than the symmetrical **21B**.

The ¹H NMR spectrum of the solid (see Figure 2.13) displays a complex pattern of signals whose integration indicates that a hydrogen is incorporated to a phenylene ring of the CNC ligand of complex [Pt(CNC)(dmsO)] (**12**), showing the characteristic signal of H9 at 8.3 ppm. The absence of a signal with platinum satellites corresponding to the methyl groups of a dmsO molecule at around 3.6 ppm points out that substitution of this ligand has taken place. Less intense signals due to the possible existence of other possible isomers are also observed. Those signals increase their intensities when the same NMR

sample tube is measured 24 hours later. A possible explanation for this observation would be that the signals obtained in a freshly prepared sample of the solid correspond to a kinetic isomer which would evolve after some time to a thermodynamic one, causing the signals observed after 24 hours and which, most likely, gives rise to the observed X-Ray crystal structure.

Furthermore, it seems that this complex is quite unstable for longer times, since more new signals appear giving a very complex ^1H NMR pattern. Indeed, it has been reported that similar platinum (II) dinuclear complexes with $\text{S}^{\wedge}\text{N}$ ligands can be oxidized in haloforms and in presence of light.³⁶

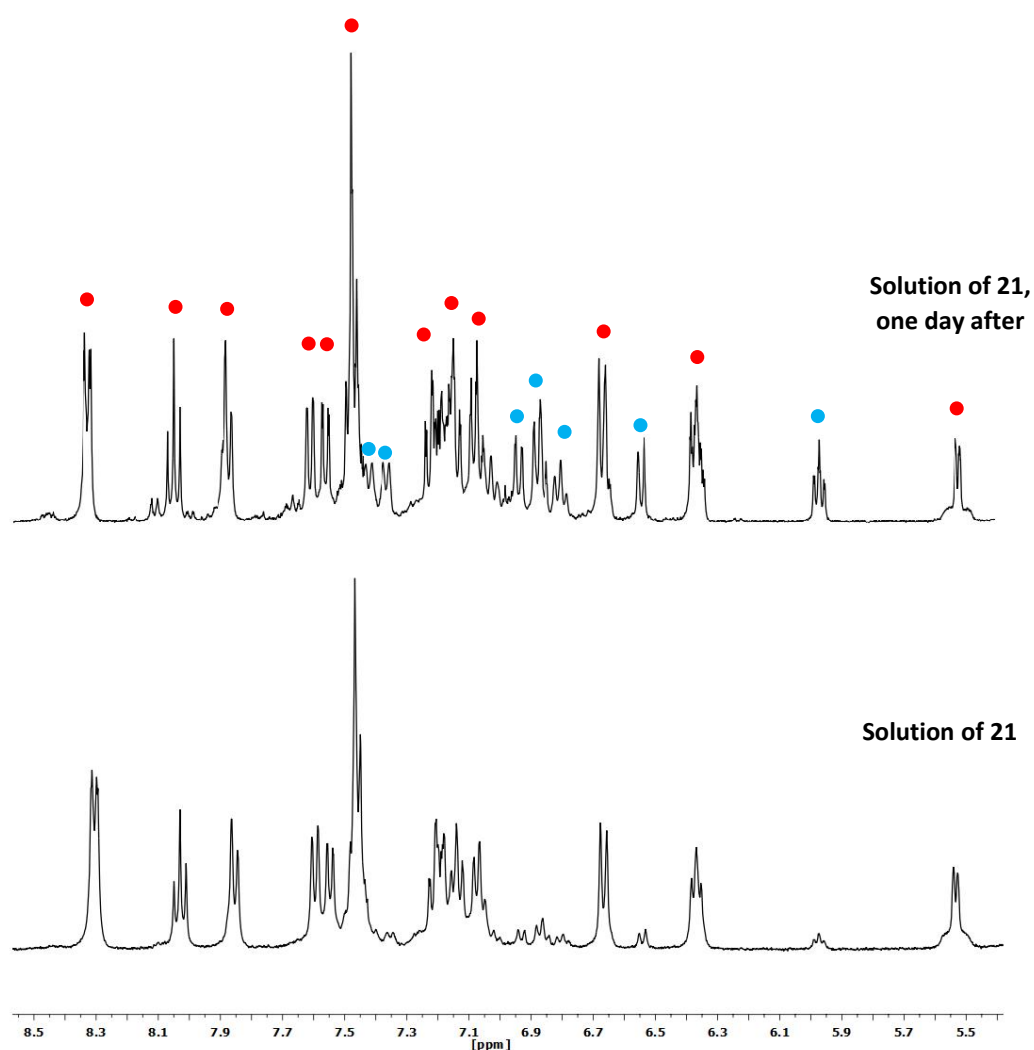
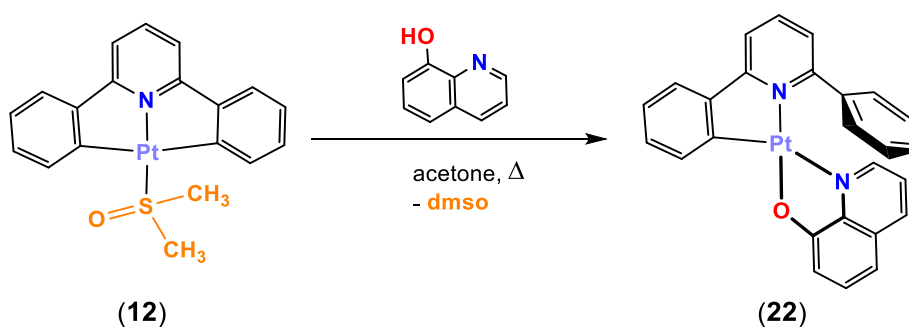


Figure 2.13. ^1H NMR spectra (CD_2Cl_2 , RT) of complex $[\text{Pt}(\text{CNC-H})(\text{S-2Py})]_2$ (**21**) (top: red and blue circles, two different sets of signals).

2.2.2. Reactions with ligands with -OH groups

Following this line of work, some P- (phosphane) or N- (pyridine) donor ligands, with an -OH group in a suitable position, were used. These ligands are *a priori* good candidates to substitute the dmsoligand of complex [Pt(CNC)(dmsol)] (**12**) and possibly form chelate rings which could stabilize the resulting compounds. Thus, 8-hydroxyquinoline (8-hqH) (Scheme 2.7, b) and (2-hydroxyphenyl)diphenylphosphane (Scheme 2.7, d) were studied as acidic substrates bearing a -OH group which could react with the platinum substrate **12**.

Reaction of **12** with 8-hydroxyquinoline was more problematic than expected. Displacement of S-donor dmsoligand by pyridines bearing -OH or -COOH groups (see below) was difficult, being necessary to keep the reaction solutions during several hours under reflux. Hence, [Pt(CNC)(dmsol)] (**12**) was reacted with 8-hydroxyquinoline in reflux of acetone for 21 hours. Shorter times of reaction resulted in high proportions of unreacted starting product **12**. After work up an orange solid with formula [Pt(CNC-H)(8-hq)] (**22**) was obtained (see Scheme 2.10).



Scheme 2.10. Synthesis of complex **22**.

X-Ray diffraction confirmed the formula of complex [Pt(CNC-H)(8-hq)] (**22**) (see Figure 2.14 for a view of the complex and Table 2.6 for a selection of distances).

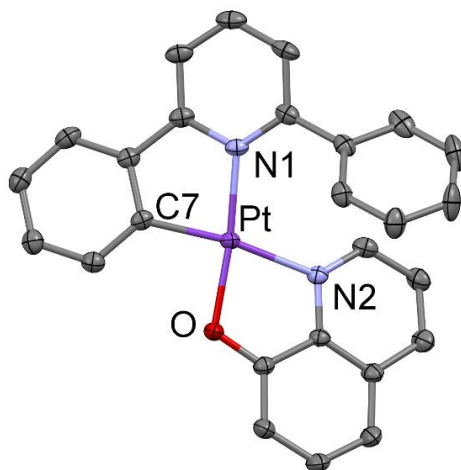
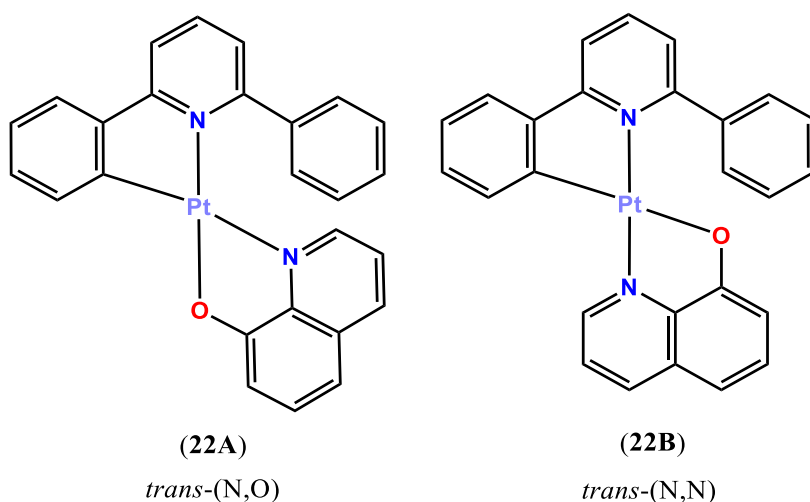


Figure 2.14. Molecular structure of complex [Pt(CNC-H)(8-hq)] (**22**).

Table 2.6. Selection of bond lengths (Å) and angles (°) for **22**.

Pt-N1	2.040(3)	Pt-N2	2.142(3)
Pt-C7	1.969(4)	C7-Pt-N2	164.43(14)
Pt-O	2.015(3)	O-Pt-N1	170.31(12)

The structure confirms the expected formula. This complex results from the protonation of a phenyl ring of complex **12** and the substitution of the dmsol ligand by a 8-hq deprotonated ligand, giving rise to a five membered chelate ring. The structure shows a *trans*-(N,O) disposition (isomer **22A**). A *trans*-(N,N) configuration (isomer **22B**) (see Scheme 2.11) could also be possible.



Scheme 2.11. Possible isomers of **22**.

In this case, steric factors should not play a key factor on the formation of the complex, as the 8-hq ligand is relatively plane. From the ^1H NMR spectrum (see below), a remarkable quantity of the other possible isomer is detected. As a matter of fact, DFT calculations revealed that both isomers **22A** and **22B** are very similar in energy (**22A**, 2.0 kcal/mol more stable). In the literature, there are some examples for similar Pt(II) complexes with C^N ligands in which the *trans*-(N,N) configuration is preferred.³⁷⁻⁴⁰ Consequently, the ^1H NMR spectrum of this complex (see Figure 2.15) shows a very complicated pattern that suggests that the two isomers are present in proportions 3 to 1. The absence of the dmsO signal of **12** and the apparition of one doublet with platinum satellites at 9.1 ppm ($^3J_{\text{H-Pt}} = 47.7$ Hz) assigned to the 8-hq ligand, confirms that the reaction had taken place. When an NMR sample of complex **22** dissolved in acetonitrile was heated at 65°C for three days, no different integration or intensity of signals was observed. In this case, it was not possible with the NMR information to assign unequivocally each set of signals to each isomer.

Indeed, one should expect that the formation of the *trans*-(N,N) isomer **22B** should be the favored one, as the substitution of the dmsO molecule by the N atom of the pyridine ligand *trans* to the N of the CNC ligand must take place at first, and after that, the deprotonation and coordination of the O center in the coordinative vacant. The *trans*-(N,O) isomer **22A** might then be formed by isomerization of complex **22B**. In this case, even more difficult mechanisms could be proposed for the formation of **22A** and **22B**.

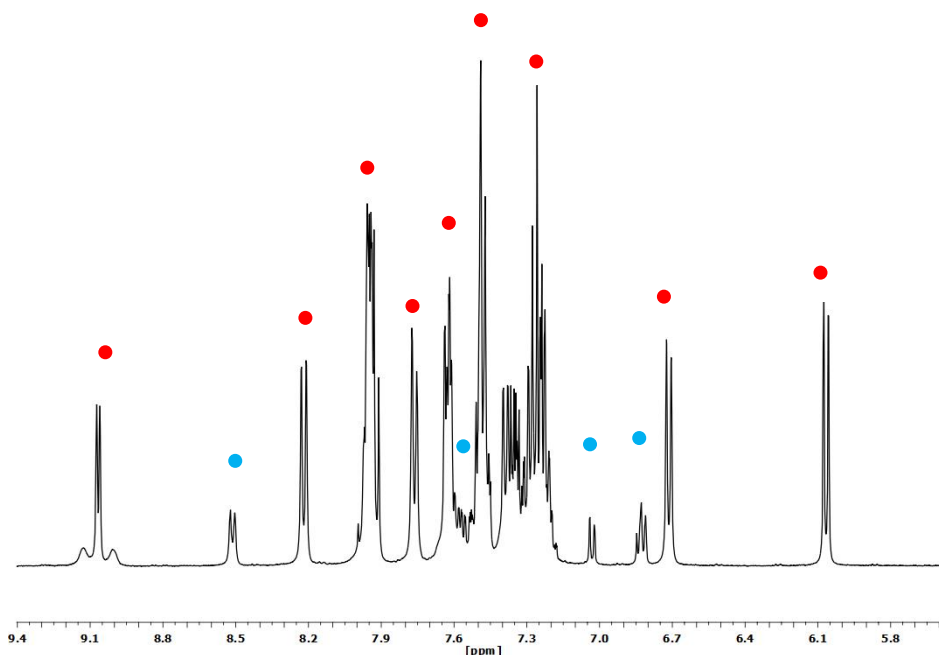
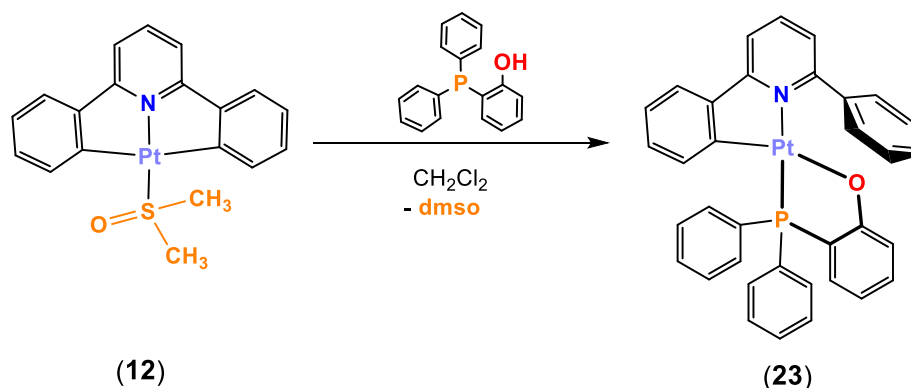


Figure 2.15. ^1H NMR spectrum (CD_2Cl_2 , RT) of complex $[\text{Pt}(\text{CNC-H})(8\text{-hq})]$ (**22**) (red and blue circles, signals of the two different isomers).

On the other hand, the reaction of $[\text{Pt}(\text{CNC})(\text{dmsO})]$ (**12**) towards a phosphane with an -OH group, (2-hydroxyphenyl)diphenylphosphane, was carried out. In a first approach, the P atom of that ligand might be more appropriate to displace the dmsO ligand of the platinum center. Thus, reaction of **12** with (2-hydroxyphenyl)diphenylphosphane in CH_2Cl_2 for 2 hours at room temperature gave rise to a complex with formula $[\text{Pt}(\text{CNC-H})\{\text{PPh}_2(\text{C}_6\text{H}_4\text{-}o\text{-O})\}]$ (**23**) (see Scheme 2.12).



Scheme 2.12. Synthesis of complex **23**.

On the other hand, reaction of $[\text{Pd}(\text{CNC})(\text{PPh}_3)]$ (**2**) with (2-hydroxyphenyl)diphenylphosphane did not give a clean product, since the substitution of

the PPh_3 ligand in the Pd precursor was not as favorable as the displacement of the dmsu molecule in the Pt starting material and mixtures of complexes were observed. In order to obtain this product as a pure solid and to compare it with its platinum analogue **23**, its preparation was tried following another procedure. Thus, reaction of $[\text{Pd}(\text{CNC-H})(\mu\text{-Cl})_2]$ with (2-hydroxyphenyl)diphenylphosphane in the presence of KOH, gave rise to $[\text{Pd}(\text{CNC-H})\{\text{PPh}_2(\text{C}_6\text{H}_4\text{-}o\text{-O})\}]$ (**24**) as a pure solid.

Crystals of $[\text{Pt}(\text{CNC-H})\{\text{PPh}_2(\text{C}_6\text{H}_4\text{-}o\text{-O})\}]$ (**23**) and $[\text{Pd}(\text{CNC-H})\{\text{PPh}_2(\text{C}_6\text{H}_4\text{-}o\text{-O})\}]$ (**24**) could be grown and their structures determined by X-Ray diffraction studies. A view of their structures is presented in Figure 2.16, while in Table 2.7 some relevant distances and angles are listed.

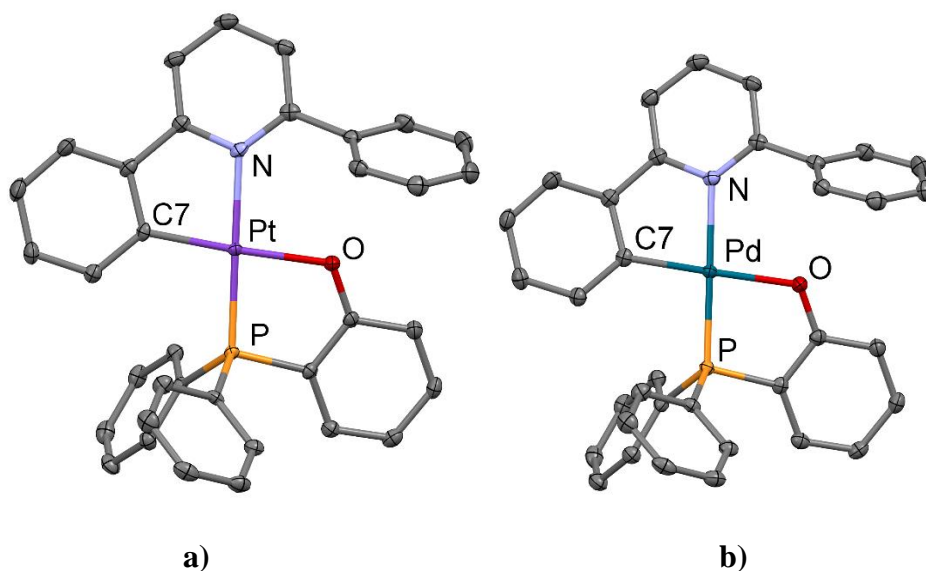


Figure 2.16. Molecular structures of complexes $[\text{Pt}(\text{CNC-H})\{\text{PPh}_2(\text{C}_6\text{H}_4\text{-}o\text{-O})\}]$ (**23**) (a) and $[\text{Pd}(\text{CNC-H})\{\text{PPh}_2(\text{C}_6\text{H}_4\text{-}o\text{-O})\}]$ (**24**) (b).

Table 2.7. Selection of bond lengths (Å) and angles (°) for **23** and **24**.

	23 (M = Pt)	24 (M = Pd)
M-N	2.132(2)	2.1497(14)
M-C7	1.993(2)	1.9981(17)
M-P	2.2044(6)	2.2250(4)
M-O	2.1011(18)	2.0964(12)
C7-M-N	81.29(9)	81.76(6)
C7-M-O	173.58(8)	173.61(6)
P-M-O	83.43(5)	83.45(3)

Structures of [Pt(CNC-H){PPh₂(C₆H₄-*o*-O)}] (**23**) and [Pd(CNC-H){PPh₂(C₆H₄-*o*-O)}] (**24**) are very similar, and can be described as mononuclear Pt(II) and Pd(II) complexes, where the phosphane ligand with an oxygen donor atom occupies two coordination sites, forming a chelate ring of five members. A bidentate C[^]N ligand completes the coordination environment of the metallic centers. The distances and angles found for this kind of complexes are in agreement with those reported in the literature.⁴¹⁻

45

Thus, the P atom is *trans* to the N and the O *trans* to the C_{ipso} of the C[^]N ligand. This disposition can be explained in terms of steric hindrance, this way the two phenylic rings of the phosphane are away from the phenyl group of the C[^]N ligand. Also, DFT calculations reveal that the *trans*-(N,O) possible isomers for **23** and **24** were higher in energy (7.9 and 10.0 kcal/mol respectively).

¹H NMR spectrum of compound [Pt(CNC-H){PPh₂(C₆H₄-*o*-O)}] (**23**) indicates that the structure in solution is consistent with the X-Ray one (see Figure 2.17). In this case only one product is detected, implying that one isomer has formed.

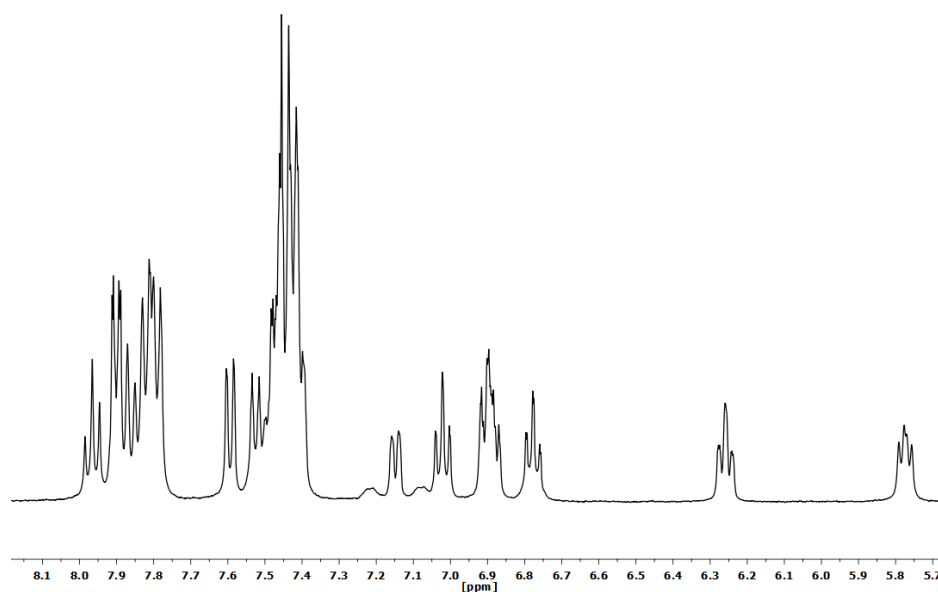


Figure 2.17. ^1H NMR spectrum (CD_2Cl_2 , RT) of complex $[\text{Pt}(\text{CNC-H})\{\text{PPh}_2(\text{C}_6\text{H}_4\text{-}o\text{-O})\}]$ (**23**).

$^{31}\text{P}\{^1\text{H}\}$ NMR experiments confirm the coordination of the new phosphane ligand. Thus, a singlet at 20.2 ppm with platinum satellites ($^1J_{\text{P-Pt}} = 4435$ Hz) is observed for **23** (see Figure S2.72, Supporting Information).

On the other hand, ^1H NMR spectrum of complex $[\text{Pd}(\text{CNC-H})\{\text{PPh}_2(\text{C}_6\text{H}_4\text{-}o\text{-O})\}]$ (**24**) (see Figure 2.18) shows a similar pattern than the one from **23**. In addition, the $^{31}\text{P}\{^1\text{H}\}$ NMR spectrum displays one singlet at 40.0 ppm (see Figure S2.80, Supporting Information).

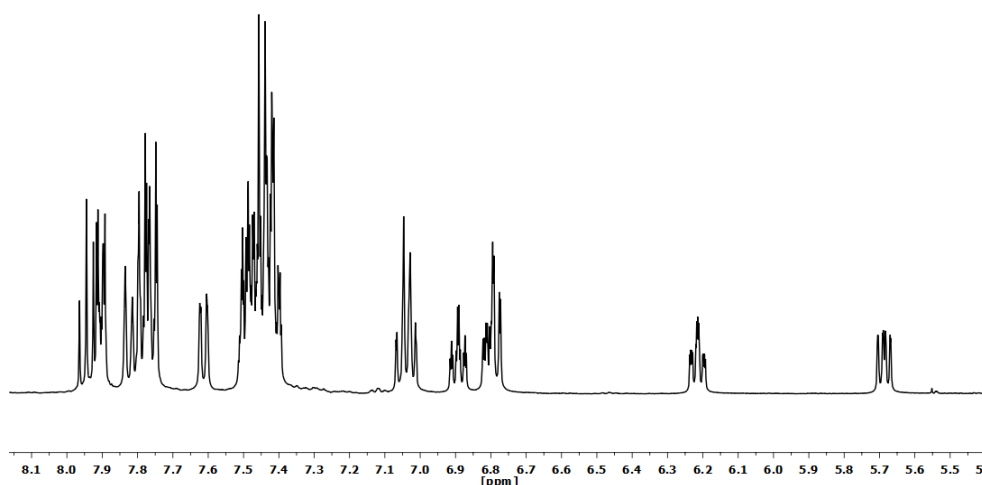


Figure 2.18. ^1H NMR spectrum (CD_2Cl_2 , RT) of complex $[\text{Pd}(\text{CNC-H})\{\text{PPh}_2(\text{C}_6\text{H}_4\text{-}o\text{-O})\}]$ (**24**).

Low temperature NMR experiments were performed to gain insight on the formation of **23**. Thus, equimolar amounts of complex [Pt(CNC)(dmsO)] (**12**) and (2-hydroxyphenyl)diphenylphosphane were dissolved in CD₂Cl₂ at low temperature and its NMR spectra immediately recorded at 223K. From the first moment, signals corresponding to free dmsO at 2.5 ppm and the final product [Pt(CNC-H){PPh₂(C₆H₄-*o*-O)}] (**23**) were detected, but also several unidentified species. Then, a row of ¹H and ³¹P{¹H} NMR experiments were recorded at different temperatures (see Figures 2.19 and 2.20). At 243K, the existence in the ¹H NMR spectrum of a remarkably deshielded singlet around 11.5 ppm (see red circle, Figure 2.19), a doublet with platinum satellites at around 8.6 ppm ($J_{\text{H-H}} = 3.9$ Hz, $J_{\text{H-Pt}} = 25.3$ Hz; see red circle, Figure 2.19), and a ³¹P{¹H} NMR singlet with platinum satellites at 10 ppm ($^1J_{\text{Pt-P}} = 3663$ Hz; see red circles, Figure 2.20) were clearly detected. After 130 minutes and rising the temperature to 293K species involved fully transformed to complex **23**.

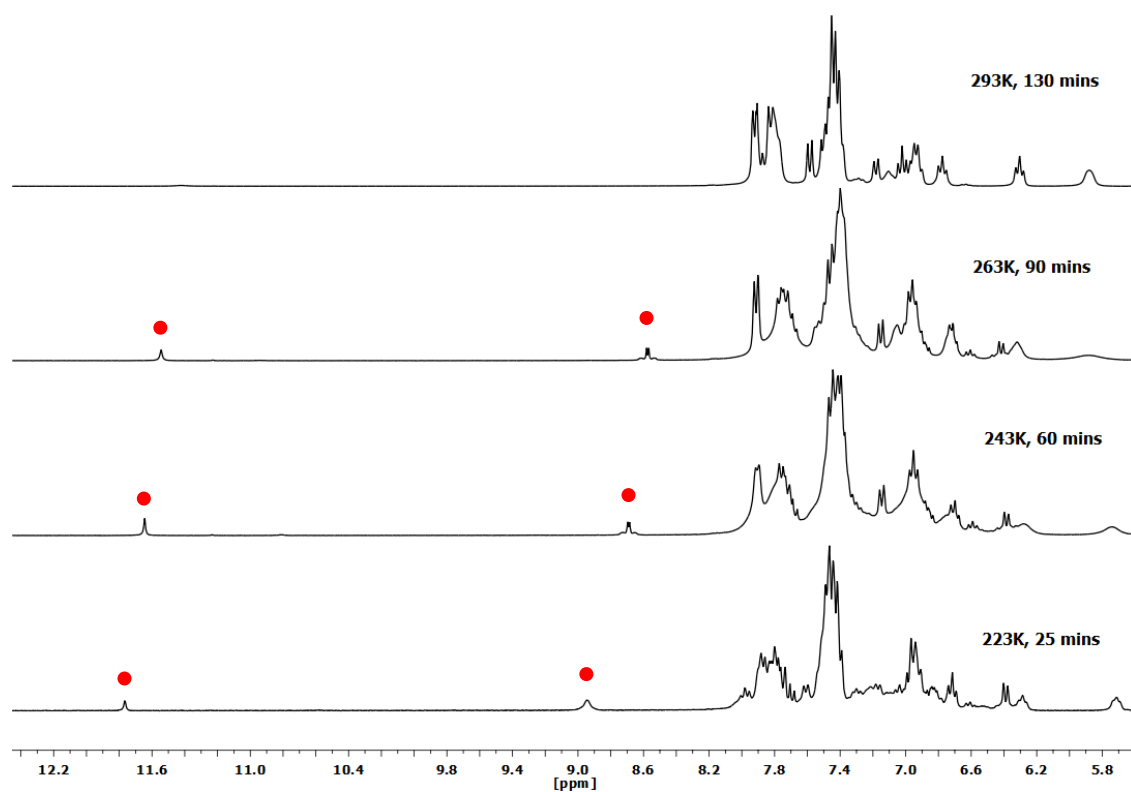


Figure 2.19. Selected ¹H VT NMR spectra (CD₂Cl₂) of reaction of complex [Pt(CNC)(dmsO)] (**12**) and (2-hydroxyphenyl)diphenylphosphane (red dots, discussed signals corresponding to an intermediate).

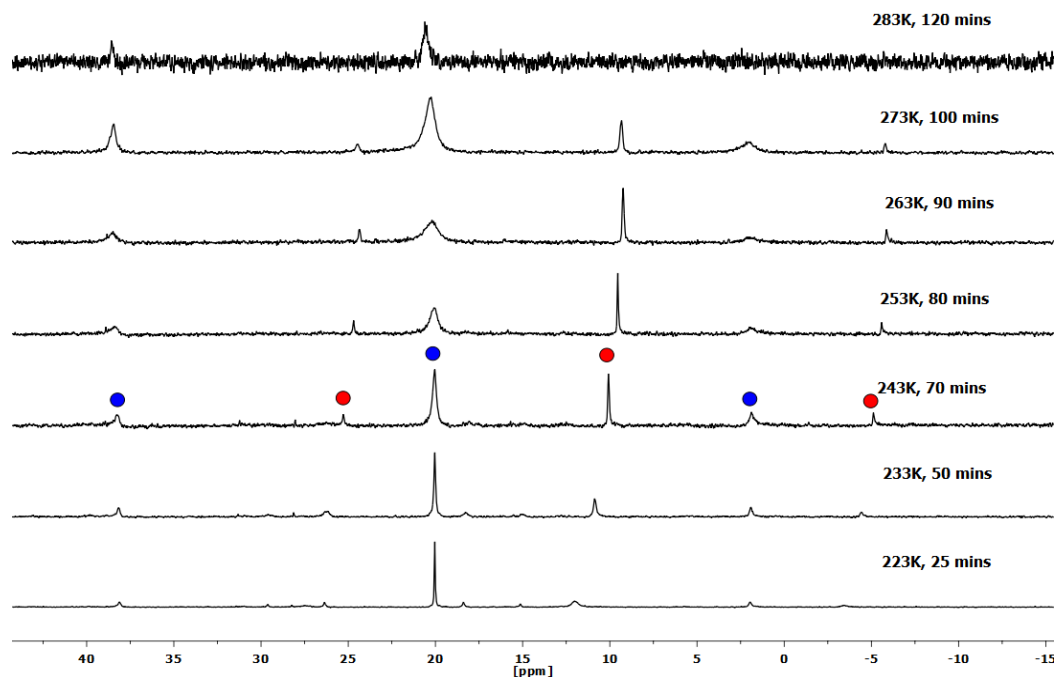


Figure 2.20. Selected $^{31}\text{P}\{^1\text{H}\}$ VT NMR spectra (CD_2Cl_2) of reaction of complex $[\text{Pt}(\text{CNC})(\text{dmsO})]$ (**12**) and (2-hydroxyphenyl)diphenylphosphane (blue circles, signals of **23**; red circles, signal of other Pt-P species).

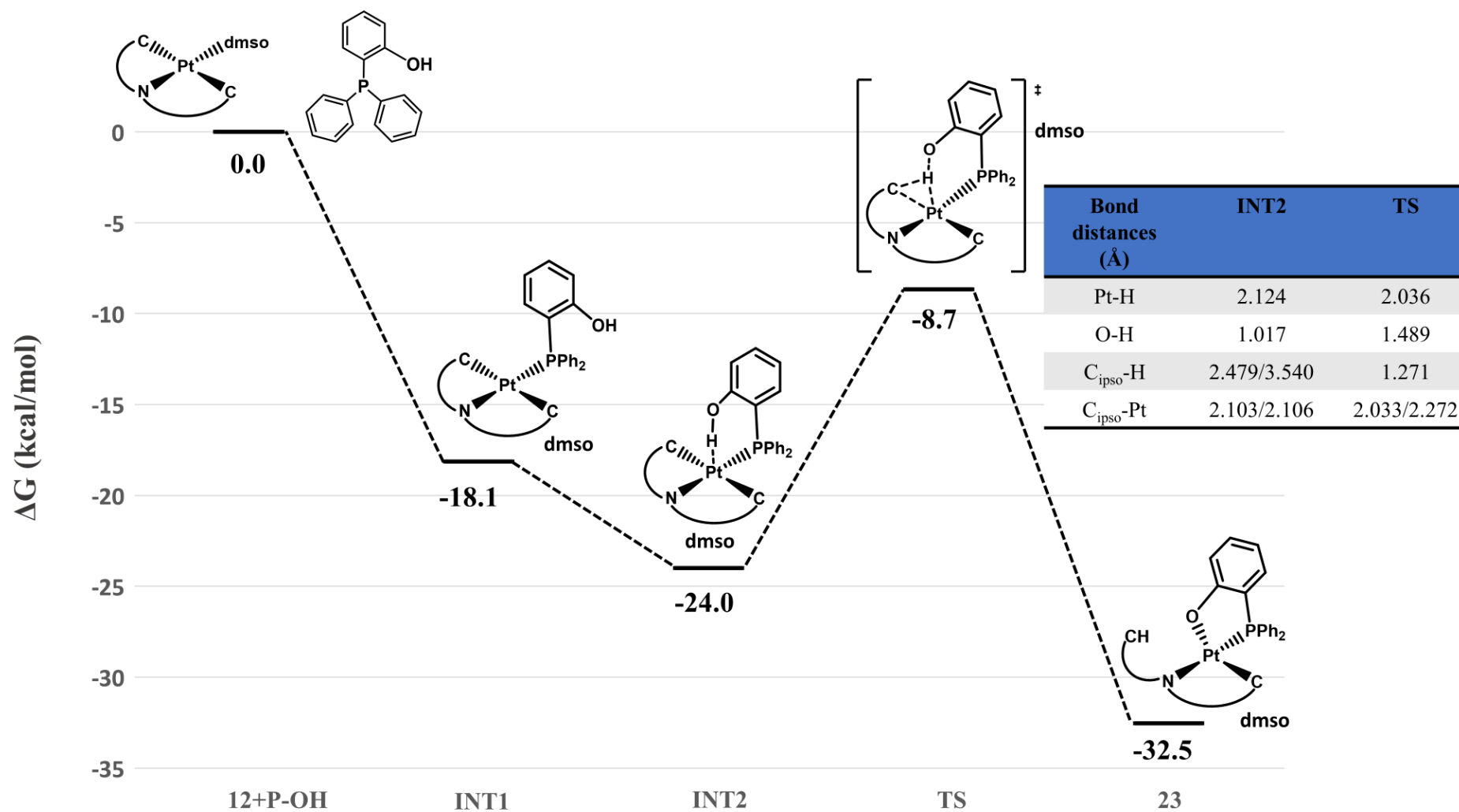
From these observations what could be inferred is, that in the first part of reaction the displacement of the dmsO ligand of complex $[\text{Pt}(\text{CNC})(\text{dmsO})]$ (**12**) must take place, as from the beginning of the experiment signals due to free dmsO were observed. On the other hand complex **12** reacts quite fast, since an appreciable amount of final product $[\text{Pt}(\text{CNC-H})\{\text{PPh}_2(\text{C}_6\text{H}_4\text{-}o\text{-}\text{O})\}]$ (**23**) was observed at first and no dmsO coordinated to platinum was detected throughout the experiment. During this process a significant amount of another species with a phosphane coordinated to the platinum center formed. Furthermore, the chemical shift of the very deshielded singlet on ^1H NMR spectroscopy can be related with the kind of signals that are observed in other type of cyclometallated complexes with -OH groups establishing hydrogen bonds with the metallic center.^{46,47} It is noteworthy that the signal of the hydroxyl group of the free phosphane ligand appears at 6.2 ppm in ^1H NMR (CD_2Cl_2). The existence of that deshielded signal could be therefore in agreement with the existence of an intermediate as the one proposed for the DFT calculations (see INT2, Scheme 2.13).

To complete this study, a plausible mechanism for the formation of $[\text{Pt}(\text{CNC-H})\{\text{PPh}_2(\text{C}_6\text{H}_4\text{O})\}]$ (**23**) in dichloromethane solution was carried out by computational

means (see in Scheme 2.13 the calculated energy profile). As shown in Scheme 2.13 the process is thermodynamically very favorable. This finding is in agreement with the experimental observations, as the reaction proceeds fast at room temperature. The first step for this reaction is the barrierless exchange of the dmsO ligand by the phosphane in the inner-sphere coordination of Pt(II). The first computed intermediate (see INT1, Scheme 2.13) has a geometry in which the hydroxyl group of the phosphane ligand is away from the metallic center.

Then, the phenyl group with the -OH group can rotate to establish a O-H...Pt interaction (see INT2, Scheme 2.13), which produces a stabilization of the complex. This can be compatible with the possibility to observe this intermediate through NMR. The existence of this intermediate can be possible given that there are similar square planar platinum (II) complexes in the literature which showed a remarkable interaction of the hydroxyl group of a 8-hydroxyquinoline ligand with the metallic center.^{46,47}

After ligand substitution, proton transfer from the hydroxyl group to the C_{ipso} (CNC) takes place (see TS, Scheme 2.13. 426i cm⁻¹; -OH bond stretching). Finally, complex **23** is formed through the dechelation of one of the arms of the tridentate ligand.

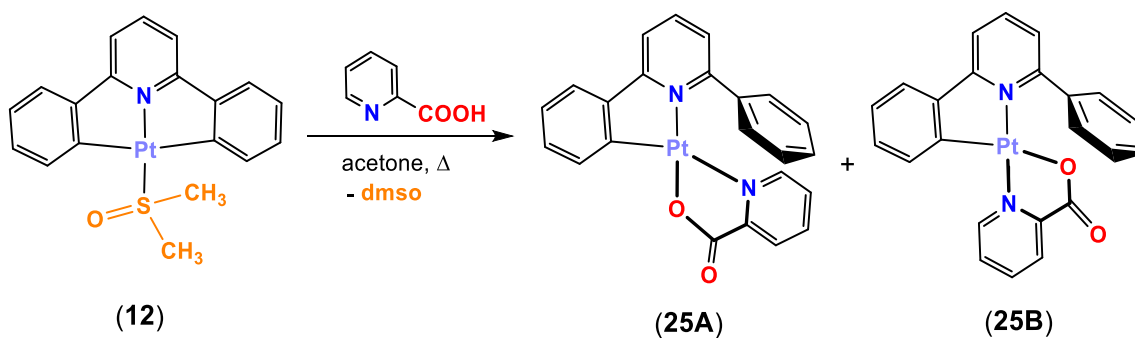


Scheme 2.13. Energy profile (DFT/BP86-D3 level, dichloromethane solution) for the reaction of **12** with (2-hydroxyphenyl)diphenylphosphane.

2.2.3. Reactions with ligands with -COOH groups

The extension of the study of reactivity of starting complexes [Pt(CNC)(dmsO)] (**12**) and [Pd(CNC)(PPh₃)] (**2**) with ligands bearing a -COOH group was also investigated. Ligands chosen for this matter were 2-pyridinecarboxylic acid and 2-(diphenylphosphino)benzoic acid.

Therefore, the behavior of mononuclear platinum complex [Pt(CNC)(dmsO)] (**12**) towards 2-pyridinecarboxylic acid was studied. As previously observed, pyridine ligands did not seem to displace easily the dimethylsulfoxide ligand. Thus, reaction of **12** with 2-pyridinecarboxylic acid in acetone (see Scheme 2.14), required longer reaction times and heating to proceed (see details in Experimental section). The resulting yellow solid was identified as a mixture of two possible isomers in similar proportions being in agreement with a formula [Pt(CNC-H)(NC₅H₄-*o*-COO)] (**25**).



Scheme 2.14. Synthesis of isomers of **25**; **A** (*trans*-(N,O)) and **B** (*trans*-(N,N)).

The structure of both isomers could be determined by X-Ray diffraction from different crystal batches of **25** with slightly different habit (Figure 2.21 depicts the structure of both isomers and Table 2.8 shows several relevant distances and angles).

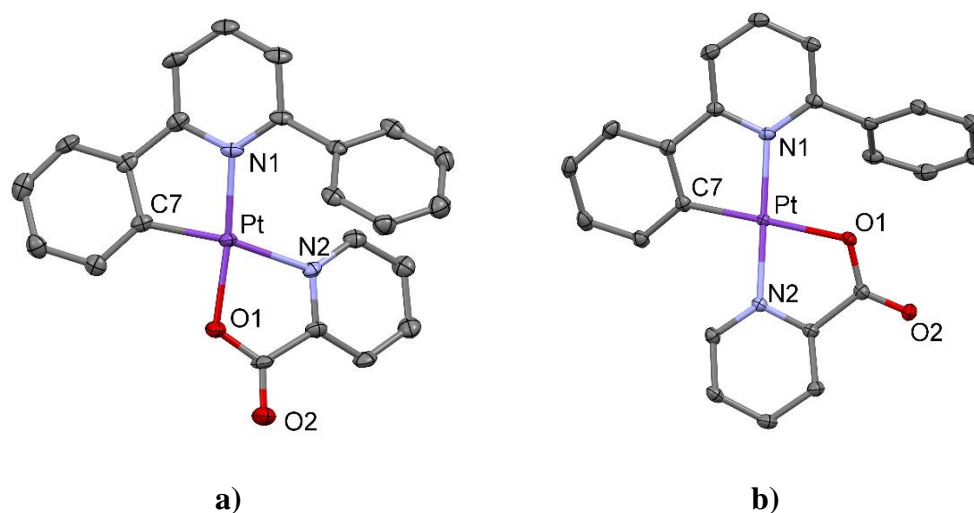


Figure 2.21. Molecular structures of isomers **25A** (a) and **25B** (b).

Table 2.8. Selection of bond lengths (Å) and angles (°) for **25A** and **25B**.

	25A	25B
Pt-N1	2.039(4)	2.0414(15)
Pt-C7	1.979(5)	1.9787(17)
Pt-N2	2.148(4)	2.0188(14)
Pt-O1	2.026(3)	2.1236(12)
C7-Pt-N1	80.70(19)	80.57(7)
C7-Pt-N2	165.40(18)	100.31(7)
C7-Pt-O1	92.62(18)	178.85(6)
O1-Pt-N2	78.94(14)	78.79(5)

Structures of **25A** and **25B** can be described as Pt(II) square planar complexes with a C^N ligand occupying two sites of the coordination sphere and a 2-pyridinecarboxylate coordinated through its N and O atoms. The two isomers are different in the way this anionic ligand coordinates to the metallic center, giving rise to two possibilities; namely isomers *trans*-(N,O) and *trans*-(N,N). Furthermore, DFT calculations reveal that both isomers are very near in energy, which could explain the similar proportions of these species obtained experimentally. The square planar environment of **25A** is distorted, exhibiting an C7-Pt-N2 angle of 165.40(18)°. In the case

of **25B**, the analogous angle of C7-Pt-O1 is $178.85(6)^\circ$, meaning that in that isomer the 2-pyridinecarboxylate ligand is almost coplanar with the Pt(II) plane. It seems that there is more steric hindrance in **25A** than in **25B**, since the pyridinic ring is closer to the phenyl group in that complex. Interestingly, in the obtention of other similar platinum (II) picolinate complexes with C^N ligands, only the *trans*-(N,N) isomer was reported.⁴⁸⁻⁵¹

Varying the reaction conditions did not affect to the proportions of these two species. Furthermore, once formed they seemed not to interconvert one on the other. ¹H NMR shows then aromatic signals corresponding to these two species, as depicted in Figure 2.22.

It was possible to separate a small batch of crystals composed mostly by isomer **25A**. The ¹H NMR of this batch allowed to identify and assign to each isomer one of the two different sets of aromatic signals (see Figure 2.22).

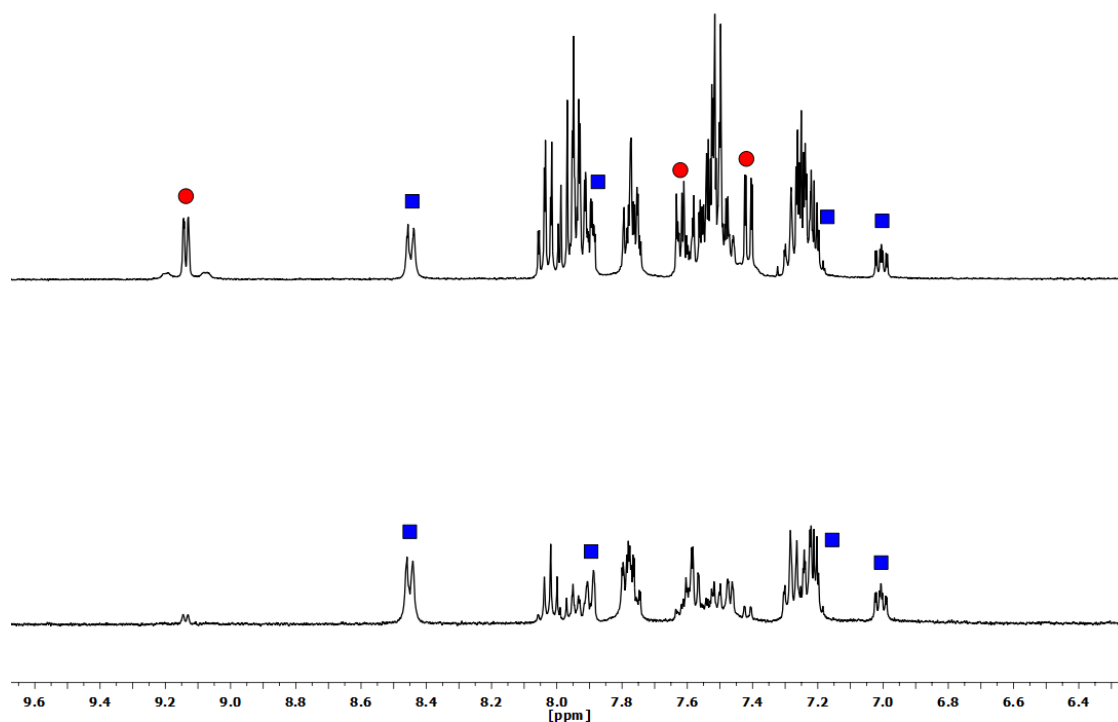
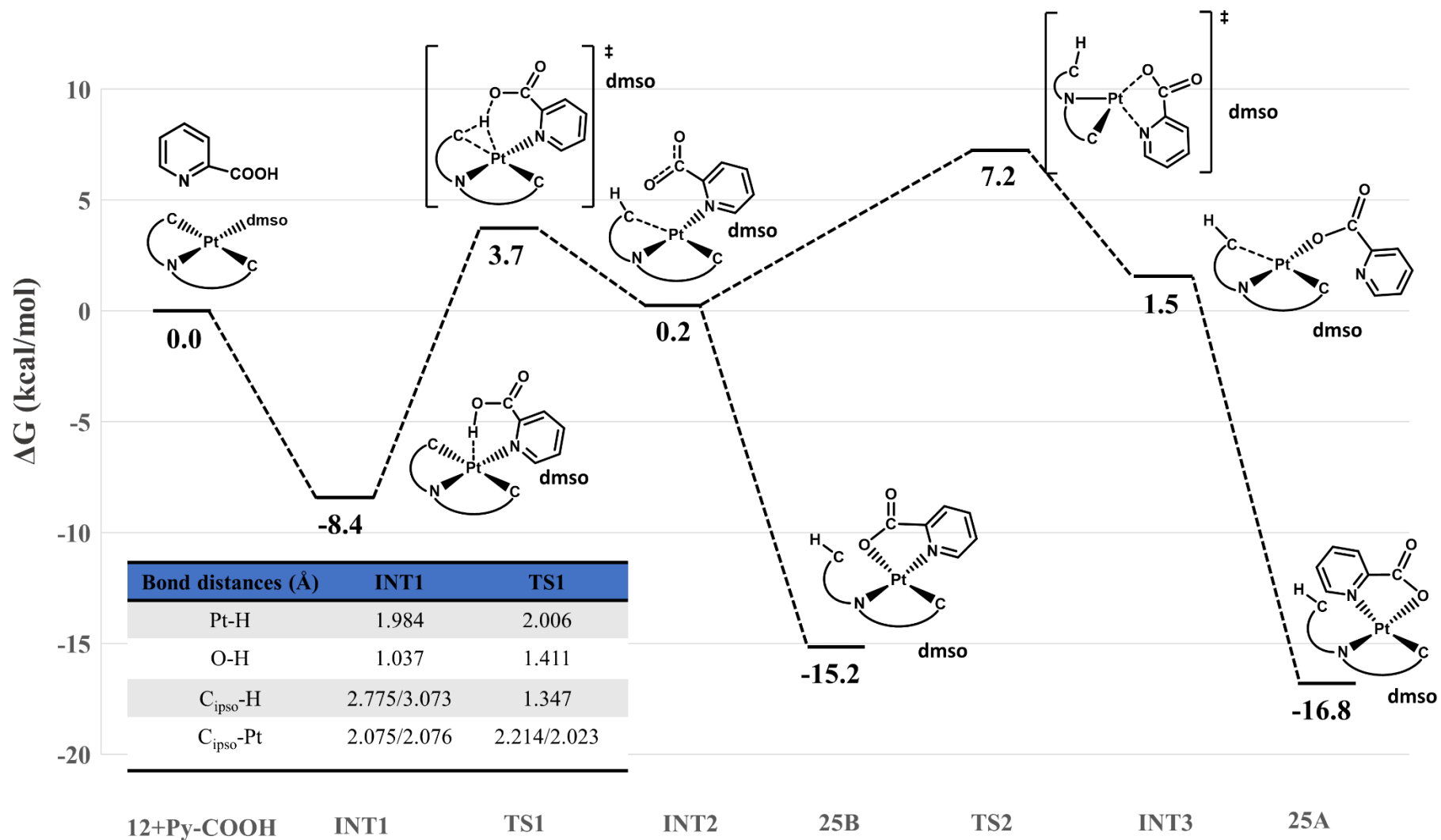


Figure 2.22. Comparison of ¹H NMR spectra (CD₂Cl₂, RT) of the raw solid **25** (top) and an enriched solution of **25A** (bottom) from the selected crystalline batch (red circles, signals of **25B**; blue squares, signals of **25A**).

DFT calculations were performed to establish a possible mechanism for the formation of isomers **25A** and **25B** in acetone solution (see Energy profile in Scheme 2.15). Thus, the first step is the barrierless substitution of the coordinated dmsol molecule

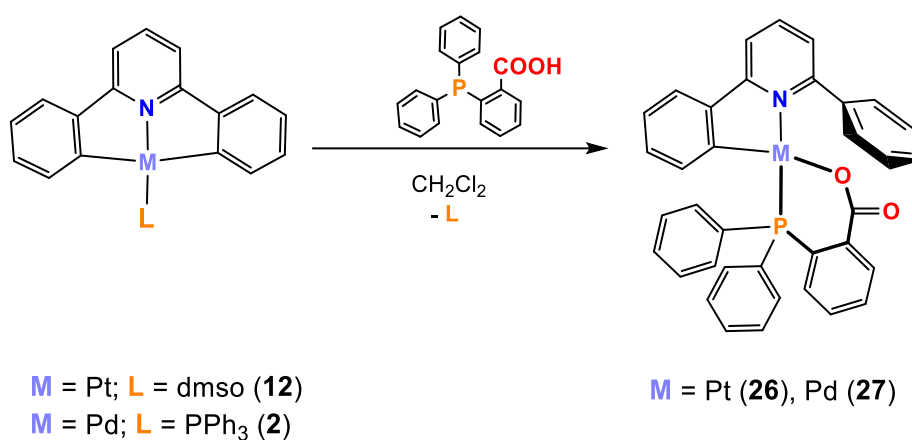
of **12** (see INT1, Scheme 2.15) with the pyridine pointing the carboxylic group towards the metallic center. In this case, it was not possible to calculate a minimum with the carboxylic group of the pyridine not pointing to the platinum, due to the proximity of this group to the metallic center.

This substitution of ligands is not as energetically favorable as the one observed for the phosphane substitution, which agrees with the more energetic reaction conditions used experimentally. Then, the proton transfer takes place, giving a transition state (see TS1, Scheme 2.15. $947i\text{ cm}^{-1}$; OH stretching). As a result of this process, an intermediate with the pyridine-2-carboxylate ligand *trans*-(N,N) (INT2, Scheme 2.15) is formed. This intermediate can evolve to isomer **25B** via coordination of the carboxylate group *trans* to the C_{ipso}. INT2 can isomerize to the coordinated *trans*-(N,O) pyridine-2-carboxylate (INT3, Scheme 2.15) via a transition state with the geometry represented in Scheme 2.15 (TS2. $106i\text{ cm}^{-1}$; N-Pt-O stretching). Finally, this intermediate can give rise to the isomer **25A**, upon coordination of the pyridine group *trans* to the C_{ipso}.



Scheme 2.15. Energy profile (DFT/BP86-D3 level, acetone solution) for the reaction of **12** with 2-pyridinecarboxylic acid.

On the other hand, the reaction times of $[\text{Pt}(\text{CNC})(\text{dmsO})]$ (**12**) and $[\text{Pd}(\text{CNC})(\text{PPh}_3)]$ (**2**) with 2-(diphenylphosphino)benzoic acid were short and no heating was necessary. Thus, dissolving $[\text{Pt}(\text{CNC})(\text{dmsO})]$ (**12**) or $[\text{Pd}(\text{CNC})(\text{PPh}_3)]$ (**2**) with 2-(diphenylphosphino)benzoic acid in CH_2Cl_2 for 20 minutes gave rise to yellow solids that after work-up were identified as species with formula $[\text{M}(\text{CNC}-\text{H})\{\text{PPh}_2(\text{C}_6\text{H}_4\text{-}o\text{-COO})\}]$ ($\text{M} = \text{Pt}$ (**26**), Pd (**27**)) (see Scheme 2.16). It is remarkable that, while in the previous study the triphenylphosphane ligand of complex $[\text{Pd}(\text{CNC})(\text{PPh}_3)]$ (**2**) could not be easily displaced with a phosphane with a -OH group, in this case reaction proceeded fast and yielded a pure solid.



Scheme 2.16. Synthesis of complexes **26** and **27**.

X-Ray diffraction studies could be carried out on well-formed crystals of **26** and **27**. See Figure 2.23 and Table 2.9 for a view of the structures and a selection of distances and angles respectively.

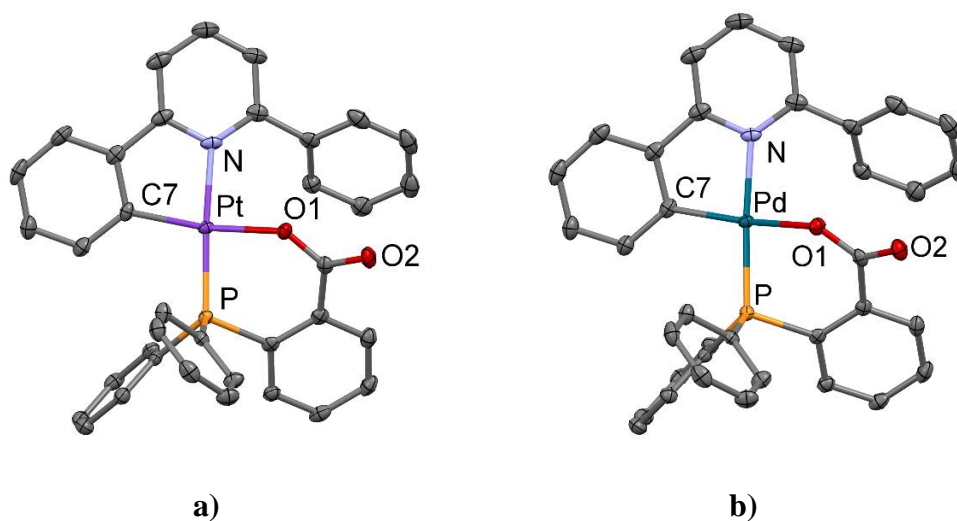


Figure 2.23. Molecular structures of complexes **26** (a) and **27** (b).

Table 2.9. Selection of bond lengths (Å) and angles (°) for **26** and **27**.

	26 (M = Pt)	27 (M = Pd)
M-N	2.101(3)	2.1147(15)
M-C7	1.990(3)	1.9968(19)
M-O1	2.103(2)	2.0998(12)
M-P	2.2067(8)	2.2244(5)
C7-M-O1	162.41(11)	161.44(7)
C7-M-N	81.07(12)	81.65(7)

Structures of **26** and **27** correspond to mononuclear Pt(II) and Pd(II) complexes in which a phosphane with a carboxylate group acts as a bidentate ligand, forming a six-membered ring. Their coordination spheres are completed by a bidentate C^N ligand, exhibiting its N atom *trans* to the P and its cyclometallated C atom *trans* to an O atom. Furthermore, possible *trans*-(N,O) isomers of **26** and **27** were studied through DFT calculations, indicating that they are higher in energy (6.1 and 8.2 kcal/mol, respectively), due to the existence of higher steric hindrance. Both structures show similar bond distances and angles, regardless of the metallic center. Angles C7-M-O1 of around 160° indicate that the chelate ring is not coplanar with the metallic square plane. This deviation from planarity can be caused by the phenyl group nearby. As expected, the phenyl ring is not coplanar with the metallic plane, showing a torsion angle with the pyridinic plane of around 40°.

¹H NMR spectrum of **26** and **27** confirms the breakage of a M-C_{ipso} (CNC) bond and the substitution of the dmsO and triphenylphosphane respectively by the phosphane ligand and the incorporation of a proton to a phenylene ring of the CNC ligand (see Figures 2.24 and 2.25).

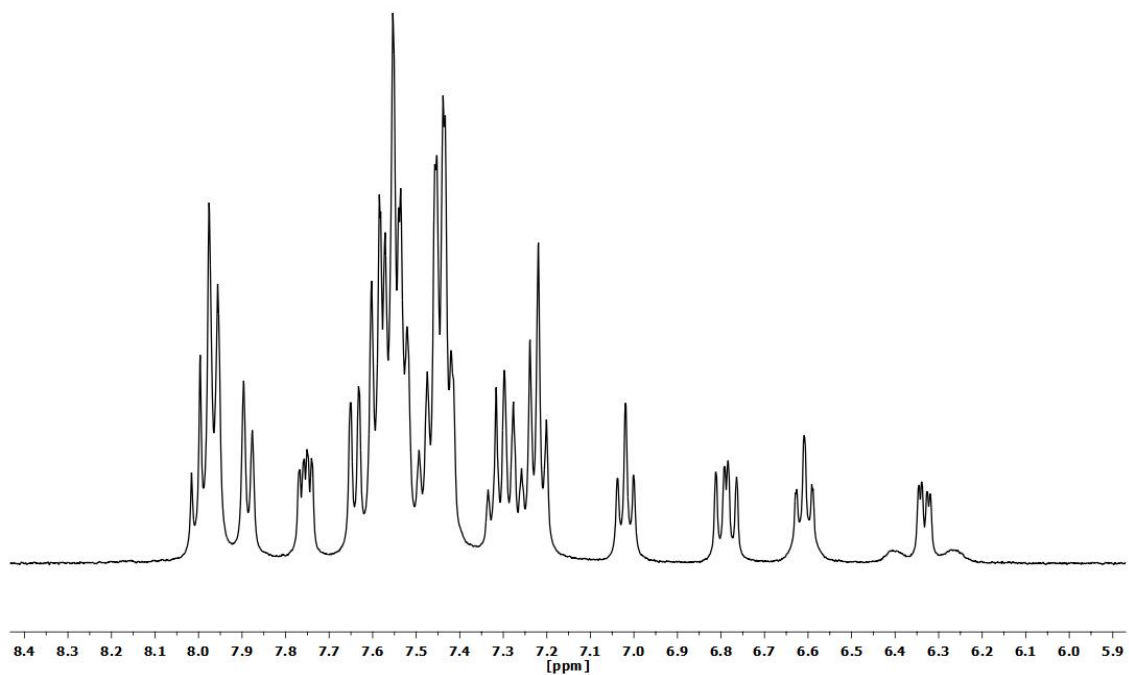


Figure 2.24. ^1H NMR spectrum (CD_2Cl_2 , RT) of complex $[\text{Pt}(\text{CNC}-\text{H})\{\text{PPh}_2(\text{C}_6\text{H}_4\text{-}o\text{-COO})\}]$ (**26**).

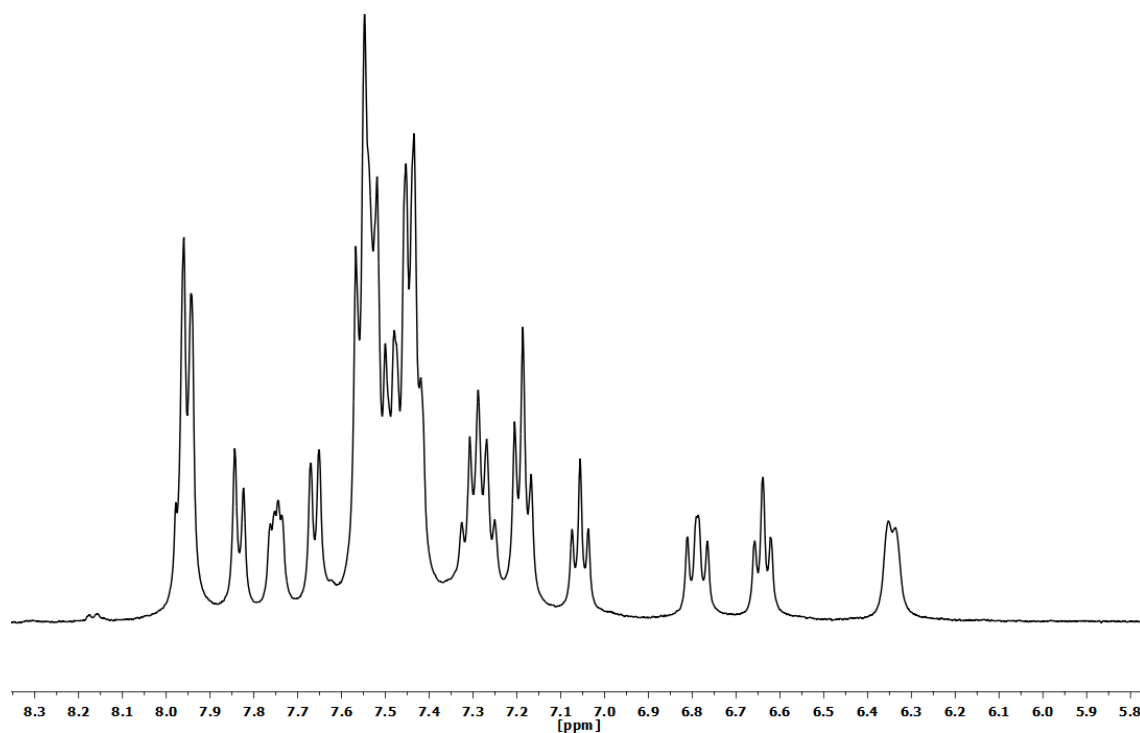


Figure 2.25. ^1H NMR spectrum (CD_2Cl_2 , RT) of complex $[\text{Pd}(\text{CNC}-\text{H})\{\text{PPh}_2(\text{C}_6\text{H}_4\text{-}o\text{-COO})\}]$ (**27**).

$^{31}\text{P}\{^1\text{H}\}$ NMR also indicated the expected substitution of ligands, showing for $[\text{Pt}(\text{CNC-H})\{\text{PPh}_2(\text{C}_6\text{H}_4\text{-}o\text{-COO})\}]$ (**26**) and $[\text{Pd}(\text{CNC-H})\{\text{PPh}_2(\text{C}_6\text{H}_4\text{-}o\text{-COO})\}]$ (**27**) one singlet with platinum satellites at 11.1 ppm ($^1J_{\text{P-Pt}} = 4388$ Hz) and one singlet at 36.0 ppm respectively (see Figures S2.95 and S2.103, Supporting Information).

It is known that the $^{31}\text{P}\{^1\text{H}\}$ NMR signal shift depends on the number of members of the ring in chelated phosphanes. Thus, five-membered rings show more deshielded signals than those with six members.⁵² In fact, it is observed that $^{31}\text{P}\{^1\text{H}\}$ NMR signals of **26** and **27** shifted upfield around 9 and 4 ppms compared to those of $[\text{Pt}(\text{CNC-H})\{\text{PPh}_2(\text{C}_6\text{H}_4\text{-}o\text{-O})\}]$ (20.2 ppm) (**23**) and $[\text{Pd}(\text{CNC-H})\{\text{PPh}_2(\text{C}_6\text{H}_4\text{-}o\text{-O})\}]$ (40.0 ppm) (**24**).

As general conclusions for this chapter, it has been confirmed that starting complexes [Pt(CNC)(PPh₃)] (**1**), [Pt(CNC)(dmsO)] (**12**) and [Pd(CNC)(PPh₃)] (**2**) act as Lewis acids towards the proton. Depending on the source of protons, different scenarios can be considered.

Protic acids cause, the breakage of a M-C_{ipso} bond, formation of a C-H bond and coordination of a ligand in the resulting free coordination site. The ligand completing the vacant can be the anion of the acid, a molecule of solvent or an added ligand additionally.

In the case of reacting starting substrates **12** or **2** with an organic ligand (P-donor or N-donor) with acidic hydrogens (with -SH, -OH or -COOH groups) the same protonation process occurs and also the coordination of the ligand in a bidentate way giving rise to a chelate ring, with one exception; pyridine-2-thiol gives rise to a dinuclear complex with bridging ligands. Remarkably, the substitution of ligands is more favored in the case of using P-donor ligands compared to N-donor ligands, needing for the latter more energetic reaction conditions and longer times to proceed. This was supported by DFT calculations, which also established a possible mechanism for two examples of these reactions. In these mechanisms the possibility of having intermediates with O-H...Pt interactions were considered, which is related with the study by NMR at low temperature of the reaction of **12** with (2-hydroxyphenyl)diphenylphosphane.

Furthermore, the use of bidentate ligands in the protonation reactions can give rise to isomers. This is not observed for the P-donor ligand reactions, due to the high sterical requirements of the phosphane ligands, which causes only the formation of the *trans*-(N,P) isomer.

2.3. Experimental section

General Comments. Literature methods were used to prepare the starting materials [Pt(CNC)(PPh₃)] (**1**) and [Pt(CNC)(dmsO)] (**12**).^{5,53} Elemental analyses were carried out with a Perkin-Elmer 2400 CHNS analyzer. IR spectra were recorded on a Perkin-Elmer Spectrum 100 FT-IR spectrometer (ATR in the range 250-4000 cm⁻¹). Mass spectrometry was performed with the Microflex matrix-assisted laser desorption ionization-time-of-flight (MALDI-TOF) Bruker or an Autoflex III MALDI-TOF Bruker instruments. ¹H, ¹³C{¹H} and ³¹P{¹H} NMR spectra were recorded on Bruker AV-300, ARX-300, AV-400 and AV-500 spectrometers using the standard references: SiMe₄, 85% H₃PO₄ and CFCl₃ for references for ¹H, ¹³C, ³¹P and ¹⁹F respectively. The signal attributions and coupling constant assessment was made on the basis of a multinuclear NMR analysis of each compound including, besides 1D spectra, ¹H-¹H COSY, ¹H-¹³C HSQC, ¹H-¹³C HMBC and ¹³C{¹H} APT.

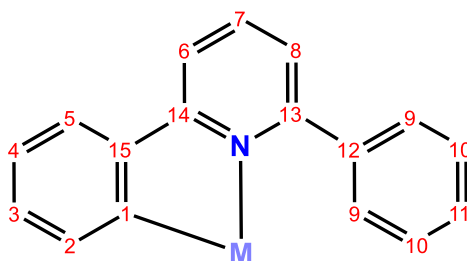


Chart 2.2. ¹H and ¹³C numbering scheme.

Preparation of the complex [Pt(CNC-H)Cl(PPh₃)] (13**).** To a solution of [Pt(CNC)(PPh₃)] (**1**) (0.060 g, 0.087 mmol) in 25 mL of CH₂Cl₂ at room temperature, 0.960 mL of a solution of HCl (0.040 M in MeOH, 0.096 mmol) were added. The bright-yellow solution was immediately evaporated to dryness and the resulting yellow solid was extracted with 10 mL of diethylether, filtered and air-dried (0.040 g, 63%). Anal. Found: C, 57.78; H, 4.00; N, 1.76. Anal. Calcd. for C₃₅H₂₇ClNPPt: C, 58.14; H, 3.76; N, 1.94. IR (ATR, cm⁻¹): 1598 (w, ν(N-C)), 1579 (w, ν(N-C)), 1562 (w, ν(N-C)), 1551 (m, ν(N-C)), 540 (vs, ν(P-C)), 516 (s, ν(P-C)), 502 (s, ν(P-C)), 281 (m, ν(Pt-Cl)). ¹H NMR (400.132 MHz, CD₂Cl₂, 293K, see Chart 2.2 for the H numbering scheme): δ = 8.06 (2H, m, H9), 7.98 (1H, t, ³J_{H7-H6} = ³J_{H7-H8} = 8.0 Hz, H7), 7.86 (1H, d, ³J_{H6-H7} = 8.0 Hz, H6), 7.75 (6H, m, *o*-PPh₃), 7.60 (1H, d, ³J_{H5-H4} = 8.0 Hz, H5), 7.57 (1H, d, ³J_{H8-H7} = 8.0 Hz, H8), 7.43 (6H, m, *p*-PPh₃, H10 and H11), 7.36 (6H, m, *m*-PPh₃), 6.98 (1H, dd, ³J_{H4-H5} =

8.0 Hz, ${}^3J_{\text{H4-H3}} = 7.5$ Hz, H4), 6.68 (1H, dd, ${}^3J_{\text{H2-H3}} = 8.0$ Hz, ${}^4J_{\text{H2-P}} = 3.2$ Hz, ${}^3J_{\text{H2-Pt}} = 52.6$ Hz, H2), 6.52 (1H, dd, ${}^3J_{\text{H3-H2}} = 8.0$ Hz, ${}^3J_{\text{H3-H4}} = 7.5$ Hz, H3) ppm. ${}^{31}\text{P}\{^1\text{H}\}$ NMR (161.923 MHz, CD_2Cl_2 , 293K): $\delta = 20.7$ (s, ${}^1J_{\text{P-Pt}} = 4525$ Hz) ppm. ${}^{13}\text{C}\{^1\text{H}\}$ NMR plus HSQC and HMBC (100.624 MHz, CD_2Cl_2 , 293K see Chart 2.2 for the C numbering scheme): $\delta = 165.3$ (d, ${}^4J_{\text{C-P}} = 3.5$ Hz, C14), 162.1 (s, C13), 146.7 (s, C15), 143.1 (d, ${}^2J_{\text{C-P}} = 5.8$ Hz, C1), 141.0 (s, C12), 139.5 (s, C7), 137.1 (d, ${}^3J_{\text{C-P}} = 6.1$ Hz, C2), 135.3 (d, ${}^2J_{\text{C-P}} = 11.1$ Hz, *o*-PPh₃), 130.9 (d, ${}^1J_{\text{C-P}} = 62.2$ Hz, *q*-PPh₃), 130.9 (d, ${}^5J_{\text{C-P}} = 4.1$ Hz, C10), 130.1 (s, C9), 129.4 (s, C11), 128.7 (d, ${}^4J_{\text{C-P}} = 3.3$ Hz, C3), 128.2 (d, ${}^3J_{\text{C-P}} = 10.9$ Hz, *m*-PPh₃), 127.9 (s, *p*-PPh₃), 124.8 (s, C5), 124.1 (d, ${}^4J_{\text{C-P}} = 4.0$ Hz, C8), 123.4 (s, C4), 116.7 (d, ${}^4J_{\text{C-P}} = 2.3$ Hz, C6) ppm. MS MALDI+ DCTB: $m/z = 723.2$ [[Pt(CNC-H)Cl(PPh₃)]+H]⁺, 687.2 [Pt(CNC-H)(PPh₃)]⁺.

Preparation of the complex [Pt(CNC-H)Cl(dmsO)] (14). To a solution of [Pt(CNC)(dmsO)] (12) (0.050 g, 0.099 mmol) in 15 mL of CH_2Cl_2 at room temperature, 0.400 mL of a solution of HCl (0.025 M in MeOH, 0.099 mmol) were added. The bright-yellow solution was immediately concentrated to *ca.* 1 mL, 20 mL of *n*-hexane were added and the resulting yellow solid was filtered and air-dried (0.035 g, 65%). Anal. Found: C, 41.97; H, 3.18; N, 2.53; S, 6.43. Anal. Calcd. for $\text{C}_{19}\text{H}_{18}\text{ClNOPtS}$: C, 42.34; H, 3.37; N, 2.60; S, 5.95. IR (ATR, cm^{-1}): 1603 (m, $\nu(\text{N-C})$), 1579 (m, $\nu(\text{N-C})$), 1561 (w, $\nu(\text{N-C})$), 1552 (w, $\nu(\text{N-C})$), 270 (s, $\nu(\text{Pt-Cl})$). ${}^1\text{H}$ NMR (400.132 MHz, CD_2Cl_2 , 293K): $\delta = 8.25$ (1H, dd, ${}^3J_{\text{H2-H3}} = 7.6$ Hz, ${}^4J_{\text{H2-H4}} = 1.4$ Hz, ${}^3J_{\text{H2-Pt}} = 44.0$ Hz, H2), 7.97 (1H, t, ${}^3J_{\text{H7-H6}} = {}^3J_{\text{H7-H8}} = 8.0$ Hz, H7), 7.95 (2H, m, H10), 7.81 (1H, dd, ${}^3J_{\text{H6-H7}} = 8.0$ Hz, ${}^4J_{\text{H6-H8}} = 1.3$ Hz, H6), 7.62 (1H, dd, ${}^3J_{\text{H5-H4}} = 7.5$ Hz, ${}^4J_{\text{H5-H3}} = 1.5$ Hz, H5), 7.48 (4H, m, H8, H9 and H11), 7.23 (1H, td, ${}^3J_{\text{H4-H3}} = {}^3J_{\text{H4-H5}} = 7.5$ Hz, ${}^4J_{\text{H4-H2}} = 1.4$ Hz, H4), 7.17 (1H, td, ${}^3J_{\text{H3-H4}} = {}^3J_{\text{H3-H2}} = 7.6$ Hz, ${}^4J_{\text{H3-H5}} = 1.5$ Hz, H3), 3.38 (6H, s, ${}^3J_{\text{Me-Pt}} = 25.0$ Hz, Me-(dmsO)) ppm. ${}^{13}\text{C}\{^1\text{H}\}$ NMR plus HSQC and HMBC (100.624 MHz, CD_2Cl_2 , 293K): $\delta = 166.2$ (s, C14), 162.6 (s, C13), 146.1 (s, C15), 141.8 (s, C1), 140.7 (s, C12), 140.2 (s, C7), 133.9 (s, C2), 130.0 (s, C10), 129.9 (s, C9 or C11), 129.4 (s, C3), 128.0 (s, C9 or C11), 125.2 (s, C4), 124.8 (s, C5), 124.0 (s, C8), 116.9 (s, C6), 46.2 (s, ${}^2J_{\text{C-Pt}} = 65.1$ Hz, Me-(dmsO)) ppm. MS MALDI+ DCTB: $m/z = 503.1$ [Pt(CNC-H)(dmsO)]⁺.

Preparation of the complex [Pt(CNC-H)(MeCN)(PPh₃)](ClO₄) (15). To a solution of [Pt(CNC)(PPh₃)] (**1**) (0.070 g, 0.102 mmol) in 20 mL of MeCN at room temperature, 0.640 mL of a solution of HClO₄ (0.175 M in MeOH, 0.112 mmol) were added. The bright-yellow solution was after 10 minutes evaporated to dryness and the resulting yellow solid was extracted with ¹PrOH (10 mL), filtered, washed with *n*-hexane (10 mL) and air-dried (0.060 g, 71%). Anal. Found: C, 53.07; H, 3.61; N, 3.12. Anal. Calcd. for C₃₇H₃₀ClN₂O₄PPt: C, 53.66; H, 3.65; N, 3.38. IR (ATR, cm⁻¹): 2321 (w, ν(CN)), 2292 (w, ν(CN)), 1605 (w, ν(N-C)), 1584 (w, ν(N-C)), 1566 (m, ν(N-C)), 1556 (m, ν(N-C)), 1081 (vs, ν(ClO₄)), 620 (s, ν(ClO₄)), 538 (s, ν(P-C)), 515 (s, ν(P-C)), 499 (s, ν(P-C)). ¹H NMR (400.132 MHz, CD₂Cl₂, 293K): δ = 8.16 (1H, t, ³J_{H7-H6} = ³J_{H7-H8} = 8.0 Hz, H7), 8.01 (1H, d, ³J_{H6-H7} = 8.4 Hz, H6), 7.95 (2H, m, H9), 7.72 (6H, m, *o*-PPh₃), 7.66 (2H, m, H5 and H8), 7.54 (6H, m, H10, H11 and *p*-PPh₃), 7.46 (6H, m, *m*-PPh₃), 7.06 (1H, td, ³J_{H4-H5} = ³J_{H4-H3} = 7.4 Hz, ⁴J_{H4-H2} = 1.0 Hz, H4), 6.67 (1H, ddd, ³J_{H2-H3} = 8.0 Hz, ⁴J_{H2-P} = 3.6 Hz, ³J_{H2-H4} = 1.0 Hz, ³J_{H2-Pt} = 50.4 Hz, H2), 6.55 (1H, dd, ³J_{H3-H2} = 8.0 Hz, ⁴J_{H3-H5} = 1.0 Hz, H3), 1.08 (3H, s, MeCN) ppm. ³¹P{¹H} NMR (161.923 MHz, CD₂Cl₂, 293K): δ = 20.9 (s, ¹J_{P-Pt} = 4297 Hz) ppm. ¹³C{¹H} NMR plus HSQC and HMBC (100.624 MHz, CD₂Cl₂, 293K): δ = 165.2 (s, C14), 161.6 (s, C13), 147.5 (s, C15), 141.3 (s, C7), 140.3 (s, C12), 138.9 (d, ³J_{C-P} = 8.6 Hz, C2), 136.4 (s, C1), 135.2 (d, ²J_{C-P} = 11.5 Hz, *o*-PPh₃), 132.4 (d, ⁴J_{C-P} = 2.6 Hz, *p*-PPh₃), 130.9 (s, C10), 129.9 (s, C9), 129.4 (s, C11), 129.3 (d, ³J_{C-P} = 11.0 Hz, *m*-PPh₃), 128.6 (d, ¹J_{C-P} = 64.0 Hz, *q*-PPh₃), 125.7 (s, C4), 125.5 (s, C3), 125.2 (s, C8), 124.6 (d, ⁴J_{C-P} = 4.0 Hz, C5), 120.4 (s, CN-(MeCN)), 118.6 (s, C6), 2.8 (s, Me-(MeCN)) ppm. MS ESI⁺: m/z = 686.5 [Pt(CNC-H)(PPh₃)]⁺.

Preparation of the complex [Pd(CNC-H)(MeCN)(PPh₃)](ClO₄) (16). To a solution of [Pd(CNC)(PPh₃)] (**2**) (0.050 g, 0.084 mmol) in 15 mL of MeCN at room temperature, 0.480 mL of a solution of HClO₄ (0.175 M in MeOH, 0.084 mmol) were added. The bright-yellow solution was immediately evaporated to dryness, and the resulting yellow solid was extracted with diethylether (5 mL), filtered and air-dried (0.034 g, 55%). Anal. Found: C, 59.69; H, 4.05; N, 3.77. Anal. Calcd. for C₃₇H₃₀ClN₂O₄PPd: C, 60.10; H, 4.09; N, 3.79. IR (ATR, cm⁻¹): 2311 (vw, ν(CN)), 2286 (vw, ν(CN)), 1597 (w, ν(N-C)), 1578 (w, ν(N-C)), 1566 (w, ν(N-C)), 1557 (m, ν(N-C)), 1082 (s, ν(ClO₄)), 621 (s, ν(ClO₄)), 529 (vs, ν(P-C)), 512 (s, ν(P-C)), 495 (s, ν(P-C)). ¹H NMR (400.132 MHz, CD₂Cl₂, 293K): δ = 8.13 (1H, t, ³J_{H7-H6} = ³J_{H7-H8} = 7.9 Hz, H7), 7.95 (2H, m, H6 and H9),

7.71 (6H, m, *o*-PPh₃), 7.66 (1H, d, ³J_{H5-H4} = 8.0 Hz, H5), 7.62 (1H, d, ³J_{H8-H7} = 7.9 Hz, H8), 7.54 (6H, m, H10, H11 and *p*-PPh₃), 7.47 (6H, m, *m*-PPh₃), 6.54 (2H, m, H2 and H3), 1.12 (3H, s, MeCN) ppm. ³¹P{¹H} NMR (161.923 MHz, CD₂Cl₂, 293K): δ = 43.3 (s) ppm. ¹³C{¹H} NMR (100.624 MHz, CD₂Cl₂, 293K): δ = 164.5 (s, C14), 161.1 (s, C13), 151.2 (s, C1), 148.3 (s, C15), 141.6 (s, C7), 140.6 (s, C12), 139.7 (d, ³J_{C-P} = 14.0 Hz, C2), 135.7 (d, ²J_{C-P} = 11.9 Hz, *o*-PPh₃), 132.7 (d, ⁴J_{C-P} = 2.8 Hz, *p*-PPh₃), 131.1 (s, C10 or C11), 130.0 (s, C10 or C11), 129.9 (d, ¹J_{C-P} = 52.2 Hz, *q*-PPh₃), 129.8 (d, ³J_{C-P} = 11.1 Hz, *m*-PPh₃), 129.7 (s, C9), 129.5 (d, ⁴J_{C-P} = 6.7 Hz, C3), 126.7 (s, C4), 126.4 (s, C5), 124.5 (d, ⁴J_{C-P} = 3.0 Hz, C8), 120.7 (s, CN), 118.7 (s, C6), 2.28 (s, Me) ppm. MS MALDI+ DCTB: m/z = 598.1 [Pd(CNC-H)(PPh₃)]⁺.

Preparation of the complex [Pt(CNC-H)(H₂O)(PPh₃)](ClO₄) (17). To a solution of [Pt(CNC)(PPh₃)] (1) (0.050 g, 0.073 mmol) in 20 mL of CH₂Cl₂ at room temperature, 0.460 mL of a solution of HClO₄ (0.175 M in MeOH, 0.080 mmol) and 0.05 ml of water (2.78 mmol) were added. The bright-yellow solution was immediately concentrated *ca.* 1 mL, 10 mL of diethylether were added and the resulting yellow solid was filtered and air-dried (0.046 g, 77%). Anal. Found: C, 52.63; H, 3.75; N, 1.70. Anal. Calcd. for C₃₅H₂₉ClNO₅PPt: C, 52.21; H, 3.63; N, 1.74. IR (ATR, cm⁻¹): 3140 (w, br. signal, ν(O-H)), 1604 (m, ν(N-C)), 1583 (m, ν(N-C)), 1564 (w, ν(N-C)), 1555 (m, ν(N-C)), 1099 (vs, ν(ClO₄)), 618 (s, ν(ClO₄)), 539 (s, ν(P-C)), 514 (s, ν(P-C)), 500 (s, ν(P-C)). ¹H NMR (400.132 MHz, CD₂Cl₂, 293K): δ = 8.16 (1H, t, ³J_{H7-H6} = ³J_{H7-H8} = 8.0 Hz, H7), 7.95 (1H, d, ³J_{H6-H7} = 8.0 Hz, H6), 7.90 (2H, d, ³J_{H9-H10} = 7.7 Hz, H9), 7.73 (7H, m, *o*-PPh₃ and H8), 7.61 (1H, d, ³J_{H5-H4} = 7.6 Hz, H5), 7.56 (3H, m, *p*-PPh₃), 7.46 (6H, m, *m*-PPh₃), 7.37 (1H, t, ³J_{H11-H10} = 7.7 Hz, H11), 7.19 (2H, t, ³J_{H10-H11} = ³J_{H10-H9} = 7.7 Hz, H10), 7.05 (1H, td, ³J_{H4-H3} = ³J_{H4-H5} = 7.6 Hz, ⁴J_{H4-H2} = 1.7 Hz, H4), 6.53 (2H, m, H2 and H3), 1.83 (2H, br. s, H₂O) ppm. ³¹P{¹H} NMR (161.923 MHz, CD₂Cl₂, 293K): δ = 23.7 (s, ¹J_{P-Pt} = 4405 Hz) ppm. ¹³C{¹H} NMR could not be recorded due to the low stability of this complex in solution for long times. MS MALDI+ DCTB: m/z = 687.1 [Pt(CNC-H)(PPh₃)]⁺.

Preparation of the complex [Pd(CNC-H)(H₂O)(PPh₃)](ClO₄) (18). To a solution of [Pd(CNC)(PPh₃)] (2) (0.050 g, 0.084 mmol) in 15 mL of CH₂Cl₂ at room

temperature, 0.480 mL of a solution of HClO₄ (0.175 M in MeOH, 0.084 mmol) and 0.05 mL of water (2.78 mmol) were added. The bright-yellow solution was immediately evaporated to dryness, and the resulting yellow solid was extracted with diethylether (10 mL), filtered and air-dried (0.043 g, 72%). Anal. Found: C, 58.45; H, 3.81; N, 2.05. Calcd. for C₃₅H₂₉ClNO₅PPd: C, 58.68; H, 4.08; N, 1.96. IR (ATR, cm⁻¹): 3290 (w, broad signal, ν(O-H)), 1597 (w, ν(N-C)), 1576 (w, ν(N-C)), 1565 (w, ν(N-C)), 1556 (m, ν(N-C)), 1098 (s, ν(ClO₄)), 621 (s, ν(ClO₄)), 529 (vs, ν(P-C)), 511 (s, ν(P-C)), 497 (s, ν(P-C)). ¹H NMR (400.132 MHz, CD₂Cl₂, 293K): δ = 8.14 (1H, t, ³J_{H7-H6} = ³J_{H7-H8} = 7.9 Hz, H7), 7.91 (3H, m, H6 and H9), 7.71 (7H, m, *o*-PPh₃ and H5), 7.65 (1H, m, H8), 7.59 (3H, m, *p*-PPh₃), 7.47 (6H, m, *m*-PPh₃), 7.29 (1H, tt, ³J_{H11-H10} = 7.4 Hz, ⁴J_{H11-H9} = 1.3 Hz, H11), 7.15 (2H, m, H10 and H4), 6.63 (1H, td, ³J_{H3-H4} = ³J_{H3-H2} = 7.5 Hz, ⁴J_{H4-H2} = 1.0 Hz, H3), 6.50 (1H, td, ³J_{H2-H3} = ⁴J_{H2-P} = 7.6 Hz, ⁴J_{H2-H4} = 1.0 Hz, H2), 1.60 (2H, s, H₂O) ppm. ³¹P{¹H} NMR (161.923 MHz, CD₂Cl₂, 293K): δ = 40.6 (s) ppm. ¹³C{¹H} NMR plus HSQC and HMBC (100.624 MHz, CD₂Cl₂, 293K): δ = 162.1 (s, C14), 159.4 (s, C13), 147.2 (s, C15), 146.8 (s, C1), 141.9 (s, C7), 139.3 (d, ³J_{C-P} = 12.8 Hz, C2), 139.1 (s, C12), 135.7 (d, ²J_{C-P} = 12.4 Hz, *o*-PPh₃), 132.9 (d, ⁴J_{C-P} = 2.7 Hz, *p*-PPh₃), 132.1 (s, C10), 131.6 (s, C11), 130.6 (d, ⁴J_{C-P} = 6.1 Hz, C3), 130.0 (d, ³J_{C-P} = 11.2 Hz, *m*-PPh₃), 128.9 (d, ¹J_{C-P} = 51.0 Hz, *q*-PPh₃), 127.3 (s, C4), 126.7 (s, C5), 125.9 (s, C9), 123.7 (d, ⁴J_{C-P} = 3.6 Hz, C8), 118.8 (d, ⁴J_{C-P} = 1.8 Hz, C6) ppm. MS MALDI+ DCTB: m/z = 598.1 [Pd(CNC-H)(PPh₃)]⁺.

Preparation of the complex [Pt(CNC-H)(tht)(PPh₃)](ClO₄) (19). To a solution of [Pt(CNC)(PPh₃)] (1) (0.100 g, 0.145 mmol) and tetrahydrothiophene (tht, 25.5 μl, 0.290 mmol) in 25 mL of CH₂Cl₂, 0.830 mL of a solution of HClO₄ (0.175 M in MeOH, 0.145 mmol) were added. The bright-yellow solution was after 1 hour evaporated to dryness, and the resulting yellow solid was extracted with diethylether (15 mL), filtered and air-dried (0.104 g, 82%). Anal. Found: C, 53.60; H, 3.85; N, 1.72; S, 3.91. Anal. Calcd. for C₃₉H₃₅ClNO₄PPtS: C, 53.52; H, 4.03; N, 1.60; S, 3.66. IR (ATR, cm⁻¹): 1600 (w, ν(N-C)), 1574 (w, ν(N-C)), 1538 (m, ν(N-C)), 1282 (w, ν(S-C)), 1235 (w, ν(S-C)), 1084 (s, ν(ClO₄)), 620 (s, ν(ClO₄)), 537 (s, ν(P-C)), 516 (s, ν(P-C)), 499 (vs, ν(P-C)). ¹H NMR (400.132 MHz, CD₂Cl₂, 293K): δ = 8.26 (1H, t, ³J_{H7-H6} = ³J_{H7-H8} = 8.0 Hz, H7), 8.21 (2H, br. s, H9), 8.09 (1H, d, ³J_{H6-H7} = 8.0 Hz, H6), 7.80 (2H, m, H5 and H8), 7.75 (6H, m, *o*-PPh₃), 7.67 (1H, t, ³J_{H11-H10} = 8.0 Hz, H11), 7.57 (5H, m, *p*-PPh₃ and H10), 7.47 (6H, m, *m*-PPh₃), 7.13 (1H, td, ³J_{H4-H5} = ³J_{H4-H3} = 7.5 Hz, ⁴J_{H4-H2} = 1.0 Hz, H4), 6.64 (1H, ddd,

$^3J_{\text{H2-H3}} = 8.0$ Hz, $^4J_{\text{H2-P}} = 3.6$ Hz, $^4J_{\text{H2-H4}} = 1.0$ Hz, $^3J_{\text{H2-Pt}} = 48.4$ Hz, H2), 6.56 (1H, dd, $^3J_{\text{H3-H2}} = 8.0$ Hz, $^4J_{\text{H3-H5}} = 1.0$ Hz, H3), 2.15 (4H, br. s, H α -tht), 1.59 (4H, br. s, H β -tht) ppm. $^{31}\text{P}\{^1\text{H}\}$ NMR (161.923 MHz, CD_2Cl_2 , 293K): $\delta = 22.2$ (s, $^1J_{\text{P-Pt}} = 4353$ Hz) ppm. $^{13}\text{C}\{^1\text{H}\}$ NMR plus HSQC and HMBC (100.624 MHz, CD_2Cl_2 , 293K): $\delta = 165.4$ (s, C14), 160.7 (s, C13), 149.8 (s, C12), 146.4 (s, C15), 145.6 (s, C1), 141.5 (s, C7), 138.3 (d, $^3J_{\text{C-P}} = 8.2$ Hz, C2), 135.2 (d, $^2J_{\text{C-P}} = 12.3$ Hz, *o*-PPh $_3$), 132.6 (d, $^4J_{\text{C-P}} = 2.6$ Hz, *p*-PPh $_3$), 131.8 (s, C10), 130.5 (s, C11), 129.8 (s, C9), 129.4 (d, $^3J_{\text{C-P}} = 11.9$ Hz, *m*-PPh $_3$), 129.4 (d, $^1J_{\text{C-P}} = 61.7$ Hz, *q*-PPh $_3$), 129.3 (s, C3), 125.8 (s, C4), 125.6 (s, C8), 124.9 (d, $^4J_{\text{C-P}} = 4.2$ Hz, C5), 118.7 (d, $^4J_{\text{C-P}} = 2.1$ Hz, $^3J_{\text{H6-Pt}} = 26.0$ Hz, C6), 41.0 (s, H α -tht), 30.2 (s, H β -tht) ppm. MS MALDI+ DCTB: $m/z = 687.1$ [Pt(CNC-H)(PPh $_3$)] $^+$.

Preparation of the complex [Pd(CNC-H)(tht)(PPh $_3$)](TfO) (20). To a solution of [Pd(CNC)(PPh $_3$)] (2) (0.050 g, 0.084 mmol) and tetrahydrothiophene (22.1 μl , 0.250 mmol) in 20 mL of CH_2Cl_2 , 7.53 μl (0.084 mmol) of HTfO were added. The bright-yellow solution was immediately evaporated to dryness, the resulting solid was dissolved with CH_2Cl_2 (4 mL) and the solution was evaporated again to dryness. The yellow solid formed was extracted *n*-hexane (10 mL), filtered and air-dried (0.039 g, 55%). Anal. Found: C, 56.92; H, 4.19; N, 1.71; S, 7.57. Anal. Calcd. for $\text{C}_{40}\text{H}_{35}\text{F}_3\text{NO}_3\text{PPdS}_2$: C, 57.45; H, 4.22; N, 1.68; S, 7.67. IR (ATR, cm^{-1}): 1597 (w, $\nu(\text{N-C})$), 1566 (w, $\nu(\text{N-C})$), 1552 (m, $\nu(\text{N-C})$), 1262 (vs, $\nu(\text{TfO})$), 529 (vs, $\nu(\text{P-C})$), 514 (s, $\nu(\text{P-C})$), 495 (s, $\nu(\text{P-C})$). ^1H NMR (400.132 MHz, CD_2Cl_2 , 293K): $\delta = 8.07$ (3H, m, H10 and H7), 7.97 (1H, d, $^3J_{\text{H6-H7}} = 8.0$ Hz, H6), 7.62 (7H, m, H5 and *o*-PPh $_3$), 7.50 (3H, t, $^3J_{\text{Hm-Hp}} = 8.2$ Hz, *p*-PPh $_3$), 7.42 (9H, m, H8, H9 and *m*-PPh $_3$), 7.12 (1H, m, H4), 6.48 (2H, m, H2 and H3), 2.45 (4H, br. s, H α -tht), 1.78 (4H, br. s, H β -tht) ppm. $^{31}\text{P}\{^1\text{H}\}$ NMR (161.923 MHz, CD_2Cl_2 , 293K): $\delta = 43.6$ (s) ppm. $^{19}\text{F}\{^1\text{H}\}$ NMR (376.489 MHz, CD_2Cl_2 , 293K): $\delta = -78.7$ (s) ppm. $^{13}\text{C}\{^1\text{H}\}$ NMR could not be recorded due to the low stability of this complex in solution for long times. MS MALDI+ DCTB: $m/z = 598.3$ [Pd(CNC-H)(PPh $_3$)] $^+$.

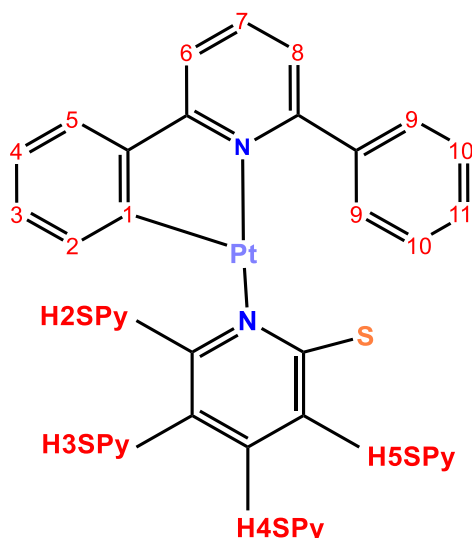


Chart 2.3. ^1H and ^{13}C numbering scheme.

Preparation of the complex $[\text{Pt}(\text{CNC-H})(\mu\text{-S-2Py})]_2$ (21). To a solution of $[\text{Pt}(\text{CNC})(\text{dmsO})]$ (**12**) (0.050 g, 0.099 mmol) in 15 mL of CH_2Cl_2 under argon at room temperature, pyridine-2-thiol (0.011 g, 0.099 mmol) was added. After 1 hour of reaction, the resulting orange solution was evaporated to dryness. To the obtained orange solid 5 mL of diethylether were added and the solution was again evaporated to dryness. After three times of washing and drying the solid it was extracted and washed with cold $^i\text{PrOH}$ (2 mL), filtered and air-dried (0.022 g, 42%). Anal. Found: C, 48.74; H, 3.00; N, 5.22; S, 5.80. Anal. Calcd. for $\text{C}_{44}\text{H}_{32}\text{N}_4\text{Pt}_2\text{S}_2$: C, 49.34; H, 3.01; N, 5.23; S, 5.99. IR (ATR, cm^{-1}): 1603 (w, $\nu(\text{N-C})$), 1581 (m, $\nu(\text{N-C})$), 1566 (w, $\nu(\text{N-C})$), 1551 (w, $\nu(\text{N-C})$). ^1H NMR (400.132 MHz, CD_2Cl_2 , 293K, see Chart 2.3 for the H numbering scheme): δ = 8.31 (4H, dd, $^3J_{\text{H9-H10}} = 8.3$ Hz, $^4J_{\text{H9-H11}} = 2.0$ Hz, H9), 8.03 (2H, t, $^3J_{\text{H7-H6}} = ^3J_{\text{H7-H8}} = 7.8$ Hz, H7), 7.83 (2H, dd, $^3J_{\text{H6-H7}} = 7.8$ Hz, $^4J_{\text{H6-H8}} = 1.0$ Hz, H6), 7.60 (2H, d, $^3J_{\text{H5S-H4S}} = 7.8$ Hz, H5S), 7.55 (2H, dd, $^3J_{\text{H8-H7}} = 7.8$ Hz, $^4J_{\text{H6-H8}} = 1.0$ Hz, H8), 7.46 (6H, m, H2S and H10), 7.20 (4H, m, H4 and H11), 7.14 (2H, dd, $^3J_{\text{H4S-H5S}} = 7.8$ Hz, $^3J_{\text{H4S-H3S}} = 7.2$ Hz, H4S), 7.07 (2H, t, $^3J_{\text{H3S-H4S}} = ^3J_{\text{H3S-H2S}} = 7.2$ Hz, H3S), 6.67 (2H, d, $^3J_{\text{H5-H6}} = 8.1$ Hz, H5), 6.37 (2H, t, $^3J_{\text{H3-H2}} = ^3J_{\text{H3-H4}} = 6.0$ Hz, H3), 5.54 (2H, $^3J_{\text{H2-H3}} = 6.0$ Hz, $^3J_{\text{H2-Pt}} = 34.6$ Hz, H2) ppm. $^{13}\text{C}\{^1\text{H}\}$ NMR could not be recorded due to the low stability of this complex in solution for long times. MS MALDI+ DCTB: m/z = 1070.4 $[[\text{Pt}(\text{CNC-H})(\mu\text{-S-2Py})]_2+\text{H}]^+$, 960.3 $[\text{Pt}(\text{CNC-H})(\mu\text{-S-2Py})(\text{CNC-H})\text{Pt}]^+$, 535.2 $[[\text{Pt}(\text{CNC-H})(\text{H2-SPy})]+\text{H}]^+$.

Preparation of the complex $[\text{Pt}(\text{CNC-H})(8\text{-hq})]$ (22). To a solution of $[\text{Pt}(\text{CNC})(\text{dmsO})]$ (**12**) (0.050 g, 0.099 mmol) in 15 mL of acetone, 8-hydroxyquinoline

(0.018 g, 0.129 mmol) was added. The reaction was refluxed for 21 hours, and the resulting orange solution was evaporated to dryness. To the resulting orange solid 5 mL of acetone were added and the solution was again evaporated to dryness. This was repeated with 5 mL of diethylether. After three times of washing and drying the solid with diethylether it was extracted with 5 mL of diethylether, filtered and air-dried (0.033 g, 58%). Anal. Found: C, 54.46; H, 2.93; N, 4.91. Anal. Calcd. for $C_{26}H_{18}N_2OPt$: C, 54.83; H, 3.19; N, 4.92. IR (ATR, cm^{-1}): 1589 (w, $\nu(N-C)$), 1570 (m, $\nu(N-C)$), 1550 (w, $\nu(N-C)$). Due to the existence of a mixture of two isomers *trans*-(N,O) (isomer **22A**) and *trans*-(N,N) (isomer **22B**) in proportions 3:1, the two sets of signals could not be assigned unequivocally. Signals of the more intense set are differenced with an asterisk. 1H NMR (400.132 MHz, CD_2Cl_2 , 293K): δ = 9.07 (d, $^3J_{H-H} = 5.7$ Hz, $^3J_{H-Pt} = 47.7$ Hz, H_{ar}^*), 8.52 (d, $^3J_{H-H} = 8.0$ Hz, H_{ar}), 8.22 (d, $^3J_{H-H} = 5.7$ Hz, $^3J_{H-Pt} = 47.7$ Hz, H_{ar}^*), 7.95 (m, H_{ar} and H_{ar}^*), 7.77 (dd, $^3J_{H-H} = 8.0$ Hz, H_{ar}^*), 7.68-7.14 (m, H_{ar} and H_{ar}^*), 7.02 (dd, $^3J_{H-H} = 8.0$ Hz, $^4J_{H-H} = 1.1$ Hz, H_{ar}), 6.83 (m, H_{ar}), 6.71 (dd, $^3J_{H-H} = 8.3$ Hz, $^4J_{H-H} = 1.1$ Hz, H_{ar}^*), 6.06 (dd, $^3J_{H-H} = 7.6$ Hz, $^4J_{H-H} = 1.1$ Hz, H_{ar}^*) ppm. $^{13}C\{^1H\}$ NMR plus HSQC and HMBC (100.624 MHz, CD_2Cl_2 , 293K): δ = 168.7 (s, C_{ar}^*), 168.2 (C_{ar}^*), 163.1 (s, C_{ar}^*), 148.2 (s, C_{ar}^*), 147.8 (s, C_{ar}^*), 146.4 (s, C_{ar}), 145.8 (s, C_{ar}^*), 144.2 (s, C_{ar}), 143.4 (s, C_{ar}^*), 140.5 (s, C_{ar}), 139.1 (s, C_{ar}), 138.8 (s, C_{ar}^*), 138.7 (s, C_{ar}), 137.9 (s, C_{ar}), 137.3 (s, C_{ar}), 132.6 (s, C_{ar}), 132.5 (s, C_{ar}^*), 131.5 (s, C_{ar}^*), 130.7 (s, C_{ar}), 130.2 (s, C_{ar}), 129.8 (s, C_{ar}), 129.6 (s, C_{ar}), 129.3 (s, C_{ar}), 129.0 (s, C_{ar}), 128.7 (s, C_{ar}), 128.3 (s, C_{ar}), 127.7 (s, C_{ar}), 124.6 (s, C_{ar}), 124.1 (s, C_{ar}), 123.7 (s, C_{ar}), 121.2 (s, C_{ar}), 120.7 (s, C_{ar}), 117.5 (s, C_{ar}), 116.7 (s, C_{ar}^*), 114.9 (s, C_{ar}^*), 114.2 (s, C_{ar}), 112.4 (s, C_{ar}), 109.9 (s, C_{ar}^*) ppm. MS MALDI+ DCTB: $m/z = 569.1$ $[Pt(CNC-H)(8-hq)]^+$.

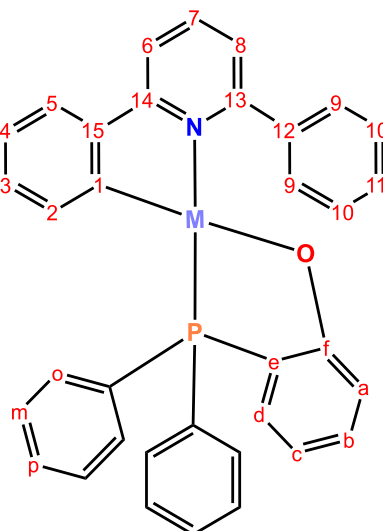


Chart 2.4. ^1H and ^{13}C numbering scheme.

Preparation of the complex [Pt(CNC-H){PPh₂(C₆H₄-o-O)}] (23). To a solution of [Pt(CNC)(dmsO)] (12) (0.070 g, 0.139 mmol) in 20 mL of CH₂Cl₂ at room temperature, (2-hydroxyphenyl)diphenylphosphane (0.039 g, 0.142 mmol) under argon was added. After 2 hours of reaction, the resulting yellow solution was concentrated to *ca.* 2 mL and 15 mL of *n*-hexane were added. The yellow solid formed was then filtered and air-dried (0.070 g, 71%). Anal. Found: C, 60.20; H, 3.73; N, 1.64. Anal. Calcd. for C₃₅H₂₆NOPPt: C, 59.83; H, 3.73; N, 1.99. IR (ATR, cm⁻¹): 1596 (w, $\nu(\text{N-C})$), 1578 (w, $\nu(\text{N-C})$), 1564 (s, $\nu(\text{N-C})$), 1551 (w, $\nu(\text{N-C})$), 532 (s, $\nu(\text{P-C})$), 509 (s, $\nu(\text{P-C})$), 489 (s, $\nu(\text{P-C})$). ^1H NMR (400.132 MHz, CD₂Cl₂, 293K, see Chart 2.4 for the H numbering scheme): δ = 7.96 (1H, t, $^3J_{\text{H7-H6}} = ^3J_{\text{H7-H8}} = 7.8$ Hz, H7), 7.90 (2H, dd, $^3J_{\text{H9-H10}} = 7.8$ Hz, $^4J_{\text{H9-H11}} = 1.5$ Hz, H9), 7.86 (1H, d, $^3J_{\text{H6-H7}} = 7.8$ Hz, H6), 7.80 (4H, m, *o*-PPh₂), 7.59 (1H, dd, $^3J_{\text{H5-H4}} = 7.6$ Hz, $^4J_{\text{H5-H3}} = 1.0$ Hz, H5), 7.53 (1H, d, $^3J_{\text{H8-H7}} = 7.6$ Hz, H8), 7.44 (8H, m, H10, H11, *m*-PPh₂ and *p*-PPh₂), 7.15 (1H, dd, $^3J_{\text{H2-H3}} = 7.6$ Hz, $^4J_{\text{H2-H4}} = 1.2$ Hz, $^3J_{\text{H2-Pt}} = 54.0$ Hz, H2), 7.02 (1H, td, $^3J_{\text{H4-H5}} = ^3J_{\text{H4-H3}} = 7.6$ Hz, $^4J_{\text{H4-H2}} = 1.2$ Hz, H4), 6.90 (2H, m, Ha and Hb), 6.78 (1H, td, $^3J_{\text{H3-H2}} = ^3J_{\text{H3-H4}} = 7.6$ Hz, $^4J_{\text{H3-H5}} = 1.0$ Hz, H3), 6.26 (1H, t, $^3J_{\text{Hc-Hd}} = ^3J_{\text{Hc-Hb}} = 7.6$ Hz, Hc), 5.77 (1H, m, Hd) ppm. $^{31}\text{P}\{^1\text{H}\}$ NMR (161.923 MHz, CD₂Cl₂, 293K): δ = 20.2 (s, $^1J_{\text{P-Pt}} = 4435$ Hz) ppm. $^{13}\text{C}\{^1\text{H}\}$ NMR plus HSQC and HMBC (100.624 MHz, CD₂Cl₂, 293K, see Chart 2.4 for the C numbering scheme): δ = 177.0 (s, Cf), 165.4 (s, C14), 162.1 (s, C13), 146.9 (s, C15), 146.9 (s, C1), 139.8 (s, C12), 139.7 (s, C7), 138.9 (d, $^3J_{\text{C-P}} = 5.7$ Hz, C2), 134.1 (d, $^2J_{\text{C-P}} = 11.7$ Hz, *o*-PPh₂), 133.4 (d, $^3J_{\text{C-P}} = 1.5$ Hz, Ca or Cb), 131.9 (s, Ca or Cb), 131.3 (d, $^4J_{\text{C-P}} = 2.6$ Hz, *p*-PPh₂), 131.1 (d, $^1J_{\text{C-P}} = 58.0$ Hz, *q*-

PPh₂), 129.9 (s, C3), 129.8 (s, C9), 129.4 (s, C11), 129.0 (d, ³J_{C-P} = 11.1 Hz, *m*-PPh₂), 127.7 (s, C10), 124.7 (s, C5), 124.4 (s, C8), 123.3 (s, C4), 119.5 (d, ³J_{C-P} = 9.2 Hz, Cc), 117.1 (s, C6), 117.0 (d, ¹J_{C-P} = 65.0 Hz, Ce), 114.3 (d, ²J_{C-P} = 9.3 Hz, Cd) ppm. MS ESI⁺: m/z = 702.5 [[Pt(CNC-H){PPh₂(C₆H₄-*o*-O)}]+H]⁺.

Preparation of the complex [Pd(CNC-H){PPh₂(C₆H₄-*o*-O)}] (24). To a solution of (2-hydroxyphenyl)diphenylphosphane (0.052 g, 0.180 mmol) in 20 mL of MeOH under argon, [Pd(CNC-H)(μ-Cl)]₂ (0.07 g, 0.094 mmol) and KOH (0.015 g, 0.24 mmol) were added. The reaction was kept under reflux for 15 mins. Then, the resulting solution was evaporated to dryness. After that, 20 mL of CH₂Cl₂ were added and the resulting solution filtered through celite. The yellow solution obtained was then evaporated to dryness and the yellow solid formed extracted with 15 mL of *n*-hexane and air-dried (0.063 g, 55%). Anal. Found: C, 68.18; H, 4.31; N, 2.01. Anal. Calcd. for C₃₅H₂₆NOPPd: C, 68.47; H, 4.27; N, 2.28. IR (ATR, cm⁻¹): 1594 (m, ν(N-C)), 1575 (m, ν(N-C)), 1553 (s, ν(N-C)), 1320 (s, ν(C-O)), 520 (s, ν(P-C)), 504 (s, ν(P-C)). ¹H NMR (400.132 MHz, CD₂Cl₂, 293K): δ = 7.94 (1H, t, ³J_{H7-H6} = ³J_{H7-H8} = 7.8 Hz, H7), 7.90 (2H, dd, ³J_{H9-H10} = 7.7 Hz, ⁴J_{H9-H11} = 1.4 Hz, H9), 7.83 (1H, d, ³J_{H6-H7} = 7.8 Hz, H6), 7.77 (3H, m, *o*-PPh₂), 7.61 (1H, dd, ³J_{H5-H4} = 7.8 Hz, ⁴J_{H5-H3} = 1.6 Hz, H5), 7.45 (10H, m, H8, H10, H11, *p*-PPh₂ and *m*-PPh₂), 7.04 (2H, m, H4 and H2), 6.89 (1H, m, Hb), 6.81 (1H, m, Ha, overlapped with H3), 6.79 (1H, td, ³J_{H3-H2} = ³J_{H3-H4} = 7.8 Hz, ⁴J_{H3-H5} = 1.6 Hz, H3), 6.21 (1H, m, Hc), 5.69 (1H, m, Hd) ppm. ³¹P{¹H} NMR (161.923 MHz, CD₂Cl₂, 293K): δ = 40.0 (s) ppm. ¹³C{¹H} NMR (100.624 MHz, CD₂Cl₂, 293K): δ = 176.5 (d, ²J_{C-P} = 17.3 Hz, Cf), 164.9 (d, ²J_{C-P} = 2.9 Hz, C14), 161.9 (s, C13), 155.1 (d, ²J_{C-P} = 1.0 Hz, C1), 148.1 (d, ³J_{C-P} = 1.5 Hz, C15), 139.8 (s, C12), 139.6 (s, C7), 139.3 (d, ³J_{C-P} = 10.5 Hz, C2), 134.2 (d, ²J_{C-P} = 13.5 Hz, *o*-PPh₂), 133.4 (d, ³J_{C-P} = 2.0 Hz, Ca), 132.3 (s, Cb), 131.4 (d, ¹J_{C-P} = 51.9 Hz, *q*-PPh₂), 131.2 (d, ⁴J_{C-P} = 2.8 Hz, *p*-PPh₂), 129.6 (s, C9), 129.4 (s, C11), 129.2 (d, ⁴J_{C-P} = 4.3 Hz, C3), 129.1 (d, ³J_{C-P} = 10.9 Hz, *m*-PPh₂), 127.8 (s, C10), 125.1 (s, C5), 124.5 (s, C4), 123.8 (d, ⁴J_{C-P} = 3.1 Hz, C8), 119.6 (d, ²J_{C-P} = 11.4 Hz, Cd), 117.4 (d, ¹J_{C-P} = 55.7 Hz, Ce), 117.2 (s, C6), 113.4 (d, ³J_{C-P} = 8.3 Hz, Cc) ppm. MS MALDI⁺ DCTB: m/z = 613.1 [Pd(CNC-H){PPh₂(C₆H₄-*o*-O)}]⁺.

Preparation of [Pt(CNC-H)(NC₅H₄-*o*-COO)] (25). To a solution of [Pt(CNC)(dmsO)] (12) (0.050 g, 0.099 mmol) in 15 mL of acetone, 2-pyridinecarboxylic acid (0.014 g, 0.114 mmol) was added. The reaction was refluxed for 16 hours, and the resulting bright yellow solution was evaporated to dryness. To the resulting orange solid 10 mL of acetone were added and the solution was again evaporated to dryness. This was repeated with 5 mL of diethylether. After three times of washing and drying the solid it was extracted with 5 mL more of diethylether, filtered and air-dried (0.041 g, 75%). Anal. Found: C, 49.99; H, 2.86; N, 4.89. Anal. Calcd. for C₂₃H₁₆N₂O₂Pt: C, 49.60; H, 2.83; N, 5.00. IR (ATR, cm⁻¹): 1662 (s, ν(C=O)), 1604 (m, ν(N-C)), 1582 (w, ν(N-C)), 1563 (m, ν(N-C)), 1552 (m, ν(N-C)), 1332 (s, ν(C-O)). Due to complexity caused by the existence of a mixture of two isomers, *trans*-(N,O) (isomer A) and *trans*-(N,N) (isomer B) in proportions 1:1, signals could not be assigned unequivocally. ¹H NMR (400.132 MHz, CD₂Cl₂, 293K): δ = 9.13 (dt, ³J_{H-H} = 5.7 Hz, ⁴J_{H-H} = 1.0 Hz, ³J_{H-Pt} = 48.3 Hz, H_{ar} isomer B), 8.45 (d, ³J_{H-H} = 8.0 Hz, H_{ar} isomer A), 7.96 (m, H_{ar} isomers A and B), 7.78 (m, H_{ar} isomers A and B), 7.52 (m, H_{ar} isomers A and B), 7.41 (dd, ³J_{H-H} = 8.3 Hz, ⁴J_{H-H} = 1.4 Hz, isomer B), 7.25 (m, H_{ar} isomers A and B), 7.01 (m, H_{ar} isomer A) ppm. ¹³C{¹H} NMR plus HSQC and HMBC (100.624 MHz, CD₂Cl₂, 293K): δ = 168.9 (s, COO), 163.5 (s, COO), 154.5 (s, C_{ar}), 150.1 (s, C_{ar}), 149.2 (s, C_{ar} isomer B), 147.9 (s, C_{ar}), 139.2 (s, C_{ar}), 138.5 (s, C_{ar}), 138.3 (s, C_{ar}), 131.0 (s, C_{ar}), 130.0 (s, C_{ar}), 129.9 (s, C_{ar} isomer A), 129.2 (s, C_{ar}), 129.0 (s, C_{ar}), 128.4 (s, C_{ar}), 128.2 (s, C_{ar}), 127.6 (s, C_{ar}), 127.3 (s, C_{ar} isomer A), 127.0 (s, C_{ar}), 126.2 (s, C_{ar}), 124.7 (s, C_{ar}), 124.6 (s, C_{ar}), 124.3 (s, C_{ar}), 123.8 (s, C_{ar} isomer B), 123.5 (s, C_{ar}), 123.4 (s, C_{ar}), 117.7 (s, C_{ar}), 116.7 (s, C_{ar}) ppm. MS MALDI+ DCTB: m/z = 547.9 [[Pt(CNC-H)(C₅H₅NCOO)]+H]⁺.

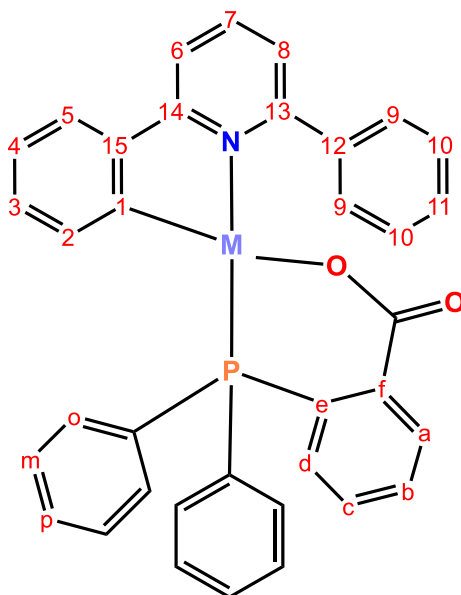


Chart 2.5. ^1H and ^{13}C numbering scheme.

Preparation of the complex [Pt(CNC-H){PPh₂(C₆H₄-*o*-COO)}] (26). To a solution of [Pt(CNC)(dmsO)] (**12**) (0.050 g, 0.099 mmol) in 20 mL of CH₂Cl₂ at room temperature, 2-(diphenylphosphino)benzoic acid (0.031 g, 0.099 mmol) was added. After 25 mins of reaction, the resulting bright yellow solution was evaporated to dryness. To the resulting yellow solid 10 mL of CH₂Cl₂ were added and the solution was again evaporated to dryness. After three times of washing and drying the solid with CH₂Cl₂ it was extracted with 10 mL of diethylether, filtered and air-dried (0.059 g, 81%). Anal. Found: C, 58.93; H, 3.62; N, 1.54. Anal. Calcd. for C₃₆H₂₆NO₂Ppt: C, 59.18; H, 3.59; N, 1.92. IR (ATR, cm⁻¹): 1623 (s, ν(C=O)), 1602 (w, ν(N-C)), 1580 (m, ν(N-C)), 1559 (w, ν(N-C)), 541 (s, ν(P-C)), 514 (s, ν(P-C)). ^1H NMR (400.132 MHz, CD₂Cl₂, 293K, see Chart 2.5 for the H numbering scheme): δ = 7.98 (3H, m, H7 and H9), 7.89 (1H, d, $^3J_{\text{H6-H7}} = 7.9$ Hz, H6), 7.75 (1H, m, Ha), 7.64 (1H, d, $^3J_{\text{H5-H4}} = 7.6$ Hz, H5), 7.56 (7H, m, *o*-PPh₂, *p*-PPh₂ and H8), 7.44 (5H, m, *m*-PPh₂ and Hb), 7.28 (2H, m, H11 and Hc), 7.22 (2H, t, $^3J_{\text{H10-H9}} = ^3J_{\text{H10-H11}} = 7.2$ Hz, H10), 7.02 (1H, t, $^3J_{\text{H4-H5}} = ^3J_{\text{H4-H3}} = 7.6$ Hz, H4), 6.79 (1H, m, Hd), 6.61 (1H, t, $^3J_{\text{H3-H2}} = ^3J_{\text{H3-H4}} = 7.6$ Hz, H3), 6.33 (1H, dd, $^3J_{\text{H2-H3}} = 7.6$ Hz, $^4J_{\text{H2-P}} = 3.0$ Hz, $^3J_{\text{H2-Pt}} = 55.4$ Hz, H2) ppm. $^{31}\text{P}\{^1\text{H}\}$ NMR (161.923 MHz, CD₂Cl₂, 293K): δ = 11.1 (s, $^1J_{\text{P-Pt}} = 4388$ Hz) ppm. $^{13}\text{C}\{^1\text{H}\}$ NMR plus HSQC and HMBC (100.624 MHz, CD₂Cl₂, 293K, see Chart 2.5 for the C numbering scheme): δ = 166.6 (s, COO), 164.4 (s, C14), 160.8 (s, C13), 146.8 (s, C15), 143.3 (s, Cf), 139.8 (s, C7), 139.3 (s, C12), 136.7 (d, $^3J_{\text{C-P}} = 4.9$ Hz, C2), 135.5 (d, $^2J_{\text{C-P}} = 4.2$ Hz, C1), 134.8 (d, $^2J_{\text{C-P}} = 13.0$ Hz, *o*-PPh₂),

133.0 (d, $^3J_{C-P} = 9.8$ Hz, Ca), 132.5 (d, $^2J_{C-P} = 5.4$ Hz, Cd), 132.1 (d, $^4J_{C-P} = 2.6$ Hz, *p*-PPh₂), 130.9 (d, $^4J_{C-P} = 2.6$ Hz, Cb), 129.6 (s, C11), 129.3 (d, $^3J_{C-P} = 11.2$ Hz, *m*-PPh₂), 129.2 (s, C9), 129.1 (s, C3), 128.9 (d, $^3J_{C-P} = 8.9$ Hz, Cc), 128.3 (s, C10), 128.2 (d, $^1J_{C-P} = 61.6$ Hz, *q*-PPh₂), 126.6 (d, $^1J_{C-P} = 60.9$ Hz, Ce), 124.8 (s, C5), 124.5 (d, $^4J_{C-P} = 4.3$ Hz, C8), 123.8 (s, C4), 116.9 (d, $^4J_{C-P} = 2.0$ Hz, C6) ppm. MS MALDI+ DCTB: $m/z = 731.2$ [[Pt(CNC-H)(C₆H₄-*o*-COO)]+H]⁺.

Preparation of the complex [Pd(CNC-H){PPh₂(C₆H₄-*o*-COO)}] (27). To a solution of [Pd(CNC)(PPh₃)] (2) (0.041 g, 0.069 mmol) in 20 mL of CH₂Cl₂ under argon at room temperature, 2-(diphenylphosphino)benzoic acid (0.023 g, 0.076 mmol) were added and the resulting solution changed to a bright yellow color. After 20 mins of stirring, the solution was evaporated to dryness. The yellow solid formed was then extracted with diethylether (10 mL), filtered and air-dried (0.032 g, 72%). Anal. Found: C, 67.08; H, 3.94; N, 1.76. Anal. Calcd. for C₃₆H₂₆NO₂PPd: C, 67.35; H, 4.08; N, 2.18. IR (ATR, cm⁻¹): 1610 (s, ν(C=O)), 1593 (s, ν(N-C)), 1576 (m, ν(N-C)), 1556 (s, ν(N-C)), 1373 (s, ν(C-O)), 533 (s, ν(P-C)), 513 (s, ν(P-C)). ¹H NMR (400.132 MHz, CD₂Cl₂, 293K): δ = 7.90 (3H, m, H7 and H6), 7.83 (1H, d, $^3J_{H6-H7} = 8.1$ Hz, H6), 7.75 (1H, m, Ha), 7.66 (1H, d, $^3J_{H5-H4} = 7.7$ Hz, H5), 7.54 (6H, m, *o*-PPh₂ and *p*-PPh₂), 7.49 (2H, m, Hb and H8), 7.44 (4H, m, *m*-PPh₂), 7.29 (3H, m, H11 and Hc), 7.19 (2H, t, $^3J_{H10-H9} = ^3J_{H10-H11} = 7.6$ Hz, H10), 7.06 (1H, t, $^3J_{H4-H5} = ^3J_{H4-H3} = 7.7$ Hz, H4), 6.79 (1H, m, Hd), 6.64 (1H, t, $^3J_{H3-H2} = ^3J_{H3-H4} = 7.6$ Hz, H3), 6.33 (1H, d, $^3J_{H2-H3} = 7.6$ Hz, H2) ppm. ³¹P{¹H} NMR (161.923 MHz, CD₂Cl₂, 293K): δ = 36.0 (s) ppm. ¹³C{¹H} NMR (100.624 MHz, CD₂Cl₂, 293K): δ = 167.6 (s, COO), 163.4 (s, C14), 160.8 (s, C13), 151.3 (s, C1), 147.9 (s, C15), 144.3 (s, Cf), 139.8 (s, C7), 139.3 (s, C12), 137.7 (d, $^3J_{C-P} = 9.8$ Hz, C2), 135.0 (d, $^2J_{C-P} = 12.5$ Hz, *o*-PPh₂), 132.9 (d, $^3J_{C-P} = 8.8$ Hz, Ca), 132.5 (d, $^2J_{C-P} = 5.8$ Hz, Cd), 132.0 (d, $^4J_{C-P} = 2.1$ Hz, *p*-PPh₂), 130.9 (d, $^4J_{C-P} = 2.5$ Hz, Cb), 129.7 (s, C11), 129.3 (d, $^3J_{C-P} = 11.2$ Hz, *m*-PPh₂), 129.0 (d, $^3J_{C-P} = 8.6$ Hz, Cc), 128.9 (s, C9), 128.8 (d, $^4J_{C-P} = 4.9$ Hz, C3), 128.6 (s, C10), 128.5 (d, overlapped, *q*-PPh₂), 126.6 (d, $^1J_{C-P} = 56.0$ Hz, Ce), 125.2 (s, C5), 124.9 (s, C4), 123.9 (s, C8), 117.1 (s, C6) ppm. MS MALDI+ DCTB: $m/z = 642.2$ [[Pd(CNC-H)(C₆H₄-*o*-COO)]+H]⁺.

2.4. References

- (1) Böttcher, H.-C.; Graf, M.; Mayer, P.; Scheer, M. Synthesis and Characterization of a Novel Triangular Rh₂Au Cluster Compound Inspired by the Isolobality Concept. *ChemistryOpen* **2020**, *9* (10), 991-995. DOI: 10.1002/open.202000217.
- (2) Hashmi, A. S. K. Homogeneous gold catalysis: The role of protons. *Catal. Today* **2007**, *122* (3), 211-214. DOI: 10.1016/j.cattod.2006.10.006.
- (3) Kickelbick, G.; Schubert, U. ClMPH₃ and [MPH₃]⁺ (M=Cu, Ag, Au); a density functional study. *Inorg. Chim. Acta* **1997**, *262* (1), 61-64. DOI: 10.1016/S0020-1693(97)05484-4.
- (4) Raubenheimer, H. G.; Schmidbaur, H. Gold Chemistry Guided by the Isolobality Concept. *Organometallics* **2012**, *31* (7), 2507-2522. DOI: 10.1021/om2010113.
- (5) Belío, Ú.; Fuertes, S.; Martín, A. Preparation of Pt-Tl clusters showing new geometries. X-ray, NMR and luminescence studies. *Dalton Trans.* **2014**, *43* (28), 10828-10843. DOI: 10.1039/c4dt00536h.
- (6) Aghakhanpour, R. B.; Nabavizadeh, S. M.; Rashidi, M.; Kubicki, M. Luminescence properties of some monomeric and dimeric cycloplatinated(II) complexes containing biphosphine ligands. *Dalton Trans.* **2015**, *44* (36), 15829-15842. DOI: 10.1039/C5DT02450A.
- (7) Sicilia, V.; Fuertes, S.; Martín, A.; Palacios, A. N-Assisted C_{Ph}-H Activation in 3,8-Dinitro-6-phenylphenanthridine. New C,N-Cyclometalated Compounds of Platinum(II): Synthesis, Structure, and Luminescence Studies. *Organometallics* **2013**, *32* (15), 4092-4102. DOI: 10.1021/om400159g.
- (8) Solomatina, A. I.; Aleksandrova, I. O.; Karttunen, A. J.; Tunik, S. P.; Koshevoy, I. O. Dibenzothiophene-platinated complexes: probing the effect of ancillary ligands on the photophysical performance. *Dalton Trans.* **2017**, *46* (12), 3895-3905. DOI: 10.1039/C7DT00349H.
- (9) Solomatina, A. I.; Chelushkin, P. S.; Abakumova, T. O.; Zhemkov, V. A.; Kim, M.; Bezprozvanny, I.; Gurzhiy, V. V.; Melnikov, A. S.; Anufrikov, Y. A.; Koshevoy, I. O.; Su, S.-H.; Chou, P.-T.; Tunik, S. P. Reactions of Cyclometalated Platinum(II) [Pt(NAC)(PR₃)Cl] Complexes with Imidazole and Imidazole-Containing Biomolecules: Fine-Tuning of Reactivity and Photophysical Properties *via* Ligand Design. *Inorg. Chem.* **2019**, *58* (1), 204-217. DOI: 10.1021/acs.inorgchem.8b02204.

- (10) Godbert, N.; Pugliese, T.; Aiello, I.; Bellusci, A.; Crispini, A.; Ghedini, M. Efficient, Ultrafast, Microwave-Assisted Syntheses of Cycloplatinated Complexes. *Eur. J. Inorg. Chem.* **2007**, 2007 (32), 5105-5111. DOI: 10.1002/ejic.200700639.
- (11) Newman, C. P.; Casey-Green, K.; Clarkson, G. J.; Cave, G. W. V.; Errington, W.; Rourke, J. P. Cyclometallated platinum(II) complexes: oxidation to, and C–H activation by, platinum(IV). *Dalton Trans.* **2007**, (29), 3170-3182. DOI: 10.1039/B705609E.
- (12) Sasaki, I.; Bijani, C.; Ladeira, S.; Bourdon, V.; Faller, P.; Hureau, C. Interference of a new cyclometallated Pt compound with Cu binding to amyloid- β peptide. *Dalton Trans.* **2012**, 41 (21), 6404-6407. DOI: 10.1039/C2DT12177H.
- (13) Stacey, O. J.; Platts, J. A.; Coles, S. J.; Horton, P. N.; Pope, S. J. A. Phosphorescent, Cyclometalated Cinchophen-Derived Platinum Complexes: Syntheses, Structures, and Electronic Properties. *Inorg. Chem.* **2015**, 54 (13), 6528-6536. DOI: 10.1021/acs.inorgchem.5b00817.
- (14) Atla, S. B.; Kelkar, A. A.; Puranik, V. G.; Bensch, W.; Chaudhari, R. V. NC palladacycles in the Heck arylation of ethylene: Synthesis, structure and their reactivity. *J. Organomet. Chem.* **2009**, 694 (5), 683-690. DOI: 10.1016/j.jorganchem.2008.11.065.
- (15) Sánchez, G.; García, J.; Meseguer, D.; Serrano, J. L.; García, L.; Pérez, J.; López, G. Synthesis and characterisation of cyclometallated palladium(II) complexes with phosphine–carboxylate and phosphine–amide ligands. *Dalton Trans.* **2003**, (24), 4709-4717. DOI: 10.1039/B310843K.
- (16) Joseph, M. C.; Swarts, A. J.; Mapolie, S. F. Phenylacetylene polymerisation mediated by cationic cyclometallated palladium(II) complexes bearing benzylidene 2,6-diisopropylphenylamine and its derivatives as ligands. *Dalton Trans.* **2018**, 47 (35), 12209-12217. DOI: 10.1039/C8DT02728E.
- (17) Shahsavari, H. R.; Babadi Aghakhanpour, R.; Nikraves, M.; Ozdemir, J.; Golbon Haghghi, M.; Notash, B.; Beyzavi, H. Highly Emissive Cycloplatinated(II) Complexes Obtained by the Chloride Abstraction from the Complex [Pt(ppy)(PPh₃)(Cl)]: Employing Various Silver Salts. *Organometallics* **2018**, 37 (17), 2890-2900. DOI: 10.1021/acs.organomet.8b00461.
- (18) Ma, J.-F.; Kojima, Y.; Yamamoto, Y. Reactions of palladium complex of N,N-dimethylbenzylamine with aromatic phosphines bearing the methoxy groups at

- the 2,6-positions. *J. Organomet. Chem.* **2000**, *616* (1), 149-156. DOI: 10.1016/S0022-328X(00)00586-6.
- (19) Monnereau, L.; Sémeril, D.; Matt, D.; Toupet, L. Cavity-Shaped Ligands: Calix[4]arene-Based Monophosphanes for Fast Suzuki–Miyaura Cross-Coupling. *Chem. Eur. J.* **2010**, *16* (30), 9237-9247. DOI: 10.1002/chem.200903390.
- (20) Jamshidi, M.; Babaghasabha, M.; Shahsavari, H. R.; Nabavizadeh, S. M. The influence of thiolate ligands on the luminescence properties of cycloplatinated(II) complexes. *Dalton Trans.* **2017**, *46* (45), 15919-15927. DOI: 10.1039/C7DT03599C.
- (21) Kim, M.; Picot, A.; Gabbai, F. P. Remarkably Efficient Hydrolysis of Methylparathion Catalyzed by [2-(2-Pyridyl)phenyl-C,N]palladium(II) Complexes. *Inorg. Chem.* **2006**, *45* (14), 5600-5606. DOI: 10.1021/ic0600578.
- (22) Niazi, M.; Shahsavari, H. R.; Haghighi, M. G.; Halvagar, M. R.; Hatami, S.; Notash, B. Reactivity of a half-lantern Pt₂(II,II) complex with triphenylphosphine: selectivity in a protonation reaction. *RSC Adv.* **2016**, *6* (80), 76463-76472. DOI: 10.1039/C6RA15604E.
- (23) Berenguer, J. R.; Lalinde, E.; Torroba, J. Synthesis, characterization and photophysics of a new series of anionic C,N,C cyclometalated platinum complexes. *Inorg. Chem.* **2007**, *46* (23), 9919-9930. DOI: 10.1021/ic701298z.
- (24) Campillo, D.; Belío, Ú.; Martín, A. New Pt → M (M = Ag or Tl) complexes based on anionic cyclometalated Pt(II) complexes. *Dalton Trans.* **2019**, *48* (10), 3270-3283. DOI: 10.1039/c9dt00121b.
- (25) El-khateeb, M.; Damer, K.; Görls, H.; Weigand, W. Pyridine- and pyrimidine-2-thiolate complexes of ruthenium. *J. Organomet. Chem.* **2007**, *692* (11), 2227-2233. DOI: 10.1016/j.jorganchem.2007.01.047.
- (26) Engelking, H.; Karentzopoulos, S.; Reusmann, G.; Krebs, B. Novel dinuclear palladium(II) complexes with the chelating ligand bis(1-methylimidazol-2-yl) ketone (bmik) and pyridine-2-thiolate, pyrimidine-2-thiolate, and 1-methylimidazole-2-thiolate as bridging secondary ligands. *Chem. Ber.* **1994**, *127* (12), 2355-2361. DOI: 10.1002/cber.19941271203.
- (27) Liaw, W.-F.; Chen, C.-H.; Lee, G.-H.; Peng, S.-M. Iron Pyridine-2-thiolate Complexes: Interconversion of [Fe⁰(CO)₄(SC₅H₄N)]⁻, *cis*-[Fe^{II}(CO)₂(SC₅H₄N)₂], and [Fe^{II}(SC₅H₄N)₃]. *Organometallics* **1998**, *17* (11), 2370-2372. DOI: 10.1021/om971004o.

- (28) Niazi, M.; Shahsavari, H. R.; Haghighi, M. G.; Halvagar, M. R.; Hatami, S.; Notash, B. Carbon-sulfur bond reductive coupling from a platinum(II) thiolate complex. *RSC Adv.* **2016**, *6* (97), 95073-95084. DOI: 10.1039/c6ra21756g.
- (29) Wächtler, E.; Gericke, R.; Zhechkov, L.; Heine, T.; Langer, T.; Gerke, B.; Pöttgen, R.; Wagler, J. Pyridine-2-thiolate bridged tin-palladium complexes with Sn(PdN₂Cl₂), Sn(PdN₂S₂), Sn(PdN₂C₂) and Sn(Pd₂N₄) skeletons. *Chem. Commun.* **2014**, *50* (40), 5382-5384. DOI: 10.1039/C3CC47912A.
- (30) Aoki, R.; Kobayashi, A.; Chang, H.-C.; Kato, M. Structures and Luminescence Properties of Cyclometalated Dinuclear Platinum(II) Complexes Bridged by Pyridinethiolate Ions. *Bull. Chem. Soc. Jpn.* **2011**, *84* (2), 218-225. DOI: 10.1246/bcsj.20100304.
- (31) Halder, P.; SantaLucia, D. J.; Park, S. V.; Berry, J. F. From Pincer to Paddlewheel: C-H and C-S Bond Activation at Bis(2-pyridylthio)methane by Palladium(II). *Inorg. Chem.* **2019**, *58* (4), 2270-2274. DOI: 10.1021/acs.inorgchem.8b03568.
- (32) Kato, M.; Omura, A.; Toshikawa, A.; Kishi, S.; Sugimoto, Y. Vapor-induced luminescence switching in crystals of the syn isomer of a dinuclear (bipyridine)platinum(II) complex bridged with pyridine-2-thiolate ions. *Angew. Chem. Int. Ed.* **2002**, *41* (17), 3183-3185. DOI: 10.1002/1521-3773(20020902)41:17<3183::Aid-anie3183>3.0.Co;2-a.
- (33) Koshiyama, T.; Omura, A.; Kato, M. Redox-controlled Luminescence of a Cyclometalated Dinuclear Platinum Complex Bridged with Pyridine-2-thiolate Ions. *Chem. Lett.* **2004**, *33* (10), 1386-1387. DOI: 10.1246/cl.2004.1386.
- (34) Ma, B.; Djurovich, P. I.; Garon, S.; Alleyne, B.; Thompson, M. E. Platinum binuclear complexes as phosphorescent dopants for monochromatic and white organic light-emitting diodes. *Adv. Funct. Mater.* **2006**, *16* (18), 2438-2446. DOI: 10.1002/adfm.200600614.
- (35) Su, N.; Meng, F.; Wang, P.; Liu, X.; Zhu, M.; Zhu, W.; Su, S.; Yu, J. Near-infrared emission from binuclear platinum (II) complexes containing pyrenylpyridine and pyridylthiolate units: Synthesis, photo-physical and electroluminescent properties. *Dyes Pigm.* **2017**, *138*, 162-168. DOI: 10.1016/j.dyepig.2016.11.037.
- (36) Sicilia, V.; Baya, M.; Borja, P.; Martín, A. Oxidation of Half-Lantern Pt₂(II,II) Compounds by Halocarbons. Evidence of Dioxygen Insertion into a Pt(III)-CH₃ Bond. *Inorg. Chem.* **2015**, *54* (15), 7316-7324. DOI: 10.1021/acs.inorgchem.5b00846.

- (37) Niedermair, F.; Trattng, R.; Mereiter, K.; Schmuck, M.; Sax, S.; List, E. J. W.; Slugovc, C. Red electrophosphorescent platinum(II) quinolinolate complexes. *Monatsh. Chem.* **2010**, *141* (8), 847-858. DOI: 10.1007/s00706-010-0345-x.
- (38) Shavaleev, N. M.; Adams, H.; Best, J.; Edge, R.; Navaratnam, S.; Weinstein, J. A. Deep-Red Luminescence and Efficient Singlet Oxygen Generation by Cyclometalated Platinum(II) Complexes with 8-Hydroxyquinolines and Quinoline-8-thiol. *Inorg. Chem.* **2006**, *45* (23), 9410-9415. DOI: 10.1021/ic061283k.
- (39) Niedermair, F.; Kwon, O.; Zojer, K.; Kappaun, S.; Trimmel, G.; Mereiter, K.; Slugovc, C. Heteroleptic platinum(II) complexes of 8-quinolinolates bearing electron withdrawing groups in 5-position. *Dalton Trans.* **2008**, (30), 4006-4014. DOI: 10.1039/B804832K.
- (40) Niedermair, F.; Sandholzer, M.; Kremser, G.; Slugovc, C. Solution Self-Assembly and Photophysics of Platinum Complexes Containing Amphiphilic Triblock Random Copolymers Prepared by ROMP. *Organometallics* **2009**, *28* (9), 2888-2896. DOI: 10.1021/om900083n.
- (41) Heinicke, J.; Kohler, M.; Peulecke, N.; Kindermann, M. K.; Keim, W.; Kockerling, M. Cationic methallylnickel and (meth)allylpalladium 2-phosphinophenol complexes: Synthesis, structural aspects, and use in oligomerization of ethylene. *Organometallics* **2005**, *24* (3), 344-352. DOI: 10.1021/om049474n.
- (42) Park, S.; Pontier-Johnson, M.; Roundhill, D. M. Novel regioselectivity and carbon-fluorine bond cleavage in the reactions of alkylplatinum(II) complexes with amide and alkoxide anions. *J. Am. Chem. Soc.* **1989**, *111* (8), 3101-3103. DOI: 10.1021/ja00190a075.
- (43) Priya, S.; Balakrishna, M. S.; Mague, J. T. Mononuclear and heterodinuclear transition metal complexes of functionalized phosphines: Crystal and molecular structures of $[\text{Mo}(\text{CO})_5(\text{RPC}_6\text{H}_4\text{OCH}_2\text{OCH}_3\text{-}o)]$ ($\text{R}=\text{Ph}$, $\text{C}_6\text{H}_4\text{OCH}_2\text{OCH}_3\text{-}o$), $[\text{Ru}(\text{Ph}_2\text{PC}_6\text{H}_4\text{O-}o)_3]$, $[\text{Pd}(\text{Ph}_2\text{PC}_6\text{H}_4\text{O-}o)_2]$ and $[\text{PdCl}(\text{Ph}_2\text{PC}_6\text{H}_4\text{O-}o)(\text{Ph}_2\text{PC}_6\text{H}_4\text{OH-}o)]$. *J. Organomet. Chem.* **2004**, *689* (21), 3335-3349. DOI: 10.1016/j.jorganchem.2004.07.041.
- (44) Sub Kim, J.; Sen, A.; Guzei, I. A.; Liable-Sands, L. M.; Rheingold, A. L. Synthesis and reactivity of bimetallic palladium(II) methyl complexes with new functional

- phosphine ligands. *J. Chem. Soc., Dalton Trans.* **2002**, (24), 4726-4731. DOI: 10.1039/B208060P.
- (45) Sun, J.-S.; Uzelmeier, C. E.; Ward, D. L.; Dunbar, K. R. Pd(II) and Pt(II) complexes with mixed phosphorus-oxygen donor ligands. *Polyhedron* **1998**, *17* (11), 2049-2063. DOI: 10.1016/S0277-5387(97)00483-X.
- (46) Baya, M.; Belío, Ú.; Martín, A. Synthesis, Characterization, And Computational Study of Complexes Containing Pt···H Hydrogen Bonding Interactions. *Inorg. Chem.* **2014**, *53* (1), 189-200. DOI: 10.1021/ic402036p.
- (47) Pérez-Bitrián, A.; Baya, M.; Casas, J. M.; Martín, A.; Menjón, B. Hydrogen bonding to metals as a probe for an inverted ligand field. *Dalton Trans.* **2021**, *50* (16), 5465-5472. DOI: 10.1039/D1DT00597A.
- (48) Ebina, M.; Kobayashi, A.; Ogawa, T.; Yoshida, M.; Kato, M. Impact of a Carboxyl Group on a Cyclometalated Ligand: Hydrogen-Bond- and Coordination-Driven Self-Assembly of a Luminescent Platinum(II) Complex. *Inorg. Chem.* **2015**, *54* (18), 8878-8880. DOI: 10.1021/acs.inorgchem.5b01343.
- (49) Ko, S.-B.; Lu, J.-S.; Kang, Y.; Wang, S. Impact of a Picolinate Ancillary Ligand on Phosphorescence and Fluoride Sensing Properties of BMes₂-Functionalized Platinum(II) Compounds. *Organometallics* **2013**, *32* (2), 599-608. DOI: 10.1021/om301112u.
- (50) Ohno, K.; Hasebe, M.; Nagasawa, A.; Fujihara, T. Change in Luminescence Induced by Solution-Mediated Phase-Transition of Cyclometalated Platinum(II) Complex with Isoquinoline Carboxylate. *Inorg. Chem.* **2017**, *56* (20), 12158-12168. DOI: 10.1021/acs.inorgchem.7b01466.
- (51) Wawrzinek, R.; Muhieddine, K.; Ullah, M.; Koszo, P. B.; Shaw, P. E.; Grosjean, A.; Maasoumi, F.; Stoltzfus, D. M.; Clegg, J. K.; Burn, P. L.; Namdas, E. B.; Lo, S.-C. Orange-Red-Light-Emitting Field-Effect Transistors Based on Phosphorescent Pt(II) Complexes with Area Emission. *Adv. Opt. Mater.* **2016**, *4* (11), 1867-1874. DOI: 10.1002/adom.201600460.
- (52) Garrou, P. E. Δ_R -ring contributions to phosphorus-31 NMR parameters of transition-metal-phosphorus chelate complexes. *Chem. Rev.* **1981**, *81* (3), 229-266. DOI: 10.1021/cr00043a002.
- (53) Baya, M.; Belío, Ú.; Fernandez, I.; Fuertes, S.; Martín, A. Unusual Metal-Metal Bonding in a Dinuclear Pt-Au Complex: Snapshot of a Transmetalation Process. *Angew. Chem. Int. Ed.* **2016**, *55* (24), 6978-6982. DOI: 10.1002/anie.201602081.

Chapter 3

Reactivity of platinum (II) and
palladium (II) cyclometallated
substrates towards sources of Me⁺

Related with the protonation studies discussed in the previous chapter, the reactivity of basic starting materials [Pt(CNC)(PPh₃)] (**1**) and [Pd(CNC)(PPh₃)] (**2**) have been investigated with other electrophile as is the methyl group. In this case, the initial idea for this line of work was to functionalize the C_{ipso} of the CNC ligand with a methyl group. This process would be analogous as the one observed in the previous chapter, involving the breakage and formation of new bonds.

In addition to this, it is also known that the methyl group is also isolobal with the proton and the [Au-PPh₃]⁺ fragment,^{1,2} being then possible to compare the reactivity of basic platinum and palladium substrates towards three different electrophiles used in this thesis.

Thus, in this third chapter the reactivity of complexes **1** and **2** towards a source of electrophilic methyl groups as iodomethane (MeI) is described.

3.1. Reactivity of [Pt(CNC)(PPh₃)] (1) and [Pd(CNC)(PPh₃)] (2) towards sources of electrophilic methyl groups

The reaction of the starting substrate [Pt(CNC)(PPh₃)] (**1**) with MeI has proven to be the easiest way to achieve the oxidative addition process, resulting in the oxidation of the Pt(II) center to Pt(IV) *via* an S_N2 process.³⁻¹⁵ A second step consisting in a reductive elimination involving C-C coupling would produce a methylation of the ligand (see Section 3.1.1).

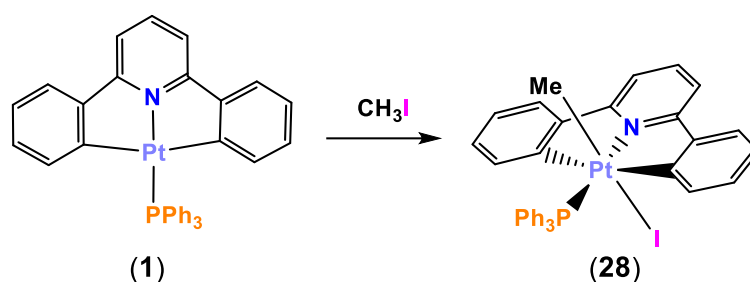
In principle, other source of electrophilic methyl groups as trimethyloxonium tetrafluoroborate, (Me₃O)(BF₄), could be used in the same way. However, no results were obtained in this case.

Thus, reaction of starting substrate [Pt(CNC)(PPh₃)] (**1**) towards (Me₃O)(BF₄) was expected to result in the obtention of a methylated “[Pt(CNC-Me)(PPh₃)]⁺” complex with a free coordination site. Several reactions were carried out under strict argon conditions, dry solvents (CH₂Cl₂ and THF) and low temperatures (ranging from -40 to -20°C; (Me₃O)(BF₄) decomposes at room temperature), but the results were unsuccessful. In some preparations, even the slight trace of water in the solvent used, caused the (Me₃O)(BF₄) to decompose forming small quantities of HBF₄, which, as described in the previous chapter, reacted with **1** protonating a phenylene ring of the CNC ligand. On the other hand, large quantities of [Pt(CNC)(PPh₃)] (**1**) and unreacted (Me₃O)(BF₄) were

found in all the preparations, indicating that the methylation process did not happen. In the presence of a coordinative solvent as THF, it could be possible the formation of a Pt(IV) species with the solvent occupying the resulting vacant. This complex could evolve *via* reductive elimination to render a methylated Pt(II) complex.

3.1.1. First methylation of the CNC ligand with MeI

The preparation of the Pt(IV) complex [PtIMe(CNC)(PPh₃)] (**28**) was achieved by stirring a solution of [Pt(CNC)(PPh₃)] (**1**) in MeI during several hours protected from light (see Experimental section for details). After workup, complex **28** was obtained as a yellow solid with good yield (see Scheme 3.1).



Scheme 3.1. Synthesis of complex **28**.

The reaction was performed in the dark because the light seems to affect the stability of **28**. That is confirmed when an NMR tube of this complex in CD₂Cl₂ is kept for 1 hour exposed to sunlight, and only signals of starting complex **1** and free MeI are detected through NMR.

The structure of **28** was determined by X-Ray. See Figure 3.1 for a view of this complex and Table 3.1 for a selection of distances and angles.

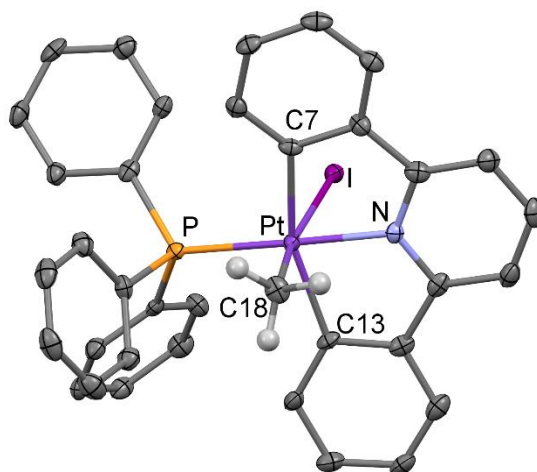


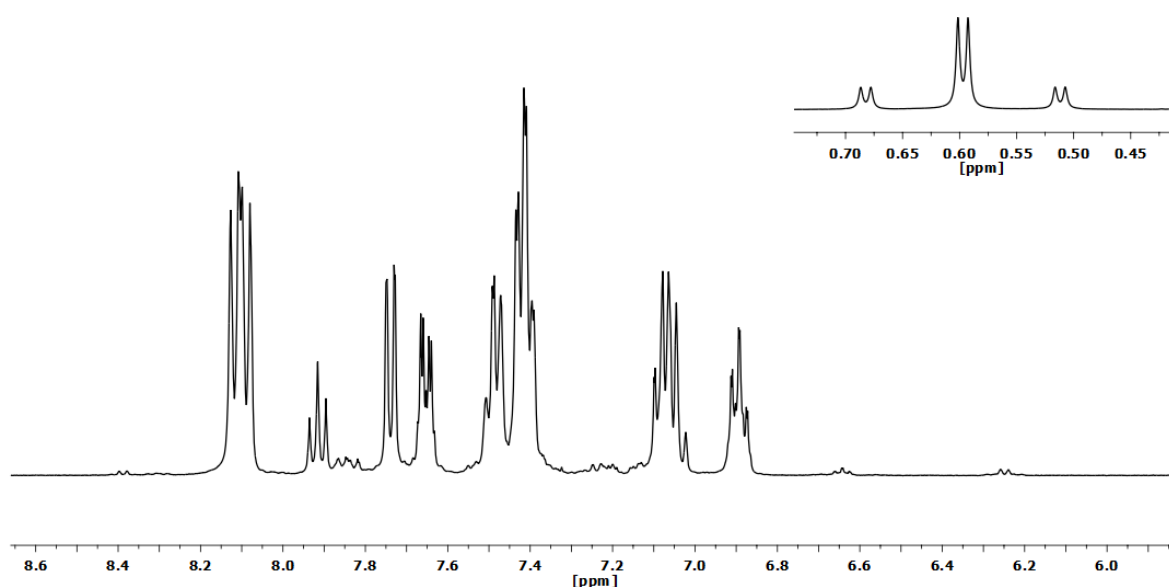
Figure 3.1. Molecular structure of complex [PtIMe(CNC)(PPh₃)] (**28**).

Table 3.1. Selection of bond lengths (Å) and angles (°) for **28**.

Pt-N	2.026(4)	Pt-C18	2.107(4)
Pt-C7	2.103(4)	C18-Pt-I	170.12(13)
Pt-C13	2.113(4)	N-Pt-C7	79.77(16)
Pt-P	2.2971(11)	N-Pt-C18	88.49(16)
Pt-I	2.8017(3)		

The X-Ray structure determined from **28** can be described as a Pt(IV) octahedral complex derived from the starting material **1** with the addition, in mutually *trans* positions, of Me and I ligands. The Pt-Me and Pt-I lines, are almost perpendicular to the “[Pt(CNC)(PPh₃)]” plane, being therefore the structure of **28**, an octahedron with little distortions apart from those caused by the CNC ligand.

The ¹H NMR spectrum of a solution of [PtMe(CNC)(PPh₃)] (**28**) in CD₂Cl₂ is in agreement with the crystal structure. It shows, along the signals corresponding to the CNC ligand in the aromatic region, a doublet at 0.6 ppm flanked by ¹⁹⁵Pt satellites (³J_{CH₃-P} = 3.5 Hz, ²J_{CH₃-Pt} = 67.8 Hz) assigned to the methyl hydrogen atoms (see Figure 3.2).

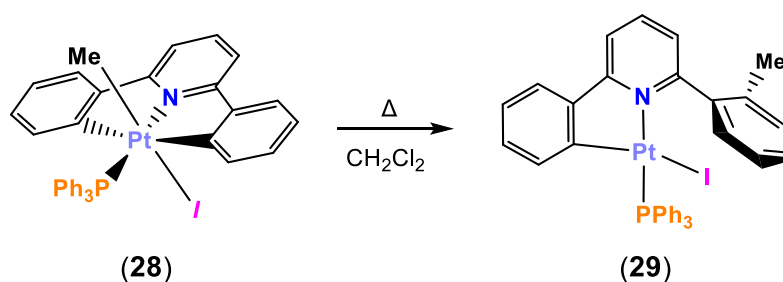
**Figure 3.2.** ¹H NMR spectrum (CD₂Cl₂, RT) of complex [PtMe(CNC)(PPh₃)] (**28**).

The $^{31}\text{P}\{^1\text{H}\}$ NMR spectrum of this sample (see Figure S3.4, Supporting Information) shows a lone singlet signal at 3.5 ppm with ^{195}Pt satellites and a coupling constant $^1J_{\text{P-Pt}}$ of 2847 Hz, corresponding to the phosphorus atom of the phosphane ligand. These parameters are again consistent with the presence of a Pt(IV) center and are similar to the ones reported for the analogous complexes $[\text{PtIme}(\text{F-CNC-F})(\text{PR}_3)]^{17}$ or $[\text{PtIme}(\text{CNC})\text{L}]^{18}$ in the literature.

Furthermore, isomerization processes seem not to take place in solution for this complex. No signals corresponding to a *cis* Pt(IV) complex are observed in the NMR spectra of solutions of **28** kept for long time at room temperature. DFT calculations revealed that the *trans* complex is very similar in energy to the *cis* isomer.

Despite the absence of an isomerization process, solutions of **28** protected from light evolve to two different complexes. After 3 days, signals assigned to starting complex **1**, complex **28**, free MeI and eliminative reduction complex $[\text{Pt}(\text{CN-}o\text{-tol})\text{I}(\text{PPh}_3)]$ (**29**) (see below) are detected.

When a CH_2Cl_2 solution of $[\text{PtIme}(\text{CNC})(\text{PPh}_3)]$ (**28**) was refluxed in the dark for two days, the reductive elimination Pt(II) complex $[\text{Pt}(\text{CN-}o\text{-tol})\text{I}(\text{PPh}_3)]$ (**29**) formed as a yellow solid with good yield (see Scheme 3.2). Thus, a reductive process with C-C coupling took place. As a result, one of the phenylene rings of the CNC ligand was methylated in *ortho* position.



Scheme 3.2. Synthesis of complex **29**.

From this reaction, a mixture of **29** and **28** in variable proportions were obtained, and thus a different, easier route was used for the reductive elimination of the methyl group (see below).

The crystal structure of **29** has been determined by X-Ray diffraction, see Figure 3.3 for a view of the structure and Table 3.2 for a selection of bond distances and angles.

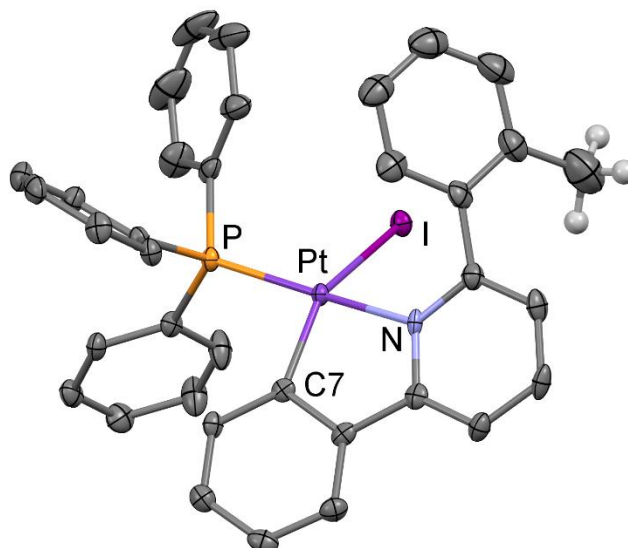


Figure 3.3. Crystal structure of complex [Pt(CN-*o*-tol)I(PPh₃)] (**29**).

Table 3.2. Selection of bond lengths (Å) and angles (°) for **29**.

Pt-N	2.104(3)	Pt-P	2.2276(10)
Pt-C7	2.010(4)	C7-Pt-I	150.20(11)
Pt-I	2.6923(3)	N-Pt-C7	80.24(14)

The structure confirms the methylation of one of the *ortho* positions of one of the phenylene rings of the CNC ligand, formally giving rise to a *o*-tolyl group. Its ring is no longer coplanar with the pyridinic ring displaying a dihedral angle of 47°. The methyl group is located away from the core of the complex in order to avoid steric repulsions. The P atom of the phosphane ligand is located *trans* with respect to the N atom of the CN-*o*-tol ligand, thus retaining the disposition found in the starting material [Pt(CNC)(PPh₃)] (**1**) and in **28**. Perhaps, the most striking feature of the structure of **29** is the remarkable small value of the C7–Pt–I angle, 150.20(11)°. The other *trans* angle, N–Pt–P (169.67(9)°), is a little bit below the theoretical value of 180°. As a consequence, the environment of the platinum center is distorted from the expected square planar disposition towards a tetrahedral geometry. This distortion has been found in some Pt(II) and Pd(II) complexes bearing cyclometallated ligand and phosphines, as well as halo ligands^{17,19-26} but the distortion found in **29** is the greatest described so far with only one exception,²¹ and it is most likely caused by the steric hindrance caused by the bulky ligands around the metal center.

The methylation of one of the phenylene rings of the CNC ligand can be confirmed by the NMR spectra of $[\text{Pt}(\text{CN-}o\text{-tol})\text{I}(\text{PPh}_3)]$ (**29**). In the ^1H NMR spectrum the signal corresponding to the methyl group appears as a singlet at 2.6 ppm with no ^{195}Pt satellites (see Figure 3.4).

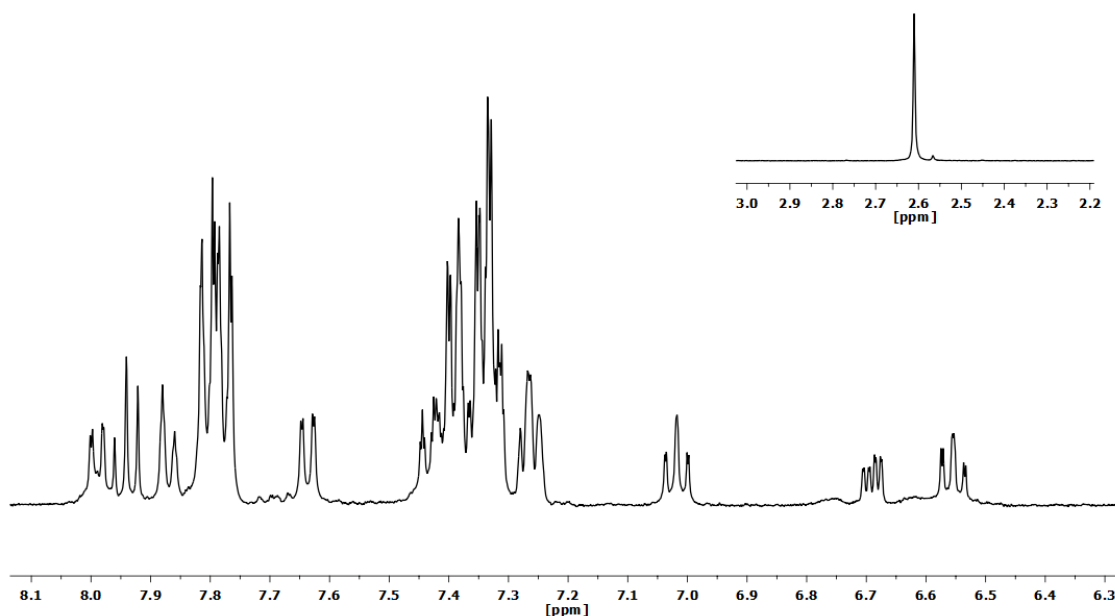
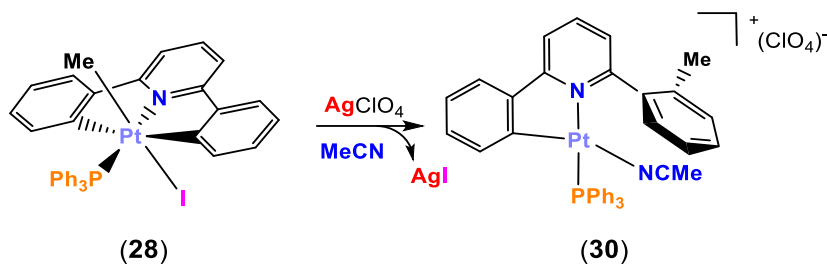


Figure 3.4. ^1H NMR spectrum (CD_2Cl_2 , RT) of complex $[\text{Pt}(\text{CN-}o\text{-tol})\text{I}(\text{PPh}_3)]$ (**29**).

Furthermore, the $^{31}\text{P}\{^1\text{H}\}$ NMR spectrum (see Figure S3.12, Supporting Information) shows only a sharp signal at 19.3 ppm, with a $^1J_{\text{P-Pt}}$ of 4388 Hz, similar to those observed for the bidentate platinum (II) $\text{C}^{\wedge}\text{N}$ complexes of the previous chapter.

On the other hand, when AgClO_4 was added to a yellow suspension of Pt(IV) complex $[\text{PtIme}(\text{CNC})(\text{PPh}_3)]$ (**28**) in MeCN, the color of the solid progressively turned to white due to the precipitation of AgI. From the solution resulting after removal of AgI, it was possible to obtain a yellow solid which was identified as $[\text{Pt}(\text{CN-}o\text{-tol})(\text{MeCN})(\text{PPh}_3)](\text{ClO}_4)$ (**30**). The simple substitution of the iodine by the MeCN in the starting material could be expected, but the resulting Pt(IV) $[\text{PtMe}(\text{CNC})(\text{MeCN})(\text{PPh}_3)]$ complex was not observed. Instead, the reduction of the Pt(IV) center to Pt(II) and methylation of the CNC ligand was directly achieved (see Scheme 3.3). On the other hand, it has been reported that in other similar reactions intermediate pentacoordinate Pt(IV) or tricoordinate Pt(II) complexes are formed,¹⁷ but such species have not been detected in this case. This reaction was cleaner than the one for the obtaining of **29**, only rendering the product $[\text{Pt}(\text{CN-}o\text{-tol})(\text{MeCN})(\text{PPh}_3)](\text{ClO}_4)$ (**30**).



Scheme 3.3. Synthesis of complex **30**.

The crystal structure of **30** has been determined by X-Ray diffraction (see Figure 3.5 for a view of its structure and Table 3.3 for a selection of distances and angles).

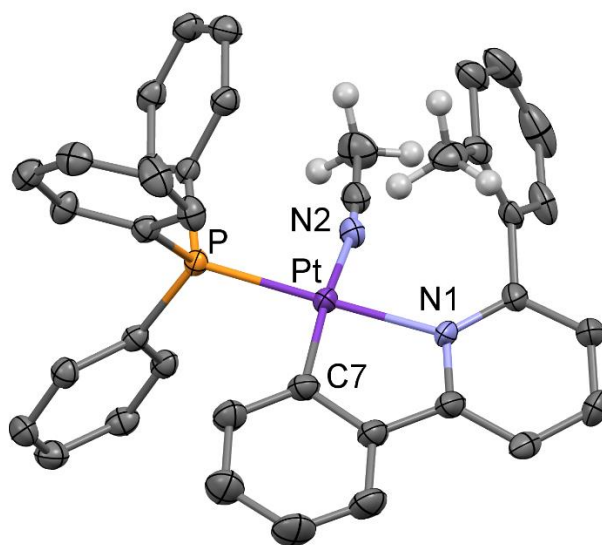


Figure 3.5. Molecular structure of complex $[\text{Pt}(\text{CN-}o\text{-tol})(\text{MeCN})(\text{PPh}_3)](\text{ClO}_4)$ (**30**).

Table 3.3. Selection of bond lengths (Å) and angles (°) for **30**.

Pt-N1	2.117(2)	C7-Pt-N2	166.69(10)
Pt-C7	2.006(3)	N1-Pt-C7	80.92(10)
Pt-N2	2.088(2)	N1-Pt-P	174.01(7)
Pt-P	2.2452(6)		

The main difference with respect to the structure of $[\text{Pt}(\text{CN-}o\text{-tol})\text{I}(\text{PPh}_3)]$ (**29**) is that the square plane around the Pt center is not so distorted. Thus, in $[\text{Pt}(\text{CN-}o\text{-tol})(\text{MeCN})(\text{PPh}_3)](\text{ClO}_4)$ (**30**) the C7–Pt–N2 angle is $166.69(10)^\circ$ and the N1–Pt–P

174.01(7)°. This might be caused by a higher steric requirement of the heavy iodine atom in **29**. Also, in **30**, the *o*-tolyl fragment is disordered over two positions (partial occupancy 0.6/0.4) with the methyl groups pointing to opposite directions. In agreement with this, DFT calculations on both possibilities revealed that these two possible conformations of the methyl group were very similar in energy, being the more stable form the conformation on Figure 3.5. This might indicate that the nearby of the metal atom is not so crowded as in **29** and therefore, there is no clear preference of one orientation or another.

The ^1H NMR spectrum of $[\text{Pt}(\text{CN-}o\text{-tol})(\text{MeCN})(\text{PPh}_3)](\text{ClO}_4)$ (**30**) confirms the methylation of one of the phenylene rings. A signal corresponding to this methyl group appears now as a singlet at 2.6 ppm with no ^{195}Pt satellites (see Figure 3.6). Besides, the methyl fragment of the coordinated MeCN ligand caused a single signal at 1.1 ppm.

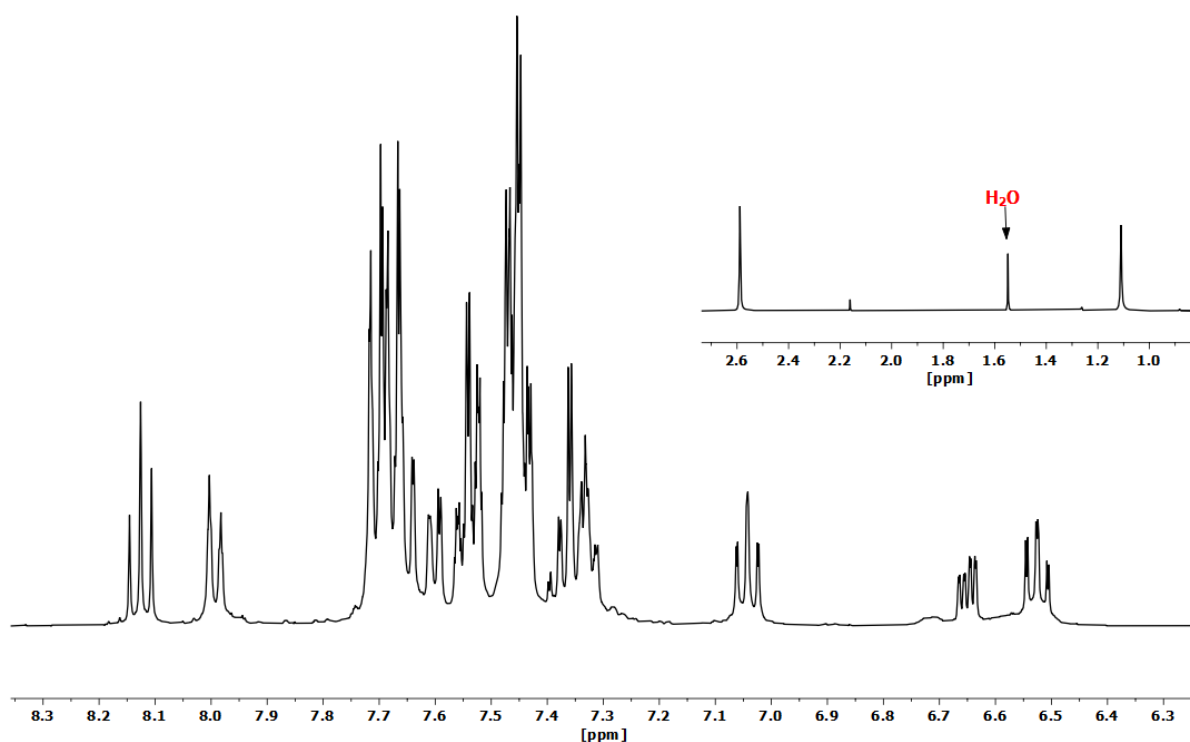


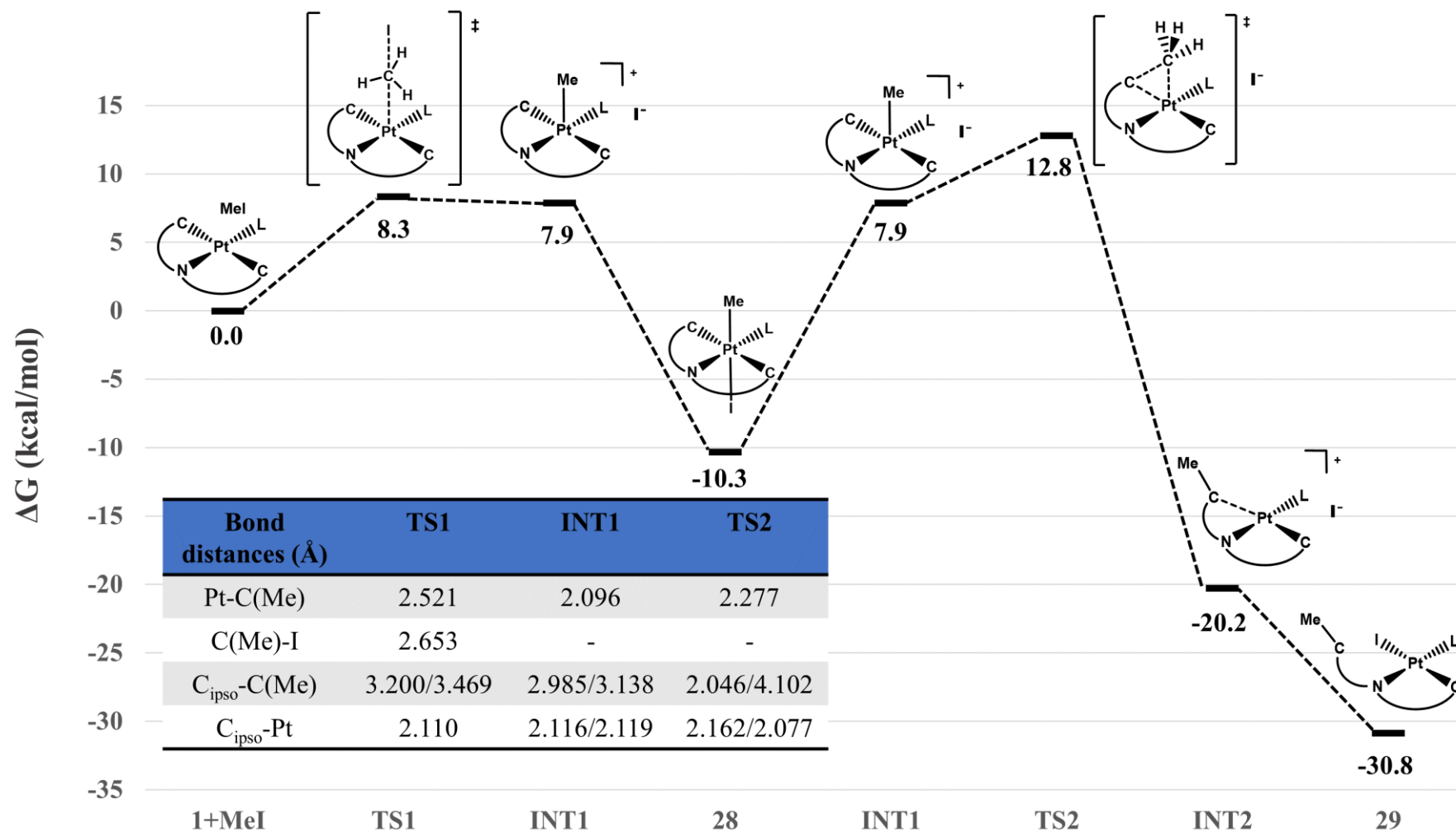
Figure 3.6. ^1H NMR spectrum (CD_2Cl_2 , RT) of complex $[\text{Pt}(\text{CN-}o\text{-tol})(\text{MeCN})(\text{PPh}_3)](\text{ClO}_4)$ (**30**).

Also, the only signal of the $^{31}\text{P}\{^1\text{H}\}$ NMR spectrum (see Figure S3.20, Supporting Information) consists of a sharp singlet at 21.5 ppm, with a $^1J_{\text{P-Pt}}$ of 4292 Hz.

DFT studies (see Computational details, Supporting Information) were carried out in order to establish the energy profile of the whole methylation process to give rise to

complex [PtI(CN-*o*-tol)(PPh₃)] (**29**) in dichloromethane solution (see Scheme 3.4 for the computed energy profile). The calculated energy value found for the oxidative addition of MeI to complex **1** to afford Pt(IV) complex [PtIme(CNC)(PPh₃)] (**28**) is 8.3 kcal/mol (see TS1, Scheme 3.4. 299i cm⁻¹; I-Me-Pt stretching). This process is proposed to follow a S_N2 mechanism as established in the literature.^{8,9,11,14,18} The value of energy for this process can be compatible with the mild conditions (RT) used in the experimental reaction.

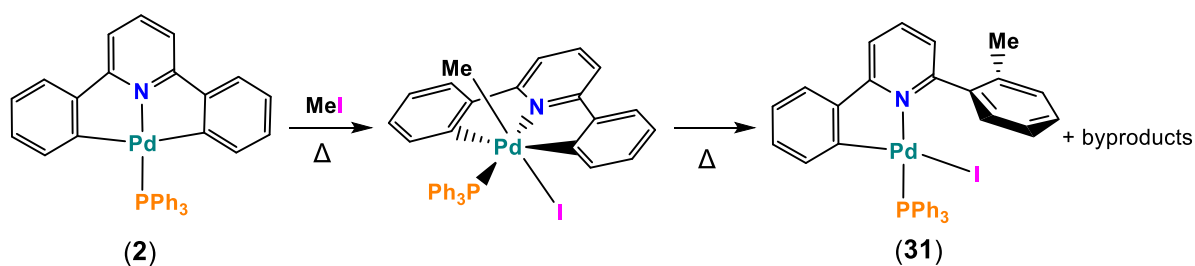
On the Pt(IV) complex, the reductive elimination of the methyl group with a C_{ipso} of the CNC cyclometallated ligand is found to be less favored energetically, needing a global value of 22.5 kcal/mol to proceed. This is again in agreement with the experimental conditions of this reaction, which needed heating (reflux in dichloromethane) in order to proceed. A possible first step for this modelled process might consist on the dissociation of an iodine ligand, which would be congruent for example, with the necessity to abstract the iodine ligand using AgClO₄ to form complex [Pt(CN-*o*-tol)(MeCN)(PPh₃)]ClO₄ (**30**). Then, on the cationic pentacoordinated Pt(IV) species (see INT1, Scheme 3.4), the reductive elimination process can take place (see TS2, Scheme 3.4. 330i cm⁻¹; C_{ipso}-Me-Pt stretching). Finally, this step gives rise to final platinum (II) species **29**, after coordination of the iodine ligand.



Scheme 3.4. Energy profile (DFT/BP86-D3 level, dichloromethane solution) for the first methylation process.

These reactions were also tried on palladium substrate [Pd(CNC)(PPh₃)] (**2**) but the reactivity of this complex could not be controlled as in the case of its platinum analogue. When complex **2** was dissolved in MeI and kept for one day at room temperature in darkness only starting substrate was detected. When the reaction was kept in reflux of MeI, complex mixtures of products were obtained (see Scheme 3.5). From those mixtures some crystals of methylated palladium (II) complex **31** could be grown (Figure 3.7 for a view of the complex and Table 3.4 for a selection of distances).

This product is rendered by the oxidative addition of a MeI molecule and the successive reductive elimination of the methyl group with the C_{ipso} of the CNC ligand. Unlike for the platinum analogues, it was impossible to establish a synthetic route to obtain palladium complex **31** as a pure solid, and thus no further reactivity was studied.



Scheme 3.5. Reaction of complex **2** with MeI.

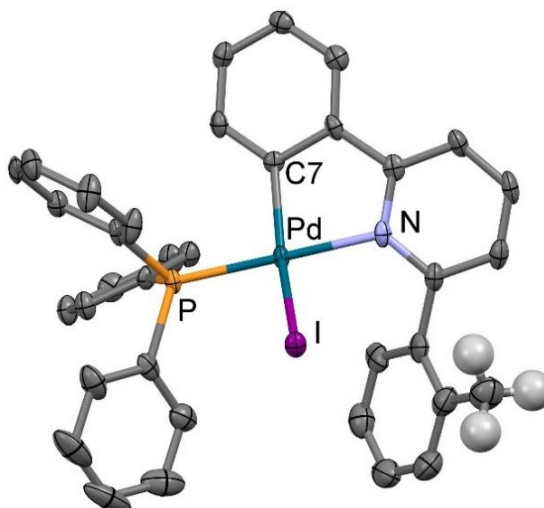
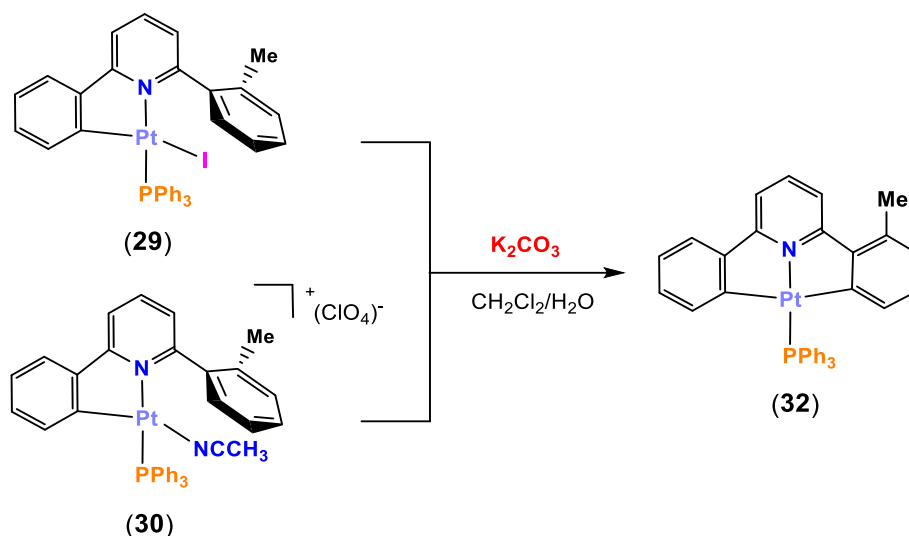


Figure 3.7. Molecular structure of complex [Pd(CN-*o*-tol)I(PPh₃)](ClO₄) (**31**).

Table 3.4. Selection of bond lengths (Å) and angles (°) for **31**.

Pd-N	2.102(4)	Pd-P	2.2499(13)
Pd-C7	2.014(5)	C7-Pd-I	148.26(13)
Pd-I	2.7027(5)	N-Pd-C7	80.69(18)

After having prepared platinum complexes [Pt(CN-*o*-tol)I(PPh₃)] (**29**) and [Pt(CN-*o*-tol)(MeCN)(PPh₃)](ClO₄) (**30**), the cyclometallation of the *o*-tolyl ring was investigated. Thus, recyclometallation of the *o*-tolyl fragment of **29** and **30** could be achieved by adding an aqueous solution of K₂CO₃ to a CH₂Cl₂ solution of these complexes (see Scheme 3.6). These mixtures were stirred for some time, and after workup, [Pt(CNC-Me)(PPh₃)] (**32**) was obtained as a yellow solid. When the starting substrate used was **30**, better yields were found and much shorter reaction times were needed (see Experimental section for details).

**Scheme 3.6.** Synthesis of complex **32**.

Crystals of **32** were obtained in order to study them through X-Ray diffraction (see Figure 3.8 for a view of the structure and Table 3.5 for a list of distances and angles).

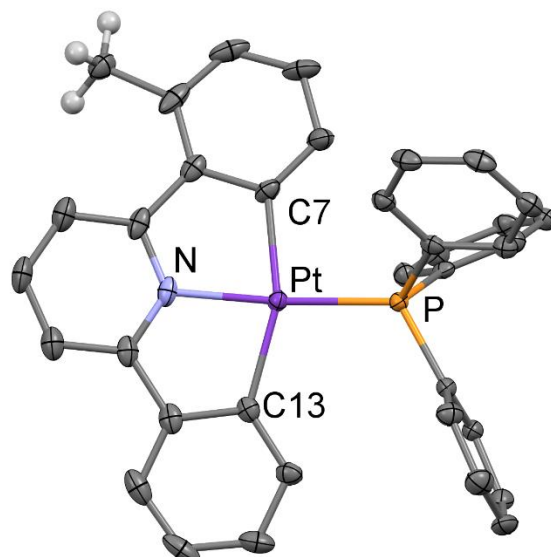


Figure 3.8. Molecular structure of complex [Pt(CNC-Me)(PPh₃)] (**32**).

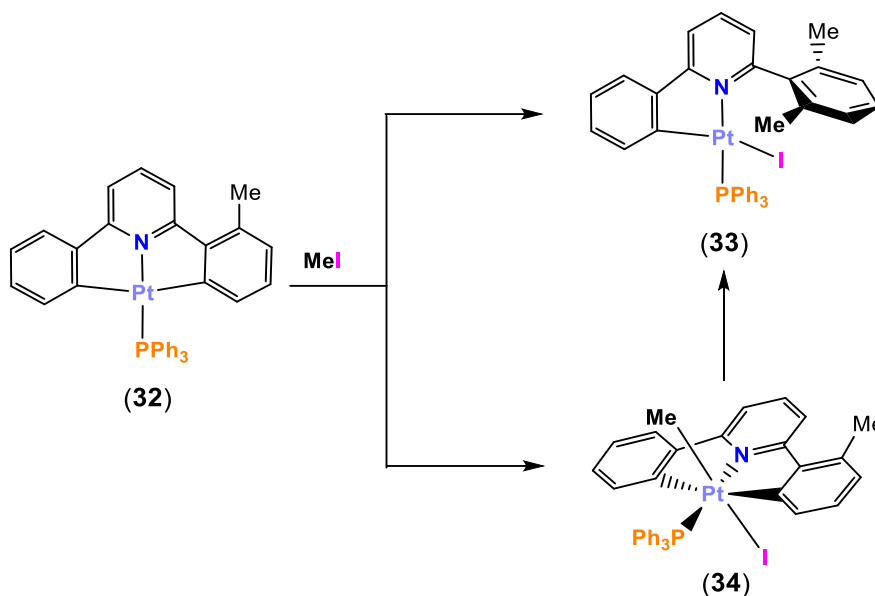
Table 3.5. Selection of bond lengths (Å) and angles (°) for **32**.

Pt-N	2.026(2)	C7-Pt-N	79.97(10)
Pt-C7	2.083(3)	C13-Pt-C7	159.28(11)
Pt-P	2.2272(7)		

The crystal structure of [Pt(CNC-Me)(PPh₃)] (**32**) confirms the recyclometallation and the tridentate nature of the CNC-Me ligand. This is essentially planar, and coplanar with the square plane of the metal center, with similar angles and distances to those of the starting material [Pt(CNC)(PPh₃)] (**1**).

The ¹H NMR spectrum of [Pt(CNC-Me)(PPh₃)] (**32**) (see Figure 3.9) shows the loss of the *ortho* H hydrogen with respect to the *o*-tolyl fragment of [Pt(CN-*o*-tol)I(PPh₃)] (**29**) and [Pt(CN-*o*-tol)(MeCN)(PPh₃)](ClO₄) (**30**) and the methyl hydrogen atoms appear again as a singlet at 2.6 ppm. As both halves of the CNC-Me ligand are inequivalent, it is remarkable the apparition of two different signals for the *ortho* protons of the cyclometallated ligand, H2 and H11 (see Chart 3.1 for the numbering of the signals) at 6.3 and 6.2 ppm respectively as doublets (³J_{H-H} = 7.4 Hz) with platinum satellites (³J_{H-Pt} = 29.0 Hz).

was not the expected Pt(IV) complex [PtMe(CNC-Me)(PPh₃)], but directly the reductive elimination Pt(II) complex [Pt(CN-2,6-xyl)I(PPh₃)] (**33**). Complex **33** was the result of a second methylation on the already methylated ring of the CNC-Me ligand of [Pt(CNC-Me)(PPh₃)] (**32**), and would be the analogous to [Pt(CN-*o*-tol)I(PPh₃)] (**29**).



Scheme 3.7. Synthesis of complex **33**.

The crystal structure of [Pt(CN-2,6-xyl)I(PPh₃)] (**33**) was determined by X-Ray diffraction (see Figure 3.10 for a view of the structure and Table 3.6 for a selection of distances and angles).

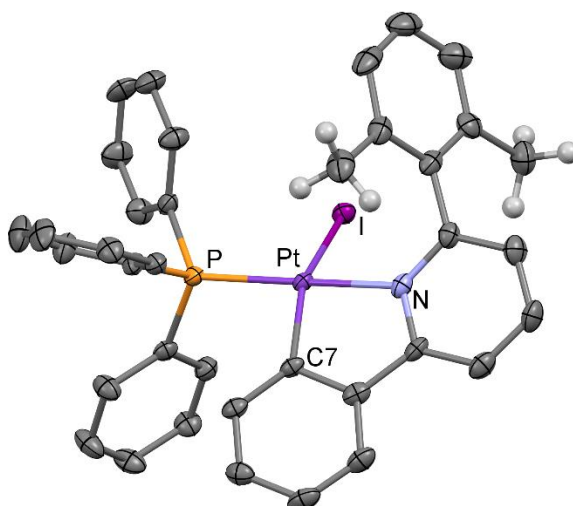


Figure 3.10. Molecular structure of complex [Pt(CN-2,6-xyl)I(PPh₃)] (**33**).

Table 3.6. Selection of bond lengths (Å) and angles (°) for **33**.

Pt-N	2.104(3)	C7-Pt-I	150.41(13)
Pt-C7	2.009(4)	C7-Pt-N	80.63(16)
Pt-I	2.6862(3)	N-Pt-P	167.71(10)
Pt-P	2.2235(11)		

This structure confirms that the second methylation of the cyclometallated ligands takes place on the ring already methylated, giving rise to a 2,6-xylyl fragment. The structure is very similar to the one found for [Pt(CN-*o*-tol)I(PPh₃)] (**29**). The dihedral angle between the dimethylated ring and the pyridinic ring is 58°. In this case, the presence of two methyl groups in *ortho* positions causes that one of them is located away from the core of the complex while the other points in the opposite direction.

The preference for the second methylation on the already methylated ring of [Pt(CNC-Me)(PPh₃)] (**32**) has been explained in terms of steric factors for a similar process.¹⁷ Nevertheless, in the structure of **33** no dramatic structural differences related with the two C₆ rings have been found. In fact, the methyl group is disordered over the two rings with partial occupancy 0.66/0.34 and thus a clear preference for one position or the other is not evident.

The ¹H NMR spectrum of [Pt(CN-2,6-xylyl)I(PPh₃)] (**33**) (see Figure 3.11) shows that at room temperature the two methyl groups of the 2,6-xylyl fragment are equivalent, appearing as a unique singlet at 2.5 ppm with relative integration of 6. This indicates that in these conditions there is free rotation of the xylyl fragment around the C(pyridine)-C(xylyl) bond.

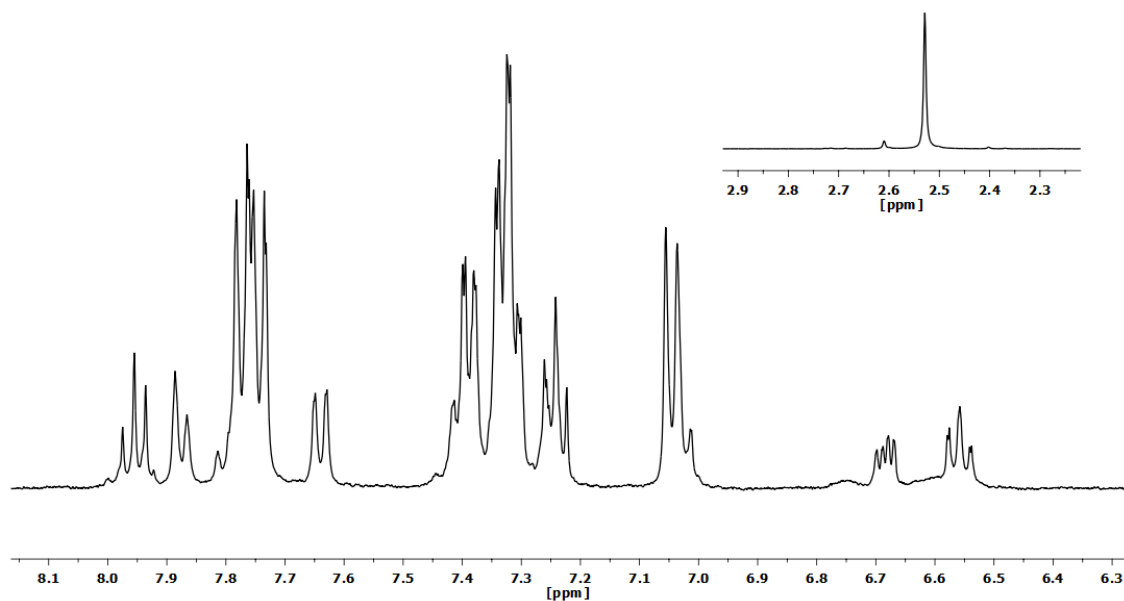


Figure 3.11. ^1H NMR spectrum (CD_2Cl_2 , RT) of complex $[\text{Pt}(\text{CN-2,6-xyI})(\text{PPh}_3)]$ (**33**).

The $^{31}\text{P}\{^1\text{H}\}$ NMR spectrum of $[\text{Pt}(\text{CN-2,6-xyI})(\text{PPh}_3)]$ (**33**) (see Figure S3.36, Supporting Information) confirmed the +2 oxidation state for the metal center, with typical parameters for the singlet signal corresponding to the P atom of the phosphane ligand (18.8 ppm, $^1J_{\text{P-Pt}} = 4432$ Hz).

On the other hand, when $[\text{Pt}(\text{CNC-Me})(\text{PPh}_3)]$ (**32**) was kept stirring in a MeI solution for less time, crudes of reaction obtained after removal of the solvent revealed the existence of a mixture of the starting material $[\text{Pt}(\text{CNC-Me})(\text{PPh}_3)]$ (**32**), the Pt(II) complex $[\text{Pt}(\text{CN-2,6-xyI})(\text{PPh}_3)]$ (**33**) and another complex which was identified as the Pt(IV) complex $[\text{PtIme}(\text{CNC-Me})(\text{PPh}_3)]$ (**34**), this latter being a minor component of the mixture. Several ^1H NMR spectra registered for crude samples of the reaction of $[\text{Pt}(\text{CNC-Me})(\text{PPh}_3)]$ (**32**) with MeI to form $[\text{Pt}(\text{CN-2,6-xyI})(\text{PPh}_3)]$ (**33**) (see Figure 3.12), reveal the existence of a low intensity doublet with platinum satellites at 0.6 ppm ($^3J_{\text{CH}_3-\text{P}} = 4.0$ Hz, $^2J_{\text{CH}_3-\text{Pt}} = 68.0$ Hz) very similar to that of complex $[\text{PtIme}(\text{CNC})(\text{PPh}_3)]$ (**28**), which would correspond to a methyl group bonded to the platinum center. Therefore, this observation would be in agreement with the existence of small quantities of Pt(IV) species $[\text{PtIme}(\text{CNC-Me})(\text{PPh}_3)]$ (**34**). The intensity of this signal was in all cases very low, indicating that this complex might be quite unstable in solution giving rise quickly to complex $[\text{Pt}(\text{CN-2,6-xyI})(\text{PPh}_3)]$ (**33**).

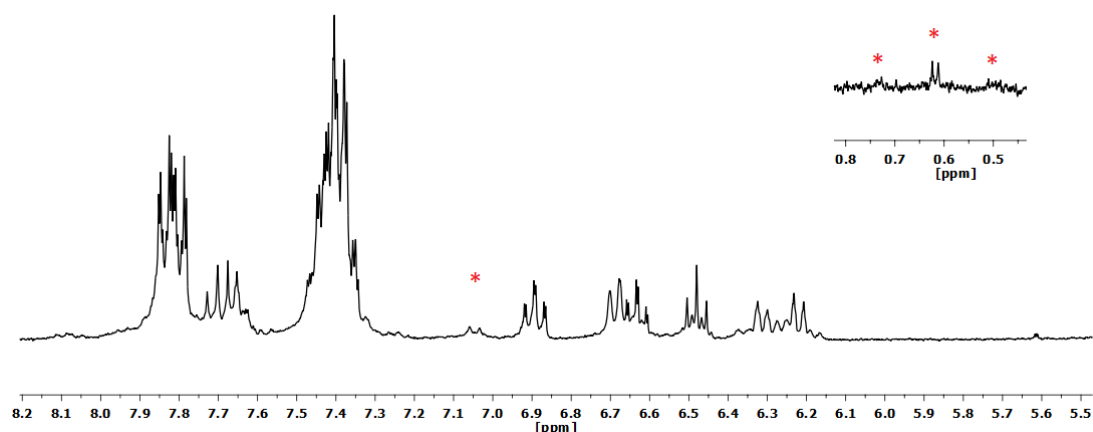


Figure 3.12. ^1H NMR spectrum (CD_2Cl_2 , RT) of the reaction of $[\text{Pt}(\text{CNC-Me})(\text{PPh}_3)]$ (**32**) with MeI (red asterisks, signals of **34**).

Unfortunately, complex **34** could not be obtained as a pure solid. Despite this, from one of these reaction mixtures some few, low quality crystals of **34** could be grown, to analyse them through X-Ray diffraction (see Figure 3.13 for a view of the structure of **34**). Due to the low quality of the crystals, the structure only allows to establish the atom connectivity.

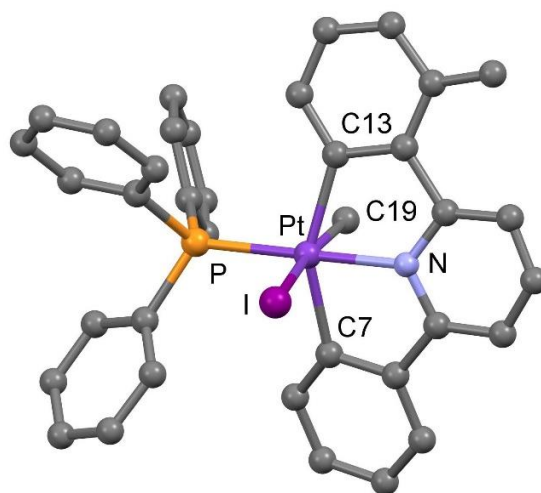


Figure 3.13. Molecular structure of complex $[\text{PtIme}(\text{CNC-Me})(\text{PPh}_3)]$ (**34**).

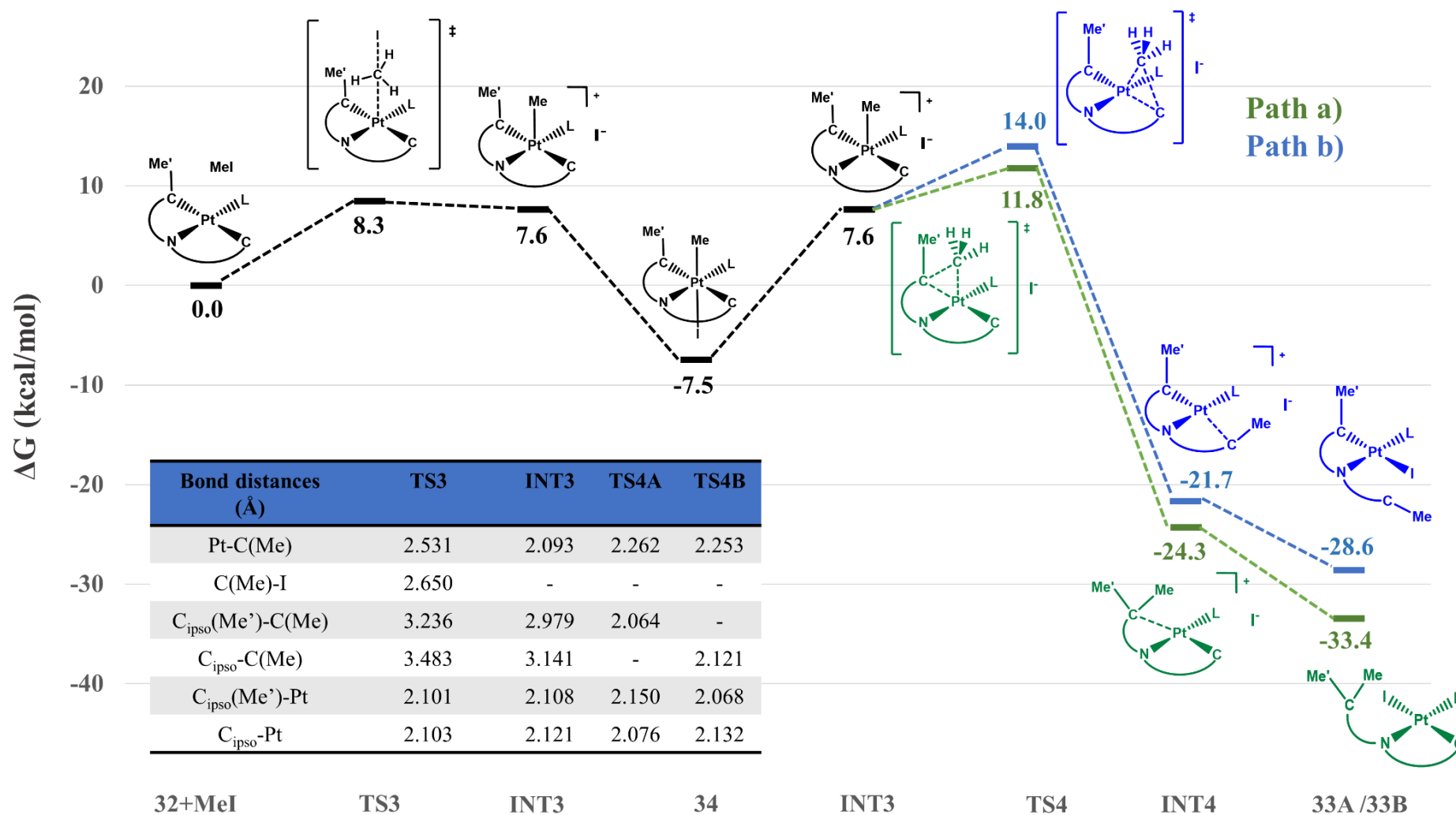
As expected, $[\text{PtIme}(\text{CNC-Me})(\text{PPh}_3)]$ (**34**) is a Pt(IV) octahedral complex with a *trans* disposition for the iodo and methyl ligands. The structural parameters are very similar to those found in the structure of $[\text{PtIme}(\text{CNC})(\text{PPh}_3)]$ (**28**), or in other similar complexes.^{17,18} The platinum-methyl and iodine lines, are again almost perpendicular to the “[Pt(CNC)(PPh₃)]” plane, being therefore, the structure of **34** an octahedron with little

distortions. The analogous *cis* Pt(IV) complex was also modelled through DFT calculations and revealed that both isomers were very near in energy.

As a global result of the reactions of this chapter the introduction of two methyl groups in the *ortho* positions of a phenylene ring of the CNC ligand of [Pt(CNC)(PPh₃)] (**1**) has been achieved, giving rise to a CN-2,6-xyI ligand.

DFT studies were also performed to build the energy profile of this second methylation process (see Scheme 3.8 for a view of the energy profile) to give rise to complex [Pt(CN-2,6-xyI)(PPh₃)] (**33**) in dichloromethane solution. The first modelled step is again the oxidative addition of MeI to complex [Pt(CNC-Me)(PPh₃)] (**32**) (see TS3, Scheme 3.8. 302i cm⁻¹; I-Me-Pt stretching), which is energetically identical to the observed for the first methylation (see Scheme 3.4 above). Global reductive elimination process on Pt(IV) complex [PtIMe(CNC-Me)(PPh₃)] (**34**) is found to be more favored than in the first methylation reaction (22.5 vs 19.3 kcal/mol). This slight difference might be in agreement with the unsuccessful attempts to obtain complex [PtIMe(CNC-Me)(PPh₃)] (**34**) as a pure solid, and the direct formation of dimethylated Pt(II) complex [Pt(CN-2,6-xyI)(PPh₃)] (**33**). As described before, the first modelled step of this process is the dissociation of the iodine ligand of [PtIMe(CNC-Me)(PPh₃)] (**34**) giving rise to a cationic five-coordinated intermediate (INT3, Scheme 3.8). Then, two possibilities can take place (see Paths a) and b), Scheme 3.8) as in the case of complex [Pt(CNC-Me)(PPh₃)] (**32**) the reductive elimination could proceed with the C_{ipso} of the methylated or the non-methylated ring of the CNC-Me ligand. Therefore, both mechanisms were investigated. Thus, the computed reductive elimination with the non-methylated ring is less favoured than the one experimentally observed, as can be seen from the energy profile of this process (see favoured green Path a) of Scheme 3.8). Thus, the two different transition states TS4A and TS4B (321i and 317i cm⁻¹ respectively; C_{ipso}-Pt-Me stretching) and intermediates (INT4A and INT4B) for both possibilities revealed that formation of complex **33A**, which is the experimentally obtained [Pt(CN-2,6-xyI)(PPh₃)] (**33**), is the preferred pathway.

Therefore, this gathered data is in agreement with the experimental observations, where only one product, [Pt(CN-2,6-xyI)(PPh₃)] (**33**), can be detected, isolated and characterized.



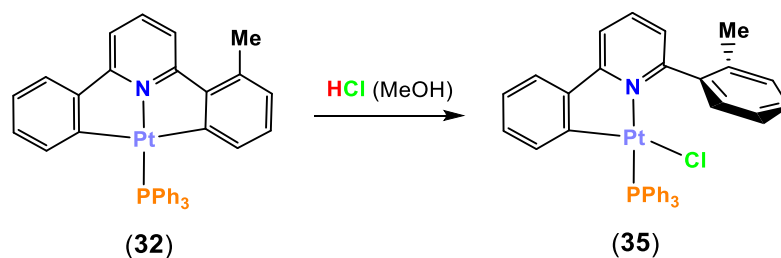
Scheme 3.8. Energy profile (DFT/BP86-D3 level, dichloromethane solution) for the second methylation process.

In order to gain insight on the different behavior of the two different C_{ipso} of $[\text{Pt}(\text{CNC-Me})(\text{PPh}_3)]$ (**32**) towards the attack of a methyl group, conceptual density functional theory (CDFT) studies were performed.²⁷ This theory contains numerous quantities that can be used to predict favorable reactive sites on chemical systems, and therefore, chemical behavior. Thus, Fukui function and dual descriptor, which are functions used to reveal reactive sites,^{28,29} can be computed on these different cyclometallated carbons. As expected, these calculations revealed that these carbons are in fact nucleophilic, but no remarkable differences between them are found giving similar negative double descriptor values (-0.018; carbon of the non-methylated ring, -0.017; carbon of the methylated ring). Therefore, their nucleophilic behavior towards an electrophilic methyl group seemed to be similar.

3.1.3. Reactivity of $[\text{Pt}(\text{CNC-Me})(\text{PPh}_3)]$ (**32**) towards HCl

As discussed before, two different results could occur from a methylation process on **32**, either the methylation on the non-methylated or the methylated ring. Only one product was rendered from that reaction, that was, $[\text{Pt}(\text{CN-2,6-xyI})(\text{PPh}_3)]$ (**33**). In the previous chapter, the behavior of $[\text{Pt}(\text{CNC})(\text{PPh}_3)]$ (**1**) towards acids was extensively studied. The similar characteristics of **1** and **32** encouraged to study also the reactivity of **32** towards HCl, to study if the electrophilic proton would distinguish between the two nucleophilic *ipso* carbons of $[\text{Pt}(\text{CNC-Me})(\text{PPh}_3)]$ (**32**).

Thus, the reaction of complex **32** in CH_2Cl_2 with a solution of HCl (MeOH) rendered immediately complex $[\text{Pt}(\text{CN-}o\text{-tol})\text{Cl}(\text{PPh}_3)]$ (**35**) (see Scheme 3.9).



Scheme 3.9. Synthesis of complex **35**.

The X-Ray structure of **35** confirmed that the protonation had taken place in the already methylated ring of the CNC-Me ligand. See Figure 3.14 for the structure of **35** and Table 3.7 for a selection of angles and distances.

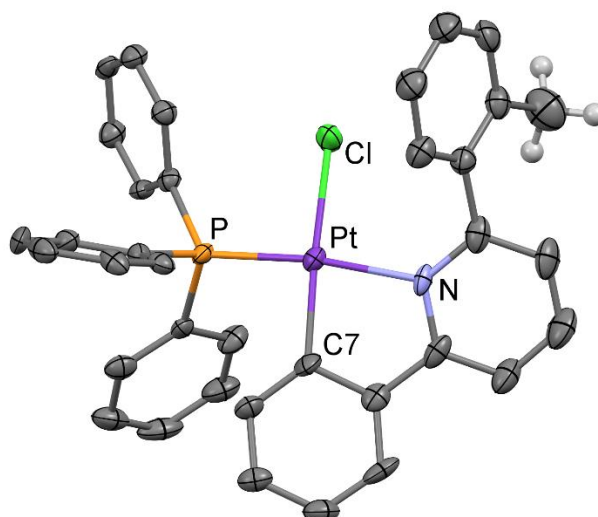


Figure 3.14. Molecular structure of complex [Pt(CN-*o*-tol)Cl(PPh₃)] (**35**).

Table 3.7. Selection of bond lengths (Å) and angles (°) for [Pt(CN-*o*-tol)Cl(PPh₃)] (**35**).

Pt-N	2.155(7)	Pt-P	2.226(2)
Pt-C7	2.029(9)	N-Pt-C7	80.6(4)
Pt-Cl	2.367(2)	Cl-Pt-C7	175.7(3)

The structure confirms the protonation of the methylated phenylene ring of [Pt(CNC-Me)(PPh₃)] (**32**) giving rise to a *o*-tolyl group. As in complex [Pt(CN-*o*-tol)I(PPh₃)] (**29**), the methyl group is observed to be away from the platinum environment, because of steric repulsions. Also, the isomer formed is the *trans*-(N,P) one, existing a chloride ligand *trans* to the carbon cyclometallated atom, which completes the coordination sphere of the platinum (II) square planar environment, displaying for example an angle Cl-Pt-C7 of 175.7(3).

NMR experiments of complex [Pt(CN-*o*-tol)Cl(PPh₃)] (**35**) are in agreement with the protonation of the methylated ring of [Pt(CNC-Me)(PPh₃)] (**32**). The ¹H NMR spectrum of **35** shows a similar pattern of signals compared to that of analogous iodo complex [Pt(CN-*o*-tol)I(PPh₃)] (**29**) (see Figure 3.15).

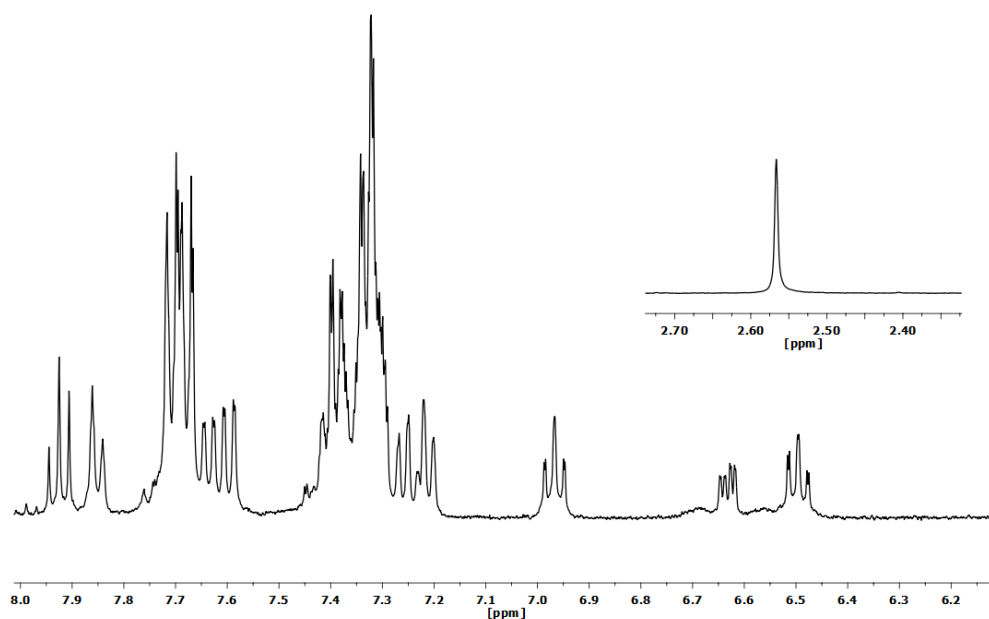
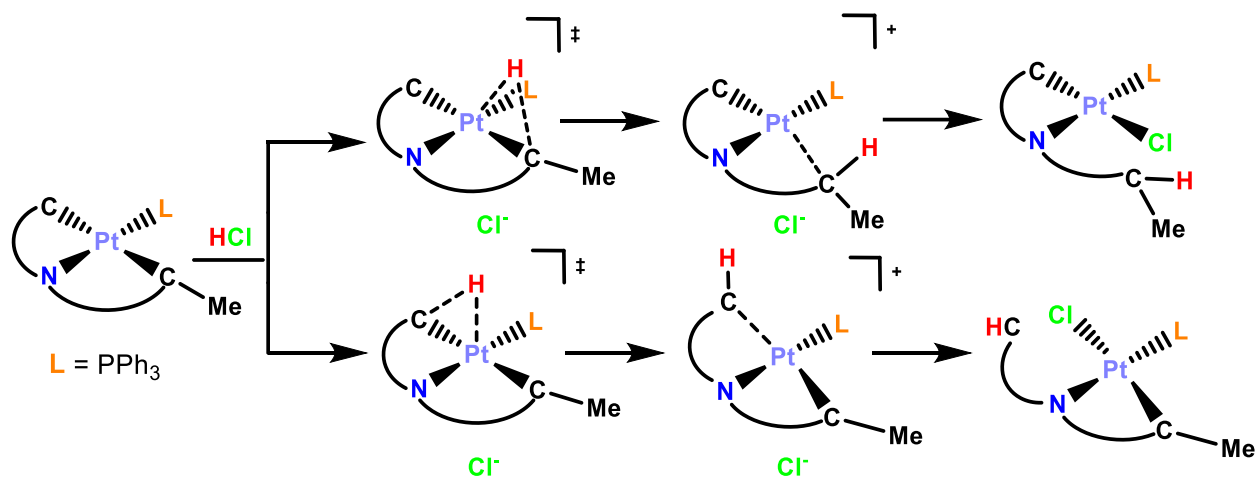


Figure 3.15. ^1H NMR spectrum (CD_2Cl_2 , RT) of complex $[\text{Pt}(\text{CN-}o\text{-tol})\text{Cl}(\text{PPh}_3)]$ (35).

Its $^{31}\text{P}\{^1\text{H}\}$ NMR spectrum (see Figure S3.44, Supporting Information) again displays a singlet with platinum satellites with chemical shifts and P-Pt coupling (20.6 ppm, $^1J_{\text{P-Pt}} = 4548$ Hz) similar to those detected for all the previously discussed C^N complexes.

DFT calculations were performed to establish the energy profile of a tentative mechanism for this protonation process, revealing that as it was found for some protonation reactions of the previous chapter, they were completely barrierless (see Scheme 3.10). Due to the fact that the proton could attack in two different possible sites of the CNC-Me cyclometallated ligand, the energy of the other possible isomer formed results to be 4.7 kcal/mol less stable than the one obtained experimentally.



Scheme 3.10. Possible mechanisms modeled for the reaction with HCl.

In this case, as the previous CDFT studies indicated for **32** (see previous Section), nucleophilicity of the two different C_{ipso} were found similar towards the attack of a proton.

As a summary for this chapter, platinum complex [Pt(CNC)(PPh₃)] (**1**) has resulted to be a proper basic substrate in the reactions with electrophilic methyl groups, using MeI as the methylating agent. On the other hand, controlling the reactivity of the analogous palladium complex [Pd(CNC)(PPh₃)] (**2**) was not possible, obtaining complex mixtures of products.

The first step on the reaction of **1** with MeI is the formation of a *trans* Pt(IV) complex which after treatment, produces a Pt(II) complex *via* reductive elimination of the methyl group with the C_{ipso} of the CNC ligand. It is remarkable that the resulting complex can be recyclometallated and reacted with MeI again, giving rise directly to the methylation of the C_{ipso} of the already methylated ligand. In this case the oxidative addition - reductive elimination process is direct, being impossible to isolate the corresponding Pt(IV) complex.

This whole methylation process has been studied in depth by DFT calculations which support the experimental observations.

Furthermore, reactivity of the recyclometallated [Pt(CNC-Me)(PPh₃)] (**32**) towards the proton (HCl) was studied, revealing that similarly to the second methylation process, the reaction of the electrophilic fragment takes place with the cyclometallated carbon of the already methylated ring. Conceptual DFT studies revealed that both carbons are nucleophilic, but very similar.

3.2. Experimental section

General Comments. Elemental analyses were carried out with a Perkin-Elmer 2400 CHNS analyzer. IR spectra were recorded on a Perkin-Elmer Spectrum 100 FT-IR spectrometer (ATR in the range 250-4000 cm^{-1}). Mass spectrometry was performed with the Microflex matrix-assisted laser desorption ionization-time-of-flight (MALDI-TOF) Bruker or an Autoflex III MALDI-TOF Bruker instruments. ^1H , $^{13}\text{C}\{^1\text{H}\}$ and $^{31}\text{P}\{^1\text{H}\}$ NMR spectra were recorded on Bruker AV-300, ARX-300 and AV-400 spectrometers using the standard references: SiMe_4 and 85% H_3PO_4 for references for ^1H , ^{13}C and ^{31}P respectively. The signal attributions and coupling constant assessment was made on the basis of a multinuclear NMR analysis of each compound including, besides 1D spectra, ^1H - ^1H COSY, ^1H - ^{13}C HSQC, ^1H - ^{13}C HMBC and $^{13}\text{C}\{^1\text{H}\}$ APT.

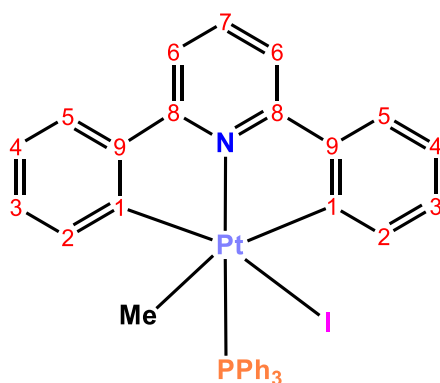


Chart 3.2. ^1H and ^{13}C numbering scheme.

Preparation of the complex [PtIME(CNC)(PPh₃)] (28). [Pt(CNC)(PPh₃)] (1) (0.070 g, 0.102 mmol) was dissolved in MeI (4 mL) and the mixture was stirred in darkness for 21 hours at room temperature. After that time the resulting yellow mixture was evaporated to dryness. Then 5 mL of diethylether were added and evaporated to dryness. This process was repeated three times. Then the resulting yellow solid obtained was extracted with 5 mL of diethylether, filtered and air dried (Yield: 0.072 g, 85%). Anal. Found: C, 51.63; H, 3.44; N, 1.69. Anal. Calcd. for $\text{C}_{36}\text{H}_{29}\text{INPpt}$: C, 52.18; H, 3.53; N, 1.69. IR (ATR, cm^{-1}): 1598 (m, $\nu(\text{N-C})$), 1581 (w, $\nu(\text{N-C})$), 1567 (w, $\nu(\text{N-C})$), 1546 (w, $\nu(\text{N-C})$), 529 (vs, $\nu(\text{P-C})$), 519 (s, $\nu(\text{P-C})$), 502 (s, $\nu(\text{P-C})$). ^1H NMR (400.132 MHz, CD_2Cl_2 , 293K, see Chart 3.2 for the H numbering scheme): δ = 8.10 (6H, m, *o*-PPh₃), 7.92 (1H, t, $^3J_{\text{H7-H6}} = 7.8$ Hz, H7), 7.74 (2H, dd, $^3J_{\text{H5-H4}} = 7.9$ Hz, $^4J_{\text{H5-H3}} = 1.0$ Hz, H5), 7.65 (2H, dd, $^3J_{\text{H6-H7}} = 7.8$ Hz, $^5J_{\text{H6-P}} = 2.6$ Hz, H6), 7.49 (3H, t, $^3J_{\text{Hp-Hm}} = 7.3$ Hz, *p*-PPh₃), 7.41 (6H, m, *m*-PPh₃), 7.07 (4H, m, H4 and H2), 6.89 (2H, td, $^3J_{\text{H3-H2}} = ^3J_{\text{H3-H4}} = 7.4$ Hz,

$^4J_{\text{H3-H5}} = 1.3$ Hz, H3), 0.60 (3H, d, $^3J_{\text{Me-P}} = 3.5$ Hz, $^2J_{\text{Me-Pt}} = 67.8$ Hz, Me) ppm. $^{31}\text{P}\{^1\text{H}\}$ NMR (161.923 MHz, CD_2Cl_2 , 293K): $\delta = 3.52$ (s, $^1J_{\text{P-Pt}} = 2847$ Hz) ppm. $^{13}\text{C}\{^1\text{H}\}$ NMR plus HSQC and HMBC (100.624 MHz, CD_2Cl_2 , 293K, see Chart 3.2 for the C numbering scheme): $\delta = 163.8$ (s, C8), 161.3 (d, $^2J_{\text{C-P}} = 5.3$ Hz, C1), 149.3 (d, $^3J_{\text{C-P}} = 2.3$ Hz, C9), 140.2 (s, C7), 137.6 (d, $^3J_{\text{C-P}} = 1.3$ Hz, $^2J_{\text{C-Pt}} = 30.0$ Hz, C2), 136.3 (d, $^2J_{\text{C-P}} = 9.4$ Hz, $^3J_{\text{C-Pt}} = 11.9$ Hz, *o*-PPh₃), 131.6 (d, $^4J_{\text{C-P}} = 2.5$ Hz, *p*-PPh₃), 129.5 (s, $^3J_{\text{C-Pt}} = 27.6$ Hz, C3), 128.3 (d, $^3J_{\text{C-P}} = 12.2$ Hz, *m*-PPh₃), 128.1 (d, $^1J_{\text{C-P}} = 60.0$ Hz, *q*-PPh₃), 126.1 (s, $^3J_{\text{C-Pt}} = 19.9$ Hz, C5), 124.3 (s, C4), 117.0 (d, $^4J_{\text{C-P}} = 4.2$ Hz, $^3J_{\text{C-Pt}} = 23.1$ Hz, C6), 16.6 (d, $^2J_{\text{C-P}} = 2.0$ Hz, $^1J_{\text{C-Pt}} = 519$ Hz, Me) ppm. MS MALDI+ DCTB: $m/z = 813.0$ [Pt(CNC)I(PPh₃)]⁺, 701.2 [PtMe(CNC)(PPh₃)]⁺.

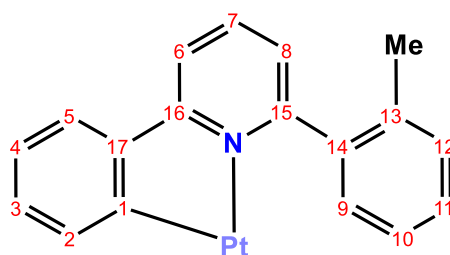


Chart 3.3. ^1H and ^{13}C numbering scheme.

Preparation of the complex [Pt(CN-*o*-tol)I(PPh₃)] (29). The complex [PtMe(CNC)(PPh₃)] (28) (0.070 g, 0.084 mmol) was dissolved in 15 mL of CH_2Cl_2 and the resulting mixture was refluxed protected from light for 2 days. Then the resulting solution was evaporated to dryness, and the yellow solid was extracted with 10 mL of *n*-hexane, filtered and air-dried (Yield: 0.045 g, 64%). Anal. Found: C, 52.26; H, 3.44; N, 1.70. Anal. Calcd. for $\text{C}_{36}\text{H}_{29}\text{INPPt}$: C, 52.18; H, 3.53; N, 1.69. IR (ATR, cm^{-1}): 1599 (w, $\nu(\text{N-C})$), 1577 (w, $\nu(\text{N-C})$), 1560 (w, $\nu(\text{N-C})$), 1550 (w, $\nu(\text{N-C})$), 538 (vs, $\nu(\text{P-C})$), 517 (s, $\nu(\text{P-C})$), 506 (s, $\nu(\text{P-C})$). ^1H NMR (400.132 MHz, CD_2Cl_2 , 293K, see Chart 3.3 for the H numbering scheme): $\delta = 7.99$ (1H, d, $^3J_{\text{H9-H10}} = 8.0$ Hz, H9), 7.94 (1H, t, $^3J_{\text{H7-H6}} = ^3J_{\text{H7-H8}} = 7.7$ Hz, H7), 7.87 (1H, d, $^3J_{\text{H6-H7}} = 7.7$ Hz, H6), 7.79 (6H, m, *o*-PPh₃), 7.64 (1H, dd, $^3J_{\text{H5-H4}} = 7.8$ Hz, $^4J_{\text{H5-H3}} = 1.5$ Hz, H5), 7.44 (1H, m, H8), 7.36 (10H, m, *p*-PPh₃, H11 and *m*-PPh₃), 7.27 (2H, m, H10 and H12), 7.02 (1H, td, $^3J_{\text{H4-H3}} = ^3J_{\text{H4-H5}} = 7.8$ Hz, $^4J_{\text{H4-H2}} = 1.2$ Hz, H4), 6.69 (1H, dd, $^3J_{\text{H2-H3}} = 7.7$ Hz, $^4J_{\text{H2-H4}} = 4.0$ Hz, H2), 6.55 (1H, dd, $^3J_{\text{H3-H2}} = ^3J_{\text{H3-H4}} = 7.7$ Hz, $^4J_{\text{H3-H5}} = 1.5$ Hz, H3), 2.61 (3H, s, Me) ppm. $^{31}\text{P}\{^1\text{H}\}$ NMR (161.923 MHz, CD_2Cl_2 , 293K): $\delta = 19.3$ (s, $^1J_{\text{P-Pt}} = 4388$ Hz) ppm. $^{13}\text{C}\{^1\text{H}\}$ NMR plus HSQC and HMBC (100.624 MHz, CD_2Cl_2 , 293K, see Chart 3.3 for the C numbering scheme): $\delta =$

164.8 (s, C16), 162.6 (s, C15), 147.1 (s, C1), 145.9 (s, C17), 143.3 (s, C14 or C13), 138.1 (s, C7), 137.4 (s, C13 or C14), 135.8 (d, $^3J_{C-P} = 7.7$ Hz, C2), 135.1 (d, $^2J_{C-P} = 11.4$ Hz, *o*-PPh₃), 132.5 (d, $^1J_{C-P} = 57.7$ Hz, *q*-PPh₃), 131.6 (s, C9), 131.2 (s, C10 or C12), 130.7 (d, $^4J_{C-P} = 2.5$ Hz, *p*-PPh₃), 129.7 (s, C11), 128.8 (d, $^4J_{C-P} = 3.1$ Hz, C3), 128.2 (d, $^3J_{C-P} = 10.7$ Hz, *m*-PPh₃), 125.7 (d, $^4J_{C-P} = 3.2$ Hz, C8), 125.4 (s, C10 or C12), 124.6 (s, C5), 123.6 (s, C4), 117.2 (d, $^4J_{C-P} = 2.0$ Hz, C6), 22.1 (s, Me) ppm. MS MALDI+ DCTB: $m/z = 701.2$ [Pt(CNC-Me)(PPh₃)]⁺.

Preparation of the complex [Pt(CN-*o*-tol)(MeCN)(PPh₃)](ClO₄) (30). To complex [PtMe(CNC)(PPh₃)] (28) (0.060 g, 0.072 mmol), AgClO₄ (0.015 g, 0.072 mmol) was added in 20 mL of MeCN. The resulting mixture was protected from light and stirred for 90 minutes at room temperature. Then, the AgI formed was removed through celite and the obtained pale-yellow solution was concentrated to 1 mL. After that, 15 mL of diethylether were added to precipitate a yellow solid, which was filtered and air-dried. (Yield: 0.042 g, 69%). Anal. Found: C, 53.62; H, 3.86; N, 3.22. Anal. Calcd. for C₃₈H₃₂ClN₂O₄PPt: C, 54.19; H, 3.83; N, 3.33. IR (ATR, cm⁻¹): 1603 (m, ν (N-C)), 1583 (w, ν (N-C)), 1568 (w, ν (N-C)), 1557 (m, ν (N-C)), 1085 (vs, ν (ClO₄)), 621 (s, ν (ClO₄)), 539 (vs, ν (P-C)), 517 (s, ν (P-C)), 500 (s, ν (P-C)). ¹H NMR (400.132 MHz, CD₂Cl₂, 293K): $\delta = 8.13$ (1H, t, $^3J_{H7-H6} = ^3J_{H7-H8} = 8.0$ Hz, H7), 7.99 (1H, d, $^3J_{H6-H7} = 8.0$ Hz, H6), 7.68 (7H, m, *o*-PPh₃ and H5), 7.60 (1H, dd, $^3J_{H-H} = 7.4$ Hz, $^4J_{H-H} = 1.8$ Hz, H9 or H12), 7.54 (3H, m, *p*-PPh₃), 7.45 (7H, m, H8 and *m*-PPh₃), 7.35 (3H, m, H9 or H12, H10, H11), 7.04 (1H, td, $^3J_{H4-H3} = ^3J_{H4-H5} = 7.8$ Hz, $^4J_{H4-H2} = 1.2$ Hz, H4), 6.65 (1H, ddd, $^3J_{H2-H3} = 7.8$ Hz, $^4J_{H2-P} = 3.8$ Hz, $^4J_{H2-H4} = 1.2$ Hz, $^3J_{H2-Pt} = 50.0$ Hz, H2), 6.53 (1H, td, $^3J_{H3-H2} = ^3J_{H3-H4} = 7.8$ Hz, $^4J_{H3-H5} = 1.4$ Hz, H3), 2.59 (3H, s, Me), 1.11 (3H, s, MeCN) ppm. ³¹P{¹H} NMR (161.923 MHz, CD₂Cl₂, 293K): $\delta = 21.5$ (s, $^1J_{P-Pt} = 4292$ Hz) ppm. ¹³C{¹H} NMR plus HSQC and HMBC (100.624 MHz, CD₂Cl₂, 293K): $\delta = 165.4$ (s, C16), 161.4 (s, C15), 147.1 (s, C17), 141.1 (s, C7), 139.8 (s, C14 or C13), 139.0 (d, $^3J_{C-P} = 7.7$ Hz, C2), 137.1 (s, C13 or C14), 136.9 (s, C1), 135.3 (d, $^2J_{C-P} = 11.6$ Hz, *o*-PPh₃), 132.4 (d, $^4J_{C-P} = 2.6$ Hz, *p*-PPh₃), 131.4 (s, C9 or C12), 131.3 (s, C9 or C12), 130.7 (s, C10 or C11), 129.5 (d, $^4J_{C-P} = 3.3$ Hz, C3), 129.3 (d, $^3J_{C-P} = 11.6$ Hz, *m*-PPh₃), 128.6 (d, $^1J_{C-P} = 63.8$ Hz, *q*-PPh₃), 126.7 (s, C10 or C11), 126.3 (d, $^4J_{C-P} = 4.3$ Hz, C8), 125.7 (s, C4), 125.1 (s, C5), 120.8 (s, CN), 118.3 (d, $^4J_{C-P} = 2.0$ Hz, C6), 21.1 (s, Me), 2.76 (s, Me (MeCN)) ppm. MS MALDI+ DCTB: $m/z = 700.2$ [[Pt(CN-*o*-tol)(PPh₃)]-H]⁺.

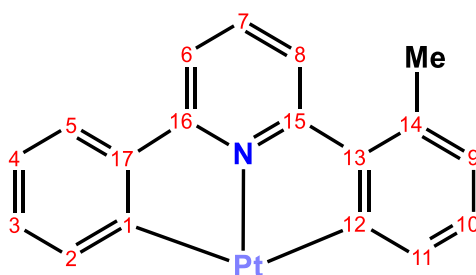


Chart 3.4. ^1H and ^{13}C numbering scheme.

Preparation of the complex [Pt(CNC-Me)(PPh₃)] (32). This complex can be prepared from different starting materials. *Pathway 1:* To a solution of [Pt(CN-*o*-tol)I(PPh₃)] (**29**) (0.040 g, 0.048 mmol) in 15 mL of CH₂Cl₂, K₂CO₃ (1M, 3 mL) was added. The resulting mixture was stirred for two days. After that time, the organic layer was separated from the aqueous layer, dried with MgSO₄ and filtered through celite. The solution was concentrated to 1 mL and 15 mL of *n*-hexane were then added. The yellow solid formed was filtered and air-dried (Yield: 0.012 g, 35%). *Pathway 2:* To a solution of [Pt(CN-*o*-tol)(MeCN)(PPh₃)](ClO₄) (**30**) (0.060 g, 0.071 mmol) in 15 mL of CH₂Cl₂, an aqueous solution of K₂CO₃ (1M, 5 mL) was added. The resulting mixture was stirred for 3 hours. After that time, the organic layer was separated from the aqueous layer, dried with MgSO₄ and filtered through celite. The solution was concentrated to 1 mL and 15 mL of *n*-hexane were added. The yellow solid formed was filtered and air-dried (Yield: 0.035 g, 70%). Anal. Found: C, 61.52; H, 3.57; N, 1.77. Anal. Calcd. for C₃₆H₂₈NPPt: C, 61.71; H, 4.03; N, 2.00. IR (ATR, cm⁻¹): 1592 (w, $\nu(\text{N-C})$), 1563 (w, $\nu(\text{N-C})$), 1548 (w, $\nu(\text{N-C})$), 541 (vs, $\nu(\text{P-C})$), 518 (s, $\nu(\text{P-C})$), 499 (s, $\nu(\text{P-C})$). ^1H NMR (400.132 MHz, CD₂Cl₂, 293K, see Chart 3.4 for the H numbering scheme): δ = 7.82 (6H, m, *o*-PPh₃), 7.70 (1H, t, $^3J_{\text{H7-H6}} = ^3J_{\text{H7-H8}} = 7.9$ Hz, H7), 7.64 (1H, d, $^3J_{\text{H-H}} = 7.9$ Hz, H6 or H8), 7.40 (11H, m, *p*-PPh₃, *m*-PPh₃ and H6 or H8), 6.89 (1H, t, $^3J_{\text{H4-H5}} = ^3J_{\text{H4-H3}} = 7.3$ Hz, H4), 6.69 (1H, d, $^3J_{\text{H9-H10}} = 7.4$ Hz, H9), 6.63 (1H, t, $^3J_{\text{H3-H2}} = ^3J_{\text{H3-H4}} = 7.3$ Hz, H3), 6.48 (1H, t, $^3J_{\text{H10-H11}} = ^3J_{\text{H10-H9}} = 7.4$ Hz, H10), 6.31 (1H, d, $^3J_{\text{H11-H10}} = 7.4$ Hz, $^3J_{\text{H11-Pt}} = 29.0$ Hz, H11), 6.22 (1H, d, $^3J_{\text{H2-H3}} = 7.4$ Hz, $^3J_{\text{H2-Pt}} = 29.0$ Hz, H2), 2.59 (3H, s, Me) ppm. $^{31}\text{P}\{^1\text{H}\}$ NMR (161.923 MHz, CD₂Cl₂, 293K): δ = 30.1 (s, $^1J_{\text{P-Pt}} = 4116$ Hz) ppm. $^{13}\text{C}\{^1\text{H}\}$ NMR plus HSQC and HMBC (100.624 MHz, CD₂Cl₂, 293K, see Chart 3.4 for the C numbering scheme): δ = 167.4 (m, C1, C12, C15, C16), 151.3 (s, C17), 150.3 (s, C13), 140.4 (s, C7), 138.8 (s, C2), 137.4 (d, $^3J_{\text{C-P}} = 3.8$ Hz, C11), 136.0 (s, C14), 135.6 (d, $^2J_{\text{C-P}} = 12.9$ Hz, *o*-PPh₃), 132.6 (d, $^1J_{\text{C-P}} = 58.0$ Hz, *q*-PPh₃), 130.8 (d, $^4J_{\text{C-P}} = 2.8$ Hz, *p*-PPh₃), 129.8 (s, C3),

129.1 (s, C10), 128.5 (m, *m*-PPh₃ and C9), 124.2 (s, C5), 123.8 (s, C4), 120.0 (s, C6 or C8), 115.1 (s, C6 or C8), 24.6 (s, Me) ppm. MS MALDI+ DCTB: $m/z = 701.4$ [Pt(CNC-Me)(PPh₃)]⁺.

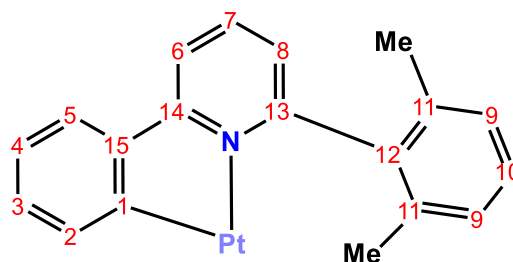


Chart 3.5. ¹H and ¹³C numbering scheme.

Preparation of the complex [Pt(CN-2,6-xy)I(PPh₃)] (33). Complex [Pt(CNC-Me)(PPh₃)] (32) (0.060 g, 0.085 mmol) was dissolved in 3 mL of MeI and stirred kept in darkness for 24 hours. The resulting yellow mixture was then evaporated to dryness and the yellow solid was extracted with 5 mL of diethylether, filtered and air-dried (Yield: 0.020 g, 55%). Anal. Found: C, 52.28; H, 3.56; N, 1.63. Anal. Calcd. for C₃₇H₃₁INPPT: C, 52.74; H, 3.71; N, 1.66. IR (ATR, cm⁻¹): 1600 (w, ν(N-C)), 1579 (w, ν(N-C)), 1567 (w, ν(N-C)), 1552 (w, ν(N-C)), 538 (vs, ν(P-C)), 516 (s, ν(P-C)), 503 (s, ν(P-C)). ¹H NMR (400.132 MHz, CD₂Cl₂, 293K, see Chart 3.5 for the H numbering scheme): δ = 7.96 (1H, t, ³J_{H7-H6} = ³J_{H7-H8} = 8.1 Hz, H7), 7.88 (1H, d, ³J_{H6-H7} = 8.1 Hz, H6), 7.76 (6H, m, *o*-PPh₃), 7.64 (1H, dd, ³J_{H5-H4} = 7.9 Hz, ⁴J_{H5-H3} = 1.2 Hz, H5), 7.39 (3H, m, *p*-PPh₃), 7.32 (6H, m, *m*-PPh₃), 7.24 (2H, m, H8 and H10), 7.04 (2H, d, ³J_{H9-H10} = 7.7 Hz, H9), 7.03 (1H, m, H4, overlapped with H9), 6.68 (1H, dd, ³J_{H2-H3} = 7.7 Hz, ⁴J_{H2-P} = 4.0 Hz, ³J_{H2-Pt} = 54.4 Hz, H2), 6.56 (1H, td, ³J_{H3-H4} = ³J_{H3-H2} = 7.7 Hz, ⁴J_{H3-H5} = 1.2 Hz, H3), 2.53 (6H, s, Me) ppm. ³¹P{¹H} NMR (161.923 MHz, CD₂Cl₂, 293K): δ = 18.8 (s, ¹J_{P-Pt} = 4432 Hz) ppm. ¹³C{¹H} NMR plus HSQC and HMBC (100.624 MHz, CD₂Cl₂, 293K, see Chart 3.5 for the C numbering scheme): δ = 162.6 (s, C13 or C14), 148.5 (s, C1), 145.9 (s, C15), 141.7 (s, C12), 138.6 (s, C7), 138.1 (s, C11), 135.7 (d, ³J_{C-P} = 8.5 Hz, C2), 135.1 (d, ²J_{C-P} = 10.4 Hz, *o*-PPh₃), 132.5 (d, ¹J_{C-P} = 62.8 Hz, *q*-PPh₃), 130.7 (d, ⁴J_{C-P} = 2.5 Hz, *p*-PPh₃), 129.0 (s, C10), 128.9 (s, C3), 128.2 (d, ³J_{C-P} = 11.2 Hz, *m*-PPh₃), 128.0 (s, C9), 126.9 (d, ⁵J_{C-P} = 4.3 Hz, C8), 124.5 (s, C5), 123.6 (s, C4), 117.8 (d, ⁵J_{C-P} = 2.7 Hz, C6), 22.7 (s, Me) ppm. MS MALDI+ DCTB: $m/z = 715.3$ [Pt(CN-2,6-xy)(PPh₃)]⁺.

Preparation of the complex [Pt(CN-*o*-tol)Cl(PPh₃)] (35). To a solution of complex [Pt(CNC-Me)(PPh₃)] (32) (0.030 g, 0.043 mmol) in 10 mL of CH₂Cl₂, a solution 0.25 M of HCl in MeOH (0.190 mL, 0.047 mmol) was added. The resulting light-yellow mixture was then concentrated to 0.5 mL and 20 mL of *n*-hexane were added. The yellow solid formed was filtered and air-dried. (Yield: 0.025 g, 79%). Anal. Found: C, 58.32; H, 3.90; N, 1.96. Anal. Calcd. for C₃₆H₂₉ClNPPt: C, 58.66; H, 3.97; N, 1.90. IR (ATR, cm⁻¹): 1596 (w, ν(N-C)), 1579 (w, ν(N-C)), 1563 (w, ν(N-C)), 1553 (w, ν(N-C)), 541 (vs, ν(P-C)), 518 (s, ν(P-C)), 502 (s, ν(P-C)), 296 (w, ν(Pt-Cl)). ¹H NMR (400.132 MHz, CD₂Cl₂, 293K, see Chart 3.3 for the H numbering scheme): δ = 7.92 (1H, t, ³J_{H7-H6} = ³J_{H7-H8} = 7.5 Hz, H7), 7.85 (1H, d, ³J_{H6-H7} = 7.5 Hz, H6), 7.69 (6H, m, *o*-PPh₃), 7.64 (1H, dd, ³J_{H9-H10} = 7.5 Hz, ⁴J_{H9-H11} = 1.3 Hz, H9), 7.60 (1H, dd, ³J_{H5-H4} = 7.8 Hz, ⁴J_{H5-H3} = 1.5 Hz, H5), 7.36 (11H, m, *p*-PPh₃, H8, H11 and *m*-PPh₃), 7.25 (1H, t, ³J_{H10-H9} = ³J_{H10-H11} = 7.5 Hz, H10), 7.21 (1H, d, ³J_{H12-H11} = 7.5 Hz, H12), 6.97 (1H, td, ³J_{H4-H3} = ³J_{H4-H5} = 7.5 Hz, ⁴J_{H4-H2} = 1.2 Hz, H4), 6.63 (1H, ddd, ³J_{H2-H3} = 7.6 Hz, ⁴J_{H2-P} = 3.5 Hz, ⁴J_{H2-H4} = 1.2 Hz, ³J_{H2-Pt} = 53.0 Hz, H2), 6.50 (1H, td, ³J_{H3-H2} = ³J_{H3-H4} = 7.6 Hz, ⁴J_{H3-H5} = 1.5 Hz, H3), 2.57 (3H, s, Me) ppm. ³¹P{¹H} NMR (161.923 MHz, CD₂Cl₂, 293K): δ = 20.6 (s, ¹J_{P-Pt} = 4548 Hz) ppm. ¹³C{¹H} NMR plus HSQC and HMBC (100.624 MHz, CD₂Cl₂, 293K, see Chart 3.3 for the C numbering scheme): δ = 162.6 (s, C16 or C15), 146.6 (s, C17), 143.5 (s, C1), 141.2 (s, C14), 138.7 (s, C7), 137.2 (d, ³J_{C2-Pt} = 7.6 Hz, C2), 137.0 (s, C13), 135.2 (d, ²J_{C-P} = 11.6 Hz, *o*-PPh₃), 131.6 (s, C9), 131.0 (d, ¹J_{C-P} = 65.0 Hz, *q*-PPh₃), 130.8 (d, ⁴J_{C-P} = 3.4 Hz, *p*-PPh₃), 130.4 (s, C12), 128.9 (s, C11), 128.73 (d, ⁴J_{C-P} = 3.4 Hz, C3), 128.1 (d, ³J_{C-P} = 10.9 Hz, *m*-PPh₃), 126.0 (d, ⁴J_{C-P} = 5.9 Hz, C8), 125.1 (s, C10), 124.6 (s, C5), 123.4 (s, C4), 116.7 (d, ⁴J_{C-P} = 3.3 Hz, C6), 21.5 (s, Me) ppm. Mass spectra MALDI+ DCTB: m/z = 737.4 [Pt(CN-*o*-tol)Cl(PPh₃)]⁺, 701.4 [Pt(CN-*o*-tol)(PPh₃)]⁺.

3.3. References

- (1) Raubenheimer, H. G.; Schmidbaur, H. Gold Chemistry Guided by the Isolobality Concept. *Organometallics* **2012**, *31* (7), 2507-2522. DOI: 10.1021/om2010113.
- (2) Stone, F. G. A. Metal-Carbon and Metal-Metal Multiple Bonds as Ligands in Transition-Metal Chemistry: The Isolobal Connection. *Angew. Chem. Int. Ed.* **1984**, *23* (2), 89-99. DOI: doi.org/10.1002/anie.198400893.
- (3) Shahsavari, H. R.; Babadi Aghakhanpour, R.; Babaghasabha, M.; Golbon Haghighi, M.; Nabavizadeh, S. M.; Notash, B. Combined Kinetic-Mechanistic and Theoretical Elucidation of the Oxidative Addition of Iodomethane to Cycloplatinated(II) Complexes: Controlling the Rate of *trans/cis* Isomerization. *Eur. J. Inorg. Chem.* **2017**, *2017* (20), 2682-2690. DOI: 10.1002/ejic.201700088.
- (4) Hosseini, F. N. Theoretical studies of methyl iodide oxidative addition to adjacent metal centers in diplatinum(II) complexes. *Polyhedron* **2015**, *100*, 67-73. DOI: 10.1016/j.poly.2015.07.041.
- (5) Jamali, S.; Nabavizadeh, S. M.; Rashidi, M. Oxidative Addition of Methyl Iodide to a New Type of Binuclear Platinum(II) Complex: a Kinetic Study. *Inorg. Chem.* **2005**, *44* (23), 8594-8601. DOI: 10.1021/ic0511064.
- (6) Hashemi, M. Comparison of reactivity of Pt(II) center in the mononuclear and binuclear organometallic diimineplatinum complexes toward oxidative addition of methyl iodide. *J. Mol. Struct.* **2016**, *1103*, 132-139. DOI: 10.1016/j.molstruc.2015.09.017.
- (7) Noori, M.; Shafaatian, B.; Notash, B. New organoplatinum complexes containing di-2-pyridyl ketone; single crystal structure determination, solvatochromism and kinetic investigations. *Inorg. Chim. Acta* **2020**, *511*, 119851. DOI: 10.1016/j.ica.2020.119851.
- (8) Nabavizadeh, S. M.; Amini, H.; Jame, F.; Khosraviolya, S.; Shahsavari, H. R.; Hosseini, F. N.; Rashidi, M. Oxidative addition of MeI to some cyclometalated organoplatinum(II) complexes: Kinetics and mechanism. *J. Organomet. Chem.* **2012**, *698*, 53-61. DOI: 10.1016/j.jorganchem.2011.10.028.
- (9) Hamidizadeh, P.; Rashidi, M.; Nabavizadeh, S. M.; Samaniyan, M.; Aseman, M. D.; Owczarzak, A. M.; Kubicki, M. Secondary kinetic deuterium isotope effect in oxidative addition reaction of cycloplatinated(II) complexes with MeI. *J. Organomet. Chem.* **2015**, *791*, 258-265. DOI: 10.1016/j.jorganchem.2015.06.001.

- (10) Habibzadeh, S.; Rashidi, M.; Nabavizadeh, S. M.; Mahmoodi, L.; Hosseini, F. N.; Puddephatt, R. J. Steric and Solvent Effects on the Secondary Kinetic α -Deuterium Isotope Effects in the Reaction of Methyl Iodide with Organoplatinum(II) Complexes: Application of a Second-Order Technique in Measuring the Rates of Rapid Processes. *Organometallics* **2010**, *29* (1), 82-88. DOI: 10.1021/om900778u.
- (11) Fatemeh, N. H.; Farasat, Z.; Nabavizadeh, S. M.; Wu, G.; Abu-Omar, M. M. N-methylation versus oxidative addition using MeI in the reaction of organoplatinum(II) complexes containing pyrazine ligand. *J. Organomet. Chem.* **2019**, *880*, 232-240. DOI: 10.1016/j.jorganchem.2018.11.002.
- (12) Dolatyari, V.; Shahsavari, H. R.; Habibzadeh, S.; Babadi Aghakhanpour, R.; Paziresh, S.; Golbon Haghighi, M.; Halvagar, M. R. Photophysical Properties and Kinetic Studies of 2-Vinylpyridine-Based Cycloplatinated(II) Complexes Containing Various Phosphine Ligands. *Molecules* **2021**, *26* (7), 2034. DOI: 10.3390/molecules26072034.
- (13) Crespo, M.; Martínez, M.; Nabavizadeh, S. M.; Rashidi, M. Kinetic-mechanistic studies on CX (X=H, F, Cl, Br, I) bond activation reactions on organoplatinum(II) complexes. *Coord. Chem. Rev.* **2014**, *279*, 115-140. DOI: 10.1016/j.ccr.2014.06.010.
- (14) Aghakhanpour, R. B.; Rashidi, M.; Hosseini, F. N.; Raoof, F.; Nabavizadeh, S. M. Oxidation of a rollover cycloplatinated(II) dimer by MeI: a kinetic study. *RSC Adv.* **2015**, *5* (82), 66534-66542. DOI: 10.1039/C5RA12201E.
- (15) Aghakhanpour, R. B.; Nabavizadeh, S. M.; Mohammadi, L.; Jahromi, S. A.; Rashidi, M. A kinetic approach to carbon-iodide bond activation by rollover cycloplatinated(II) complexes containing monodentate phosphine ligands. *J. Organomet. Chem.* **2015**, *781*, 47-52. DOI: 10.1016/j.jorganchem.2015.01.015.
- (16) Shaw, P. A.; Rourke, J. P. Selective C-C coupling at a Pt(IV) centre: 100% preference for sp^2 - sp^3 over sp^3 - sp^3 . *Dalton Trans.* **2017**, *46* (14), 4768-4776. DOI: 10.1039/C7DT00328E.
- (17) Shaw, P. A.; Clarkson, G. J.; Rourke, J. P. Long-Lived Five-Coordinate Platinum(IV) Intermediates: Regiospecific C-C Coupling. *Organometallics* **2016**, *35* (21), 3751-3762. DOI: 10.1021/acs.organomet.6b00697.
- (18) Hamidzadeh, P.; Nabavizadeh, S. M.; Hoseini, S. J. Effects of the number of cyclometalated rings and ancillary ligands on the rate of MeI oxidative addition

- to platinum(II)–pincer complexes. *Dalton Trans.* **2019**, 48 (10), 3422-3432. DOI: 10.1039/C9DT00205G.
- (19) Baik, C.; Han, W.-S.; Kang, Y.; Kang, S. O.; Ko, J. Synthesis and photophysical properties of luminescent platinum(II) complexes with terdentate polypyridine ligands: [Pt(bpqb)X] and [Pt(tbbppy)X](PF₆) (bpqb-H=1,3-bis(4'-phenyl-2'-quinolinyl) benzene; tbbppy=4-tert-butyl-1,3-bis(4'-phenyl-2'-quinolinyl) pyridine; X=Cl, CCC₆H₅, CCC₆H₄NMe₂, CCC₆H₄NO₂). *J. Organomet. Chem.* **2006**, 691 (26), 5900-5910. DOI: 10.1016/j.jorganchem.2006.09.062.
- (20) Gong, G.; Cao, Y.; Wang, F.; Zhao, G. Planar Chiral Ferrocene Cyclopalladated Derivatives Induce Caspase-Dependent Apoptosis and Antimetastasis in Cancer Cells. *Organometallics* **2018**, 37 (7), 1103-1113. DOI: 10.1021/acs.organomet.7b00897.
- (21) Ito, Y.; Miyake, T.; Hatano, S.; Shima, R.; Ohara, T.; Suginome, M. Asymmetric Synthesis of Helical Poly(quinoxaline-2,3-diyl)s by Palladium-Mediated Polymerization of 1,2-Diisocyanobenzenes: Effective Control of the Screw-Sense by a Binaphthyl Group at the Chain-End. *J. Am. Chem. Soc.* **1998**, 120 (46), 11880-11893. DOI: 10.1021/ja982500m.
- (22) Shaw, P. A.; Clarkson, G. J.; Rourke, J. P. Reversible C–C bond formation at a triply cyclometallated platinum(IV) centre. *Chem. Sci.* **2017**, 8 (8), 5547-5558. DOI: 10.1039/C7SC01361B.
- (23) Solomatina, A. I.; Chelushkin, P. S.; Abakumova, T. O.; Zhemkov, V. A.; Kim, M.; Bezprozvanny, I.; Gurzhiy, V. V.; Melnikov, A. S.; Anufrikov, Y. A.; Koshevoy, I. O.; Su, S.-H.; Chou, P.-T.; Tunik, S. P. Reactions of Cyclometalated Platinum(II) [Pt(NAC)(PR₃)Cl] Complexes with Imidazole and Imidazole-Containing Biomolecules: Fine-Tuning of Reactivity and Photophysical Properties *via* Ligand Design. *Inorg. Chem.* **2019**, 58 (1), 204-217. DOI: 10.1021/acs.inorgchem.8b02204.
- (24) Štěpnička, P.; Solařová, H.; Císařová, I. Synthesis and structural characterization of 1'-(diphenylphosphino)ferrocene-1-carboxamide, its corresponding hydrazide, some heterocycles derived from the hydrazide and palladium(II) complexes with these functional phosphinoferrocene ligands. *J. Organomet. Chem.* **2011**, 696 (23), 3727-3740. DOI: 10.1016/j.jorganchem.2011.08.043.
- (25) Xu, C.; Li, H.-M.; Wang, Z.-Q.; Fu, W.-J. Synthesis, crystal structures and catalytic activity of three cyclopalladated 6-bromo-2-ferrocenylquinoline

- complexes with N-heterocyclic carbenes (NHCs) and triphenylphosphine. *Inorg. Chim. Acta* **2014**, *423*, 11-15. DOI: 10.1016/j.ica.2014.07.037.
- (26) Xu, C.; Zhang, Y.-P.; Wang, Z.-Q.; Liang, T.; Fu, W.-J.; Hao, X.-Q.; Xu, Y.; Ji, B.-M. Synthesis, characterization and crystal structures of monocyclopalladated and biscyclopalladated 1,1'-bisferrocenylpyrimidine–monophosphine complexes. *Inorg. Chim. Acta* **2011**, *365* (1), 469-472. DOI: 10.1016/j.ica.2010.08.046.
- (27) Shu-Bin, L. Conceptual Density Functional Theory and Some Recent Developments. *Acta Phys.-Chim. Sin.* **2009**, *25* (03), 590-600. DOI: 10.3866/pku.Whxb20090332.
- (28) Morell, C.; Grand, A.; Toro-Labbé, A. New Dual Descriptor for Chemical Reactivity. *J. Phys. Chem. A* **2005**, *109* (1), 205-212. DOI: 10.1021/jp046577a.
- (29) Parr, R. G.; Yang, W. Density functional approach to the frontier-electron theory of chemical reactivity. *J. Am. Chem. Soc.* **1984**, *106* (14), 4049-4050. DOI: 10.1021/ja00326a036.

Conclusions

Conclusiones

Conclusions

1. Neutral substrates [Pt(CNC)(PPh₃)] (**1**) and [Pd(CNC)(PPh₃)] (**2**) have proven to be proper starting materials in the obtention of bimetallic complexes with M-M' donor-acceptor bonds (M' = Ag(I), Au(I)). Depending on the proportion and the acidic metal substrate used either dinuclear or trinuclear clusters are rendered.
2. In all the M-M' clusters a short interaction between the acidic metal M' and the C_{ipso} of the CNC cyclometallated ligand is detected, not only in the solid state but also in solution. In the latter case, M' is able to alternate between the C_{ipso} of the CNC ligand, breaking and forming M'-C_{ipso} interactions, giving rise to an intramolecular dynamic process; a "metronome-like" movement. This interesting behavior in solution could be carefully studied by VT NMR experiments.
3. In the solid state, it is observed for some clusters a remarkable distortion of a phenylene ring of the ligand interacting with the acidic metal with respect to the square planar environment of the Pt(II) or Pd(II) centers. Greater deviations from planarity are observed for the gold complexes, detecting the greatest in the Pd-Au complexes.
4. The previous results allow to regard these bimetallic complexes as models of a transmetallation process, representing a frozen snapshot of a frustrated phenyl group transfer between the metals. DFT calculations have played an important role in the further study of the bonding situation and the strength of the interaction between the metallic fragments. Thus, with all the gathered information, a series for the degree of transfer of the phenyl group between the metals can be established; Pd-Au > Pt-Au > Pd-Ag > Pt-Ag.
5. To study the reactivity of basic platinum and palladium substrates towards another electrophile as the proton, starting complexes [Pt(CNC)(PPh₃)] (**1**), [Pt(CNC)(dmsO)] (**12**) and [Pd(CNC)(PPh₃)] (**2**) have been reacted toward protic acids and organic ligands with donor atoms (N, P) and acidic hydrogens (-SH, -OH or -COOH groups). When a protic acid is used, breakage of a M-C_{ipso} bond,

formation of a C-H bond and coordination of a ligand in the resulting vacant is observed. Depending on the situation, the ligand completing the free coordination site generated can be the anion of the acid used, a molecule of solvent or an added ligand additionally. On the other hand, if an organic ligand with acidic hydrogens is reacted with [Pt(CNC)(dmsO)] (**12**) or [Pd(CNC)(PPh₃)] (**2**), not only the same protonation process is observed but also the coordination of the ligand in a bidentate way giving rise to a chelate ring. Exceptionally, when the ligand used is pyridine-2-thiol a dinuclear complex with bridging ligands is rendered.

6. In these reactions in which there is a substitution of ligands, the process is more favored in the case of using P-donor ligands compared to N-donor ligands, needing for the latter more energetic reaction conditions and longer times to proceed. In addition, the use of bidentate ligands in the protonation reactions can give rise to isomers. This is not observed for the P-donor ligands, due to their steric requirements.
7. Intermediates with Pt...H-O interactions may play an important role in some of these reactions, as detected for the reaction of [Pt(CNC)(dmsO)] (**12**) with (2-hydroxyphenyl)diphenylphosphane at low temperature and given some examples in the literature of similar complexes containing these interactions.
8. Furthermore, reactivity of basic [Pt(CNC)(PPh₃)] (**1**) and [Pd(CNC)(PPh₃)] (**2**) substrates towards sources of electrophilic methyl groups, as MeI or (Me₃O)(BF₄) has been explored. In the case of palladium (II) complex **2** not conclusive results are obtained. Complex **1** does not react with (Me₃O)(BF₄), but on the other hand oxidative addition of MeI to **1** gives rise to the expected *trans* Pt(IV) complex [PtIme(CNC)(PPh₃)] (**28**). No isomerization *trans-cis* is observed for this complex.
9. Reductive elimination of the methyl group of complex **28** with the C_{ipso} of the CNC ligand gives rise to a C-C coupling and the methylation of the ligand. If the Pt(IV) complex **28** is treated with a silver salt, the reductive elimination process with precipitation of AgI takes place in milder reaction conditions. Methylated Pt(II) complexes [Pt(CN-*o*-tol)I(PPh₃)] (**29**) and [Pt(CN-*o*-tol)(MeCN)(PPh₃)](ClO₄) (**30**) can be recyclometallated in the presence of basic

media and reacted again with MeI. In this case, the Pt(IV) complex could not be isolated and the reductive elimination product is directly rendered. The second methylation process takes place in the already methylated ligand.

10. As a global result of these reactions a phenylene ring of the CNC ligand is methylated in *ortho* positions.
11. Reaction of complex [Pt(CNC-Me)(PPh₃)] (**32**) towards a source of protons as HCl gives rise to the protonation of the already methylated ring.

Conclusiones

1. Los sustratos neutros [Pt(CNC)(PPh₃)] (**1**) y [Pd(CNC)(PPh₃)] (**2**) han resultado ser productos de partida adecuados en la obtención de complejos bimetálicos con enlaces M-M' dador-aceptor (M'= Ag(I), Au(I)). Dependiendo de la proporción y el sustrato del metal ácido utilizado se obtienen clústeres dinucleares o trinucleares.
2. En todos los clústeres M-M' se observa una interacción corta entre el metal M' y el C_{ipso} del ligando ciclometalado CNC, tanto en estado sólido como en disolución. En este último caso, M' es capaz de interactuar alternativamente con los C_{ipso} del ligando CNC, rompiendo y formando interacciones M'-C_{ipso}, dando lugar a un proceso dinámico intramolecular; un movimiento "de tipo metrónomo". Este interesante comportamiento en disolución pudo ser cuidadosamente estudiado mediante experimentos de RMN de temperatura variable.
3. En estado sólido, se observa para algunos clústeres una importante distorsión del anillo fenilénico del ligando interactuando con el metal ácido con respecto al entorno planocuadrado de los centros de Pt(II) y Pd(II). Se observan mayores desviaciones con respecto a la planaridad para los complejos de oro, siendo detectadas las mayores en los complejos Pd-Au.
4. Los resultados anteriores permiten considerar a estos complejos bimetálicos como modelos de un proceso de transmetalación, representando un intermedio congelado de una transferencia de un grupo fenilo entre metales. Los cálculos DFT juegan un papel importante a la hora de profundizar en el estudio de la situación de enlace y en la fortaleza de la interacción entre los fragmentos metálicos de los clústeres. Por tanto, con toda la información obtenida se puede establecer una progresión en el grado de transferencia del grupo fenilo entre metales; Pd-Au > Pt-Au > Pd-Ag > Pt-Ag.
5. Para estudiar la reactividad de los complejos básicos de platino y paladio frente a un electrófilo como es el protón, se hicieron reaccionar los complejos de partida

[Pt(CNC)(PPh₃)] (**1**), [Pt(CNC)(dmsO)] (**12**) y [Pd(CNC)(PPh₃)] (**2**) con ácidos próticos y ligandos orgánicos con átomos dadores (N, P) e hidrógenos ácidos (grupos -SH, -OH o -COOH). Cuando se utiliza un ácido prótico, se observa la ruptura de un enlace M-C_{ipso}, la formación de un enlace C-H y la coordinación de un ligando en la vacante resultante. Dependiendo de la reacción, el ligando que completa la vacante coordinativa puede ser el anión del ácido utilizado, una molécula de disolvente o un ligando añadido adicionalmente. Por otro lado, cuando se hace reaccionar un ligando orgánico con hidrógenos ácidos con los complejos [Pt(CNC)(dmsO)] (**12**) o [Pd(CNC)(PPh₃)] (**2**), se produce tanto la reacción de protonación como la coordinación del ligando de manera bidentada, formando un anillo quelato. Excepcionalmente, cuando el ligando utilizado es la piridina-2-tiol, se obtiene un complejo dinuclear con ligandos puente.

6. En estas reacciones en las que se produce una sustitución de ligandos, el proceso está más favorecido con los ligandos P-dador que con ligandos N-dador, siendo necesarios para el último caso condiciones de reacción más energéticas y tiempos más largos. Además, el uso de ligandos bidentados en las reacciones de protonación puede dar lugar a la formación de isómeros. Esto no fue observado para los ligandos P-dador debido a sus elevados requerimientos estéricos.
7. Intermedios con interacciones Pt...H-O podrían jugar un papel importante en algunas de estas reacciones, como pudo ser observado en la reacción de [Pt(CNC)(dmsO)] (**12**) con (2-hidroxifenil)difenilfosfano a baja temperatura y dado que existen complejos similares en la bibliografía con este tipo de interacciones.
8. Además, se ha explorado la reactividad de los sustratos básicos [Pt(CNC)(PPh₃)] (**1**) y [Pd(CNC)(PPh₃)] (**2**) con fuentes de grupos metilo electrófilo, como MeI o (Me₃O)(BF₄). En el caso del complejo de paladio (II) **2**, no se pudieron obtener resultados concluyentes. El complejo **1** no reacciona con (Me₃O)(BF₄). Por otro lado, la adición oxidante de MeI a **1** da lugar al complejo esperado *trans* de Pt(IV) [Pt(IV)Me(CNC)(PPh₃)] (**28**). No se observó isomerización *trans-cis* para este complejo.

9. La eliminación reductora del grupo metilo del complejo **28** con el C_{ipso} del ligando CNC da lugar a un acoplamiento C-C y a la metilación del ligando. Si se trata el complejo **28** con una sal de plata, la eliminación reductora con precipitación de AgI tiene lugar en condiciones más suaves de reacción. Los complejos metilados de Pt(II) [Pt(CN-*o*-tol)I(PPh₃)] (**29**) y [Pt(CN-*o*-tol)(MeCN)(PPh₃)](ClO₄) (**30**) pueden ser ciclometalados de nuevo en presencia de medio básico y hechos reaccionar de nuevo con MeI. En este caso, el complejo de Pt(IV) correspondiente no pudo ser aislado, y se obtuvo directamente el producto de eliminación reductora. La segunda metilación tiene lugar en el anillo previamente metilado.
10. Como resultado global de estas reacciones un anillo fenilénico del ligando CNC es metilado en posiciones *orto*.
11. La reacción del complejo [Pt(CNC-Me)(PPh₃)] (**32**) con una fuente de protones como el HCl da lugar a una protonación en el anillo ya metilado.

